COORDINATION CHEMISTRY AND FUNCTIONALIZATION OF BENZANNULATED N-HETEROCYCLIC CARBENES

TENG QIAOQIAO

NATIONAL UNIVERSITY OF SINGAPORE

2014

COORDINATION CHEMISTRY AND FUNCTIONALIZATION OF BENZANNULATED N-HETEROCYCLIC CARBENES

TENG QIAOQIAO

(*B.SC.*, SOOCHOW UNIVERSITY)

A THESIS SUBMITTED FOR THE DEGREE OF DOCTOR OF PHILOSOPHY

DEPARTMENT OF CHEMISTRY

NATIONAL UNIVERSITY OF SINGAPORE

2014

DECLARATION

I hereby declare that this thesis is my original work and it has been written by me in its entirety, under the supervision of A/P Huynh Han Vinh, Department of Chemistry, National University of Singapore.

I have duly acknowledged all the sources of information which have been used in this thesis.

This thesis has also not been submitted for any degree in any university previously.

Teng Qiaoqiao	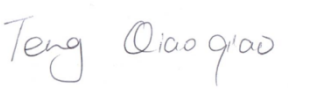	1/8/2014
Name	Signature	Date

Acknowledgements

I would like to express my deepest thanks to my supervisor, Dr. Huynh Han Vinh, for all his patient guidance throughout my research. He is a professor who cares about his students very much and devotes abundant time to teaching and discussing with the students. It is such a fortune for me to be his student. During the last four years, I do have learnt a lot from him; not only the specific skill of doing experiment, but also the positive attitude for research and life as well.

I thank the National University of Singapore and Singapore Ministry of Education for giving me the opportunity and scholarship to pursue my Ph. D degree in Singapore.

I would also like to thank my past and present colleagues, Dr. Han Yuan, Dr. Yuan Dan, Jan Christopher Bernhammer, Xie Xiao Ke for their discussion and advice. Special thanks were given to Haresh S/O Sivaram and Guo Shuai for their help along my research.

The staff at X-ray diffraction, Nuclear Magnetic Resonance, Mass spectrometry and Elemental Analysis in the chemistry department is greatly thanked for their technical support and discussion.

Last but not least, I thank my family and friends for their unconditional love and support.

Table of Contents

Table of Contents I
Summary III
Compounds Synthesized in this Work IV
List of Tables and Charts X
List of Figures XI
List of Schemes XIV
List of Abbreviations XVI
1. Introduction 1
1.1 Carbenes and N-heterocyclic Carbenes 1
1.1.1 Singlet and Triplet Carbenes 1
1.1.2 N-heterocyclic Carbenes 2
1.2 Carbenes as Ligands in Transition Metal Complexes 5
1.2.1 Fischer and Schrock Carbene Complexes 5
1.2.2 NHC Complexes 6
1.3 NHC as a Probe in Ligands Donor Strengths Determination 8
1.4 Functionalized-NHC Metal Complexes 11
1.4.1 Synthetic Approaches to Functionalized-NHC Metal Complexes 11
1.4.2 Functionalized-NHC in Metallosupramolecular Chemistry 14
2. Donor Strengths Determination of Monodentate and Bidentate Ligands Using Their Palladium(II) 1,3-diisopropylbenzimidazolin-2-ylidene Complexes 17
2.1 Donor Strengths Determination of Monodentate Ligands 17
2.1.1 Electron Donor Strengths of Substituted Pyridines 17
2.1.2 Electron Donor Strengths of Other N, P, As, Sb, S and O Ligands 22
2.2 Donor Strengths Determination of Bidentate Ligands 33
2.2.1 Electron Donor Strengths of Diimines 33
2.2.2 Electron Donor Strengths of Dicarbenes 38
3. Synthesis of Functionalized-NHC Palladium(II) Complexes Via a Postmodification Approach 50
3.1 Synthesis of Parent Complexes 50

3.1.1 Synthesis of Mono(NHC)-Pd(II) Parent Complex 50
3.1.2 Synthesis of Bis(NHC)-Pd(II) Parent Complex 54
3.2 Synthesis of Functionalized-NHC Palladium Complexes 58
3.2.1 Synthesis of Mono(functionalized NHC)-Pd(II) Complexes 58
3.2.2 Synthesis and Catalytic Activities of Bis(functionalized NHC)-Pd(II) Complexes 68
4. Multi-metallic Complexes Bearing Dipropyl-pyridine-2,6-dicarboxamide bridged diNHC Ligands 80
4.1 Synthesis and Characterization of Ligand Precursors 80
4.2 Synthesis and Characterization of Gold Complexes 83
4.2.1 Synthesis and Characterization of Metallocyclic NHC-Silver(I), Gold(I) and Gold(III) Complexes 83
4.2.2 Synthesis and Characterization of a Macrocyclic Bimetallic Trinuclear [Au(I), Co(III)] Double Helical Complex 89
4.3 Synthesis and Characterization of Palladium(II) complexes 92
5. Conclusion 104
6. Experimental Section 110
7. Selected Crystallographic Data 171
Appendix 180
References 194

Summary

N-heterocyclic carbenes (NHC) are state of the art ligands in organometallic chemistry. They have been widely used as supporting ligands for transition metals to obtain complexes with diverse and interesting structural or catalytic properties.

Using a NHC as a reporter ligand in complexes of the type *trans*-[$PdBr_2(^iPr_2$-bimy)L], the Huynh group recently developed a new ^{13}C NMR based electronic parameter for the evaluation of Werner-type and organometallic ligands L in terms of their net electron donating properties. In continuation of this study, one topic of this thesis addresses the extension of this electronic parameter to a wider scope of monodentate ligands. Moreover, a general ^{13}C NMR based methodology for the evaluation of bidentate ligands has been developed.

The functionalization of NHC complexes, which may lead to complexes with better chemical, physical and biological properties, is one of the important topics for NHC chemists. As a second topic in this work, a versatile and modular postmodification strategy to access functionalized-NHC complexes is described. In comparison to the traditional method, where metalation of individually pre-functionalized NHC precursors is required, this methodology represents a substantial improvement in terms of cost, labor, time and waste reduction.

Only recently has NHCs been applied as building blocks in metallosupramolecular chemistry. As the third major topic and our contribution to this field, we designed a multi-topic pro-ligand by functionalizing NHC precursors with a dipropyl-pyridine-dicarboxamide unit. The resulting potential pentadentate ligands showed interesting coordination chemistry with gold, cobalt and palladium.

The new compounds synthesized in this work are depicted in the following section (see Compounds Synthesized in this Work).

Compounds Synthesized in this Work

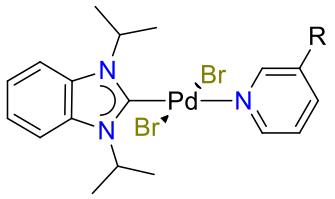

R = F, **1**; Cl, **2**; Br, **3**
I, **4**; OH, **5**; Ph, **6**

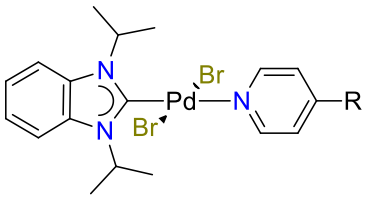

R = Cl, **7**; Br, **8**; I, **9**;
OH, **10**; Ph, **11**

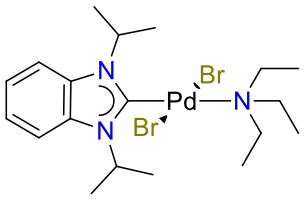

12

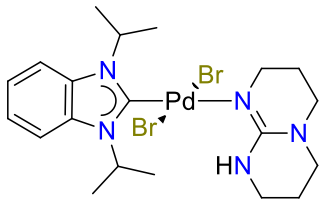

13

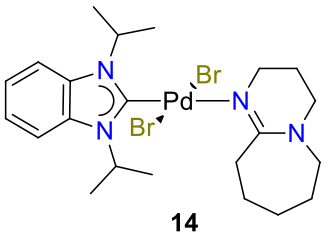

14

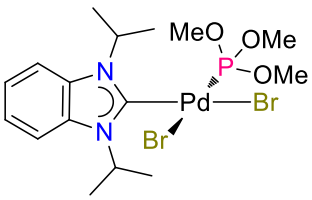

***cis*-15**

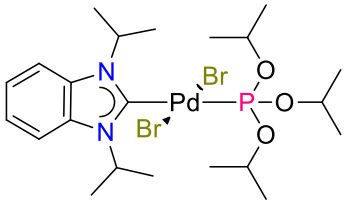

***trans*-16**

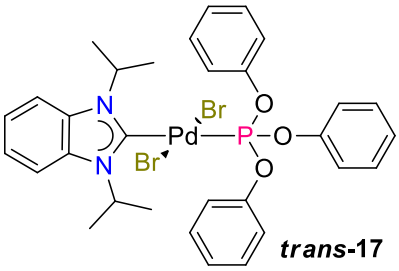

***trans*-17**

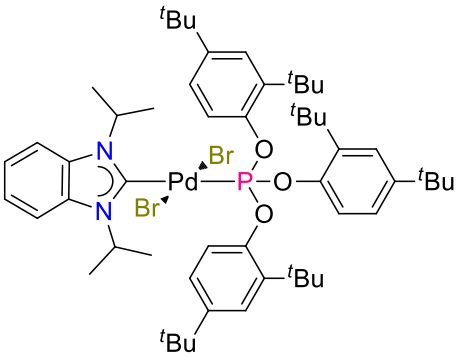

18

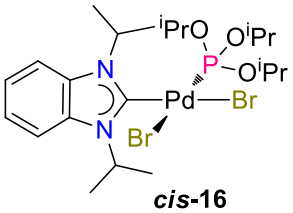

***cis*-16**

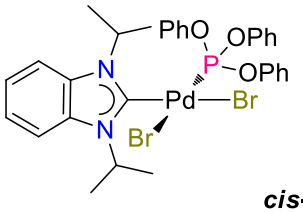

***cis*-17**

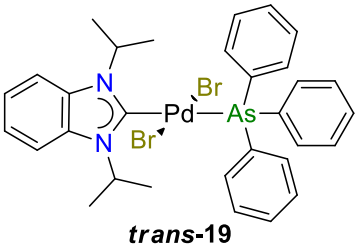

***trans*-19**

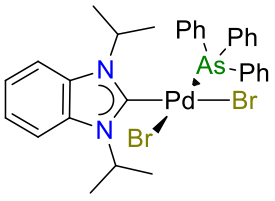

***cis*-19**

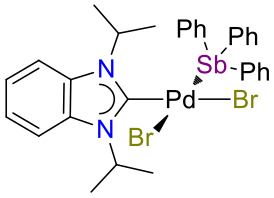

20

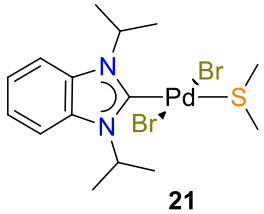

21

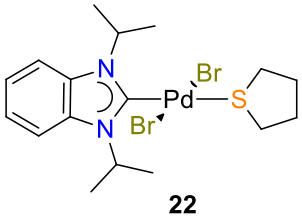

22

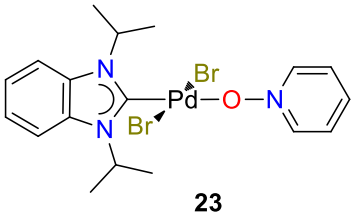

23

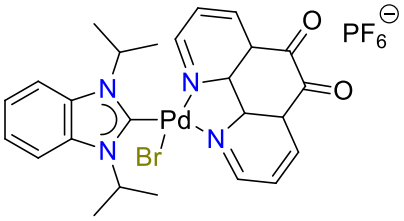

24

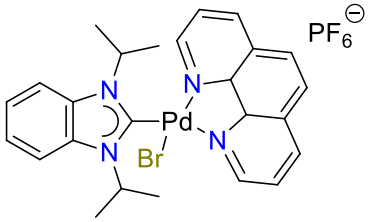

25

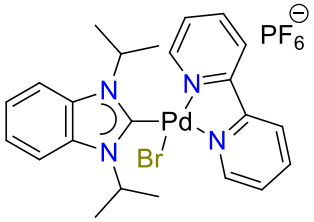

26

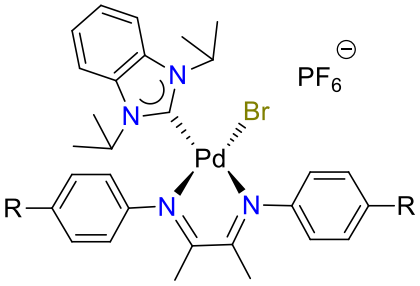

R = Br, **27**; H, **28**; Me, **29**
OMe, **30**; ^{t}Bu, **31**

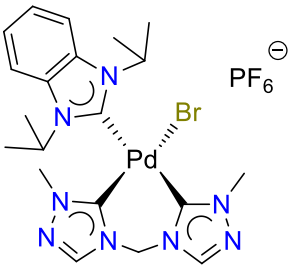

32

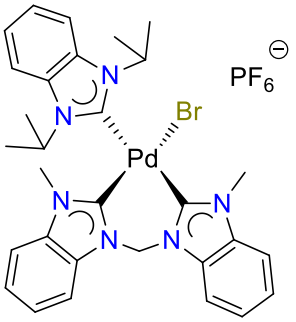

33

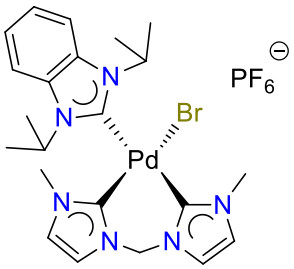

34

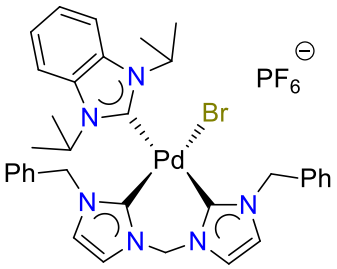

35

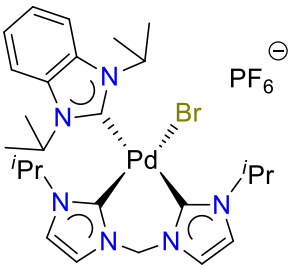

36

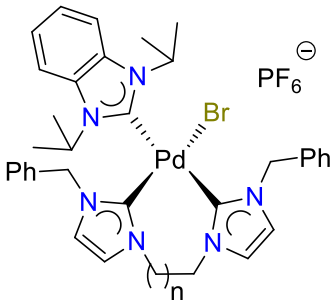

n = 1, **37**; 2, **38**

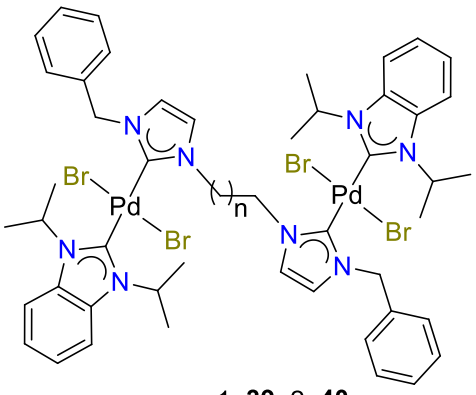

n = 1, **39**; 2, **40**

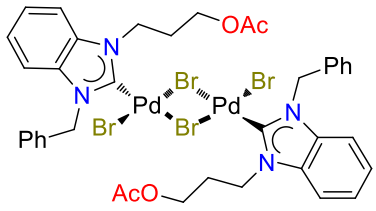

41

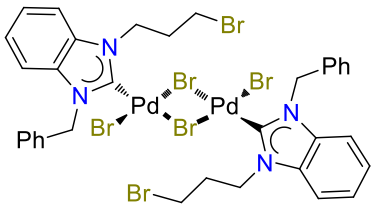

42

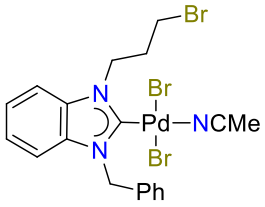

43

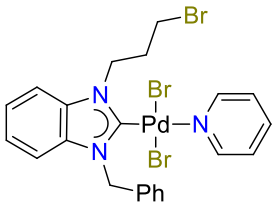

44

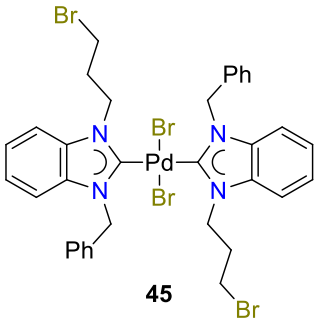

45

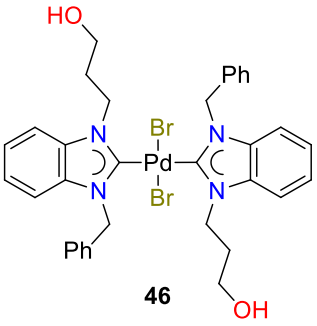

46

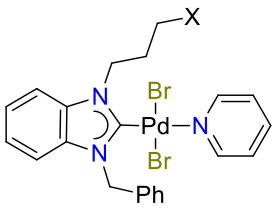

X = OAc, **47**; N_3, **48**

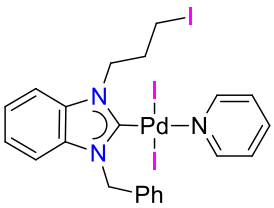

49

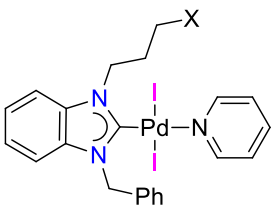

X = N_3, **50**; SCN, **51**; SAc, **52**

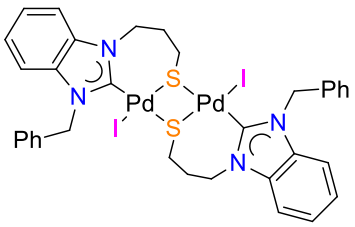

53

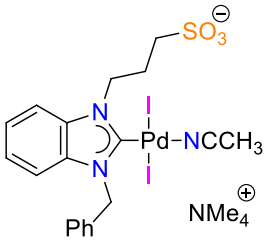

54

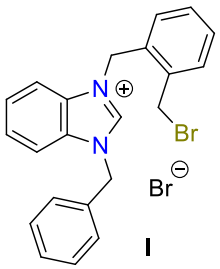

I

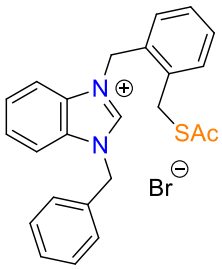

J

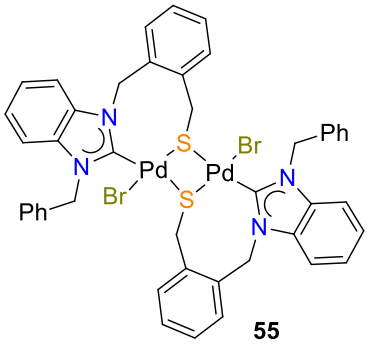

55

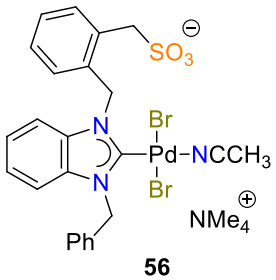

56

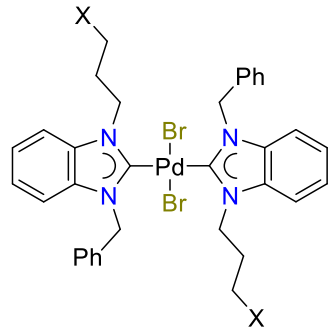

X = OAc, **57**; NEt_2, **58**; N_3, **59**

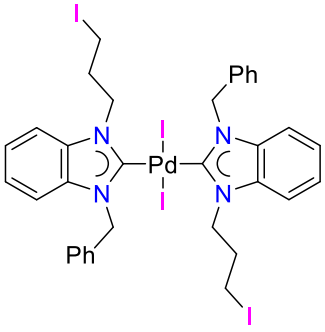

60

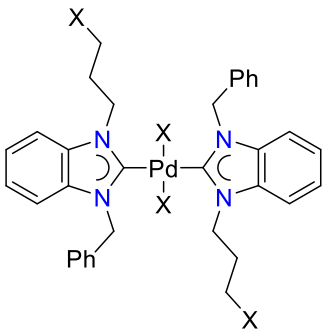

X = SPh, **61**; SCN, **62**

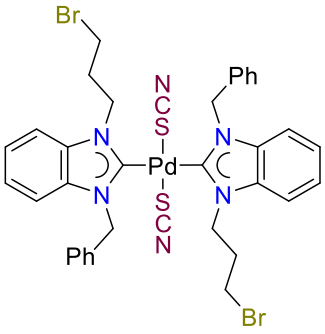

63

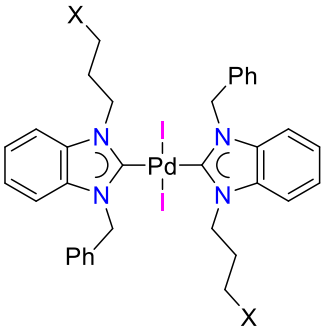

X = N_3, **64**; SPh, **65**;
SAc, **66**; SCN, **67**

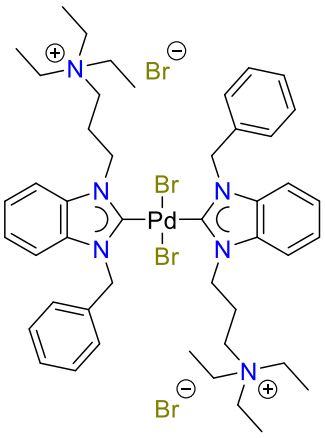

68

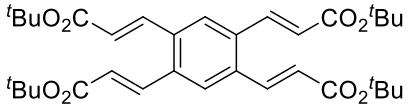

69

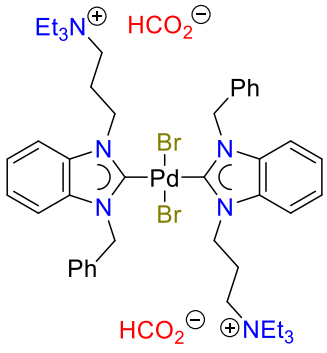

70

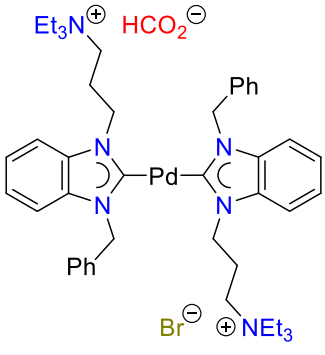

71

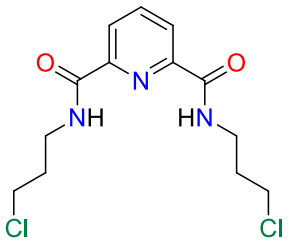

K

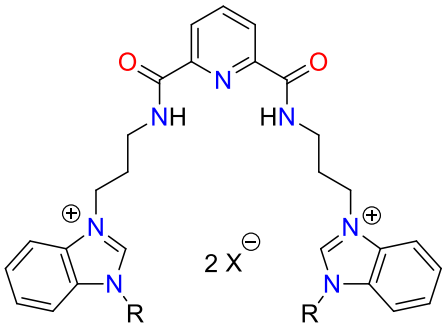

X = I; R = Bn, **L_{Bn}**; Me, **L_{Me}**
X = BF_4; R = Bn, **M_{Bn}**; Me, **M_{Me}**

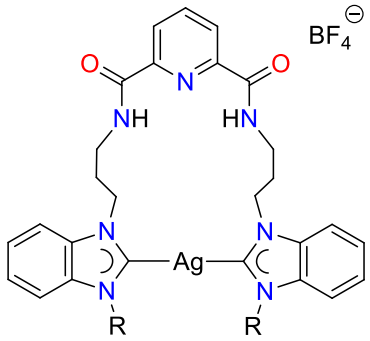

R = Bn/Me, **$72_{Bn/Me}$**

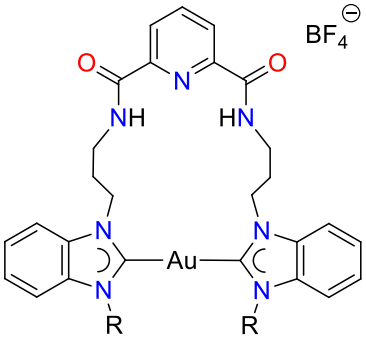

$73_{Bn/Me}$

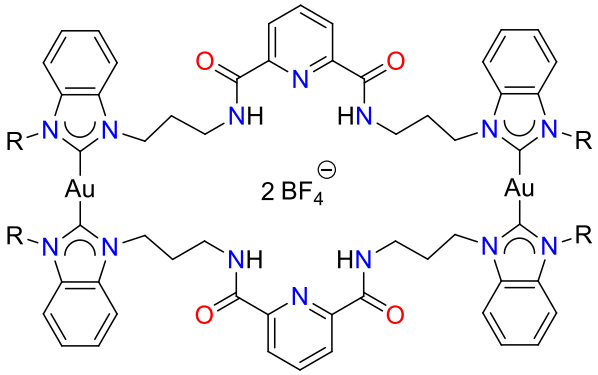

$74_{Bn/Me}$

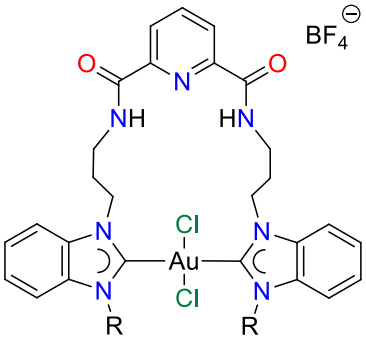

$75_{Bn/Me}$

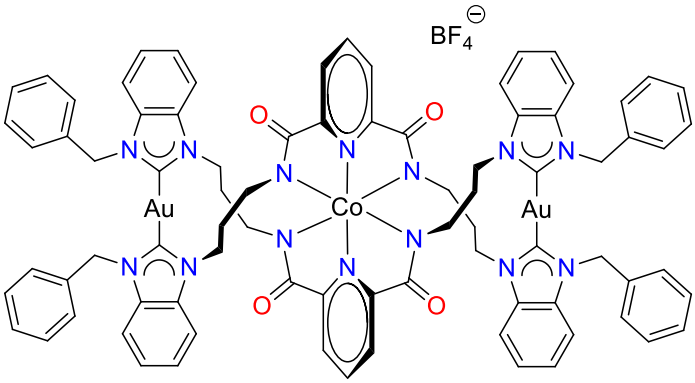

76

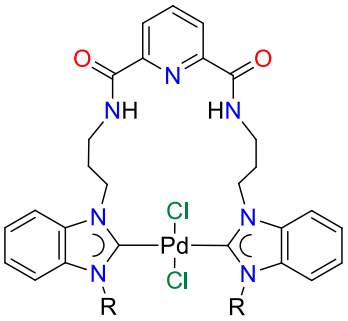

$77_{Bn/Me}$

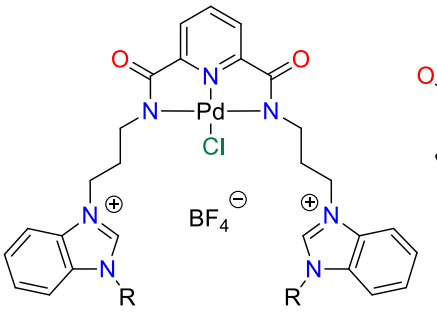

$78_{Bn/Me}$

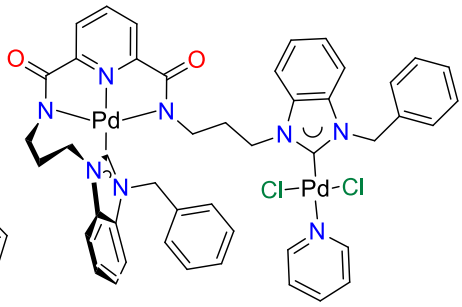

80

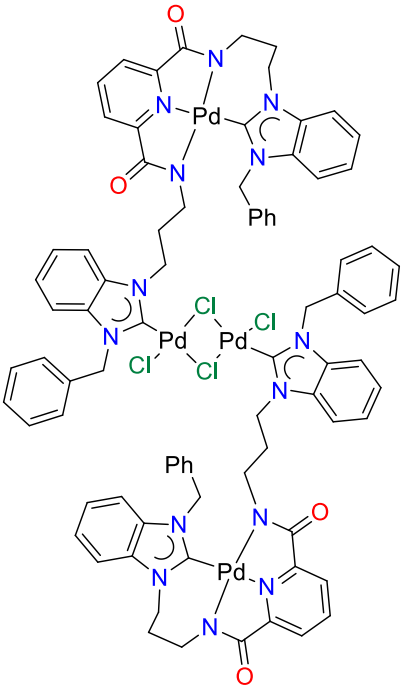

79

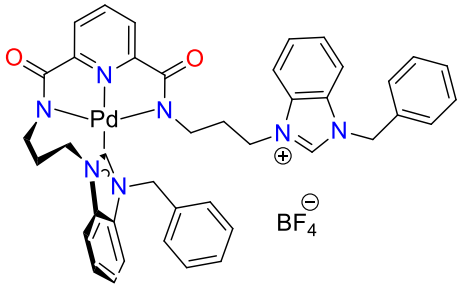

81

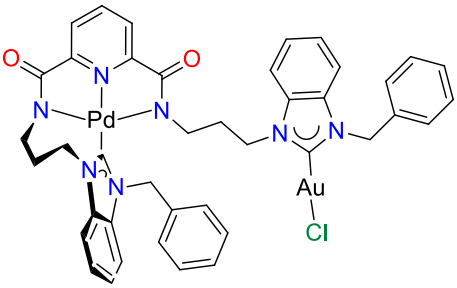

82

List of Tables and Charts

Table 2.1. $^{1}H_{NCH}$ and $^{13}C_{carbene}$ NMR resonances of complexes *trans*-[$PdBr_2$($^{i}Pr_2$-bimy)(R-Py)] (**1**–**11**) and Hammett σ constants for the respective substituent

Table 2.2. Selected NMR data of complexes [$PdBr_2$($^{i}Pr_2$-bimy)(L)] (L = phosphites, triphenylarsine, triphenylantimony, **15**–**20**)

Table 2.3. Summary of $^{i}Pr_2$-bimy carbenoid resonances in complexes bearing diimines

Table 2.4. Summary of $^{i}Pr_2$-bimy carbenoid resonances in complexes bearing diNHC chelators

Table 3.1. α-CH_2, $C_{carbene}$ NMR resonances of complexes *trans*-[PdY_2(C_3X-bimy)(Py)] (**41**–**44**, **47**–**52**)

Table 3.2. α-CH_2, $C_{carbene}$ NMR resonances and ESI mass signals of complexes *trans*-[PdY_2(C_3X-bimy)$_2$] (**45**, **46**, **57**–**63**)

Table 3.3. α-CH_2, $C_{carbene}$ NMR resonances and ESI mass signals of complexes *trans*-[PdI_2(C_3X-bimy)$_2$] (**60**, **64**–**67**)

Table 3.4. Mizoroki-Heck coupling reactions

Table 4.1. Selected NMR data of salts $\mathbf{M_{Bn/Me}}$, their Ag(I)-complexes $\mathbf{72_{Bn/Me}}$, and Pd(II)-complexes **77**–**82**

Chart 2.1. Sketches of the three nitrogen organic bases

Chart 2.2. Lewis structures of 7 classical diNHCs

List of Figures

Figure 1.1. Singlet and triplet state of carbenes

Figure 1.2. Representative electronic configuration and resonance structures of NHCs

Figure 1.3. Three major types of NHCs and their properties

Figure 1.4. Fischer and Schrock type carbene complexes

Figure 1.5. Ligand donor strengths reflected by TEP and LEP

Figure 1.6. Donor abilities of Werner and organometallic ligands on a ^{13}C NMR scale

Figure 1.7. Selection of metallosupramolecular structures featuring NHC moieties

Figure 1.8. Reported double stranded-helicates NHC complexes

Figure 2.1. ^{1}H NMR spectra of complexes *trans*-[$PdBr_2$($^{i}Pr_2$-bimy)(3-Br-Py)] (**3**) and *trans*-[$PdBr_2$($^{i}Pr_2$-bimy)(4-Br-Py)] (**8**)

Figure 2.2. Resonance structures of OH-pyridines

Figure 2.3. Molecular structure of complex *trans*-[$PdBr_2$($^{i}Pr_2$-bimy)(TBD)] (**13**)

Figure 2.4. Conjugation of the protonatedTBD and DBU ammonium ions

Figure 2.5. Molecular structures of complexes *cis*-[$PdBr_2$($^{i}Pr_2$-bimy)(L)] (L = phosphites, **15**–**17**; triphenylarsine, **19**; trihenylantimony, **20**)

Figure 2.6. Molecular structures of complexes *trans*-[$PdBr_2$($^{i}Pr_2$-bimy)(SMe_2)] (**22**) and *trans*-[$PdBr_2$($^{i}Pr_2$-bimy)(PNO)] (**23**)

Figure 2.7. Donor abilities of P, As, N, S and O donors on a unified ^{13}C NMR scale

Figure 2.8. Donor abilities of aromatic and aliphatic diimines on the ^{13}C NMR scale

Figure 2.9. Molecular structures of complexes [PdBr($^{i}Pr_2$-bimy)(phen)]PF_6 (**25**) and [PdBr($^{i}Pr_2$-bimy)(Br-DAB)]PF_6 (**30**)

Figure 2.10. Variable temperature ^{1}H NMR spectra of complex [PdBr($^{i}Pr_2$-bimy)(ditazy)]PF_6 (**32**) in the region of 4.5–9.0 ppm

Figure 2.11. Section of the 2D ^{1}H,^{13}C-HMBC NMR spectrum of complex [PdBr($^{i}Pr_2$-bimy)(dibimy)]PF_6 (**33**)

Figure 2.12. Donor abilities of dicarbenes on the ^{13}C NMR scale

Figure 2.13. Molecular structures of complexes [PdBr($^{i}Pr_2$-bimy)(diNHC)]PF_6 (**32**, **34**, **37** and **38**)

Figure 2.14. Molecular structure of dinuclear complex [Pd_2Br_4($^{i}Pr_2$-bimy)$_2$(diNHC)] (**40**)

Figure 3.1. Molecular structure of complex [$PdBr_2$(C_3OAc-bimy)]$_2$ (**41**)

Figure 3.2. Molecular structure of complex [$PdBr_2$(C_3Br-bimy)(CH_3CN)] (**43**)

Figure 3.3. ^{1}H NMR spectrum for the *trans*-[$PdBr_2$(C_3Br-bimy)(Py)] complex **44**

Figure 3.4. ^{1}H NMR spectrum for the *trans*-[$PdBr_2$(C_3Br-bimy)$_2$] complex **45** in the aliphatic region

Figure 3.5. Molecular structure of complex *trans*-[$PdBr_2$(C_3Br-bimy)$_2$] (**45**)

Figure 3.6. Molecular structures of complexes *trans*-[PdI_2(C_3I-bimy)(Py)] (**49**) and *trans*-[PdI_2(C_3SCN-bimy)(Py)] (**51**)

Figure 3.7. Molecular structure of propyl-thiolato-bridged complex **53**

Figure 3.8. Isotopic pattern of the [M – NMe_4 – CH_3CN]$^-$ fragment of complex *trans*-(NMe_4)[PdI_2(C_3SO_3-bimy)(CH_3CN)] (**54**) in the negative ESI mass spectrum (left) and a simulated pattern (right)

Figure 3.9. Molecular structure of xylenyl-thiolato-bridged complex **55**

Figure 3.10. Molecular structure of xylenyl-sulfonate complex **56**

Figure 3.11. Molecular structures of complexes *trans*-[PdY_2(C_3X-bimy)$_2$] (**57**, **61**–**63**)

Figure 3.12. Molecular structure of complex *trans*-[PdI_2(C_3SCN-bimy)$_2$] (**67**)

Figure 4.1. Molecular structure and perspective view of dipropyl-pyridine-2,6-dicarboxamide bridged dibenzimidazolium salt precursor $\mathbf{M_{Bn}}$

Figure 4.2. ^{1}H NMR spectra of monogold $\mathbf{73_{Bn}}$ and digold $\mathbf{74_{Bn}}$ complexes in the range of 2.2 to 10.0 ppm ($CDCl_3$)

Figure 4.3. Isotopic pattern of the base peaks belonging to monogold $\mathbf{73_{Bn}}$ and digold $\mathbf{74_{Bn}}$ complexes in the respective positive ESI mass spectrum

Figure 4.4. Molecular structure of monogold complex $\mathbf{73_{Me}}$

Figure 4.5. Molecular structure of digold complex $\mathbf{74_{Bn}}$

Figure 4.6. Possible spin states of d^6 metal complexes

Figure 4.7. Molecular structure of mixed [Au(I)/Co(III)] complex **76**

Figure 4.8. ^{1}H and ^{13}C NMR spectra of salt precursor $\mathbf{M_{Bn}}$ (CD_3CN) and *trans*-[$PdCl_2$(diNHC)] complex $\mathbf{77_{Bn}}$ ($CDCl_3$)

Figure 4.9. Molecular structures of complexes *trans*-[$PdCl_2$(diNHC)] ($\mathbf{77_{Bn,Me}}$)

Figure 4.10. ^{1}H and ^{13}C NMR spectra of [PdCl(N',N,N')]BF_4 complex $\mathbf{78_{Bn}}$ ($CDCl_3$)

Figure 4.11. Molecular structure of [PdCl(N',N,N')]BF_4 complex ($\mathbf{78_{Me}}$)

Figure 4.12. ^{1}H and ^{13}C NMR spectra of tetra-Pd(II) complex **79** (CD_3CN)

Figure 4.13. Section of the 2D $^{1}H,^{13}C$-HMBC NMR spectrum of hetero-bimetallic [Pd(II)/Au(I)] complex **82**

Figure 4.14. Molecular structure of complex **82**

List of Schemes

Scheme 1.1. Attempts of preparing a free NHC by Wanzlick

Scheme 1.2. Synthesis of the first free NHC by Arduengo

Scheme 1.3. Synthesis of the first NHC metal complex

Scheme 1.4. Synthesis of functionalized-NHC complexes via the traditional and postmodification routes

Scheme 1.5. Isolation of unexpected thiolato-bridged dimeric complex via metalation of thioester-functionalized-azolium salt

Scheme 2.1. Cleavage reactions of $[PdBr_2(^{i}Pr_2\text{-bimy})]_2$ (**I**) to afford *trans*/*cis*-$[PdBr_2(^{i}Pr_2\text{-bimy})(L)]$ complexes

Scheme 2.2. Synthesis of $[PdBr(^{i}Pr_2\text{-bimy})(diimine)]PF_6$ complexes (**24**–**31**)

Scheme 2.3. Synthesis of $[PdBr(^{i}Pr_2\text{-bimy})(diNHC)]PF_6$ complexes (**32**–**38**) and $[Pd_2Br_4(^{i}Pr_2\text{-bimy})_2(diNHC)]$ complexes (**39**–**40**)

Scheme 3.1. Synthesis of complex precursors $[PdBr_2(C_3OAc\text{-bimy})]_2$ (**41**) and $[PdBr_2(C_3Br\text{-bimy})]_2$ (**42**)

Scheme 3.2. Cleavage of complex **42** to $[PdBr_2(C_3Br\text{-bimy})(CH_3CN)]$ (**43**)

Scheme 3.3. Synthesis of mono(NHC)-Pd(II) parent complex **44**

Scheme 3.4. Synthesis of bis(NHC)-Pd(II) parent complex **45**

Scheme 3.5. Hydrolysis of *trans*-$[PdBr_2(C_3Br\text{-bimy})_2]$ (**45**) to *trans*-$[PdBr_2(C_3OH\text{-bimy})_2]$ (**46**)

Scheme 3.6. Postmodifications of mono(NHC)-Pd(II) complex **44**

Scheme 3.7. Synthesis of propyl-thiolato-bridged complex **53**

Scheme 3.8. Synthesis of propyl-sulfonate complex **54**

Scheme 3.9. Synthesis of xylenyl-thiolato-bridged complex **55**

Scheme 3.10. Synthesis of xylenyl-sulfonate complex **56**

Scheme 3.11. First generation postmodifications of bis(NHC)-Pd(II) complex **45**

Scheme 3.12. Second generation postmodifications of bis(NHC)-Pd(II) complex **60**

Scheme 3.13. Synthesis of *trans*-[$PdBr_2(C_3NEt_3$-bimy$)_2]Br_2$ (**68**)

Scheme 3.14. Reduction of **68** to [$Pd(C_3NEt_3$-bimy$)_2]X_2$ (**71**)

Scheme 4.1. Synthesis of dipropyl-pyridine-2,6-dicarboxamide bridged dibenzimidazolium ligand precursors

Scheme 4.2. Synthesis of silver and gold complexes

Scheme 4.3. Synthesis of mixed [Au(I)/Co(III)] complex **76**

Scheme 4.4. Synthesis of *trans*-[$PdCl_2$(diNHC)] complexes $\mathbf{77_{Bn/Me}}$

Scheme 4.5. Synthesis of pincer type [$PdCl(N^{'},N,N^{'})]BF_4$ complexes $\mathbf{7_{Bn/Me}}$

Scheme 4.6. Synthesis of tetra-Pd(II) **79** and di-Pd(II) pyridine adduct **80**

Scheme 4.7. Synthesis of intermediate complex **81**

Scheme 4.8. Synthesis of tetra-Pd(II) complex **79** and heterobimetallic [Pd(II)/Au(I)] complex **82** from complex **81**

Scheme 5.1. [$PdBr_2(^{i}Pr_2$-bimy)(L)] and [$PdBr(^{i}Pr_2$-bimy)$(L_2)]PF_6$ complexes

Scheme 5.2. Mono- and bis-(functionalized NHC) Pd(II) complexes

Scheme 5.3. Complexes bearing dipropyl-pyridine-2,6-dicarboxamide bridged dibenzimidazolin-2-ylidene ligands

List of Abbreviations

Anal. Calcd	Analysis calculated
Ar	Aryl
AT	Ambient temperature
Bn	Benzyl
br	Broad
δ	NMR chemical shift in ppm
d	Doublet
dd	Doublet of doublet
DMSO	Dimethylsulfoxide
DMF	Dimethylfornsmide
e.g.	For example
equiv	Equivalent
ESI	Electrospray Ionisation
et al	and others
etc.	and so on
h	Hour
I	Inductive effect
i.e.	that is
^{i}Pr	Isopropyl
J	Coupling constant
m	Multiplet
M	Mesomeric effect
Me	Methyl
MS	Mass spectrometry
m/z	Mass to charge ratio
NMR	Nuclear Magnetic Resonance
Ph	Phenyl
s	Singlet
t	Triplet
THF	Tetrahydrofurane

1. Introduction

1.1 Carbenes and N-heterocyclic Carbenes

1.1.1 Singlet and Triplet Carbenes

According to the International Union of Pure and Applied Chemistry (IUPAC) a carbene is "*the electrically neutral species H_2C: and its derivatives, in which the carbon is covalently bonded to two univalent groups of any kind or a divalent group and bears two nonbonding electrons*."[1] Most carbenes contain an sp^2-hybridized carbon center and therefore are bent. A free carbene may have two spin states, singlet and triplet.[2] In the singlet carbene, the two nonbonding electrons are paired up in the frontier σ orbital. Hence, the total spin is zero and the multiplicity is one. In contrast, the two electrons could also remain unpaired occupying the σ and p_π orbitals, which results in a total spin of one and multiplicity of three (Figure 1.1).

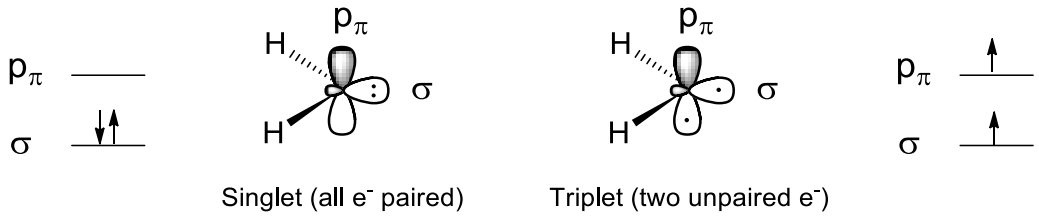

Figure 1.1. Singlet and triplet state of carbenes.

As described by Hund's rule, the singlet state will have a higher energy than the triplet state due to spin pair energy in the σ orbital (Δ = 8 kcal/mol). Hence, for a simple CH_2: carbene, the triplet carbene is the more stable (ground) state and singlet is the excited state. However, the ground state would change from triplet state to singlet upon substituent variations. Harrison et al. showed that electron withdrawing substituents could inductively stabilize the σ orbital by

enriching the s character and leaving the p_π orbital unchanged.[3] Hoffmann and Baird, on the other hand, described that π-electron donor substituents could increase the empty p_π orbital energy owing to their mesomeric effects, without affecting the σ orbital to a great extent.[4] Both these substituent effects would increase the energy gap between the σ and p_π orbitals, and therefore the singlet ground state would be favored.

1.1.2 N-heterocyclic Carbenes

For a few decades, carbenes were considered highly reactive transient intermediates in organic transformations. Isolation of a free carbene seemed impossible due to the incomplete electron octet and coordinative unsaturation. Although carbene chemistry was advanced with matrix-isolation of short-lived triplet carbenes,[5] the discovery of N-heterocyclic carbenes (NHCs), which are able to survive under normal condition and in bulk, makes the carbene chemistry develop rapidly.[6]

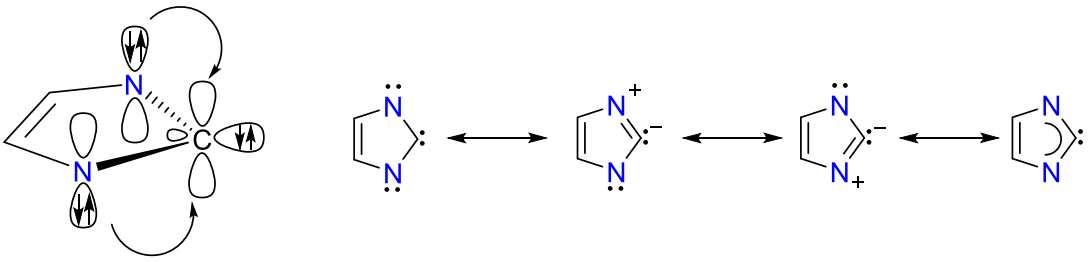

Figure 1.2. Representative electronic configuration, resonance structures and Lewis structure of NHCs.

NHCs are, as the name suggests, neutral, cyclic species with at least one nitrogen atom within the ring and one divalent carbene atom bearing a lone pair of electrons. On one hand, the N atoms pull electrons away from the carbene carbon, but on the other hand, they also push

electrons to the empty p_π orbital of the carbene carbon center (Figure 1.2). This overall "push-pull" effect greatly stabilizes the carbene center in the singlet state, and hence NHCs are exclusively singlet carbenes in the ground state.[7]

Isolation of a free NHC was initially attempted by Wanzlick in 1962.[8] The reaction was designed to give the imidazolidin-2-ylidene by elimination of chloroform from the imidazoline derivative (Scheme 1.1). However, an enetetramine compound was isolated instead due to dimerization of the transient carbene. The generation of the free carbene was corroborated by the successful trapping with transition metals afterwards (*vide infra*).

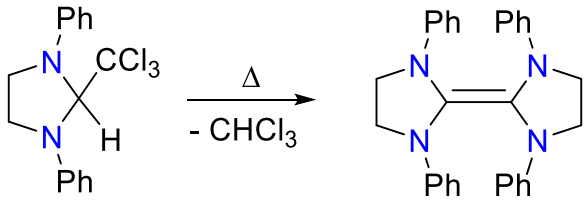

Scheme 1.1. Attempts of preparing a free NHC by Wanzlick.

Only in 1991 was the first free NHC successfully isolated by Arduengo et al via the deprotonation of a 1,3-diadamantyl imidazolium salt with NaH in the catalytic amount of DMSO in THF (Scheme 1.2).[9]

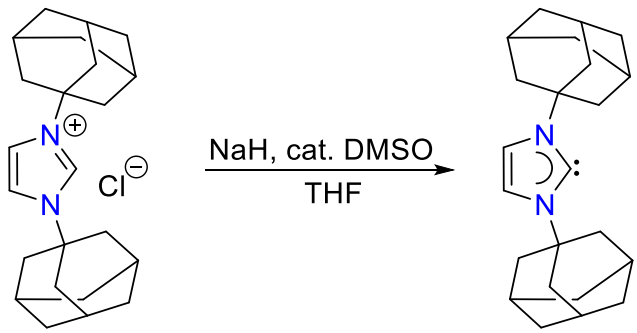

Scheme 1.2. Synthesis of the first free NHC by Arduengo.

This “bottle-able” species is stable at ambient temperature in the absence of oxygen and moisture. The stability of this NHC was initially attributed to the two bulky N-adamantyl groups, which help to kinetically stabilize the species by sterically disfavouring dimerization to the corresponding olefin. Later on, it was found that the partial aromaticity arising from a certain extent of electron delocalization in the five-membered ring would account for a more important degree of stabilization at the carbene center.

The isolation of the first Arduengo NHC marked the renaissance of NHCs and led to a great increase of experimental and theoretical studies with a large number of NHCs being synthesized and analyzed.[10] Among them, three major types, namely imidazolin-2-ylidene, benzimidazolin-2-ylidene and imidazolidin-2-ylidene, were studied the most extensively (Figure 1.3).

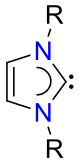

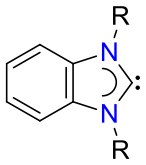

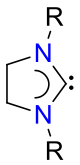

	imidazolin-2-ylidene	**benzimidazolin-2-ylidene**	**imidazolidin-2-ylidene**
Tendency to dimerize	no	depends on R	depends on R
Topology	unsaturated, aromatic	benzannulated	saturated, nonaromatic
$^{13}C_{carbene}$ (ppm)	205-215	223-231	238-244
N-C-N angle (°)	101.2-102.2	103.5-104.3	104.7-106.6

Figure 1.3. Three major types of NHCs and their properties.

The unsaturated imidazolin-2-ylidenes benefit from aromatic stabilization in comparison to the saturated imidazolidin-2-yidenes (*vide supra*), which allows for a lesser demand for proximal steric bulk. Interestingly, benzimidazolin-2-ylidenes have the topology of an

unsaturated NHC. However, they show similar stability to the saturated imidazolidin-2-ylidenes and tend to dimerize when R is a less bulky substituent (Figure 1.3). This indicates that in benzimidazolin-2-ylidenes, the electron delocalization in the five-membered ring is reduced due to the already fully delocalized 6π aryl system. Hence, a smaller aromatic stabilization is present as compared to that of the unsaturated imidazolin-2-ylidenes. Notably, the sequences of increasing downfield shift for the $^{13}C_{carbene}$ resonances and enlarging N–C–N bond angles are the same as that observed for the decrease of aromatic characters of these three NHCs.

Increasing attention has been paid to benzannulated NHCs since the isolation of the first representative by Hahn and co-workers.[10h] However, they are still far less established than the other two counterparts in literature. Hence, it is of our interest to explore the chemistry of benzimidazolin-2-ylidene and their transition metal complexes. In this work, most of the NHCs are derived from benzimidazole.

1.2 Carbenes as Ligands in Transition Metal Complexes

1.2.1 Fischer and Schrock Carbene Complexes

Carbenes have already been used as ligands to form metal complexes in the early 1960s. Generally, the resulting complexes were classified into Fischer and Schrock types, as named after the two respective chemists who isolated the first example of each (Figure 1.4). In the Fischer type complex, the metal-carbene bond contains two types of interaction, i.e. σ-donation from the electron lone pair of the carbon to an empty p-orbital of the metal and π-back bonding of a filled orbital on the metal to the empty p_π orbital of the carbon. The C→M donation predominates and hence the carbon atom tends to be more positively charged. In the Schrock carbene complex,

however, two covalent bonds are formed with each polarized to the carbon giving it a partially negative charge.

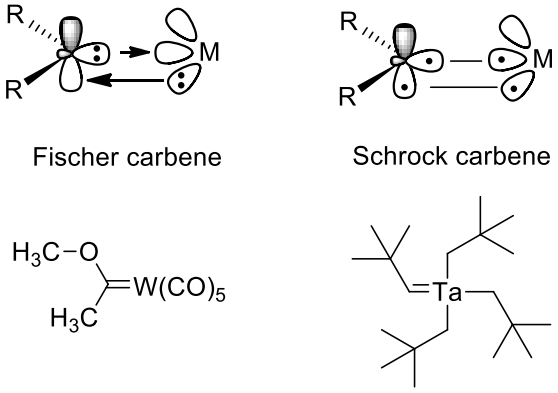

Figure 1.4. Fischer and Schrock type carbene complexes.

In the Fischer type complex, the substituents on the carbon donor are π-donating groups, such as -OMe and $–NMe_2$. The metal centers are usually late transition metals in low oxidation states with other π-acceptor ligands such as CO. In the most common model, the carbene ligand is considered as a 2e donor derived from a singlet carbene. In contrast, the Schrock type complexes have no π-donor substitutes bonded to the carbene carbon and no π-acceptor ligands coordinated to the early transition metal in high oxidation state. In the most common model of this type, the carbene is often considered to act as X_2-type bis-alkyl ligand, formally derived from the triplet carbene.

1.2.2 NHC Complexes

N-heterocyclic carbene complexes can be regarded as a special subclass of Fischer type complexes, in which the strong metal carbene bonds are mainly attributed to the strong electron donation of NHCs to the metal center with little back donation from the metal to the NHCs. The

first NHC complex was prepared by Wanzlick early in 1968 (Scheme 1.3, A).[11] At almost same time, Öfele reported a similar NHC-Cr(0) complex (B).[12]

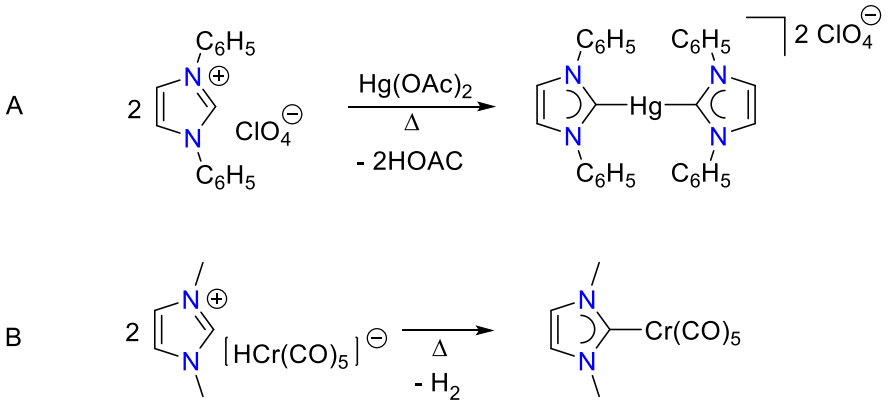

Scheme 1.3. Synthesis of the first NHC metal complex.

The interest in NHC complexes rapidly increased particularly after Arduengo's discovery. In the last two decades, the coordination chemistry of NHCs has covered almost all the transition metals, be it in low or high oxidation states. A straightforward way to prepare NHC complexes is to replace ligands on a metal complex by free NHCs. [10e-f,j-k,m,o,13] However, the synthesis needs to be carried out under an inert atmosphere, and more importantly, the free NHC intermediate must be stable as a monomer. This limits the feasibility of the method, especially for the access of complexes bearing benzimidazolin-2-ylidenes and imidazolidin-2-ylidenes with non-bulky substituents. The second method is based on the reaction of an azolium salt precursor with a basic metal complex, which was originally employed by Wanzlick and Öfele. This method circumvents the handling of air/moisture sensitive free carbene, and thus it is largely used nowadays.[14] Notably, some of the resulting NHC complexes are able to serve as carbene-transfer agents due to the labile metal–$C_{carbene}$ bonds. In this regard, Lin and coworkers have developed the silver-carbene transfer method.[15] This method makes use of Ag_2O as the base to deprotonate azolium

salts with formation of the Ag NHC complexes. Via subsequent reactions, the NHC ligands have been transferred to a wide range of metals such as Pd(II), Au(I), Pt(II), Rh(I), Rh(III), Ir(I), Ir(III), Ru(II), Ru(III), and Ru(IV).[16] In this work, the last two methods are used to synthesize complexes with benzimidazolin-2-ylidenes.

Another attractive feature of NHCs as ligands for complexes is their good performances in homogeneous catalysis, which was firstly studied by Herrmann in 1995.[17] By comparing the performances of the well-known Pd/organophosphane catalysts with a Pd/NHC catalyst in Heck coupling reaction, they found that Pd/NHC complexes showed higher thermal and hydrolytic stabilities due to the stronger metal−carbene bonds. Hence, addition of excess ligand, often 100 times than the metal, is avoided. Since then, complexes of NHCs become prevalent catalysts in organic reactions including Heck, Suzuki, Sonogashira, Kumada coupling, olefin metathesis, hydroamination, hydrogenation and C-H activation.[18]

1.3 NHC as a Probe in Ligands Donor Strengths Determination

The knowledge of the electron donating ability of a ligand is of utmost importance in coordination chemistry, since it is one of the key factors affecting the complex's property and reactivity.[19] For decades, a flurry of innovative research endeavors has been initiated with the intention to evaluate a ligand's relative electronic properties experimentally,[13a, 20] mostly considering monodentate ligands. In summary, there are two widely used methods. The dominating one in organometallic chemistry is the Tolman's electronic parameter (TEP), which is the A_1 IR stretching frequency of the carbonyl ligands in complexes of the type $[Ni(CO)_3L]$, where L is the ligand being studied (Figure 1.5).[20a] The second method, more widely used in classical coordination chemistry and introduced by Lever, is based on assessment of

electrochemical E_0 values of a redox couple, e.g., $Ru^{II/III}$, in analogous complexes differing solely in the ligand of interest to be compared. From these values, individual ligand electrochemical parameters (LEP) were derived.[21] Although LEP values are not a direct measure for the donating ability, they can be used to predict redox-potentials of metal complexes, which are related to the donor strength of their ligands (Figure 1.5).

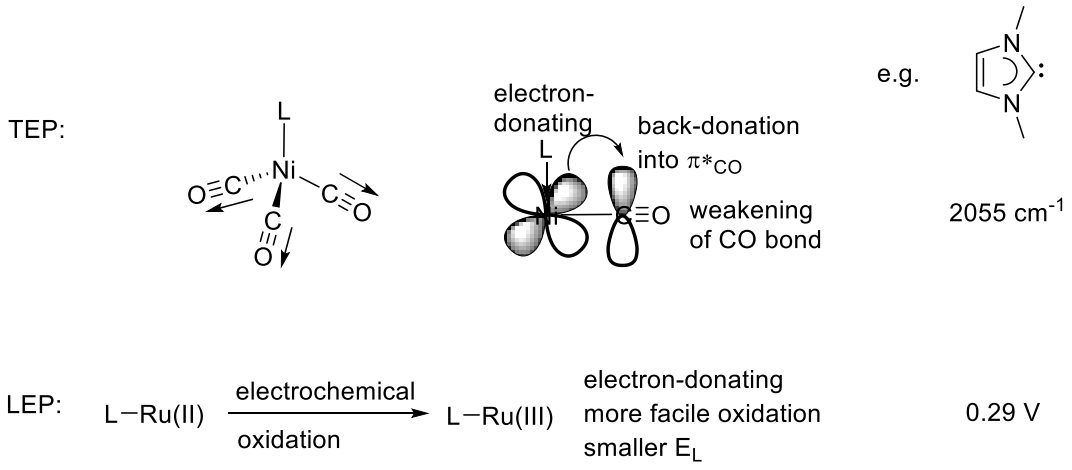

Figure 1.5. Ligands donor strengths reflected by TEP[22] and LEP[23].

More recently, Huynh et al. have reported a new electronic parameter that is based on the evaluation and comparison of $^{13}C_{carbene}$ signals in complexes of the type *trans*-[$PdBr_2$($^{i}Pr_2$-bimy)(L)] ($^{i}Pr_2$-bimy = 1,3-diisopropylbenzimidazolin-2-ylidene).[24] It is known that the carbene carbon of free NHCs resonates at > 200 ppm and a significant upfield shift of this signal is observed upon binding to a transition metal. As has been noted by Lappert in an early work, the deshielding effect of this *trans* co-ligand on the carbene carbon increases with its *trans* influence, which in turn is related to its donating ability.[25] Similar trend was observed in these complexes that a stronger donating ligand L gives rise to a more downfield ^{13}C NMR resonance of the $^{i}Pr_2$-bimy carbene carbon. Hence, using the $^{i}Pr_2$-bimy as a constant probe and based on the $^{13}C_{carbene}$

resonances of the respective complexes, the electron donating abilities of a series of Werner type and organometallic ligands have been ranked on a unified scale (Figure 1.6).

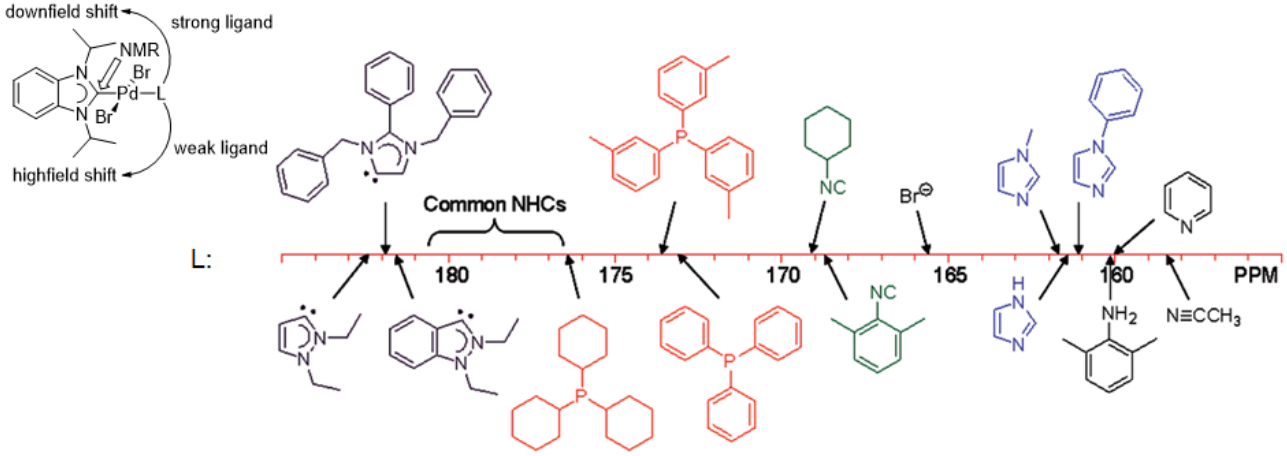

Figure 1.6. Donor abilities of Werner and organometallic ligands on a ^{13}C NMR scale.[24a]

Compared to TEP and LEP, this method can place both organometallic and classical Werner-type ligands on a unified scale, and the enhanced sensitivity allows for the detection of small differences within the same class of ligands, which are primarily due to subtle differences in inductive and mesomeric effects of substituents. Moreover, preparation of the generally air- and moisture-stable complex probes is much safer and more convenient. The non-destructive analysis by solution NMR for the determination ligands' donating power, also allows for further derivatizations or applications, e.g. in catalysis, of the complex probes.[24b,d,26]

Compared to monodentate donors, bidentate ligands (L_2) can impart greater stabilities in their complexes due to the chelate effect, which is highly beneficial and desirable in transition metal chemistry. However, the electronic properties of bidentate ligands have been far less studied. Notably, Crabtree and co-workers evaluated carbonyl stretching frequencies of *cis*-$[Mo(CO)_4L_2]$ type complexes. These were converted to TEP using a conversion equation, that was based on the correlation of bis(monodentate) complexes *cis*-$[Mo(CO)_4(L)_2]$ with $[Ni(CO)_3L]$.

For ligands, which complexes could not be prepared, DFT calculations were conducted, and scaling factors had to be applied.[27,28,29] The necessity for scaling factors and conversion equations based on monodentate ligands in this indirect methodology complicates donor strength evaluation and may limit reliability. Apart from these, several groups have compared the relative donor strengths of L_2 ligands by simple comparisons of carbonyl stretching frequencies in metal carbonyl complexes. However, different transition metals, e.g. Rh, W, Mn, and Cr, with different oxidation states were used in these studies.[30,31,32,33,34,35] Similarly, the relative electron donating abilities of bidentate ligands have been assessed via comparing the oxidation potentials of analogous complexes.[36] Although Lever's equation $E = S_M(\Sigma E_L) + I_M$, where E is the measured oxidation potential (in V vs. NHE), ΣE_L is the sum of the E_L values for all the ligands, and S_M and I_M are standard parameters depending on the the metal redox couple, spin state and stereochemistry, has been established to calculate the LEP values E_L,[21] one should be very cautious with the estimated values since, it is just based on a single complex. To the best of our knowledge, there is not a general and unified system for the direct determination of electron donating abilities of bidentate ligands.

Hence, one of the objectives of this thesis is the extension of Huynh's parameter to other monodentate and bidentate ligands as well. The results will be discussed in Chapter 2.

1.4 Functionalized-NHC Metal Complexes

1.4.1 Synthetic Approaches to Functionalized-NHC Metal Complexes

The nitrogen atoms in the NHCs offer ample possibilities for tuning the ligand structure. Through changing the N-substituents, steric demands and electronic properties of the ligand can

be altered to provide complexes with enhanced catalytic performances.[37] More interestingly, various functional groups can also be introduced resulting in complexes with wider applications.[38] For example, introduction of a suitable donor group could lead to versatile structures in ditopic complexes or enhanced catalytic performance of complexes with hemilabile ligands.[39] Potentially antibacterial compounds have also been made by the introduction of a biologically active function.[40] In addition, complexes of bifunctional ligands were immobilized or their solubilities altered by suitable functionalization to afford recoverable catalysts.[41]

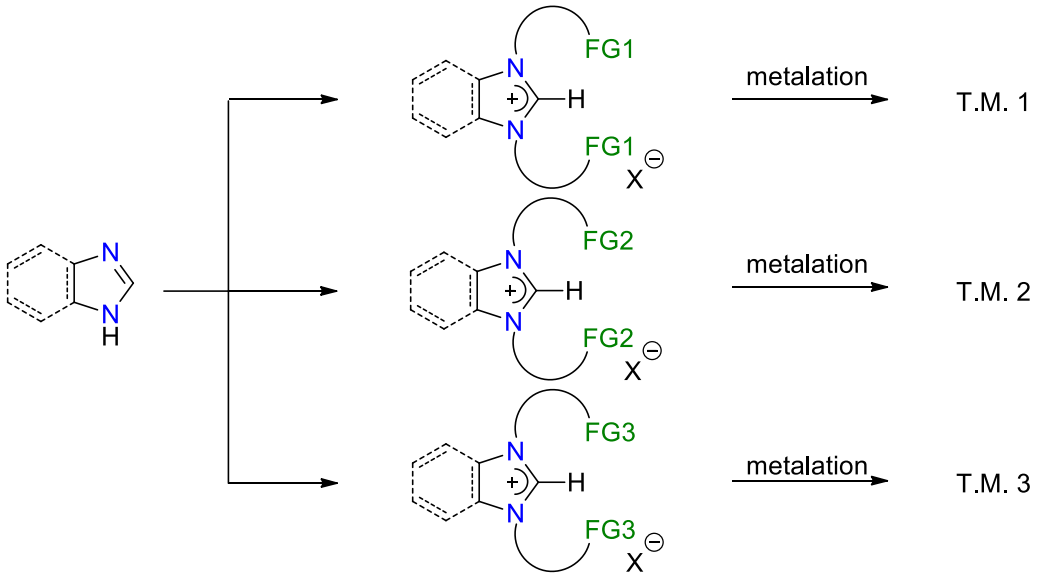

(A) Traditional way, a total steps of 6

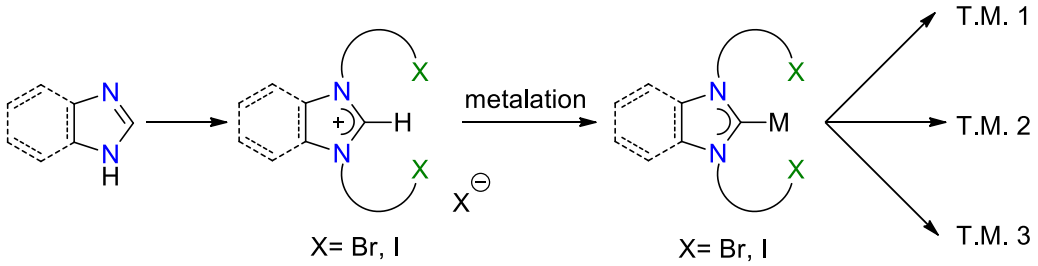

(B) Postmodification method, a total steps of 5

Scheme 1.4. Synthesis of functionalized-NHC complexes via the traditional and postmodification routes.

Routinely, functionalized NHC complexes are obtained by metalation of an already pre-functionalized NHC precursor (Scheme 1.4, A).[42] In this "linear" approach, the functional group may interfere negatively with the coordination process leading to the unexpected formation of by-products and lower yields (Scheme 1.5).[42c,43] Furthermore, versatility and modularity are limited, and only a small number of complexes can be obtained from a single functionalized ligand precursor.

An alternative and "divergent" approach, where functional group transformations can be conducted with a single and easily accessible NHC complex would represent a substantial improvement in terms of cost, labor, time and waste reduction (Scheme 1.4, B).[40b,44] Moreover, new complexes might be envisaged, which are not accessible via the traditional way due to incompatibility of the desired functional group with the conditions required for complexation.

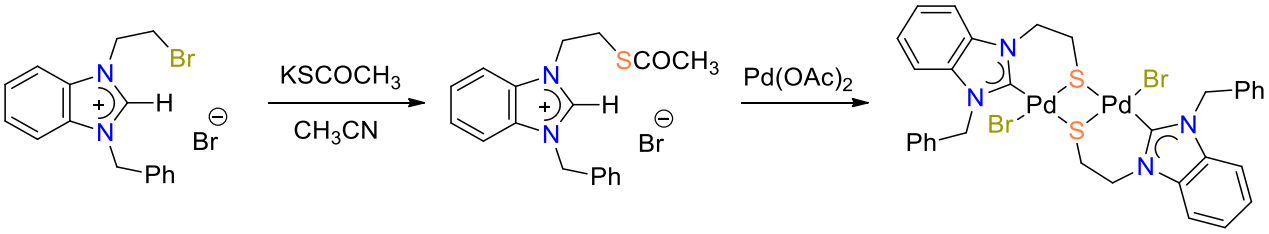

Scheme 1.5. Isolation of unexpected thiolato-bridged dimeric complex using via metalation of thioester-functionalized-azolium salt.

Therefore, the second aim of this thesis is to synthesize suitable parent complexes, which will allow further postmodifications to give a large library of newly functionalized NHC complexes. The results will be presented in Chapter 3.

1.4.2 Functionalized-NHC in Metallosupramolecular Chemistry

Nowadays, NHCs have become standard ligands in organometallic chemistry and particularly in the field of homogeneous catalysis (vide supra). In addition, they have also been used to form photoluminescent[45] and biologically active[46] complexes. However, only recently has their application been extended to metallosupramolecular chemistry.[47] To date, only a small number of homo- and hetero-multimetallic complexes with one, two or three dimensional architectures were reported by Hahn,[48] Bielawski,[49] Peris,[50] Huynh,[42c,43,51] and others[52] based on polydentate ligands featuring NHC moieties.

Among the reported architectures, the most common motifs are molecular rectangles and squares. As an early example in this field, Hahn reported the construction of a Ni(II) cornered molecular rectangle with so-called "Janus type" (facially opposed) di(NHC)s and 4,4'-bipyridine ligands.[53] Subsequently, a number of similar structures were prepared with different NHC linkers or metal corners. One representative is the molecular square with pure N,O-carbene bridges.[54] Huynh et al reported a rectangular motif bearing mesoionic and remote NHC ligands, in which the corners are not formed by the metal atoms, but by the CH_2-spacer of the dicarbene and the bridging iodido ligands. In addition, they also reported several rare tetranuclear complexes, which feature a 8-membered square consisting of alternating four Pd(II) and four S atoms. A few examples of star-shaped complexes were developed by Bielawski and Peris using rigid tris(NHC) ligands. Metallo- and NHC based supramolecular chemistry was pushed further by Hahn, who reported a rare cylindrical structure containing six silver atoms sandwiched between two hexa-NHC ligands.[55] Although rotaxanes are very common motifs in supramolecular chemistry, there is so far only one example that contains NHC ligands, which was reported by Huynh et al (Figure 1.7).

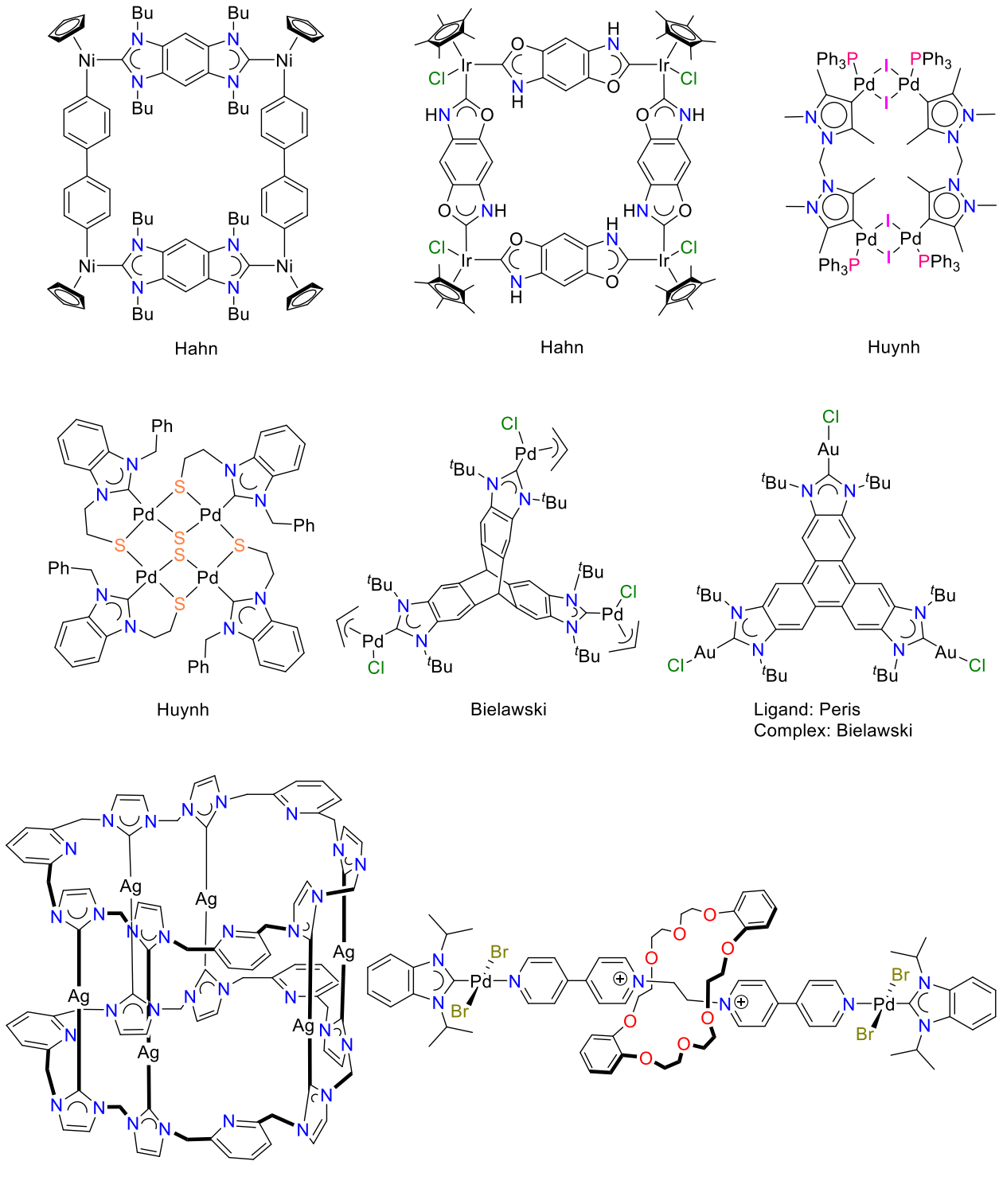

Figure 1.7. Selection of metallosupramolecular structures featuring NHC moieties.

In addition to the above mentioned architectures, double stranded-helices are common structures found in nature such as α-helical polypeptides and double-helical nucleic acids. In the last few decades, chemists have contributed great efforts to make artificial helices, and one of most important results was made by Lehn, who demonstrated the spontaneous formation of a double-helical complex (helicate) from bipyridine and Cu(I).[56] Although a large library of helicates is available in literature now, it is worth noting that almost all of them were built from Werner-type ligands. Lin and Meyer reported the only two examples of double stranded-helicates with NHCs that were obtained via simple coordination of pyridine- or pyridazine-bridged dicarbenes to Hg(II) centers (Figure 1.8).[57]

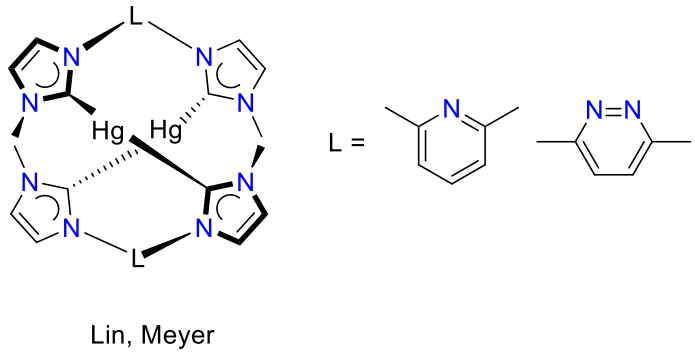

Lin, Meyer

Figure 1.8. Reported double stranded-helicates NHC complexes.

Intrigued by the versatile and interesting structures, and given the fact that NHCs could be easily functionalized, the last objective of this thesis is to design a polydentate ligand precursor and explore its coordination chemistry to build metallosupramolecules. The result will be discussed in detail in Chapter 4.

2. Donor Strengths Determination of Monodentate and Bidentate Ligands Using Their Palladium(II) 1,3-diisopropylbenzimidazolin-2-ylidene Complexes

2.1 Donor Strengths Determination of Monodentate Ligands

The reactivity of the dimeric [$PdBr_2$(^{i}Pr_2-bimy)]$_2$ complex **I** towards a wide range of Werner-type and organometallic monodentate ligands has been well explored previously.[24] With addition of two equiv pro-ligand (L), the bromido-bridges were straightforwardly cleaved resulting in the formation of [$PdBr_2$(^{i}Pr_2-bimy)(L)] complexes (Scheme 2.1). Notably, both *trans*- and *cis*-arrangements are possible, depending on the nature of the pro-ligand. However, only the *trans*-[$PdBr_2$(^{i}Pr_2-bimy)(L)] complexes will be suitable for the determination of electron donating abilities of the L ligands.

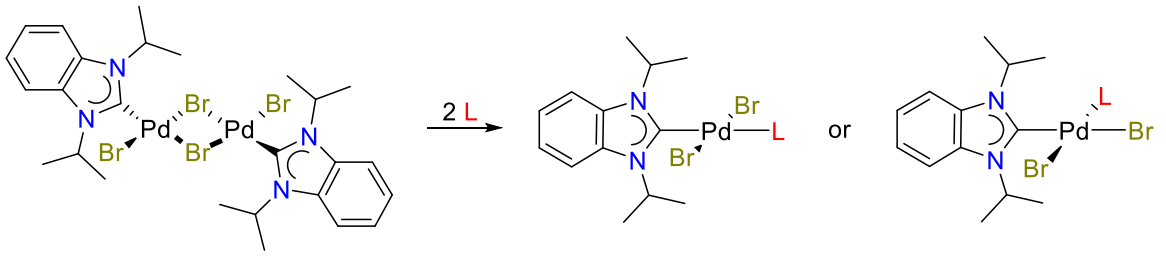

Scheme 2.1. Cleavage reactions of [$PdBr_2$(^{i}Pr_2-bimy)]$_2$ (**I**) to afford *trans*/*cis*-[$PdBr_2$(^{i}Pr_2-bimy)(L)] complexes.

2.1.1 Electron Donor Strengths of Substituted Pyridines

Cleavage reactions of [$PdBr_2$(^{i}Pr_2-bimy)]$_2$ with 11 commercially available pyridines smoothly yield two types of complexes *trans*-[$PdBr_2$(^{i}Pr_2-bimy)(3-R-Py)] (R = F, **1**; Cl, **2**; Br, **3**; I,

4; OH, **5**; Ph, **6**) and *trans*-[$PdBr_2$($^{i}Pr_2$-bimy)(4-R-Py)] (R = Cl, **7**; Br, **8**; I, **9**; OH, **10**; Ph, **11**). Pro-ligand 4-F-Py was not included due to its limited availability. In comparison to the parent complex, the solubilities of the resulting complexes **1**–**11** in common organic solvents, with the exception of nonpolar hexane and diethyl ether, have improved significantly. A distinct color change from orange to yellow was observed for all the eleven complexes. Formation of complexes **5** (3-OH), **10** (4-OH), **6** (3-Ph) and **11** (4-Ph) were evidenced by their ESI mass spectra, which show base peaks at *m*/*z* 525 or 697 assignable to the $[M - Br + CH_3CN]^+$ or $[M + CH_3CN + MeOH + H]^+$ fragments. However, the base peaks for the other complexes are consistently observed at *m*/*z* 469 attributed to the $[M - Py + H]^+$ fragment due to the loss of the halo-pyridine ligand when subjected to ESI MS conditions. The halo-pyridine ligand dissociation serves as an indirect sign of their weaker donation (*vide infra*), and it also demonstrates the strong *trans effect* of the $^{i}Pr_2$-bimy ligand.

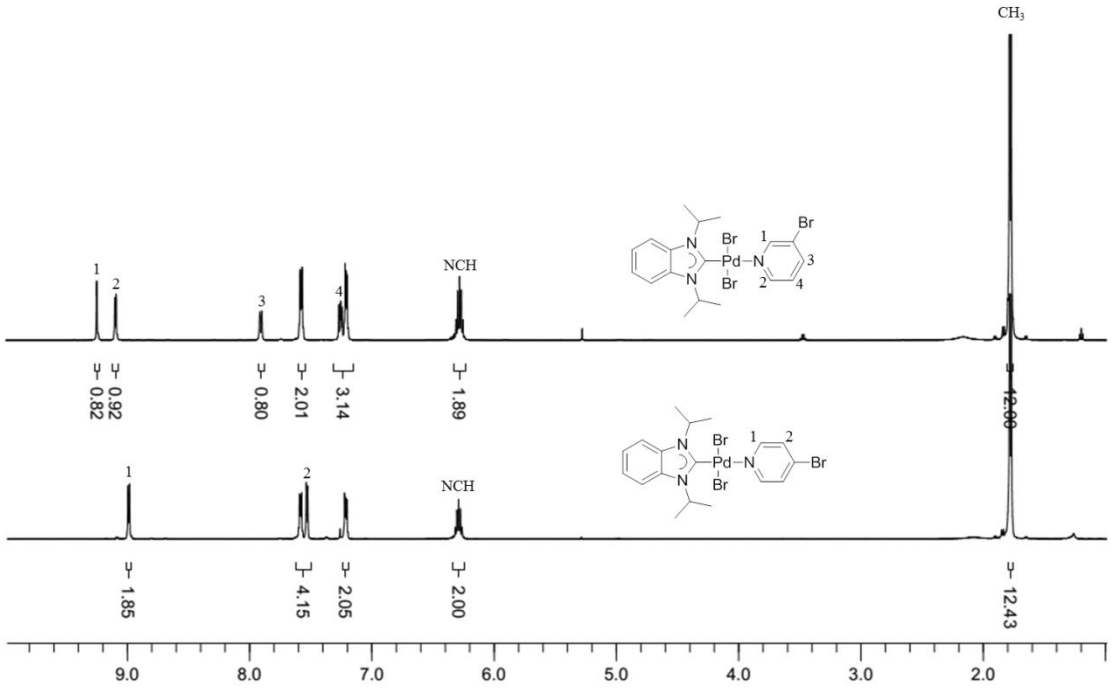

Figure 2.1. ^{1}H NMR spectra of complexes *trans*-[$PdBr_2$($^{i}Pr_2$-bimy)(3-Br-Py)] (**3**) and *trans*-[$PdBr_2$($^{i}Pr_2$-bimy)(4-Br-Py)] (**8**).

NMR spectroscopy confirms the formation of all complexes as evidenced by the additional signals assignable to the pyridine ligands. ^{1}H NMR spectra of complexes *trans*-[PdBr$_2$(^{i}Pr$_2$-bimy)(3-Br-Py)] (**3**) and *trans*-[PdBr$_2$(^{i}Pr$_2$-bimy)(4-Br-Py)] (**8**) are displayed in Figure 2.1 as a representative for each type. Four additional signals are observed assignable for the 3-Br-Py ligand in complex **3**, while only two are found for the 4-Br-Py ligand in complex **8** due to symmetry. The hydrogen signals of the ^{i}Pr$_2$-bimy are not much affected by the positioning of the substituent. However, they do shift slightly upfield compared to the analogous resonances of the parent dinuclear complex. Anagostic C–H···Pd interactions in solution exist in these complexes as indicated by the more downfield ^{1}H NMR shifts of the NCH protons in comparisons to that of the ^{i}Pr$_2$-bimy·HBr salt ($\Delta\delta$ = 1.07–1.16 ppm).[58] Such interaction has been explored in depth for (^{i}Pr$_2$-bimy)-metal (Pd, Pt and Ni) complexes by Huynh's group.[37b,59]

Table 2.1. $^{1}H_{NCH}$ and $^{13}C_{carbene}$ NMR resonances of complexes **1**–**11**[a] and Hammett σ constants for the respective substituent.

complex	R	$^{1}H_{NCH}$	$^{13}C_{carbene}$	σ_m	complex	R	$^{1}H_{NCH}$	$^{13}C_{carbene}$	σ_p
1	3-F	6.30	158.65[b]	0.34	-	-	-	-	-
2	3-Cl	6.30	158.72[b]	0.37	**7**	4-Cl	6.29	158.98[b]	0.23
3	3-Br	6.29	158.63[b]	0.39	**8**	4-Br	6.29	159.03[b]	0.23
4	3-I	6.29	158.68[b]	0.35	**9**	4-I	6.28	159.2	0.18
5	3-OH	6.32	159.6	0.12	**10**	4-OH	6.32	160.21[b]	-0.37
6	3-Ph	6.37	159.8	0.06	**11**	4-Ph	6.38	160.16[b]	-0.01

[a]Measured in $CDCl_3$ and internally referenced to the solvent signal at 7.26 and 77.7 ppm, respectively, relative to tetramethylsilane (TMS) in the ^{1}H and ^{13}C NMR spectra. [b]2 decimal placings are given to highlight the small, but discernable differences.

With the substituents being five or six bonds away, the $^{13}C_{carbene}$ resonances of the ^{i}Pr$_2$-bimy are still able to tell the differences and shed light on the donor strengths of these pyridine

ligands (Table 2.1). Generally, the 4-R-Pys have stronger donating abilities than the respective 3-R-Py ligands. The OH- and Ph-pyridines are stronger donors than the halo-pyridines within both series.

Substituents may exert two effects on its adjacent aromatic ring, i.e. inductive and mesomeric effects. Relative inductive effects of various substituents have been experimentally measured and those discussed herein are with decreasing negative inductive effect (*–I*) in the order of F > Cl > Br > I > OH > Ph. Strong evidence shows that inductive effects in the *meta*- and *para*-positions are very similar. Mesomeric effects, on the other hand, are largely position-dependent, which is highlighted in Figure 2.2 using the OH-pyridine as a model. The positive mesomeric effect (*+M*) is brought about by the overlapping of the filled p orbital of the oxygen atom with the π system, which leads to extra electron density on the ring. Notably, the additional electron density is selectively located at the *ortho*- and *para*-positions with respect to the C–OH atom. As shown in the resonance structures, one of the three partial negative charges is located on the N atom in the *para*-OH-pyridine, while all of them are on the C atoms in the *meta*-OH-pyridine. This explains the stronger donation of the 4-R-Pys than that of the respective 3-R-Py ligands.

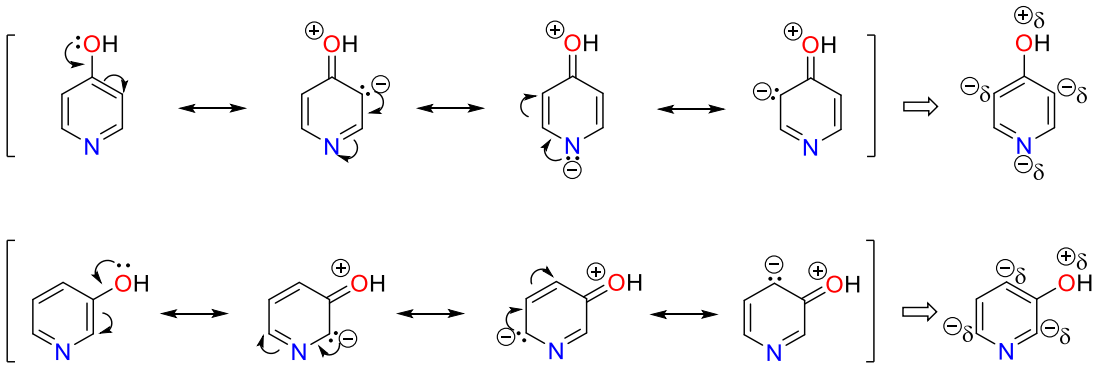

Figure 2.2. Resonance structures of OH-pyridines.

The OH- and Ph-substituents have smaller *–I* effects and stronger *+M* effects, both of which account for the stronger donating abilities of their pyridines. Interestingly, the relative donating abilities of the OH- and the Ph-pyridines are reversed in the two series. In the *meta*-case, the inductive effect dominates; hence the 3-Ph-Py is a reasonably stronger donor. However, in the *para*-analogues, the stronger *+M* of the OH group overcomes the stronger *–I* effect, giving rise to a slightly stronger 4-OH-Py ligand.

A closer inspection of the carbene resonances of complexes **7**–**9** involving the 4-halo-pyridines reveals decreasing donation powers in the order 4-I-Py > 4-Br-Py ≥ 4-Cl-Py. Notably, the *+M* effects of halogen substituents are in the order of F > Cl > Br > I due to the decreasing p-π orbital overlap of the pyridine ring with increasingly larger halogen atoms. Hence, the result obtained above indicates that the smallest *–I* of iodine atom balances its weakest *+M* effect, giving rise to a stronger net electron donor than the chlorine and bromine analogues. However, the stronger *+M* of Cl is compensated by its more negative *–I* effect in comparison to those of Br, resulting in two comparable electron donors of 4-Br-Py and 4-Cl-Py on this scale. Overall, the *para*-substituted pyridines have decreasing electron-donating properties in the order 4-OH-Py > 4-Ph-Py > 4-I-Py > 4-Br-Py ≥ 4-Cl-Py.

The $^{13}C_{carbene}$ signals of the *meta*-halo-pyridine series are scarcely distinguishable with differences of less than 0.05 ppm, indicating fairly similar electronic effects of the different halogen atoms at the *meta*-positions. The net electron donating abilities can still be ranked in the order of 3-Ph-Py > 3-OH-Py > 3-Cl-Py ≥ 3-I-Py ≥ 3-F-Py ≥ 3-Br-Py.

In physical organic chemistry, such substituent electronic effects have been established by Hammett, based on conductance measurements of ionisation constants of the appropriately substituted benzoic acid. Hammett constants σ_p and σ_m are derived from an equation: $\sigma = \log K_X$

– logK_H, where K_H = ionisation constant for benzoic acid in water at 25 ℃ and K_X = ionisation constant for a *para*- and *meta*-substituted benzoic acid.[60] An electron-withdrawing substituent would cause the benzoic acid to be more acidic, thus giving rise to a positive value of the Hammett σ constant; while an electron-donating group would lead to a more negative value.

The Hammett σ_p constants of 4-R substituents relevant to this work are as following: 4-OH (-0.37) > 4-Ph (-0.01) > 4-I (0.18) > 4-Br (0.23) ≥ 4-Cl (0.23).[61] Notably, the electron donor strengths trend obtained by the ^{13}C NMR method is in well agreement with it. The *meta*-substituent effects to the overall donor abilities, on the other hand, only correlate to σ_m constants for different types: 3-Ph (0.06) > 3-OH (0.12) > 3-X (0.34–0.39).

2.1.2 Electron Donor Strengths of Other N, P, As, Sb, S and O Ligands

Nitrogen donors. Triethylamine (NEt_3), 1,5,7-Triazabicyclo[4.4.0]dec-5-ene (TBD) and 1,8-diazabicyclo[5.4.0]undec-7-ene (DBU) are widely used as organic bases in catalytic reactions (Chart 2.1). In certain cases, they outperform the inorganic bases due to the better solubilities in organic solvents, and the fact that they can coordinate and therefore stabilize the active metal species.[62] It is to our surprise that their electron donating abilities to metal centers have not been compared. Hence, we herein prepared the analogous $^{i}Pr_2$-bimy/nitrogen base complexes in an attempt to reveal their relative net electron donation to palladium, which will be reflected by the $^{13}C_{carbene}$ resonances. Two equiv TBD and DBU reacted smoothly with **I** affording the yellow solid products *trans*-[$PdBr_2$($^{i}Pr_2$-bimy)(TBD)] (**13**) and *trans*-[$PdBr_2$($^{i}Pr_2$-bimy)(DBU)] (**14**). However, an excess of triethylamine and prolonged stirring were required to fully convert complex **I** to *trans*-[$PdBr_2$($^{i}Pr_2$-bimy)(NEt_3)] (**12**).

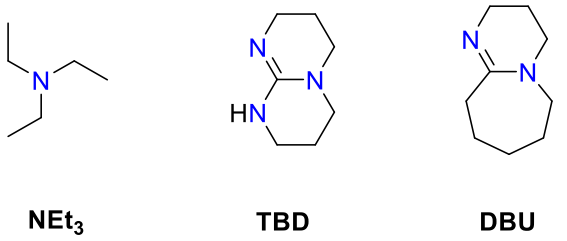

Chart 2.1. Sketches of the three nitrogen organic bases.

Notably, TBD is a bicyclic guanidine derivative in which one imine and one secondary amine nitrogen donor are available for coordination. However, the ligand shows selective coordination of the imine nitrogen donor to metal centers such as Pd, Cu, Fe and Li.[63] Indeed, the *trans*-[$PdBr_2$(^{i}Pr_2-bimy)(TBD)] (**13**) complex with imine coordination was obtained, which is evidenced by X-ray diffraction on a single crystal obtained by slow evaporation of a saturated solution in $CHCl_3$/hexane.

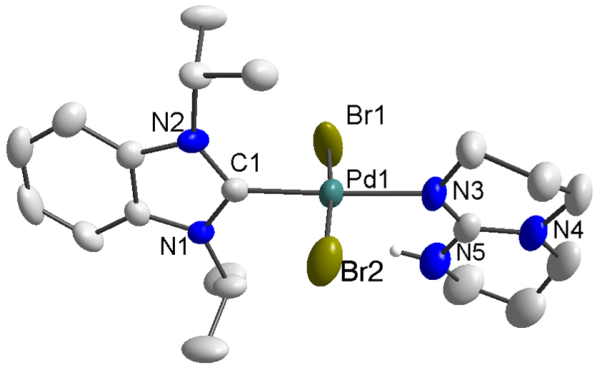

Figure 2.3. Molecular structure of **13** showing 50% probability ellipsoids; hydrogen atoms are omitted for clarity. Selected bond length [Å] and bond angles [°]: Pd1–C1 1.967(4), Pd1–Br1 2.4380(7), Pd1–Br2 2.4341(7), Pd1–N3 2.075(4); C1–Pd1–Br1 86.29(13), C1–Pd1–Br2 89.20(13), Br1–Pd1–N3 93.43(12), Br2–Pd1–N3 91.21(12); $PdCBr_2N$/NHC dihedral angle 88.1 °.

The solid state structure depicted in Figure 2.3 confirms the square planar connectivity of the ^{i}Pr_2-bimy, TBD and two bromido ligands to the Pd(II) center. Both the NHC and TBD ligands rotate almost perpendicular to the coordination plane to relieve steric congestion. Interestingly, a

short contact of the NH proton and the Pd(II) center is noted with N–H···Pd angle of 123.2° and distance of 2.619 Å in the solid state. However, retention of such interaction in solution is uncertain as the corresponding hydrogen signal is not resolved in the ^{1}H NMR spectrum. The two *trans*-arranged bromido ligands slightly tilt towards the carbene ligand possibly indicating electron donation to the formally vacant p-orbital of the carbene center.[58] All related bond parameters are as expected and hence will not be further commented upon.

The three base adducts have good solubilities in most organic solvents. Similar ^{1}H NMR spectra and ESI MS characteristics were found for these complexes as discussed previously for the mixed NHC/Py complexes. In the ^{13}C NMR spectra, the three carbene carbon atoms resonate in the order of **12** (NEt_3, 158.0 ppm) < **14** (TBD, 165.8) < **13** (DBU, 166.3). This trend indicates that the saturated amine NEt_3 is a weaker donor compared to the unsaturated imines. In addition, DBU is a stronger ligand than TBD, which is reasonable by considering the additional –*I* effect from the third nitrogen atom in the TBD ligand.

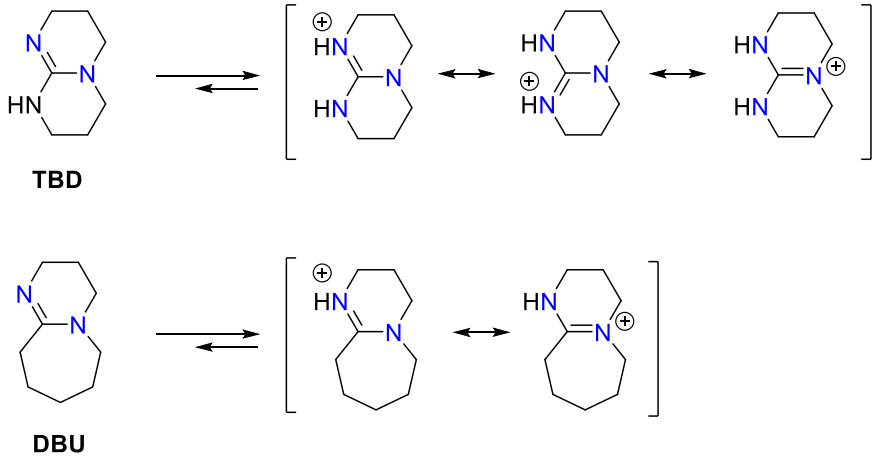

Figure 2.4. Conjugation of the ammonium ions.

The pK_a values of the conjugated acids of the three organic bases are: NEt_3, ~11; DBU, ~12 and TBD, > 12. Notably, the stronger basicity of the two imines is due to a highly effective conjugated system after protonation under reversible conditions, which is reflected by the number of resonance forms (Figure 2.4).[64] The three versus two resonances structures found for TBD and DBU, respectively, explain the stronger basicity of TBD. Correlation of the donor strengths to the basicity values shows a consistent result of between the amine and the imines.

Phosphine, arsine and antimony donors. Previously, Huynh et al have used the ^{13}C NMR spectroscopy to rank the electron donating properties of three phosphine ligands in the order of PPh_3 < P(*m*Tol)$_3$ < PCy_3.[24a] Herein, the scope was extended to phosphites, including $P(OMe)_3$, P(O^{i}Pr)$_3$, $P(OPh)_3$ and P(O-2,4-^{t}Bu-Ph)$_3$. In addition, evaluation of NPh_3, $AsPh_3$ and $SbPh_3$ was also attempted to test the feasibility of this method in differentiating the donor strengths of ligands from the same group. Besides their electron donating properties, it will also be interesting to study the physical and chemical properties of the resulting complexes, as they are relatively rare.

Instant color changes from orange to pale yellow were observed for most reaction mixtures indicative of successful bridge cleavage. Initially, the reactions were stirred in CH_2Cl_2 and stopped after 30 min to ensure complete consumption of complex **I**. Notably, the reaction with NPh_3 did not proceed at all regardless of different reaction time, substance ratios, solvents and reaction temperature.

Similarly to complexes of phosphine, those of phosphite complexes underwent *trans*-*cis* isomerizations. In comparison to *trans*-configured amine and imine complexes, the *cis*-arrangement is thermodynamically preferred in these cases, due to the so-called "*transphobia*

effect" of phosphorus donors.[65] *Transphobia* is the term used to describe the difficulty of placing a P ligand and a C donor *trans* to each other.[66] The isomerization is fast for the $P(OMe)_3$ and $P(O^iPr)_3$ supported complexes. Hence, only the *cis*-[$PdBr_2$(^{i}Pr_2-bimy){$P(OMe)_3$}] (**15**) and *cis*-[$PdBr_2$(^{i}Pr_2-bimy){$P(O^iPr)_3$}] (**16**) complexes were isolated. The process is slower for $P(OPh)_3$ complex, and signals for both *trans*/*cis*-[$PdBr_2$(^{i}Pr_2-bimy){$P(OPh)_3$}] (**17**) were captured in the NMR spectra. The complex *trans*-[$PdBr_2$(^{i}Pr_2-bimy){P(O-2,4-^{t}Bu-Ph)$_3$}] (**18**) resists isomerization apparently due to the enhanced steric bulk.

As noted earlier, *trans*-configured complex probes are required for the determination of donor strengths using this method. Hence, direct NMR scale reactions were attempted to capture the initially formed *trans*-isomers for the complexes with $P(OMe)_3$, $P(O^iPr)_3$ and $P(OPh)_3$ ligands. Complex **I** and the respective phosphite were mixed in NMR tubes, and the samples were immediately measured after addition of $CDCl_3$. Indeed, only one set of signals due to the *trans*-[$PdBr_2$(^{i}Pr_2-bimy){$P(O^iPr)_3$}] (**16**) or *trans*-[$PdBr_2$(^{i}Pr_2-bimy){$P(OPh)_3$}] (**17**) complex was observed in the respective ^{1}H NMR spectra. ^{31}P and ^{13}C NMR spectroscopy were measured immediately thereafter. All the signals were successfully resolved for complex **17** before isomerization. However, a mixture of signals due to both *trans*- and *cis*-isomers was detected for **16** in the ^{13}C NMR spectrum. To resolve the carbene signal of *trans*-**16** in a shorter time, the NMR reaction was repeated with $^{13}C_{carbene}$-labeled complex **I**.[24a] The ^{i}Pr_2-bimy carbene signal was detected even with a single scan. Unfortunately, the signals of *trans*-**15** complex could not be captured even within such a short time.

Similar isomerizations were also observed for the $AsPh_3$ and $SbPh_3$ complexes due to the *transphobia effect*, with the latter being faster. Only *cis*-[$PdBr_2$(^{i}Pr_2-bimy)($SbPh_3$)] (**20**) was

observed. Complex *trans*-[$PdBr_2$(^{i}Pr_2-bimy)($AsPh_3$)] (**19**), on the other hand, isomerizes slower and could be fully characterized by direct NMR reaction.

After obtaining the carbene signals of the *trans*-configured complexes **16**–**19**, the isomerization processes were purposely monitored by ^{1}H NMR spectroscopy. For the $P(OPh)_3$ complexes **17**, 17% of the *trans*-isomer converted to the *cis*-complex after 8 days. However, the ^{1}H NMR spectrum of the product mixture obtained from the initial reaction (30 min stirring in CH_2Cl_2) shows a *trans*-*cis* conversion of up to 50%. Besides the stirring, which might help in the conversion by a better mixing, the different solvents would be the key factor in influencing the isomerization rate. The more polar CH_2Cl_2 versus $CDCl_3$ favors the formation of the *cis*-isomer with a larger dipole moment. Hence, by repeating the reaction in a more polar organic solvent MeOH, the *cis*-[$PdBr_2$(^{i}Pr_2-bimy){$P(OPh)_3$}] (**17**) was exclusively obtained after 10 hours of stirring.

^{1}H NMR monitoring of the other *trans*-complexes in $CDCl_3$ showed that the $P(O^iPr)_3$ complex *trans*-**16** fully converted to *cis*-**16** within two hours. The P(O-2,4-^{t}Bu-Ph)$_3$ complex *trans*-**18** did not change at all after 10 days. The same NMR sample was then heated in a hot oil bath (65 °C) for several days. No conversion to *cis*-isomer but decomposition to Pd(0) black was detected instead. The isomerization of the $AsPh_3$ complex **19** seems to reach equilibrium after six days giving rise to a *trans*/*cis* mixture with a ratio of 1:3.5.

The formation of a *trans*- or *cis*-configured product could be best identified by the ^{1}H NMR signals of methyl groups in the ^{i}Pr_2-bimy ligand. In the *trans*-isomers, the structure is symmetrical and hence only one doublet is observed. However, they become non-equivalent in the *cis*-isomers and two doublets assignable for the NCH(CH_3)$_2$ are found. Moreover, for the phosphite complexes, the carbene signals are found as doublets due to C–P coupling. The ^2J(C,P)

coupling constants are over 280 Hz in the *trans*-isomers, but less than 25 Hz in the *cis*-isomers (Table 2.2).[67]

Table 2.2. Selected NMR data of complexes **15**–**20**.[a]

complex	co-ligand	$^{1}H_{Me}$	$^{13}C_{carbene}$	^{2}J(C,P)
cis-**15**	$P(OMe)_3$	1.74, 1.66	170.8	21.4
trans-**16**	$P(O^{i}Pr)_3$	1.74	**175.3**	287.1
cis-**16**	$P(O^{i}Pr)_3$	1.71, 1.69	172.0	22.9
trans-**17**	$P(OPh)_3$	1.51	**171.7**	289.8
cis-**17**	$P(OPh)_3$	1.57, 1.14	169.3	22.9
trans-**18**	$P(O\text{-}2,4\text{-}^{t}Bu\text{-}Ph)_3$	1.59	**171.5**	289.6
trans-**19**	$AsPh_3$	1.79	**169.2**	-
cis-**19**	$AsPh_3$	1.66, 0.90	169.3	-
cis-**20**	$SbPh_3$	1.66, 1.04	167.5	-

[a]Measured in $CDCl_3$ and internally referenced to the solvent signal at 7.26 and 77.7 ppm, respectively, relative to tetramethylsilane (TMS) in the ^{1}H and ^{13}C NMR spectra.

The $^{13}C_{carbene}$ signals of the *trans*-complexes **16**–**18** indicates an increasing donating powers of $P(O\text{-}2,4\text{-}^{t}Bu\text{-}Ph)_3 < P(OPh)_3 < P(O^{i}Pr)_3$. The strong electron donation of the $P(O^{i}Pr)_3$ is reasonable due to the strong *+I* effects of the isopropyl substituents. The weakest donor strength of the $P(O\text{-}2,4\text{-}^{t}Bu\text{-}Ph)_3$ ligand compared to $P(OPh)_3$, however, seems questionable. The additional electron donating groups of ^{t}Bu should lead to a stronger electron donor. The steric bulk of this ligand may offer an explanation for the irregularity, as it surely affects the

coordination of all other ligands to the Pd(II) center. The difficulty in determining the donor strengths of very bulky ligands accurately represents one limitation of the ^{13}C NMR based method to be studied in future. In comparison to the evaluated phosphine ligands (PPh_3, 173.1; P(*m*Tol)$_3$, 173.6; PCy3, 176.4 ppm), phoshites are generally weaker donors due to the *–I* effects of the oxygen atoms. However, they are all stronger than $AsPh_3$ (*trans*-**19**), in line with the results obtained by TEP values.[68]

Single crystals of complexes **15**, **16**, **17**, **19** and **20** were obtained by slow evaporation of their solutions in $CHCl_3$/hexane. As a consequence of the *transphobia*, all complexes crystallize in *cis*-configurations, although the *trans*-complexes of **16**, **17** and **19** were initially dissolved (Figure 2.5).

The Pd(II) centers adopt square planar geometries in all cases. The Pd–$C_{carbene}$ lengths of the $AsPh_3$ and $SbPh_3$ complexes are essentially equal and shorter than those observed in the phosphite complexes with differences beyond the 3σ limit. The Pd–Br bond lengths *trans* to P/As/SbPh3 (2.4761(4)[58] /2.4624(3)/2.4699(4) Å) indicate *trans*-influences of the three ligands following in the sequence: $AsPh_3$ < $SbPh_3$ < PPh_3, which deviates from the sequence, $SbPh_3$ < $AsPh_3$ < PPh_3, reported by Wendt.[69] Due to the various differences in parameters of different since crystal data, this deviation is understandable. The corresponding Pd–Br bond in the P(OPh)$_3$ complex is lightly shorter than that of the PPh_3 complex, while those of the P(OMe)$_3$, P(O^{i}Pr)$_3$ complexes are longer. The ^{i}Pr$_2$-bimy ligand in all cases is almost perpendicular to the coordination plane with dihedral angles of 82.8–89.6 º.

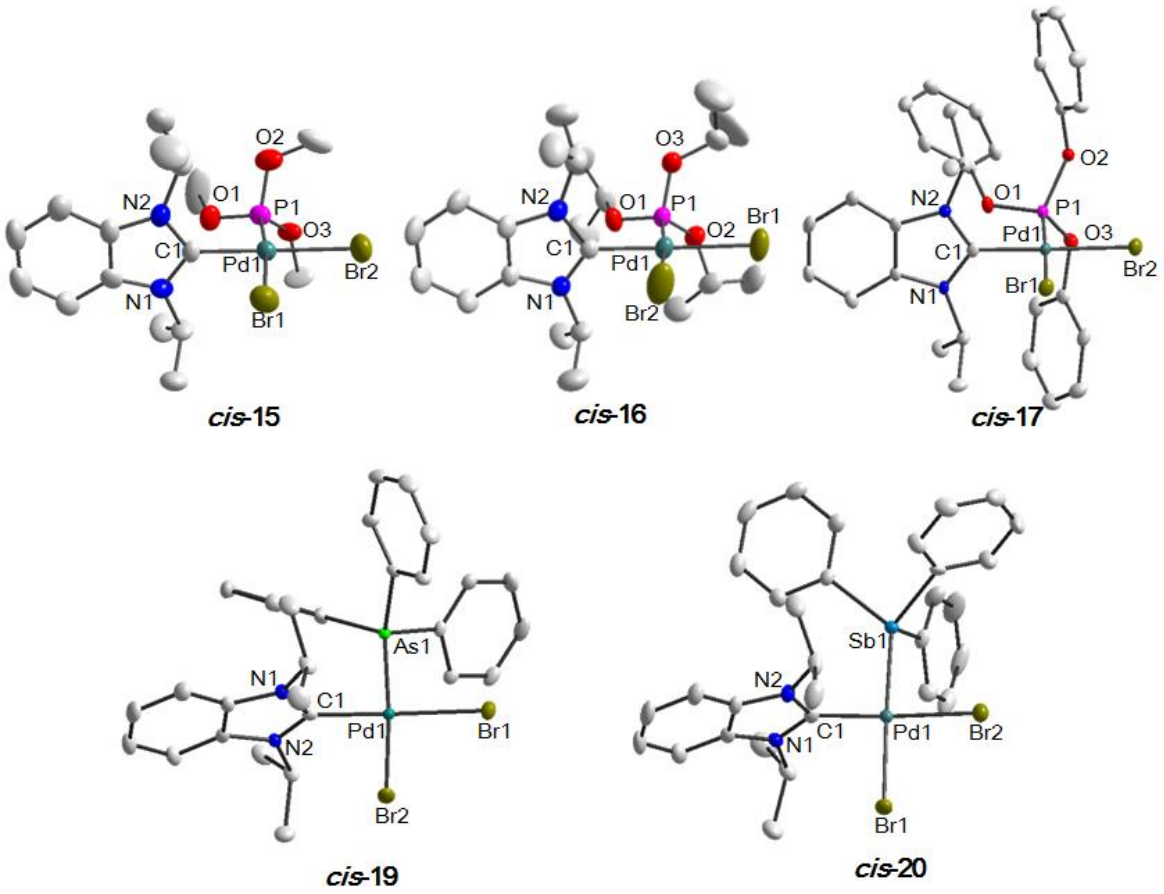

Figure 2.5. Molecular structure of *cis*-**15**, **16**, **17**, **19** and **20** showing 50% probability ellipsoids; hydrogen atoms are omitted for clarity. Selected bond length [Å] and bond angles [°]: *cis*-**15**, Pd1–C1 1.980(7), Pd1–Br1 2.4914(9), Pd1–Br2 2.4724(10), Pd1–P1 2.2044(19); C1–Pd1–Br1 84.78(19), C1–Pd1–P1 89.70(19), Br1–Pd1–Br2 94.21(3), Br2–Pd1–P1 91.30(6); $PdCBr_2N$/NHC dihedral angle 89.6°. *cis*-**16**, Pd1–C1 1.988(3), Pd1–Br1 2.4853(4), Pd1–Br2 2.4779(4), Pd1–P1 2.2133(8); C1–Pd1–Br2 85.90(8), C1–Pd1–P1 90.41(8), Br1–Pd1–Br2 92.221(15), Br1–Pd1–P1 91.33(2); $PdCBr_2N$/NHC dihedral angle 83.8°. *cis*-**17**, Pd1–C1 1.992(4), Pd1–Br1 2.4751(5), Pd1–Br2 2.4767(5), Pd1–P1 2.2040(10); C1–Pd1–Br1 88.05(11), C1–Pd1–P1 90.43(11), Br1–Pd1–Br2 94.642(17), Br2–Pd1–P1 86.88.33(3); $PdCBr_2N$/NHC dihedral angle 82.8°. *cis*-**19**, Pd1–C1 1.970(2), Pd1–Br1 2.4818(3), Pd1–Br2 2.4624(3), Pd1–As1 2.3568(3); C1–Pd1–Br2 85.44(6), C1–Pd1–As1 90.40(6), Br1–Pd1–Br2 93.915(10), Br1–Pd1–As1 90.094(10); $PdCBr_2N$/NHC dihedral angle 88.4°. *cis*-**20**, Pd1–C1 1.971(3), Pd1–Br1 2.4699(4), Pd1–Br2 2.4771(4), Pd1–Sb1 2.4967(3); C1–Pd1–Br1 86.44(9), C1–Pd1–Sb1 95.66(9), Br1–Pd1–Br2 95.552(14), Br2–Pd1–Sb1 82.489(12); $PdCBr_2N$/NHC dihedral angle 84.2°.

Sulfur and oxygen donors. Thioethers are known to form weak bonds with metal centers, which can be important for catalysis as they would dissociate from the metal center and provide free coordination sites for substrate activation.[70] However, less attention has been paid to the

measurement of their electron donating abilities compared to those of the other ligands. Herein, two common thioethers, i.e. dimethylthioether (SMe_2) and tetrahydrothiophene (THT) were studied.

Besides, we were also interested in studying the coordination chemistry and electron donating properties of analogous neutral oxygen donors. Unfortunately, similar dialkyl ethers were not able to cleave the dimeric complex **I** due to their weak donor properties. Pyridine *N*-oxide (PNO) as a formally neutral oxygen donor derivative was prepared by the oxidation of pyridines. The increased dipole moment due to charge separation leads to a stronger nucleophilic property of the oxygen atom, which may allow the cleavage reaction to proceed. Hence, it was chosen for this study.

The two dialkyl thioether smoothly cleaved complex **I**, affording complexes *trans*-[$PdBr_2$(^{i}Pr_2-bimy)(SMe_2)] (**21**) and *trans*-[$PdBr_2$(^{i}Pr_2-bimy)(THT)] (**22**). However, an excess of PNO had to be heated with complex **I** to afford the desired complex *trans*-[$PdBr_2$(^{i}Pr_2-bimy)(PNO)] (**23**). Their solubilities and spectroscopic properties are very similar to those of other *trans*-configured complexes, and hence no further comments are required.

The two thioethers have very close electron donating properties. However, ^{13}C NMR spectroscopy could still resolve the small difference as indicated by the $^{13}C_{carbene}$ resonances of complexes **21** and **22** at 163.5 and 163.6 ppm, respectively. As expected, the cyclic THT ligand is slightly stronger than the SMe_2 ligand. Complex **23** shows a very upfield $^{13}C_{carbene}$ at 155.7 ppm indicating a weak donor property of the PNO ligand, which in turn explains the difficulty met in the preparation of this complex.

Single crystals of complexes **22** and **23** were obtained by slow evaporation of their saturated solutions in $CHCl_3$/hexane. The molecular structures depicted in Figures 2.6 confirm

the coordination of the co-ligands to the Pd(II) metal in *trans*-arrangements. The stronger THT ligand in complex **22** leads to a longer Pd–$C_{carbene}$ bond than that of complex **23**.

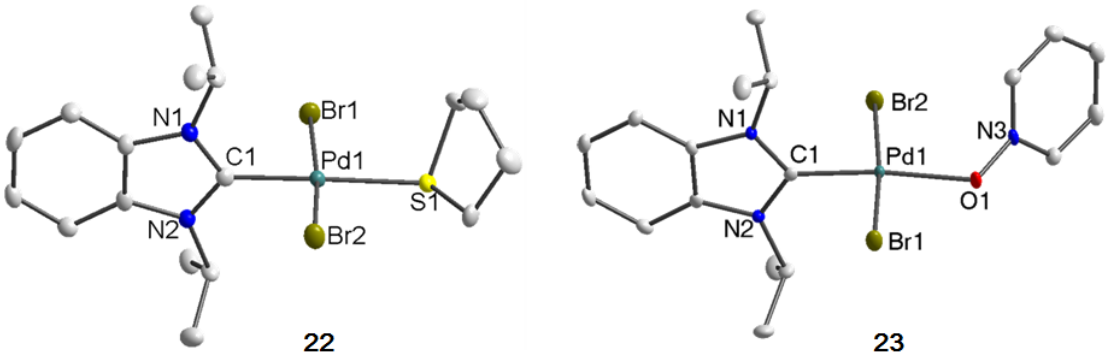

Figure 2.6. Molecular structures of complexes **22** and **23** showing 50% probability ellipsoids; hydrogen atoms are omitted for clarity. Selected bond length [Å] and bond angles [°]: **22**, Pd1–C1 1.969(3), Pd1–Br1 2.4286(4), Pd1–Br2 2.4342(4), Pd1–S1 2.3784(7); C1–Pd1–Br1 86.85(8), C1–Pd1–Br2 87.63(8), Br1–Pd1–S1 87.13(2), Br2–Pd1–S1 98.76(2); $PdCBr_2N$/NHC dihedral angle 87.1 °. **23**, Pd1–C1 1.935(2), Pd1–Br1 2.4213(3), Pd1–Br2 2.4201(3), Pd1–O1 2.1126(15); C1–Pd1–Br1 88.42(6), C1–Pd1–Br2 86.46(6), Br1–Pd1–O1 88.86(4), Br2–Pd1–O1 96.39(4); $PdCBr_2N$/NHC dihedral angle 88.2 °.

Overall, the donor strengths of the different monodentate ligands can be ranked on a unified scale based on the $^{13}C_{carbene}$ resonances of the respective complexes (Figure 2.7). Generally, the phosphite ligands are the strongest among the ligands studied followed by $AsPh_3$. The thioethers have medium donating powers in between some nitrogen donors, and pyridine *N*-oxide has the lowest donating ability in this series.

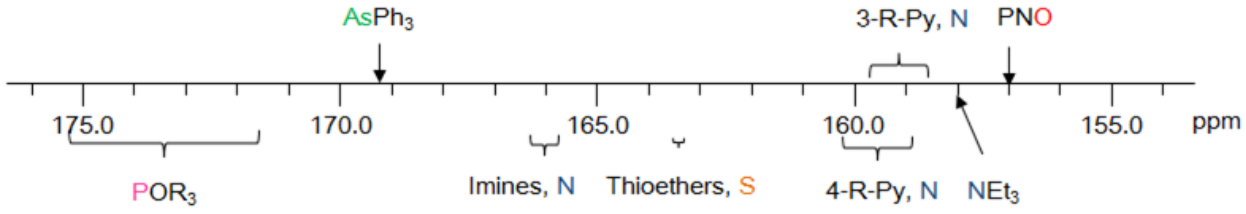

Figure 2.7. Donor abilities of P, As, N, S and O donors on a unified ^{13}C NMR scale.

2.2 Donor Strengths Determination of Bidentate Ligands

2.2.1 Electron Donor Strengths of Diimines

1,2-bidentate nitrogen ligands such as aromatic and aliphatic α-diimines have acquired immense importance in coordination chemistry due to the diverse photochemical properties and catalytic activities of their complexes. Importantly, it has been reported that the electron donating potential of these ligands have prominent influence on these applications.[71] Thus, in extension of the Huynh electronic parameter to bidentate ligands, the electron donating abilities of aromatic and aliphatic diimine ligands will be determined.

The synthesis of the respective $^{i}Pr_2$-bimy/diimine complexes involves again the bridge-cleavage reaction of complex **I** and concurrent chelate formation by ligand displacement of one bromido ligand with the suitable 1,2-diimines[72] {1,10-Phenanthroline-5,6-dione (phen-dione), phen, bipy, and 1,4-di(4-R-phenyl)-2,3-dimethyl-1,4-diazabutadienes (R-DAB: R = Br, H, Me, OMe, ^{t}Bu)}. Subsequent anion metathesis reaction with KPF_6 affords the desired [PdBr($^{i}Pr_2$-bimy)(diimine)]PF_6 complexes **24**–**31** (Scheme 2.2). With the exception of [PdBr($^{i}Pr_2$-bimy)(Br-DAB)]PF_6 (**27**), all complexes were obtained in spectroscopically pure form in high yields of >80% by simply washing with a non-polar solvent such as hexane or diethyl ether. Complex **27** had to be purified by column chromatography, and was isolated in a moderate yield of 40%.

All complexes are pale-yellow solids and stable to air and moisture. Most complexes have fairly good solubilities in common polar organic solvents, such as $CHCl_3$, CH_2Cl_2, CH_3CN, DMF and DMSO. Two exceptions are compounds [PdBr($^{i}Pr_2$-bimy)(phen-dione)]PF_6 (**24**) and [PdBr($^{i}Pr_2$-bimy)(bipy)]PF_6 (**26**), which sparingly dissolve in $CHCl_3$ hampering full NMR spectroscopic characterization in $CDCl_3$ (*vide infra*).

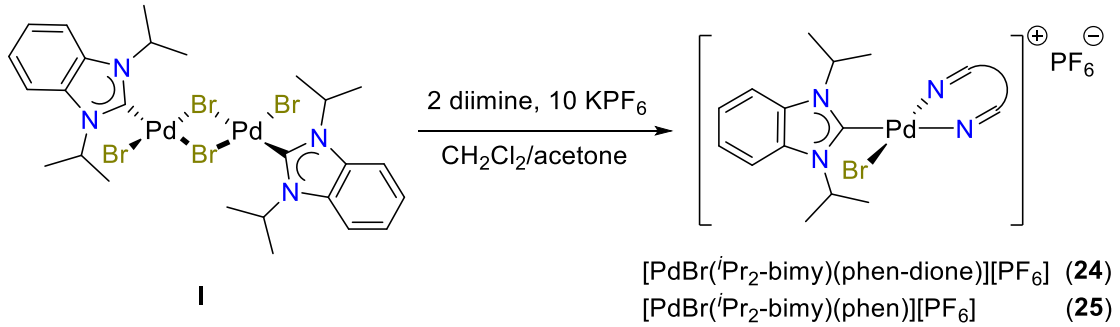

I

[PdBr(^{i}Pr$_2$-bimy)(phen-dione)][PF$_6$] (**24**)
[PdBr(^{i}Pr$_2$-bimy)(phen)][PF$_6$] (**25**)
[PdBr(^{i}Pr$_2$-bimy)(bipy)][PF$_6$] (**26**)
[PdBr(^{i}Pr$_2$-bimy)(R-DAB)][PF$_6$] (**27-31**)

Scheme 2.2. Synthesis of [PdBr(^{i}Pr$_2$-bimy)(diimine)]PF$_6$ complexes **24**–**31**.

Formation of these complexes is indicated by positive mode ESI-MS, which shows base peaks owing to the [M – PF$_6$]$^+$ fragments. In their ^{1}H and ^{13}C NMR spectra, signals of the respective diimine ligands are observed. As expected, a doubling of ligand signals was observed after coordination, which led to inequivalent "*transoid*" and "*cisoid*" parts of the diimine ligands with respect to the NHC.

The aromatic signals of the ^{i}Pr$_2$-bimy ligand remain largely unchanged upon cleavage of complex **I** and subsequent coordination of the diimine ligands. In the ^{1}H NMR spectra, the isopropyl C–H resonances are shifted upfield by 0.4–0.7 ppm as compared to that in the precursor complex **I**, and the isopropyl CH$_3$ resonances split into two doublets, indicating a restricted rotation of the ^{i}Pr$_2$-bimy ligands about the Pd–C bond in complexes **24**–**31**. This is also observed in their ^{13}C NMR spectra, where two singlets were detected for the isopropyl CH$_3$ groups. With exception of complexes **24** and **26**, the carbene carbon signals of all complexes were successfully obtained in short time due to their good solubilities in CDCl$_3$ (Table 2.3). The poor solubility of the phen-dione, bipy complexes **24** and **26**, however, hampers the data collection. This problem was resolved by ^{13}C labeling their carbene donors via cleavage reaction using the ^{13}C$_{carbene}$-

labeled complex **I**. By doing so, detection of the carbene signals of **24** and **26** in $CDCl_3$ was accomplished in a short time (Table 2.3).

Table 2.3. Summary of $^{i}Pr_2$-bimy carbenoid resonances in complexes bearing diimines.

complex	L_2	$\delta\ C_{carbene}$ [a]
24	phen-dione	160.0 [b]
25	phen	161.4
26	bipy	162.7 [b]
27	Br-DAB	160.5
28	H-DAB	162.2
29	Me-DAB	162.6
30	OMe-DAB	162.8
31	^{t}Bu-DAB	163.4

[a] Measured in $CDCl_3$ and internally referenced to the solvent signal at 77.7 ppm relative to tetramethylsilane (TMS). [b] Carbene signal obtained from the $^{13}C_{carbene}$-labeled analogue.

The $^{13}C_{carbene}$ resonances of aromatic diimine complexes **24**–**26** are observed at 160.0, 161.4 and 162.7 ppm, respectively, indicating increasing donor strengths from phen-dione to phen followed by bipy ligand, which is in agreement with *–I* effects originating from the two electron withdrawing carbonyl groups in the phen-dione or the additional benzannulation in the phen ligand compared to the bipy parent. The $^{13}C_{carbene}$ shifts of DAB complexes **27**–**29** range from 160.5 to 162.6 ppm, showing the intermediate donating ability of the R-DAB chelators (R = Br, H, Me) compared to phen-dione and bipy. The OMe-DAB and ^{t}Bu-DAB ligands possess

stronger donating power than the bipy ligand with their complexes' carbene signals found at 162.8 and 163.4 ppm.

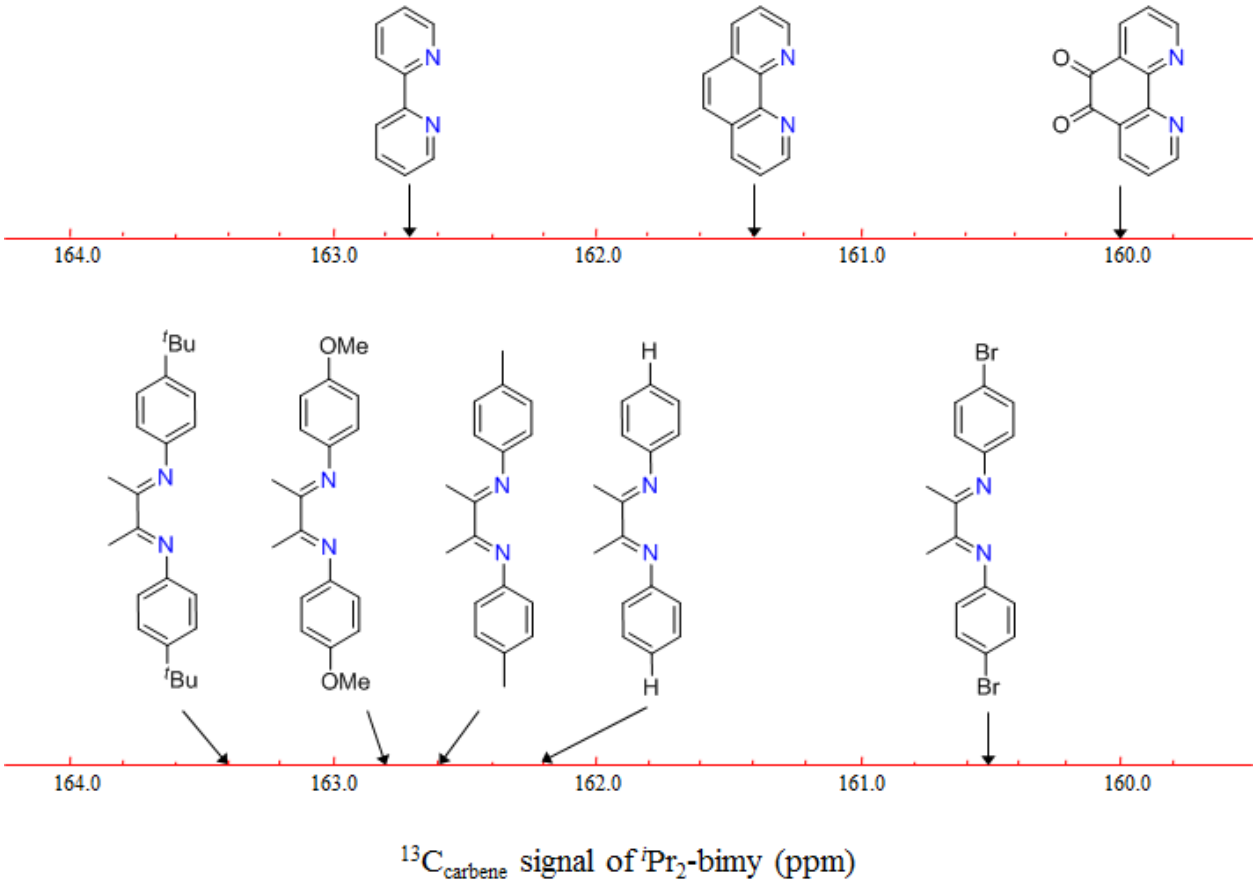

Figure 2.8. Donor abilities of aromatic and aliphatic diimines on the ^{13}C NMR scale.

Notably, this method can discern differences within the five R-DAB ligands, which only differ in their *para*-substituents five bonds away from the N-donor and seven bonds away from the reporter nuclei. Based on the $^{13}C_{carbene}$ resonances, the five DAB ligands were clearly ranked according to their decreasing donor abilities in the order ^{t}Bu-DAB > OMe-DAB > Me-DAB > H-DAB > Br-DAB. This order is reasonable and consistent with the decreasing positive inductive (+*I*) effect of the *para*-substituent in the order ^{t}Bu > Me > H > Br (Figure 2.8). The positioning of the OMe-DAB ligand can be explained by the +*M* effect of the methoxy group, which not only

compensates its –*I* effect, but even increases electron density via p-π conjugation of its lone pairs with the aromatic rings. These results demonstrate that the ^{13}C based electronic parameter can be extended to the evaluation of bidentate ligands. The method's unprecedented sensitivity, which allows detection of small electronic differences within the same class brought about remote ligand modifications not only applies for monodentate ligands, but for bidentate ligands as well.

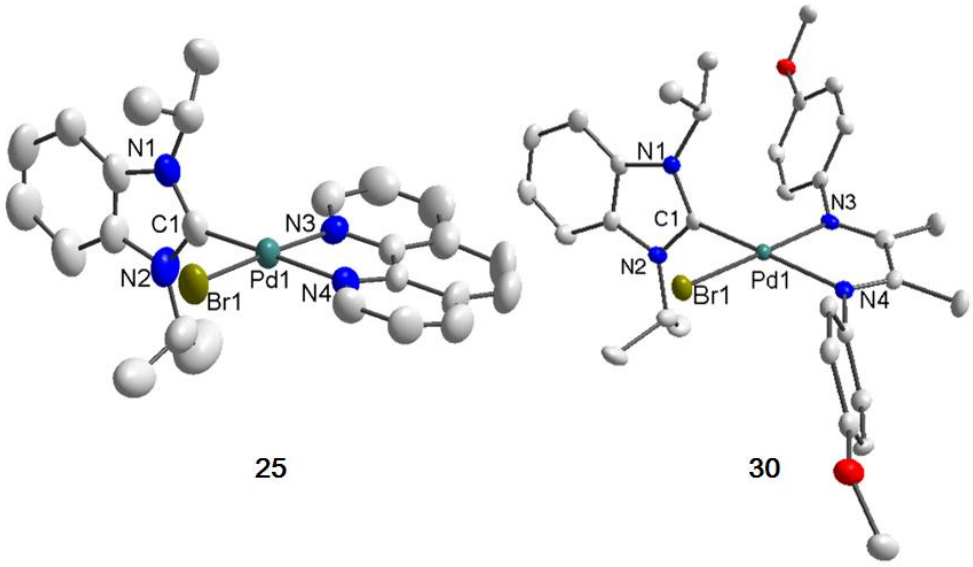

Figure 2.9. Molecular structures of **25** and **30** in the solid state (hydrogen and counter ion atoms are omitted for clarity; ellipsoids drawn at 50% probability). Selected bond lengths [Å] and angles [deg] of **25**: Pd1–C1 1.977(7), Pd1–N3 2.044(5), Pd1–N4 2.071(5), Pd1–Br1 2.3925(10), C1–Pd1–Br1 85.7(2), C1–Pd1–N3 96.9(3), N4–Pd1–N3 81.0(2), N4–Pd1–Br1 96.31(16); $PdCBr_2N$/NHC dihedral angle 89.4°. **30**: Pd1–C1 1.976(3), Pd1–N3 2.035(3), Pd1–N4 2.087(3), Pd1–Br1 2.4119(5), C1–Pd1–Br1 84.01(10), C1–Pd1–N3 99.30(12), N4–Pd1–N3 78.56(11), N4–Pd1–Br1 98.32(8); $PdCBr_2N$/NHC dihedral angle 81.3°.

Slow evaporation of concentrated solutions of complex **25** and **30** in $CHCl_3$/hexane afforded single crystals, which were analyzed by X-ray diffraction. Figures 2.9 depicts their molecular structures, in which both palladium centers are coordinated by one NHC, one bromido and one chelating diimine ligand. The NHC planes in both complexes are perpendicular to the $PdCN_2Br$ coordination plane with dihedral angles of 89 ° and 81 ° in complexes **25** and **30**, respectively. In complex **30**, the two N-aryl rings tilt towards different directions about the

chelating plane with dihedral angles of 63 ° and 67 °. The N3–Pd1–N4 bite angle in complex **25** (81 °) and **30** (79 °) are very similar. The similarity is also observed for their Pd–$C_{carbene}$ bond lengths of 1.977(7) and 1.976(3) Å.

2.2.2 Electron Donor Strengths of Dicarbenes

In addition to the evaluation of the ubiquitous bidentate diimine ligands, particularly interest are being paid to the donor strength determination of chelating dicarbenes due to their increasing importance as ligands in catalytic reactions and organometallic chemistry in general.

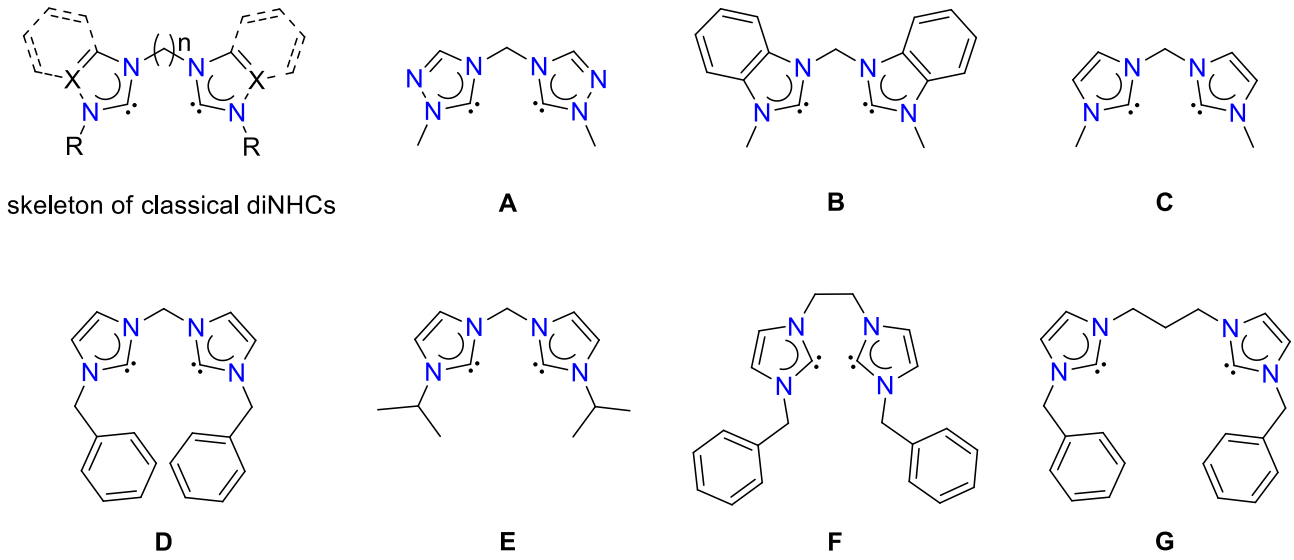

Chart 2.2. Lewis structures of 7 classical diNHCs.

Simple dicarbenes formed by bridging two classical NHCs can differ in their heterocyclic backbones, their external N-substituents (R groups) and finally the nature of their linkers (Chart 2.2). Changes in any of these three parameters may affect their electron donating abilities. In

order to study if all these effects can be accurately determined, seven diNHCs were targeted (Chart 2.2, **A**–**G**), the precursors of which were prepared according to literature procedures.[73] Overall, these salts, and consequently their diNHCs, form three comparable groups, each differing in only one parameter: (i) heterocyclic backbone (**A**·2HBr, **B**·2HBr, **C**·2HBr), (ii) N3-substituent (**C**·2HBr, **D**·2HBr, **E**·2HBr), and (iii) linker length (**D**·2HBr, **F**·2HBr, **G**·2HBr).

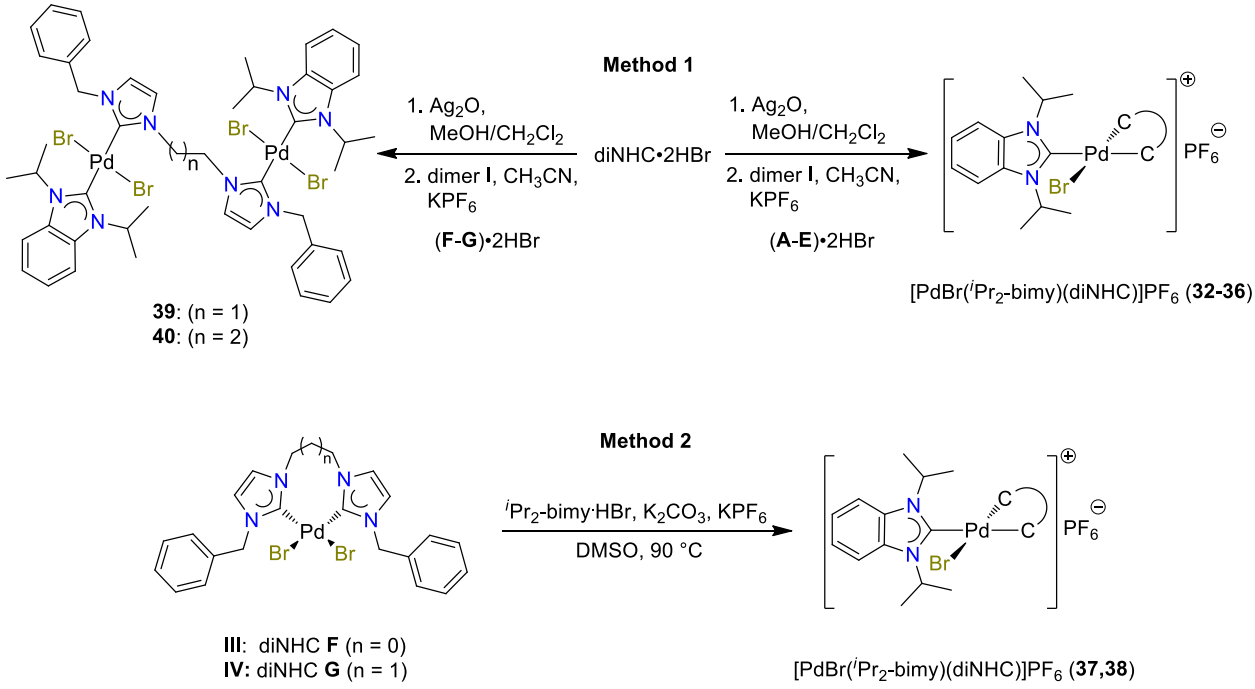

Scheme 2.3. Syntheses of [PdBr(^{i}Pr$_2$-bimy)(diNHC)]PF$_6$ complexes **32**–**38** and [Pd$_2$Br$_4$(^{i}Pr$_2$-bimy)$_2$(diNHC)] complexes **39**–**40**.

Generally, the carbene precursors were first reacted with Ag_2O to obtain the intermediate Ag NHC species, which subsequently transfers the diNHC to the Pd center in *trans*-[PdBr$_2$(^{i}Pr$_2$-bimy)(CH$_3$CN)][58] (**II**), under displacement of the CH_3CN and one bromido ligand. Anion exchange using KPF_6 gave the [PdBr(^{i}Pr$_2$-bimy)(diNHC)]PF$_6$ complexes **32**–**36** bearing diNHCs **A**–**E**, respectively, in moderate to decent yields of over 60% (Scheme 2.3, method 1). Complexes **37** and **38** with ethylene and propylene bridged diNHCs **F** and **G**, however, were only isolated as

minor by-products in low yields of 8% (**37**) and 18% (**38**) through this route. The major products isolated were the dipalladium species **39** and **40** (Scheme 2.3, method 1), in which the diNHCs are bridging two palladium(II) centers, instead of chelating to one palladium(II) Lewis acid as required for the formation of complexes **37** and **38**. The low yields of the latter were attributed to the difficult formation of the less stable 7- and 8-membered palladacycles during the transmetalation step as opposed to the more stable 6-membered cycles in complexes **32**–**36**.

To circumvent this, a reversed protocol was attempted for the preparation of **37** and **38**, whereby the known diNHC complexes **III** and **IV** were preformed,[74] and then subjected to attack by the $^{i}Pr_2$-bimy ligand generated *in situ* by deprotonation of the 1,3-diisopropylbenzimidazolium salt with K_2CO_3. Salt KPF_6 was again added to replace the bromide anion affording complexes **37** and **38** in higher yields of 56% and 85%, respectively (Scheme 2.3, method 2). To the best of our knowledge, these hetero-tris(NHC) palladium(II) complexes are the first of their kind to contain a metal center that is simultaneously coordinated by both a monodentate NHC and a bidentate diNHC.[75]

Monopalladium complexes **32**–**38** are off-white solids, while the two bridged dipalladium species **39** and **40** are yellow powders. These two neutral complexes have very good solubilities in common organic solvents such as diethyl ether, ethyl acetate, $CHCl_3$, CH_2Cl_2, CH_3CN, DMSO, etc. On the other hand, the cationic complexes **32**–**38** are insoluble in ethers and only well soluble in polar organic solvents. Surprisingly, the solubilities of **37** and **38** bearing the longer ethylene and propylene linked diNHCs are significantly poorer in $CHCl_3$ and CH_2Cl_2, but remain good in CH_3CN and DMSO. ESI-MS revealed base peaks from *m/z* 565 to 745 for the $[M - PF_6]^+$ cations of complexes **32**–**38**, while strong isotopic envelopes centered at *m/z* 1199 and 1213 were recorded for the $[M - Br]^+$ fragments of the dinuclear species **39** and **40**.

NMR spectra of the complexes were recorded in $CDCl_3$ (**32**–**36**, **39**, **40**) or CD_3CN (**37**, **38**) at 298 K. Most complexes give rise to well-resolved spectra at this temperature with the exception of the [PdBr($^{i}Pr_2$-bimy)(**A**)]PF_6 complex (**32**), where only broad signals are observed in its ^1H NMR spectrum. At room temperature, the $^{i}Pr_2$-bimy NCH and bridging NCH_2N protons are not resolved due to a fast fluxional behavior. Cooling the sample to 273 K improves the resolution, and a well-resolved spectrum was finally obtained when the temperature was further decreased to 243 K (Figure 2.10).

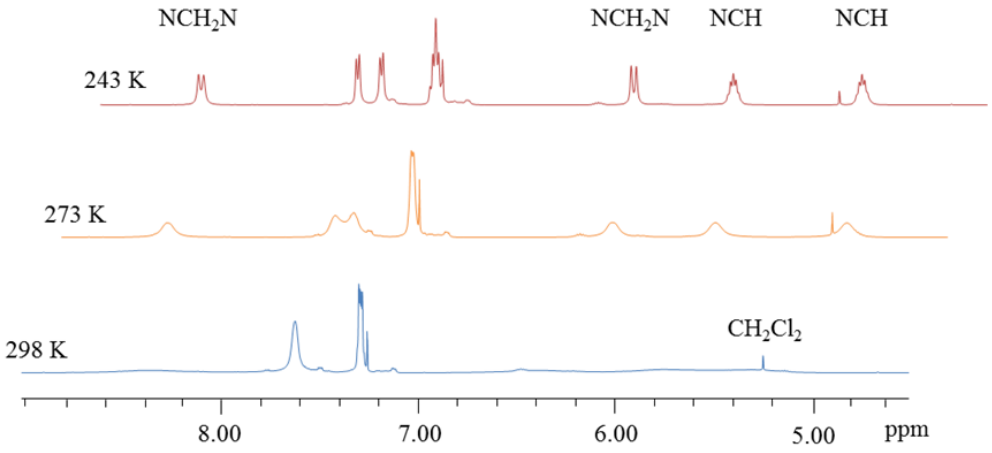

Figure 2.10. Variable temperature ^1H NMR spectra of complex **32** in the region of 4.5–9.0 ppm.

When sufficiently resolved, complexes **32**–**38** share very similar ^1H and ^{13}C NMR spectra. Besides the doubling of the diNHC signals upon coordination as observed for the diimine complexes, further splitting due to diastereotopy of N3-substituents is noted for complexes with benzyl and isopropyl groups. For example, complex **36** shows four doublets in its ^1H NMR spectrum, which are attributed to the inequivalent isopropyl CH_3 signals of the diNHC ligand. Similarly, four AM patterned doublets are observed in the ^1H NMR spectra of complexes **35**, **37** and **38**, assignable to the benzylic protons. In most cases, the linker protons become

diastereotopic upon complexation as well. As a representative, two doublets at 8.48 and 6.29 ppm are observed for the methylene spacer in the spectrum of complex **32** (Figure 2.10). The coupling pattern for the $^{i}Pr_2$-bimy ^{1}H NMR signals in these complexes are more complicated than those found in the diimine derivatives, showing two septets at 5.25 and 6.02 ppm for the NCH protons. This indicates a restricted rotation of the N-substituents in the $^{i}Pr_2$-bimy probe after diNHC coordination.

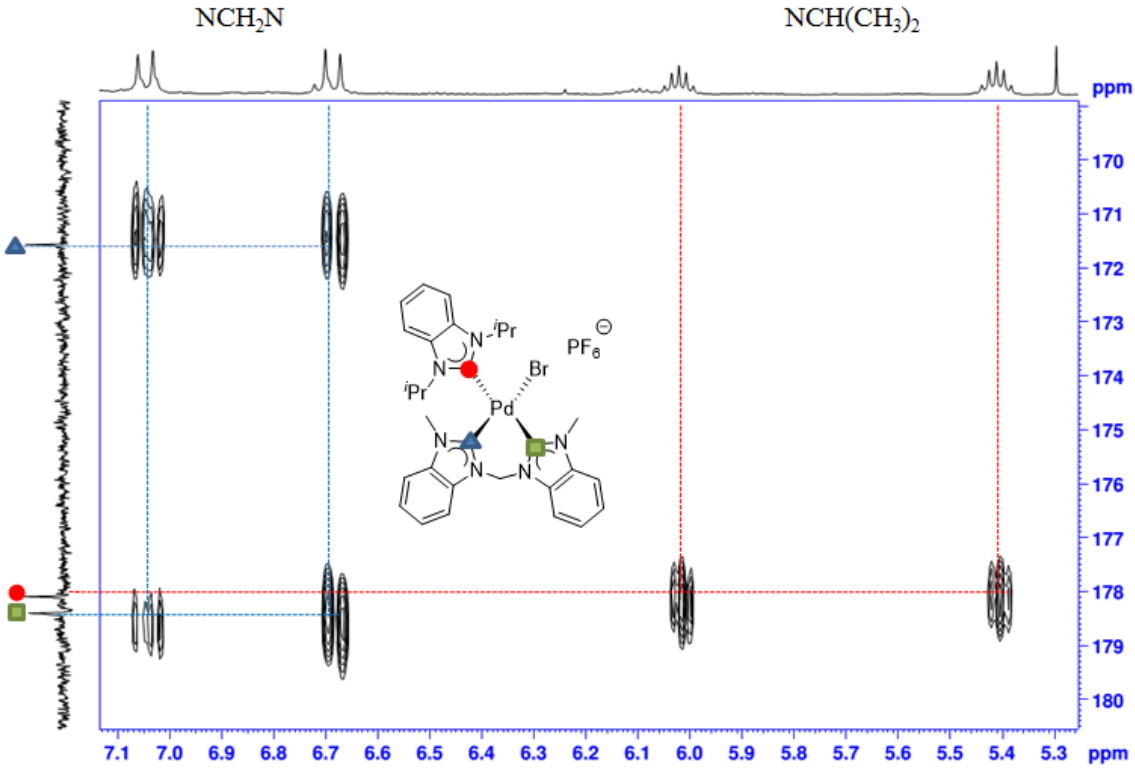

Figure 2.11. Section of the 2D ^{1}H,^{13}C-HMBC NMR spectrum of complex **33**.

The reduced symmetry also leads to a doubling of the ^{13}C NMR signals for the diNHC ligands and the $^{i}Pr_2$-bimy probe. As expected, three downfield carbene signals are detected in these seven complexes, most of which are sufficiently different to be properly assigned in accordance to literature values for related complexes.[74] Complex **33** bearing the

dibenzimidazolin-2-ylidene chelator, on the other hand, shows three carbene resonances in a very narrow range. Here, HMBC NMR experiments were conducted to assist the correct assignment (Figure 2.11). 2D cross-peak correlations between the carbene carbon atoms with the protons in the respective N-substituents allow for an unambiguous assignment to the correct carbene atom. The detection of the $^{i}Pr_2$-bimy carbene signals in $CDCl_3$ of the poorly soluble complexes **37** and **38** was accomplished by using the ^{13}C-labeled 1,3-diisopropylbenzimidazolium salt[24a] in their syntheses.

The NMR spectra of the dipalladium complexes **39** and **40** are much simpler, with the benzylic protons resonating as one singlet at 5.80 and 5.76 ppm, respectively. The equivalent ethylene protons in **39** show one singlet and the propylene protons in **40** give rise to a triplet and a multiplet in a 4:2 integral ratio. Restricted rotation of the $^{i}Pr_2$-bimy ligand about the Pd–C bond in both complexes is evidenced by two septets and doublets assignable to the isopropyl substituents. Each complex exhibits only two carbene signals in its ^{13}C NMR spectrum, and the more downfield signal at 178.8 ppm (**39**) or 179.1 ppm (**40**) is assigned to the $^{i}Pr_2$-bimy ligand.

Table 2.4 summarizes the diagnostic $^{13}C_{carbene}$ resonances of the $^{i}Pr_2$-bimy probe in complexes **32**–**38**. Generally, they are much more downfield than those in the diimine counterparts confirming stronger donating abilities of the diNHC ligands. The group (i) diNHCs **A**–**C** (ditriazolin-5-ylidenes (ditazy), dibenzimidazolin-2-ylidene (dibimy) and diimidazolin-2-ylidene (diimi)) in complexes **32**–**34** differ only in their heterocyclic backbone, and by comparison of the $^{i}Pr_2$-bimy reporter signals, an increasing electron donating ability in the order of **A** (ditazy) < **B** (dibimy) < **C** (diimi) can be deduced. This backbone influence is consistent with that reported for monodentate NHCs, i.e. benzannulation in **B** and introduction of an electronegative nitrogen atom in **C** result in a successive increase of *–I* effect and weakening of

the respective donors. This trend also agrees with that obtained from the CO stretches calculated by Crabtree and coworkers based on a [Mo(CO)$_4$(diNHC)] (diNHC = diimi, ditazy) system[29] and the CO stretches measured by Veige *et al*. from a [Rh(CO)$_2$(diNHC)]OTf (diNHC = diimi, dibimy) system.[33]

Table 2.4. Summary of ^{i}Pr$_2$-bimy carbenoid resonances in complexes bearing diNHC chelators.

complex	L_2	δ $C_{carbene\text{-}probe}$ [a]
32	**A**	177.1
33	**B**	178.7
34	**C**	179.9
35	**D**	179.51
36	**E**	180.0
37	**F**	179.54[b]
38	**G**	180.3[b]

[a]Measured in $CDCl_3$ and internally referenced to the solvent signal at 77.7 ppm relative to TMS. [b]Carbene signal obtained from the carbene ^{13}C-labeled analogue.

In addition, comparison among group (ii) ligands (i.e. **C**–**E**) in complexes **34**–**36** reveals that the electronic parameter can also detect N3-substituent effects of diNHCs in the order of **D** (Bn) < **C** (Me) < **E** (^{i}Pr) in line with their increasing +*I* effects. Effects induced by the linkers as a special type of N-substituent effect in diNHCs of group (iii) have rarely been investigated. From increasing downfield shifts of the ^{i}Pr$_2$-bimy $^{13}C_{carbene}$ resonances in complexes **35** < **37** < **38**, it is concluded that simple lengthening of the linkers by a CH_2 group leads to a detectable increase of

donor strength in the order of **D** (methylene) < **F** (ethylene) < **G** (propylene). The very small difference between **D** and **F** is understandable, since all carbon atoms in the bridges experience *–I* effects of at least one electron withdrawing nitrogen atom. In ligand **G** the situation is different, as the central CH_2 group in the bridge exerts a *+I* effect, which can effectively increase electron density. Generally, this result is in line with the fact that the *+I* effect of an alkyl group increases with the chain length, which has also been testified by Ito's Group via comparing the CO stretches of $[Mo(CO)_4(diNHC)]$ (diNHC = methylene and ethylene bridged imidazolin-2-ylidenes).[34] However no clear trend was detected when similar carbonyl-based methods using *fac*-$[(CO)_3ReBr(diNHC)]$ type complexes were employed.[35] This highlights the better sensitivity and broader applicability of this ^{13}C NMR based electronic parameter.

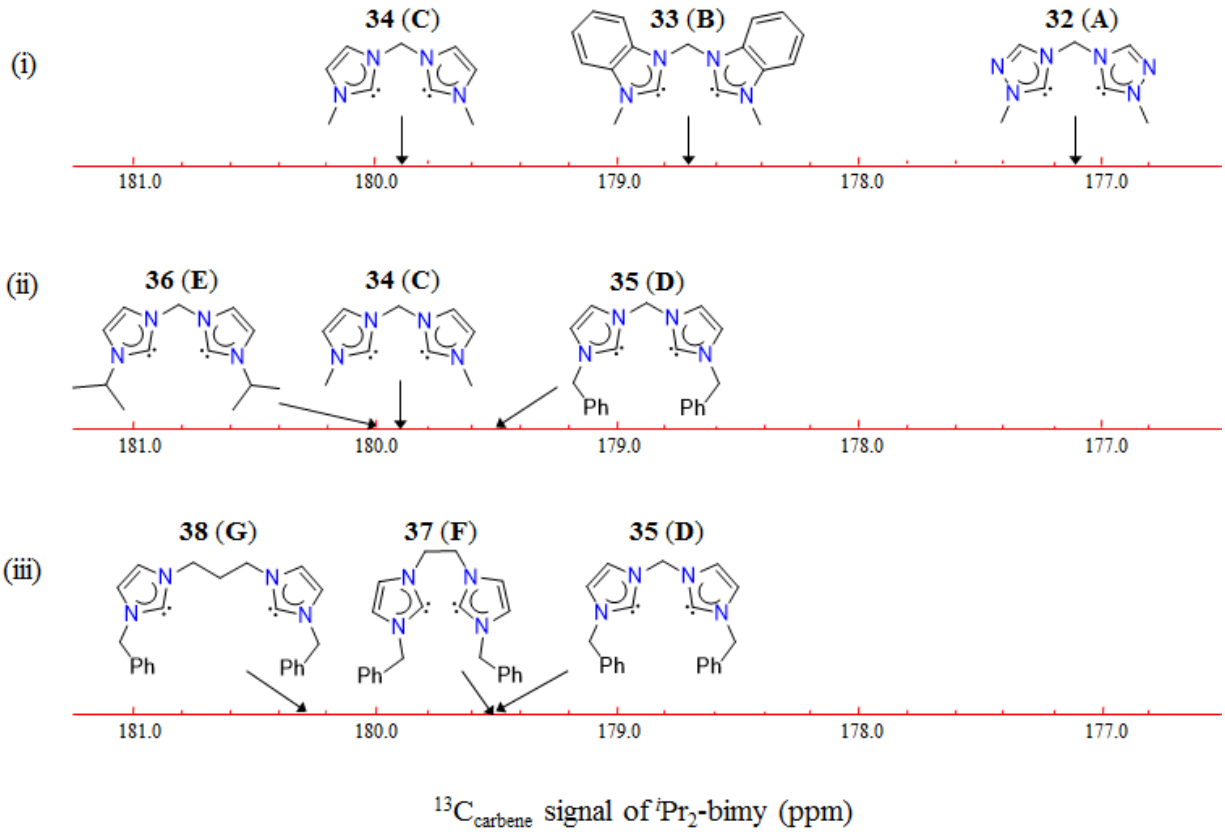

Figure 2.12. Donor abilities of dicarbenes on the ^{13}C NMR scale.

Overall, as can be seen from Figure 2.12, the NHC backbone has the most significant influence among the three parameters studied with chemical shift differences > 1.0 ppm. Different N3-substituents and linkers within the imidazole-derived system give rise to diNHCs (**C**–**G**) with varying donating potentials in the order of **G** (propylene, Bn) > **E** (methylene, iPr) > **C** (methylene, Me) > **F** (ethylene, Bn) > **D** (methylene, Bn). The results obtained provide useful information for the electronic fine-tuning of ligands, which is one of the key factors for complex stability and their applications.

Single crystals of **32**, **34**, **37** and **38** can easily be grown upon standing of concentrated solutions (DMSO for **32**, CH_2Cl_2/hexane for **34**, $CHCl_3$/hexane for **38**) or from diffusion of diethyl ether into a solution of **37** in CH_3CN.

The molecular structures are shown in Figure 2.13 along with selected bond parameters. The asymmetric unit of complex **34** contains two independent molecules, which have essentially identical structure except for several bond parameter differences slightly over 3σ, and therefore only one of them is shown. The cationic complexes **32**, **34**, **37** and **38** crystallize as mononuclear species, in which one $^{i}Pr_2$-bimy, one diNHC and one bromido ligand coordinate the palladium centers in distorted square–planar geometries. Complex **34** bearing the methylene bridged diNHC ligand **C** and complex **37** with ethylene-bridged diNHC ligand **F** have very similar bite angles (85.9º *vs* 84.9º). The bite angle in complex **38** with a propylene-bridged diNHC is only slightly bigger with 87.7º. The six- to eight-membered palladacycles all adopt boat-like conformations similar to those reported for simple dihalido-diNHC complexes.[74,73,76,77,78]

Among the three carbene donors in each complex, the $^{i}Pr_2$-bimy ring plane always has the largest dihedral angle with respect to the PdC_3Br coordination plane (**32**, 70.2º; **34**, 74.3º; **37**, 78.6º; **38**, 76.2º). The short methylene bridge of the diNHC ligands prevents an otherwise

preferred perpendicular orientation, which result in small dihedral angles ranging from 39.2º to 52.7º in complexes **32** and **34**. Elongation of the spacer in the diNHCs of complexes **37** and **38** increases the flexibility leading to larger dihedral angles of 62.9º to 74.3º.

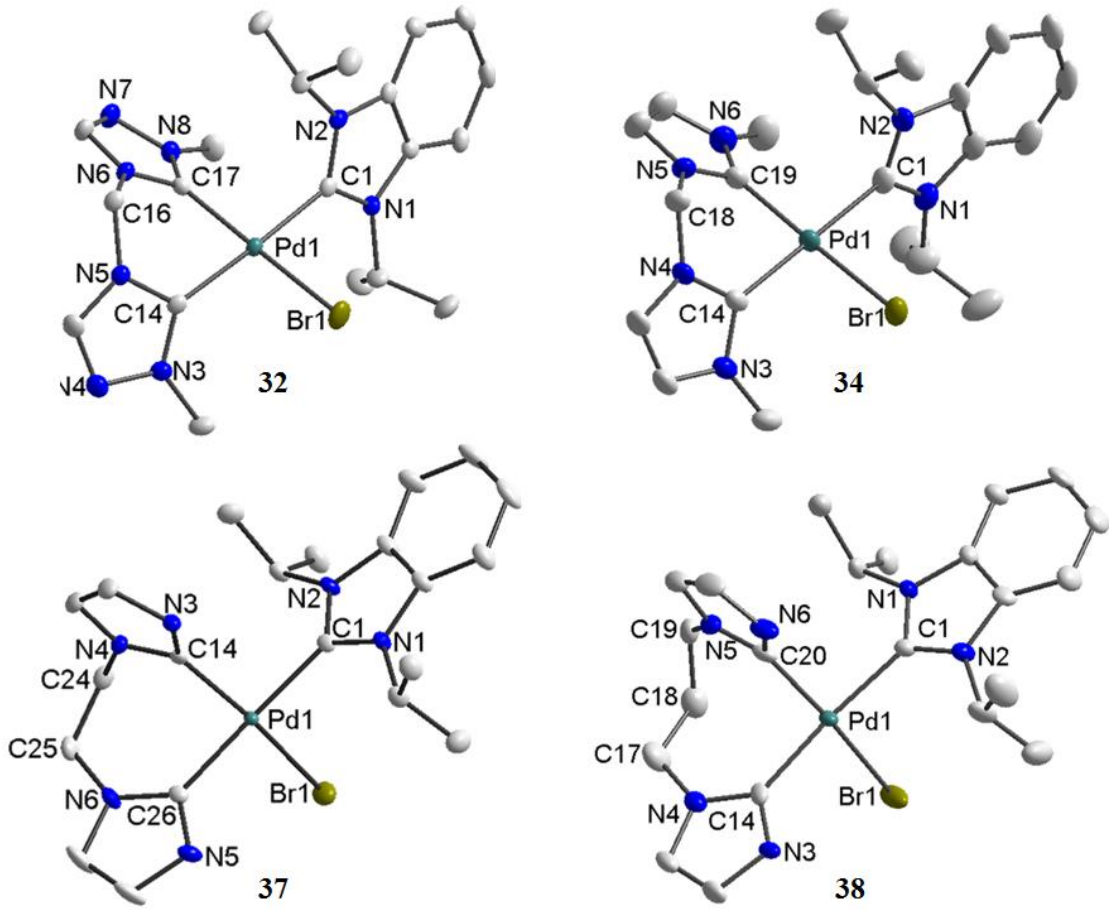

Figure 2.13. Molecular structures of **32**, **34**, **37** and **38** in the solid state (hydrogen atoms, counter ions, solvent molecules and N-benzyl substituents in complexes **37** and **38** are omitted for clarity; ellipsoids drawn at 50% probability). Selected bond lengths [Å] and angles [deg]: **32**, Pd1–C1 2.0251(19), Pd1–C17 1.9977(18), Pd1–C14 2.0190(19), Pd1–Br1 2.4576(3); C1–Pd1–C17 92.30(7), C14–Pd1–C17 84.14(7), C14–Pd1–Br1 93.01(5), C1–Pd1–Br1 90.77(5). **34**, Pd1–C1 2.038(4), Pd1–C19 2.003(4), Pd1–C14 2.033(4), Pd1–Br1 2.4556(16); C1–Pd1–C19 94.52(17), C14–Pd1–C19 85.89(16), C14–Pd1–Br1 91.63(12), C1–Pd1–Br1 87.83(13). **37**, Pd1–C1 2.044(2), Pd1–C14 1.995(2), Pd1–C26 2.026 (2), Pd1–Br1 2.4646(3); C1–Pd1–C14 94.24(9), C14–Pd1–C26 84.88(10), C26–Pd1–Br1 91.31(7), C1–Pd1–Br1 90.56(7). **38**, Pd1–C1 2.055(4), Pd1–C20 1.998(4), Pd1–C14 2.036(4), Pd1–Br1 2.4623(6); C1–Pd1–C20 93.88(15), C14–Pd1–C20 87.69(15), C14–Pd1–Br1 89.91(10), C1–Pd1–Br1 89.79(11).

The Pd–C ($^{i}Pr_2$-bimy) distances in these four complexes fall in a narrow range of about 2.0 Å, which are generally longer than those found in the diimine analogues. This is due to less Lewis-acidic metal centers resulting from the coordination of the stronger donating diNHC ligands, although no clear correlation between these distances and the electron-donating powers among diNHCs was found.

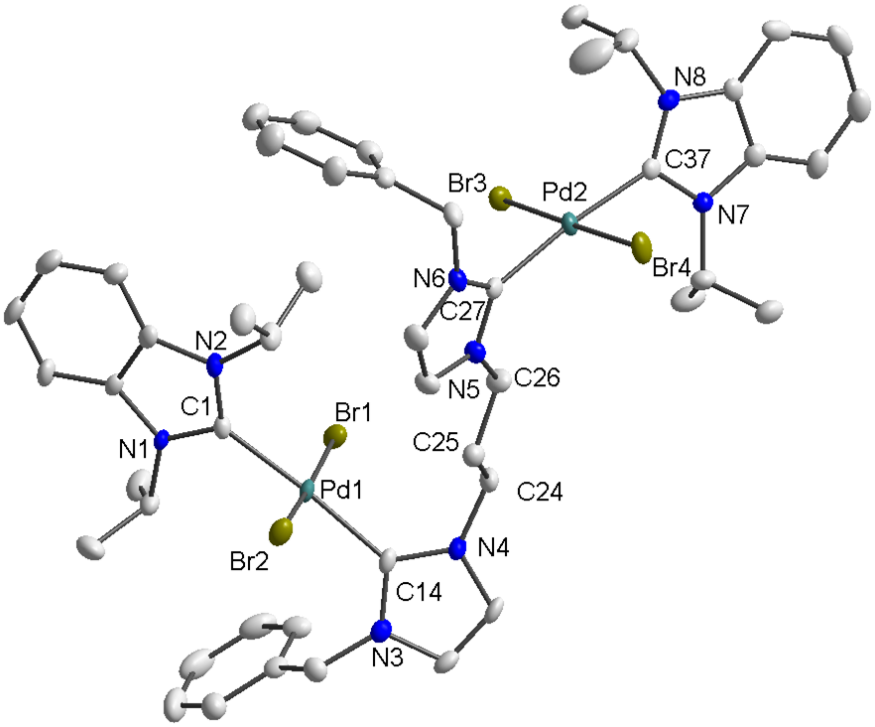

Figure 2.14. Molecular structures of **40** in the solid state (hydrogen atoms are omitted for clarity; ellipsoids drawn at 50% probability). Selected bond lengths [Å] and angles [deg]: Pd1–C1 2.014(3), Pd1–Br1 2.4473(5), Pd1–C14 2.042(3), Pd1–Br2 2.4370(5), Pd2–C37 2.031(3), Pd2–Br3 2.4346(4), Pd2–C27 2.031(3), Pd2–Br4 2.4530(5); C1–Pd1–Br1 87.84(10), C14–Pd1–Br1 91.66(10), C14–Pd1–Br2 91.61(10), C1–Pd1–Br2 89.34(10), C37–Pd2–Br3 89.63(9), C27–Pd2–Br3 92.20(9), C27–Pd2–Br4 88.90(9), C37–Pd2–Br4 89.27(9).

Single crystals of dipalladium complex **40** were grown by slow evaporation of a saturated solution in diethyl ether. As depicted in Figure 2.14, the complex features two neutral *trans* configured palladium(II) centers. The propylene linked diNHC coordinates in a bridging manner.

The dihedral angles between the NHC and the PdC_2Br_2 coordination planes are generally larger for the $^{i}Pr_2$-bimy ligands (78.4º, 85.3º) compared to those of the bridging diNHC ligand (69.9º and 66.9º). The Pd–C ($^{i}Pr_2$-bimy) bond lengths do not differ significantly from those of the cationic chelates **32**, **34**, **37** and **38**, indicating that the *cis*-positioned co-ligand (Br *vs* NHC) does not affect these distances much regardless of the overall charge of the complex.

3. Synthesis of Functionalized-NHC Palladium(II) Complexes Via a Postmodification Approach

3.1 Synthesis of Parent Complexes

Parent complexes should have reactive sites (i) which have relatively good tolerance during preparation; and (ii) that allow easy functionalizations. Palladium-NHC complexes featuring bromopropyl N-substituents fulfill these requirements and thus were designed as the parent complexes to achieve the goal of postmodifications.

3.1.1 Synthesis of Mono(NHC)-Pd(II) Parent Complex

The suitable ligand precursor **H** that contains a C_3Br N-substituent can be prepared according to literature, by reacting 1-benzylbenzimidazole with an excess of 1,3-dibromopropane.[37d] Initially, it was mixed with one equiv of $Pd(OAc)_2$ and four equiv of NaBr in DMSO and stirred at 90 °C in an attempt to prepare a dimeric monocarbene–Pd(II) species.[58] However, the main product isolated by column chromatography turned out to be an ester-functionalized dimeric complex $[PdBr_2(C_3OAc\text{-}bimy)]_2$ (**41**, Scheme 3.1). Apparently, one equiv of acetate deprotonated the benzimidazolium salt, while the 2nd equiv underwent a S_N2 reaction with the bromopropyl arm forming the ester function.

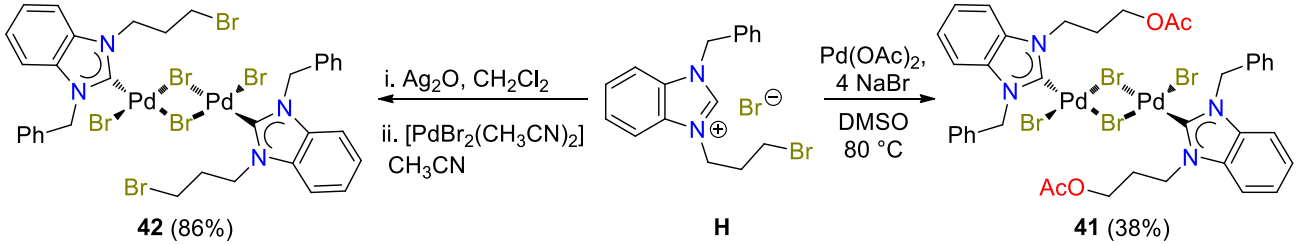

Scheme 3.1. Synthesis of ligand precursor **H** and complex precursors **41** and **42**.

Complex **41** is a dark orange solid, with poor solubilities in common organic solvents such as CH_2Cl_2, CH_3CN and DMSO. The identity of this product was supported by its ^{1}H and ^{13}C NMR spectra, where signals characteristic of the $COCH_3$ group are found. Its formation was further corroborated by the IR spectrum, in which a band at $\tilde{\nu}$ = 1738 cm^{-1} assignable to the C=O double bond is observed.

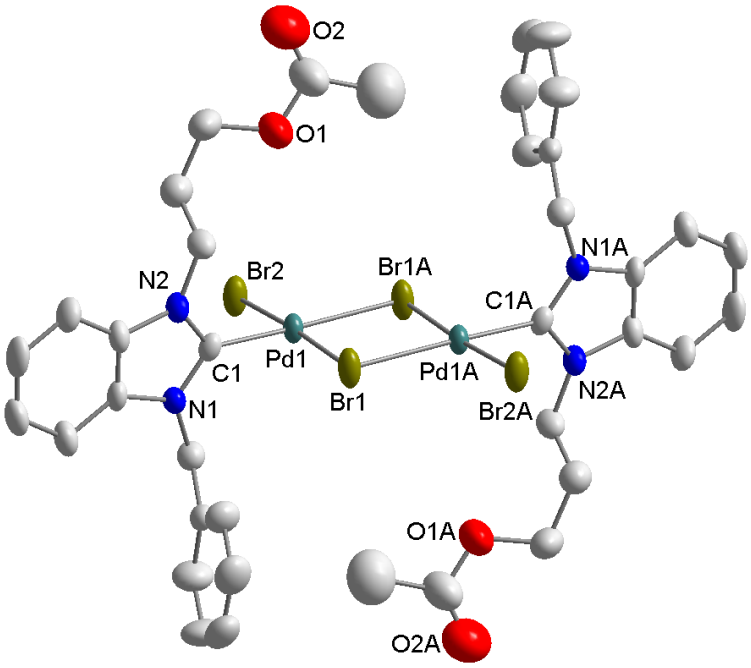

Figure 3.1. Molecular structure of **41** showing 50% probability ellipsoids; hydrogen atoms are omitted for clarity. Selected bond lengths [Å] and bond angles [deg]: Pd1-C1 1.943(5), Pd1-Br1 2.4421(7), Pd1-Br1A 2.5330(7), Pd1-Br2 2.3992(7); C1-Pd11-Br1 90.65(16), Br1-Pd1-Br1A 88.42(2), Br1A-Pd1-Br2 93.49(2), Br2-Pd1-C1 87.57(16); $PdCBr_3$/NHC dihedral angle: 82.8 °.

The identity of **41** was additionally ascertained by X-ray diffraction analysis on a single crystal obtained by slow evaporation of a CH_2Cl_2/hexane solution (Figure 3.1). As expected, complex **41** is a dimeric monocarbene–Pd(II) complex with two bridging bromido ligands. The molecule lies at an inversion center. The coordination sphere at each square planar Pd center is completed by an ester–NHC and a terminal bromido ligand. The two alkyl ester N-substituents

point in different directions resulting in an *anti*-arrangement with respect to the coordination plane. The carbene plane deviates from the coordination plane with a dihedral angle of ~83 °.

In order to prevent the ester-substitution, the milder Ag-carbene transfer was investigated (Scheme 3.1). Salt **H** was hence reacted with Ag_2O to afford the Ag NHC intermediate. Without isolation, the product was directly added to $[PdBr_2(CH_3CN)_2]$ in a 1:1 ratio to afford the desired product $[PdBr_2(C_3Br\text{-}bimy)]_2$ (**42**) in 86% yield.

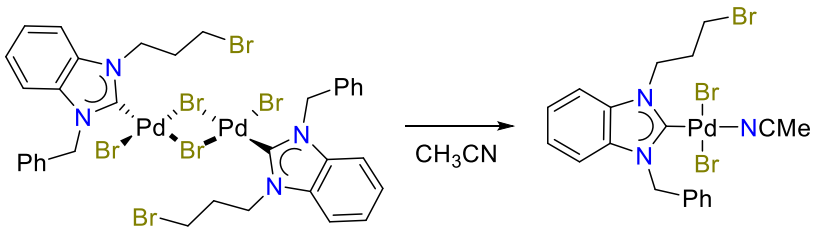

42 **43** (90%)

Scheme 3.2. Cleavage of complex **42** to **43**.

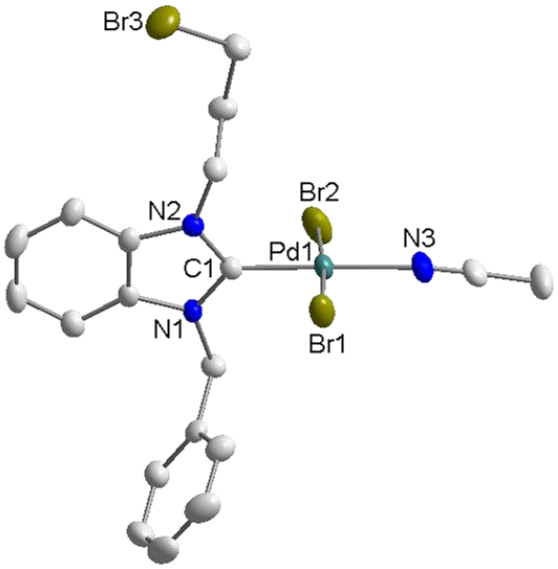

Figure 3.2. Molecular structure of **43** showing 50% probability ellipsoids; hydrogen atoms are omitted for clarity. Selected bond lengths [Å] and bond angles [deg]: Pd1-C1 1.939(3), Pd1-Br1 2.4276(5), Pd1-N3 2.071(3), Pd1-Br2 2.4299(5); C1-Pd11-Br1 87.75(9), Br1-Pd1-N3 93.44(8), N3-Pd1-Br2 90.52(8), Br2-Pd1-C1 88.23(9); $PdCNBr_2$/NHC dihedral angle: 75.0 °.

Compared to **41**, the target complex **42** is a red brown solid with poorer solubilities in the chlorinated solvents. Its ^{1}H NMR spectrum in d_6-DMSO shows the absence of the acidic NCHN proton as found in the salt **H**. Further evidence was obtained by X-ray diffraction analysis on a single crystal obtained by slow evaporation of a concentrated solution in CH_3CN. As depicted in Figure 3.2, the dinuclear complex **42** was cleaved by CH_3CN during crystallization (Scheme 3.2), giving rise to a mononuclear CH_3CN adduct *trans*-[$PdBr_2$(C_3Br-bimy)(CH_3CN)] (**43**). As expected, the Pd(II) center is square planar with the CH_3CN ligand arranged *trans* to the NHC ligand.

Similarly, dimeric complex **42** could undergo bridge-cleavage reaction with pyridine affording the more stable pyridine adduct *trans*-[$PdBr_2$(C_3Br-bimy)(Py)] (**44**, Scheme 3.3), which was anticipated to be better suitable for postmodifications. Complex **44** is soluble in most organic solvents excluding hexane and diethyl ether.

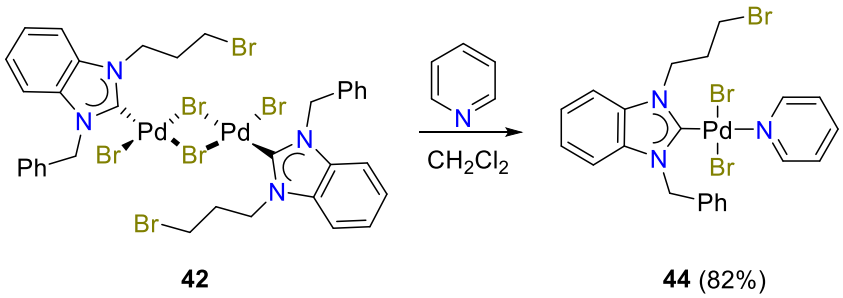

42 **44** (82%)

Scheme 3.3. Synthesis of mono(NHC)-Pd(II) parent complex **44**.

An isotopic pattern at *m/z* 594 in the positive mode ESI mass spectrum assignable to the cationic $[M - Br]^+$ fragment corroborates its formation. Its ^{1}H NMR spectrum shows pyridine signals, which are shifted downfield in comparison to the free pro-ligand. The benzylic and propylene protons resonate as one singlet, two triplets and one quintet, respectively (Figure 3.3).

The carbene carbon resonates at 164.6 ppm in the ^{13}C NMR spectrum, which falls in the range typically observed for analogous complexes.

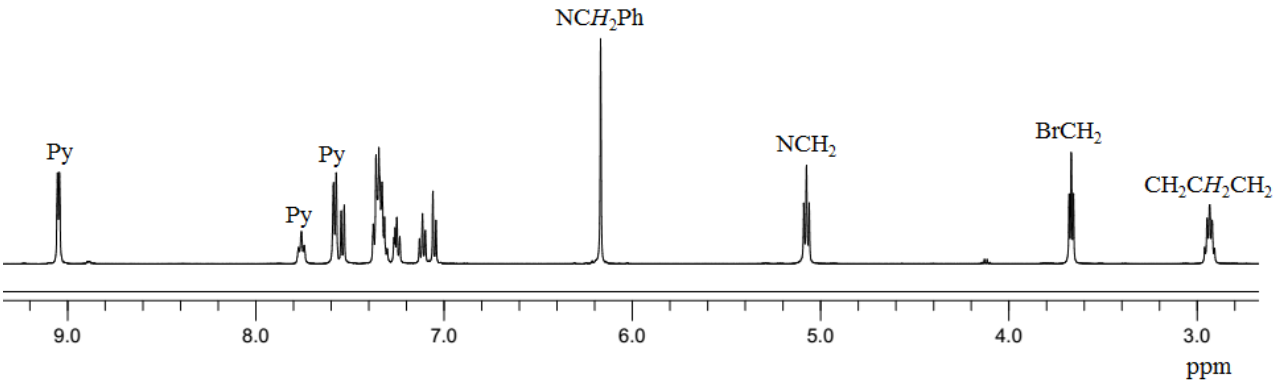

Figure 3.3. ^{1}H NMR spectrum for the *trans*-[$PdBr_2(C_3Br$-bimy)(Py)] complex **44**.

3.1.2 Synthesis of Bis(NHC)-Pd(II) Parent Complex

In order to obtain a bis(NHC) complex for postmodifications, the ratio of the Ag-carbene intermediate to [$PdBr_2(CH_3CN)_2$] was increased to 2:1 to afford the *trans*-[$PdBr_2(C_3Br$-bimy$)_2$] complex **45** as the major product (Scheme 3.4).

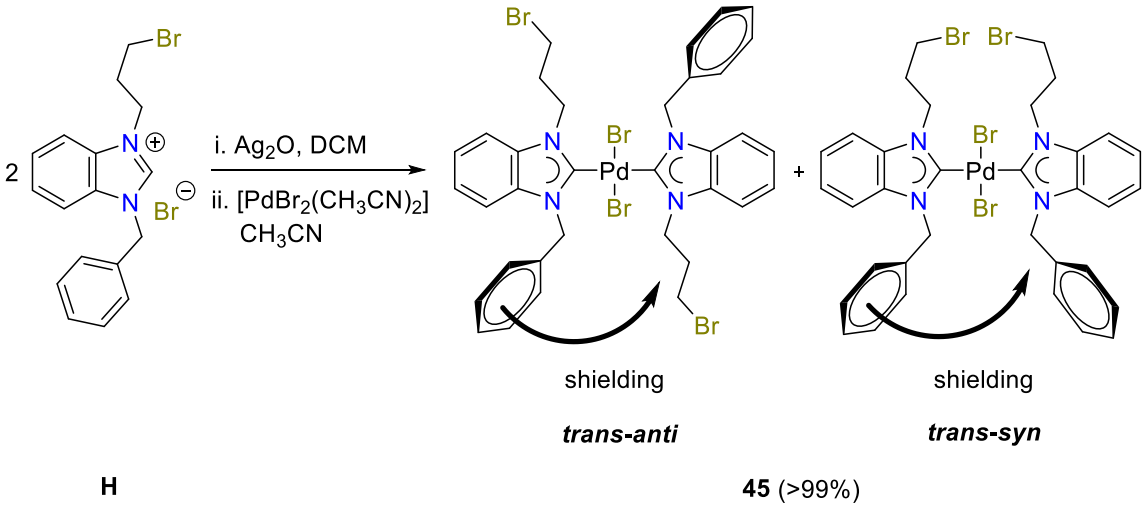

Scheme 3.4. Synthesis of bis(NHC)-Pd(II) parent complex **45**.

Notably, the sequence of addition showed a significant influence on the product yield. When the Ag species was added into the solution of $[PdBr_2(CH_3CN)_2]$ in CH_3CN, only 50% of the bis(NHC) complex **45** was isolated. The dinuclear $[PdBr_2(C_3Br\text{-}bimy)]_2$ complex **42** was isolated as the side product in 43% yield. However, the yield of **45** was quantitative when the $[PdBr_2(CH_3CN)_2]$ was added dropwise to the Ag-NHC.

Complex **45** is a pale-yellow powder with good solubilities in THF, CH_2Cl_2, DMSO, and DMF, but it is poorly soluble in ethanol and non-polar solvents, such as hexane and diethyl ether. In its ESI mass spectrum, a base peak at *m/z* 843 is observed for the $[M - Br]^+$ fragment.

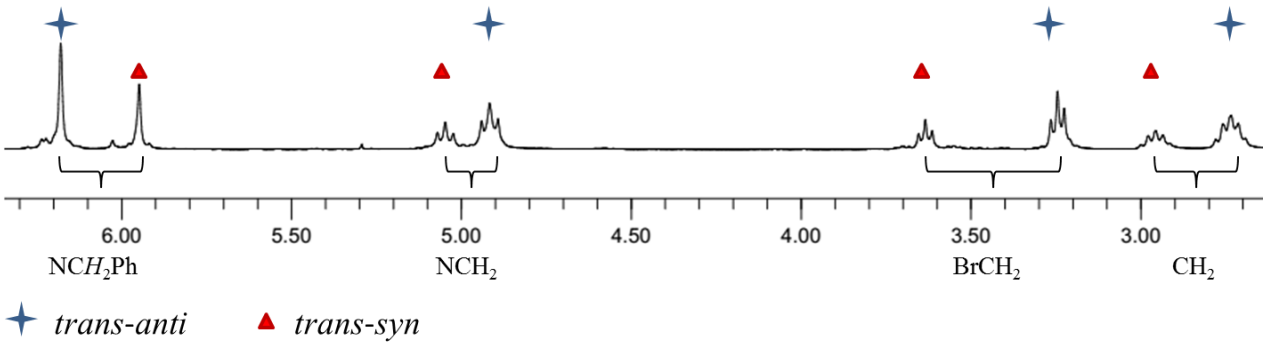

Figure 3.4. ^1H NMR spectrum for the *trans*-$[PdBr_2(C_3Br\text{-}bimy)_2]$ complex **45** in the aliphatic region.

Due to the unsymmetrical nature of the NHC ligands, two sets of signals with slightly different integrals are observed in both ^1H and ^{13}C NMR spectra.[79] Two closely spaced carbene signals are observed at 182.6/182.5 ppm. These values are indicative of *trans* configured dibromido-bis(benzimidazole-derived NHC) complexes,[59a] while more highfield values are expected for their *cis* isomer. The more intense signal at 182.6 is assigned to the *trans-anti* rotamer, while the weaker signal at 182.5 is attributed to the *trans-syn* form. This assignment is further corroborated by their ^1H NMR spectra, where two sets of well separated signals are

observed for the aliphatic protons. These can be unambiguously assigned by considering the shielding effect exerted by phenyl ring of the benzyl substituent.[80] In the *anti*-rotamer the bromopropyl arm is situated in the shielded area of the phenyl ring giving rise to more upfield signals (Figure 3.4, small signals of impurities were possible due to hydrolysis products). The benzylic CH_2 protons in the *anti*-rotamer, on the other hand, do not experience this shielding effect and appear more downfield. In the *syn* form, the situation is reversed, and the bromopropyl signals are more downfield, while the benzylic protons are more upfield. The chemical shift differences of equivalent groups in the *anti*- and *syn*-rotamers decrease in the order of $BrCH_2$ (0.39 ppm) > NCH_2Ph (0.23 ppm) > CH_2 (0.22 ppm) > NCH_2 (0.13 ppm), indicating the relative sensitivity of these functions to the shielding effect of the phenyl ring. This trend is generally observed for most of the complexes (*vide infra*). As expected, the *anti*-rotamer was generated as the major product due to steric reasons.

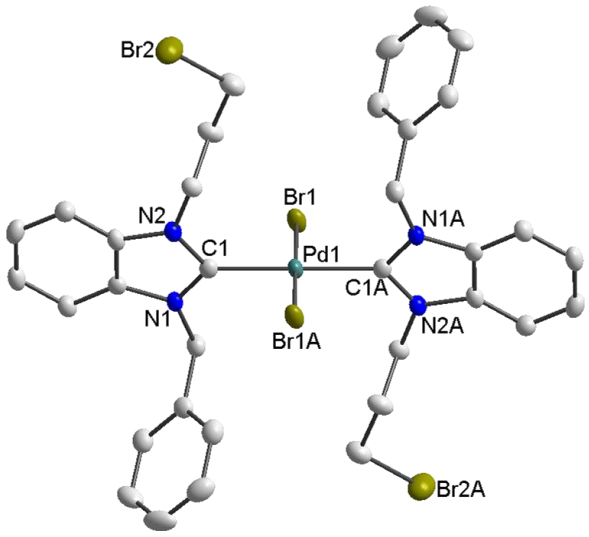

Figure 3.5. Molecular structure of **45** showing 50% probability ellipsoids; hydrogen atoms are omitted for clarity. Selected bond length [Å] and bond angles [°]: Pd1–C1 2.024(4), Pd1–Br1 2.4334(4); C1–Pd1–Br1 88.34(10), C1–Pd1–Br1A 91.66(10); PdC_2Br_2/NHC dihedral angle 75.0 °.

Single crystals of **45** were grown by slow evaporation of a saturated solution in CH_2Cl_2, and the molecular structure determined by X-ray diffraction analysis is shown in Figure 3.5. The Pd(II) center is coordinated by two *trans-anti* oriented carbene and two bromido ligands in a square-planar geometry. The two benzimidazolin-2-ylidene rings are coplanar as a result of symmetry, but twisted from the coordination plane with a dihedral angle of 75 º.

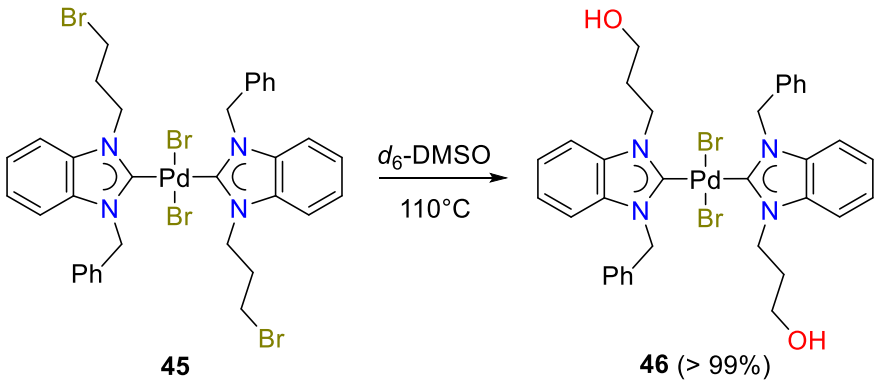

Scheme 3.5. Hydrolysis of *trans*-[$PdBr_2(C_3Br\text{-}bimy)_2$] (**45**) to *trans*-[$PdBr_2(C_3OH\text{-}bimy)_2$] (**46**).

Coalescence of *trans-anti* and *trans-syn* rotamers in a similar bis(NHC)-Pd(II) complex has been previously observed at ~107 ℃ by high temperature ^{1}H NMR spectroscopy,[80] and a similar study was conducted on complex **45** in $CDCl_3$. However, no change was observed upon raising the temperature to 50 °C. To achieve higher temperatures, d_6-DMSO was used as the solvent instead. No ratio change or coalescence was recorded up to 100 °C suggesting a higher rotational barrier about the Pd–C bond in this case. With further increase of the temperature to 110 °C, two sets of new signals close to the original ones appeared, which remained after cooling the sample back to room temperature indicating the formation of a new rotameric pair. In order to achieve full conversion, the same sample was heated at 110 °C for one day. Subsequent NMR

analysis showed that the original signals due to complex **45** were completely replaced by two new sets of signals indicating rotamers of a new species. Notably, a new triplet is observed at 4.62 ppm, which upon successful hydrogen-deuterium exchange by addition of D_2O was assigned to OH protons. Additional evidence was found in the positive mode ESI mass spectrum of the sample, where a new base peak was observed at *m/z* 719 with the correct isotopic pattern for the $[M - Br]^+$ fragment of the alcohol-functionalized complex **46** (Scheme 3.5, only the *trans-anti* rotamers are presented for clarity).

3.2 Synthesis of Functionalized-NHC Palladium Complexes

3.2.1 Synthesis of Mono(functionalized NHC)-Pd(II) Complexes

Postmodifications by nucleophilic substitution were first conducted on the mono(NHC)-Pd(II) parent complex **44**. The treatment with KOAc or NaN_3 exclusively yielded the respective ester- and azido-functionalized NHC complexes *trans*-[$PdBr_2$(C_3OAc-bimy)(Py)] (**47**) and *trans*-[$PdBr_2$(C_3N_3-bimy)(Py)] (**48**) in high yields without affecting the bromido ligands (Scheme 3.6). Notably, possible olefinic byproducts due to base-catalyzed HBr elimination of the bromopropyl side arm were not observed. Complex **47** can also be obtained by bridge-cleavage reaction of dimer [$PdBr_2$(C_3OAc-bimy)]$_2$ (**41**) with pyridine.

Reaction with NaI on the other hand is expected to affect both bromo-substituents as well as the bromido ligands. In order to avoid halide scrambling in this reaction, 10 equiv of NaI was added to **44**, which cleanly afforded the *trans*-[PdI_2(C_3I-bimy)(Py)] (**49**) complex bearing an iodo-functionalized NHC. The combination of a better iodo leaving group at the sidearm with stronger coordinating iodido ligands makes **49** an even better precursor for (here 2nd generation) postmodifications. Thus, its S_N2 reactions with the nucleophiles NaN_3, KSCN and KSAc yielded

three new derivative complexes *trans*-[PdI_2(C_3X-bimy)(Py)] (X = N_3, (**50**), SCN (**51**), SAc (**52**)). Notably, complexes **51** and **52** are not obtainable via palladation of the respective pre-functionalized azolium salts.[81] This fact highlights the importance of the current postmodification protocol, which not only complements the traditional methodology, but also provides functionalized NHC compounds that are otherwise not accessible.

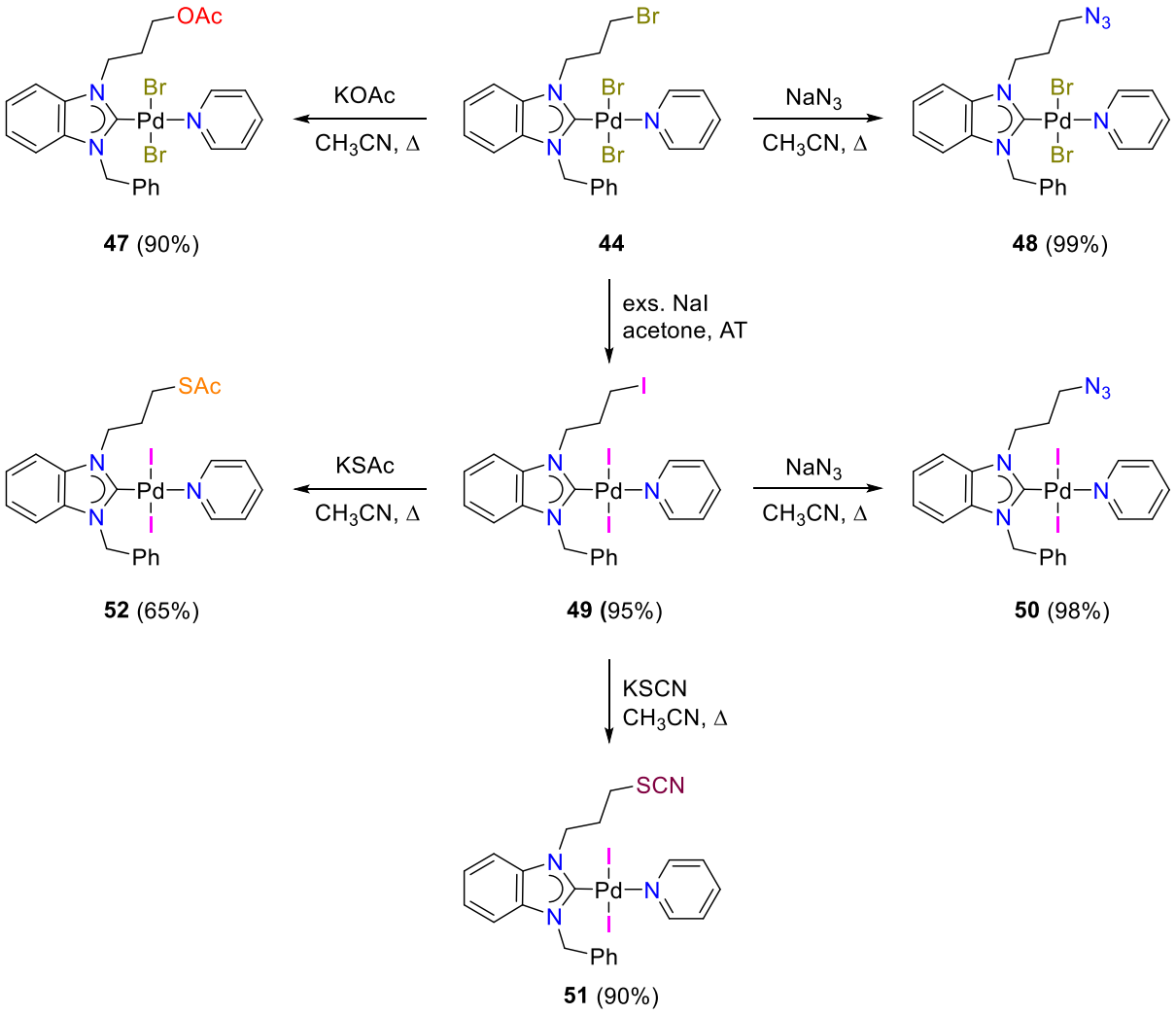

Scheme 3.6. Postmodifications of mono(NHC)-Pd(II) complex **44**.

Complexes **48**–**51** are yellow to orange powders, while complexes **47** and **52** are brownish solids. All these complexes remain well soluble in common polar organic solvents.

Apart from the spectroscopic signatures of the functional group itself, such postmodifications can be best traced by monitoring the ^{1}H NMR signal of the α-methylene group with respect to the reactive site. Other resonances of the ligands remain largely unaffected by the postmodifications.

Table 3.1. α-CH_2, $C_{carbene}$ NMR resonances of complexes **41**–**44**, **47**–**52**. [a]

complex	X	δ (^{1}H)	δ ($^{13}C_{carbene}$)
41	OAc	4.26	160.6
42[b]	Br	3.76	/[d]
43[c]	Br	3.65	161.8
44	Br	3.67	164.6
47	OAc	4.31	164.3
48	N_3	3.60	164.4
49	I	3.43	163.3
50	N_3	3.60	163.0
51	SCN	3.28	163.9
52	SAc	3.14	162.9

[a]Measured in $CDCl_3$. [b]Measured in d_6-DMSO. [c]Measured in CD_3CN. [d]$C_{carbene}$ signal could not be resolved.

Table 3.1 summarizes and compares the α-CH_2 ^{1}H NMR resonances for complexes **41**–**44** and **47**–**52**. Comparing those of the dimers **41** and **42** reveals that the ester group in **41** is more deshielding than the bromo substituent in **42**, which reflects their inductive effects. The same trend can be observed for their respective mononuclear pyridine adducts **44** and **47**. The reduced –*I* effect of the azido group in **48** and **50**, on the other hand, leads to an upfield shift. The identical α-CH_2 chemical shift for complexes **48** and **50** also reveals that substitution of bromido versus iodido ligands has no significant effect on the postmodifications. Overall, the negative inductive effects of the functional groups investigated here can be ranked in the order SAc < SCN < I < N_3 < Br < OAc based on the comparison of the α-CH_2 ^{1}H NMR signals of their respective complexes. The ^{13}C NMR signals for the carbene carbon atoms of the pyridine complexes **44**,

47–**52** are found in the narrow range of 162.9–164.6 ppm. Generally, the *trans*-[PdI_2(C_3X-bimy)(Py)] complexes have higher field $^{13}C_{carbene}$ resonances than the *trans*-[$PdBr_2$(C_3X-bimy)(Py)] analogous. Apparently, the carbene carbon atoms in the former are more shielded by the more electron rich iodido ligands, and hence, more upfield $^{13}C_{carbene}$ resonances are found. Those of the dimeric complexes **41** and **43** are shifted upfield indicating more Lewis acidic metal centers.

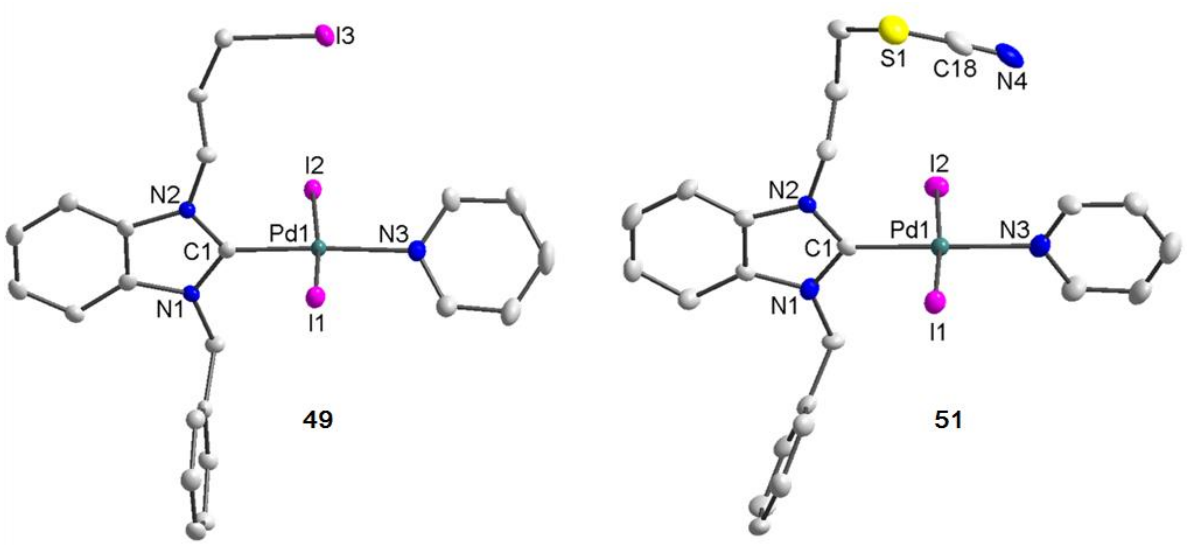

Figure 3.6. Molecular structures of **49** and **51** showing 50% probability ellipsoids; solvent molecules and hydrogen atoms are omitted for clarity. Selected bond length [Å] and bond angles [°]: **49**, Pd1-C1 1.960(3), Pd1-I1 2.6112(4), Pd1-N3 2.102(3), Pd1-I2 2.6115(4); C1-Pd1-I1 88.18(9), I1-Pd1-N3 92.71(8), N3-Pd1-I2 91.63(8), C1-Pd1-I2 87.78(9); $PdCNI_2$/NHC dihedral angle 81.8 °. **51**, Pd1-C1 1.959(6), Pd1-I1 2.6061(13), Pd1-N3 2.100(5), Pd1-I2 2.6049(13); C1-Pd1-I1 89.24(18), I1-Pd1-N3 90.63(16), N3-Pd1-I2 93.08(16), C1-Pd1-I2 87.03(18); $PdCNI_2$/NHC dihedral angle 81.5 °.

The solid state molecular structures of complexes **49** and **51** have also been determined by single crystal X-ray diffraction and are depicted in Figure 3.6. Apart from the different functional groups, the mononuclear complexes have a very similar structure. Both contain a square planar Pd(II) center that is coordinated by one functionalized benzimidazolin-2-ylidene, two *trans*-

iodido and one pyridine ligand. As expected the carbene planes are oriented almost perpendicularly to the coordination planes by angles of ~82 °.

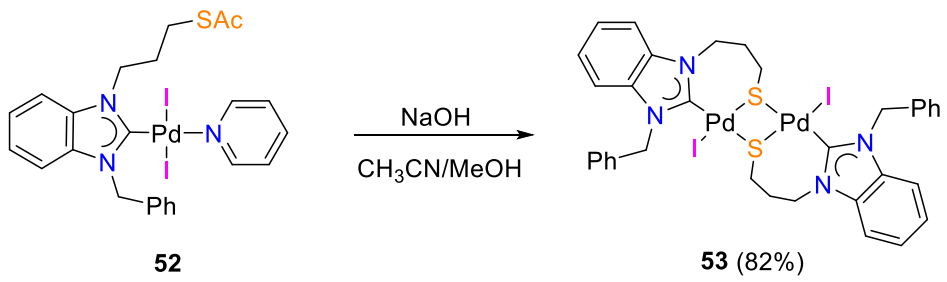

Scheme 3.7. Synthesis of propyl-thiolato-bridged complex **53**.

It is conceivable that the functional groups in complexes **50**–**52** could be subjected to a 3rd generation postfunctionalization. To demonstrate such feasibility, complex **52** was chosen for a NaOH base-assisted hydrolysis reaction, which led to the formation of the anticipated thiolato-donor functionalized NHC complex dimer **53** in a good yield (Scheme 3.7). This complex is an orange solid, which is well soluble in chlorinated solvents such as $CHCl_3$, CH_2Cl_2, but slightly soluble in DMSO. Its formation is supported by ESI-MS, which shows a base peak at *m*/*z* 903 for the $[M - I]^+$ fragment. In the ^{1}H NMR spectrum, the benzylic protons become diasterotopic upon dimerization and resonate as two doublets centered at 6.37 and 5.32 ppm, respectively, with a coupling constant of ^2J(H,H) = 15.8 Hz. All six methylene protons of each propyl-thiolato-bridge are also diasterotopic, giving rise to multiplets ranging from 6.25–1.72 ppm. In comparison to the aformentioned functionalized complexes, the electron rich thiolato donors in this complexes lead to a more downfield shift of the $^{13}C_{carbene}$ resoance at 174.8 ppm.[43]

Single crystals of **53** were grown by slow evaporation in $CHCl_3$/hexane, and the molecular structure determined by X-ray diffraction analysis is shown in Figure 3.7. Complex **53**

is a dimeric species, in which the two Pd(II) centres are coordinated and bridged by two μ-thiolato-functionalized NHCs in a chelating fashion. The square-planar coordination sphere at each Pd(II) is completed by one terminal iodido ligand. Both dihedral angles between these [$PdCS_2I$] coordination planes and the carbene ring planes amount to ~63 °, which deviate substantially from the favored perpendicular orientation (90 °) due to the chelating binding mode of the S-functionalized carbene ligand. The [Pd_2S_2] core of **53** is significantly bent with a hinge angle of ~128 °, which is slightly larger than the reported value of ~119 ° for a similar complex bearing a shorter ethyl-thiolato-chelate.[43]

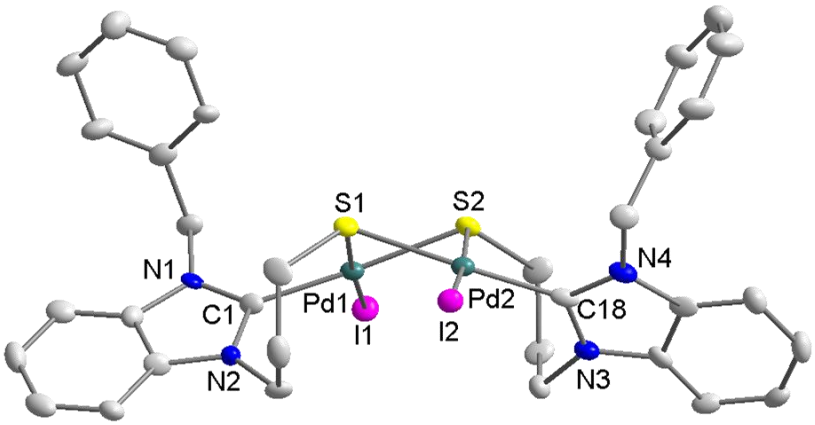

Figure 3.7. Molecular structures of **53** showing 50% probability ellipsoids; solvent molecules and hydrogen atoms are omitted for clarity. Selected bond length [Å] and bond angles [°]: Pd1-C1 2.000(8), Pd1-I1 2.6345(11), Pd1-S2 2.357(2), Pd1-S1 2.311(2), Pd2-C18 1.998(9), Pd2-I2 2.6471(12), Pd2-S2 2.311(2), Pd1-S1 2.354(2); C1-Pd1-I1 92.4(2), I1-Pd1-S2 98.16(6), S2-Pd1-S1 77.93(8), C1-Pd1-S1 91.6(2), C18-Pd2-I2 92.9(2), I2-Pd2-S1 98.02(6), S1-Pd2-S2 77.98(8), C18-Pd2-S2 91.2(2); $PdCS_2I$/NHC dihedral angle 63.2 °.

The oxidation of the thiolato-bridges of complex **53** may lead to the formation of a dinuclear or mononuclear complex bearing sulfur donors of higher oxidation states, such as sulfinate, sulfenate, or sulfonate. Oxidation of the thiolato group of a Ni(II) complex to the sulfinate ligand by aerial oxygen or H_2O_2 has been reported.[82] A previous study by Huynh's group also showed that the thioether function of a dibenzimidazolium salt was easily oxidized to

a sulfoxide group by 3 equiv of H_2O_2 in acetic acid at ambient temperature.[83] Complex **53** was therefore treated with the same reagents, and DMF was added to ensure a homogeneous reaction. However, the compound remained intact below 70 °C and started to decompose to palladium black at higher temperatures. The fact that **53** is resistant to oxidation by H_2O_2 may be ascribed to the lower electron density at the sulfur atoms in the bridging mode, which calls for a stronger oxidant.

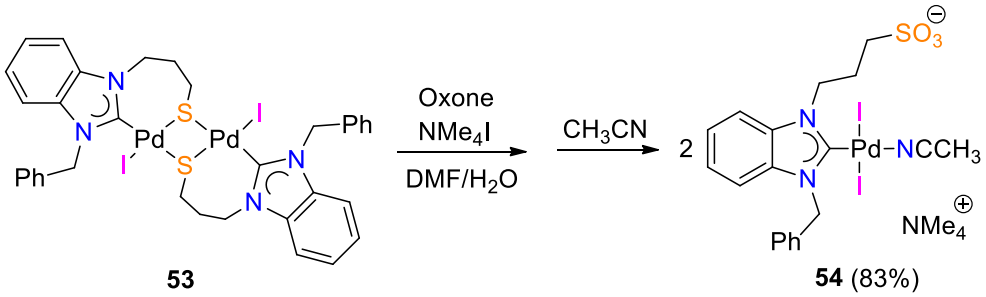

Scheme 3.8. Synthesis of propyl-sulfonate complex **54**.

Indeed, thiolato to sulfonate oxidation occurs with complex **53** when Oxone ($KHSO_5$) is used, which is a cheap and strong oxidant. The reaction proceeds smoothly at ambient temperature with 3 equiv of Oxone in a DMF/H_2O mixture with excess of NMe_4I, which provides additional iodido ligands as well as a suitable counter cation (Scheme 3.8). Other alkali or ammonium salts proved less suitable for the isolation and crystallization of the product. With 2 equiv of Oxone a lower yield of the sulfonate species was obtained, and no sulfinate or sulfenate intermediates could be detected. In contrast, Oxone was reported to be a chemoselective reagent for the oxidation of organic sulfides to sulfoxides and further to sulfones.[84]

Presumably, a dinuclear complex was obtained after oxidation, which was subsequently cleaved by CH_3CN, resulting in the formation of the mononuclear complex *trans*-$(NMe_4)[PdI_2(C_3SO_3\text{-bimy})(CH_3CN)]$ (**54**). Complex **54** is a red solid, which is moderately

soluble in DMF, CH_3CN, and DMSO, and slightly soluble in H_2O. Its negative ion ESI mass spectrum shows a predominant signal at *m*/*z* 689 attributed to the $[M - NMe_4 - CH_3CN]^-$ fragment (Figure 3.8).

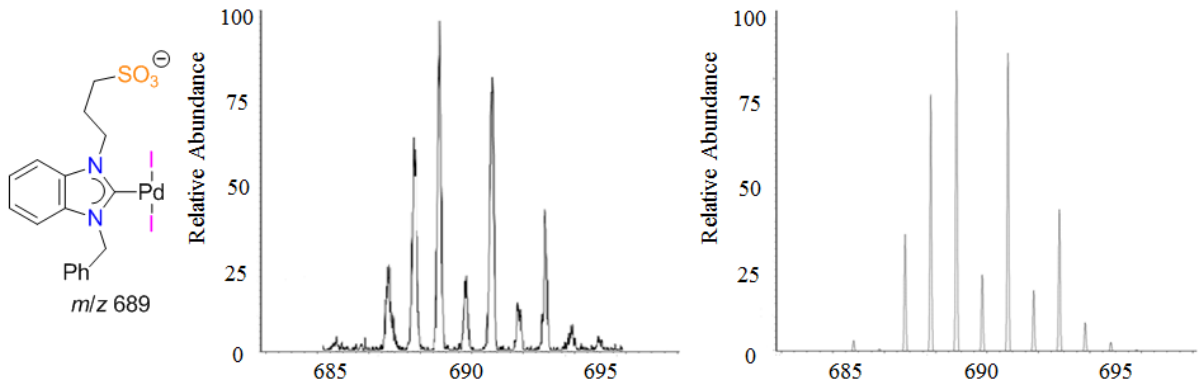

Figure 3.8. Isotopic pattern of the $[M - NMe_4 - CH_3CN]^-$ fragment of complex **54** in the negative ESI mass spectrum (left) and a simulated pattern (right).

The ^1H NMR spectrum of complex **54** recorded in CD_3CN shows a similar pattern to that of the CH_3CN adduct complex *trans*-[$PdBr_2$(C_3Br-bimy)(CH_3CN)] (**43**). All the methylene signals do not show the diastereotopic patterns of **53**, implying a pendant sulfonate moiety. A singlet at 3.10 ppm attributed to NMe_4^+ supports the successful incorporation of the ammonium cation. Moreover, a triplet was observed for the cation at 56.2 ppm in the ^{13}C NMR spectrum due to the coupling with the NMR-active ^{14}N nucleus. The carbene carbon atom resonates at 159.9 ppm, which is shifted upfield in comparison to that of the dimeric thiolato complex **53**.

This new template-assisted methodology was expanded to make sulfonate NHC complexes with different linkers. Of particular interest is the synthesis of a complex with a xylenyl linker, which is not obtainable via the conventional route (*vide supra*). Since only the corresponding dimeric thiolato complex was targeted, the compound was prepared using the

traditional route in analogy to the literature procedure. Ligand precursor **J** was prepared from the reaction of KSAc with the bromo-*o*-xylenyl-substituted benzimidazolium salt **I**, which was in turn synthesized by reacting 1-benzylbenzimidazole with *o*-xylene dibromide. Subsequent reaction of **J** with $Pd(OAc)_2$ smoothly gave rise to complex **55** in a yield of 76% (Scheme 3.9).

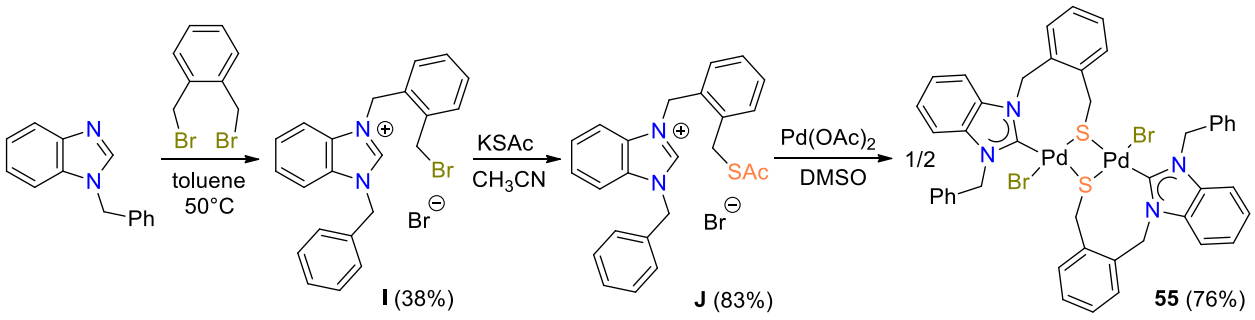

Scheme 3.9. Synthesis of xylenyl-thiolato-bridged complex **55**.

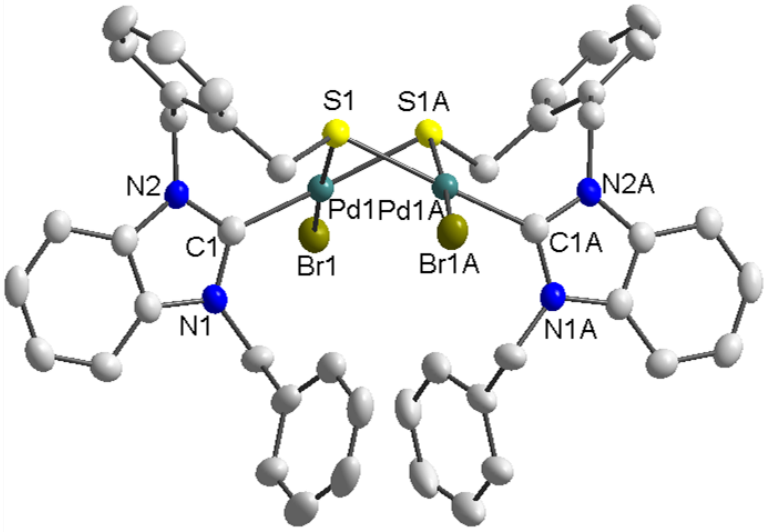

Figure 3.9. Molecular structure of **55** showing 50% probability ellipsoids; solvent molecules and hydrogen atoms are omitted for clarity. Selected bond lengths [Å] and bond angles [deg]: Pd1−C1 2.002(8), Pd1−Br1 2.4641(12), Pd1−S1A 2.363(2), Pd1−S1 2.300(2); C1−Pd1−Br1 94.79(6), C1−Pd1−S1 92.2(2), Br1−Pd1−S1A 96.79(6), S1A−Pd1-S1 76.47(9), C1−Pd1−S1A 168.3(2), Br1−Pd1−S1 172.41(6).

Similar to **53**, complex **55** shows poor solubility in DMSO and precipitated from the reaction mixture. It was isolated as a yellow powder after simple filtration and washing with H_2O. The solid is slightly soluble in $CHCl_3$, CH_2Cl_2, and DMF. The formation is corroborated by positive ESI-MS, where a predominant signal at *m*/*z* 979 is observed for the $[M - Br]^+$ fragment. The aliphatic protons again become diastereotopic upon complex formation. Due to insufficient solubility, its ^{13}C NMR spectrum could not be obtained. The identity of complex **55** was further confirmed by X-ray diffraction of a single crystal obtained via slow evaporation of a saturated $CHCl_3$/toluene solution. As depicted in Figure 3.9, the solid state structure is similar to that of complex **53** with a butterfly shape.

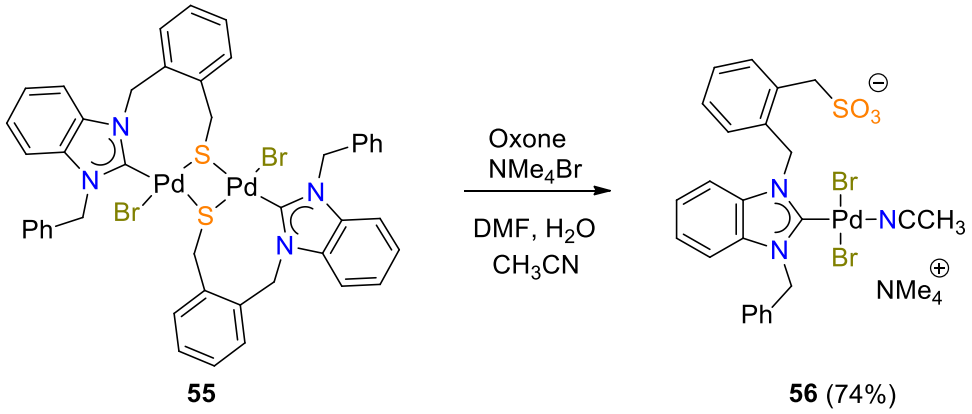

Scheme 3.10. Synthesis of xylenyl-sulfonate complex **56**.

Subsequent oxidation of complex **55** using the same condition established for **54**, straightforwardly afforded complex **56** with a xylenyl-sulfonate function (Scheme 3.10). Similarly, a distinct base peak at *m*/*z* 659 was recorded in its negative ESI mass spectrum owning to the $[M - NMe_4 - CH_3CN]^-$ fragment. In the ^1H NMR spectrum, three singlets are found at 6.41, 6.13, and 4.17 ppm due to the SCH_2 protons and the two NCH_2 protons. The NMe_4 signal is

not much affected by the different complex anions, and remains at ~3.1 ppm. In its ^{13}C NMR spectrum, the chemical shift of the carbene carbon atom is found at 162.6 ppm, which is more downfield than that of propyl sulfonate complex **54** (159.9 ppm).

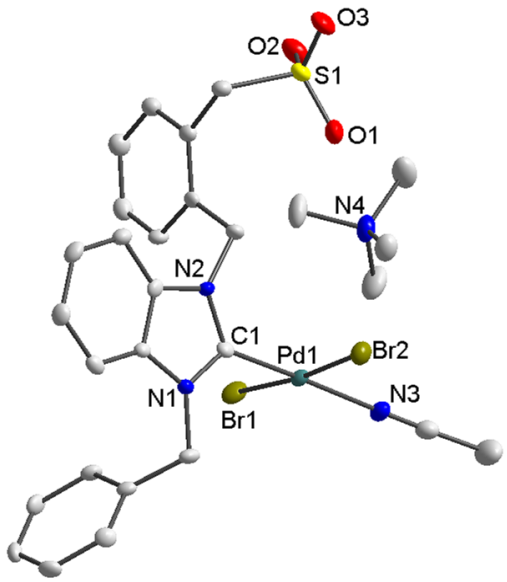

Figure 3.10. Molecular structure of **56** showing 50% probability ellipsoids; hydrogen atoms are omitted for clarity. Selected bond lengths [Å] and bond angles [deg]: Pd1−C1 1.949(5), Pd1−Br1 2.4280(10), Pd1−N3 2.077(5), Pd1−Br2 2.4409(10); C1−Pd1−Br1 88.23(15), C1−Pd1−Br2 88.03(15), Br1−Pd1−N3 93.45(15), Br2−Pd1−N3 90.44(15), C1−Pd1−N3 177.28(2), Br1−Pd1−Br2 174.52(2); PdCNBr2/NHC dihedral angle 85.7(8) °.

Single crystals of complex **56** were obtained by diffusion of diethyl ether to a CH_3CN solution. Figure 3.10 shows the expected molecular structure. Notably, the phenyl ring of the linker is almost perpendicular to the carbene ring with a dihedral angle of 89°.

3.2.2 Synthesis and Catalytic Activities of Bis(functionalized NHC)-Pd(II) Complexes

First generation postfunctionalizations of the bis(NHC) parent complex **45** were conducted with various nucleophiles (Scheme 3.11). In general, the exposure of the complex to

nucleophiles can lead to two types of reactions, i.e. (i) nucleophilic substitution at C-Br, and (ii) ligand displacement at the Pd(II) center. Since Pd–NHC bonds are strong, displacements of the bromido ligands are more likely in the latter case.

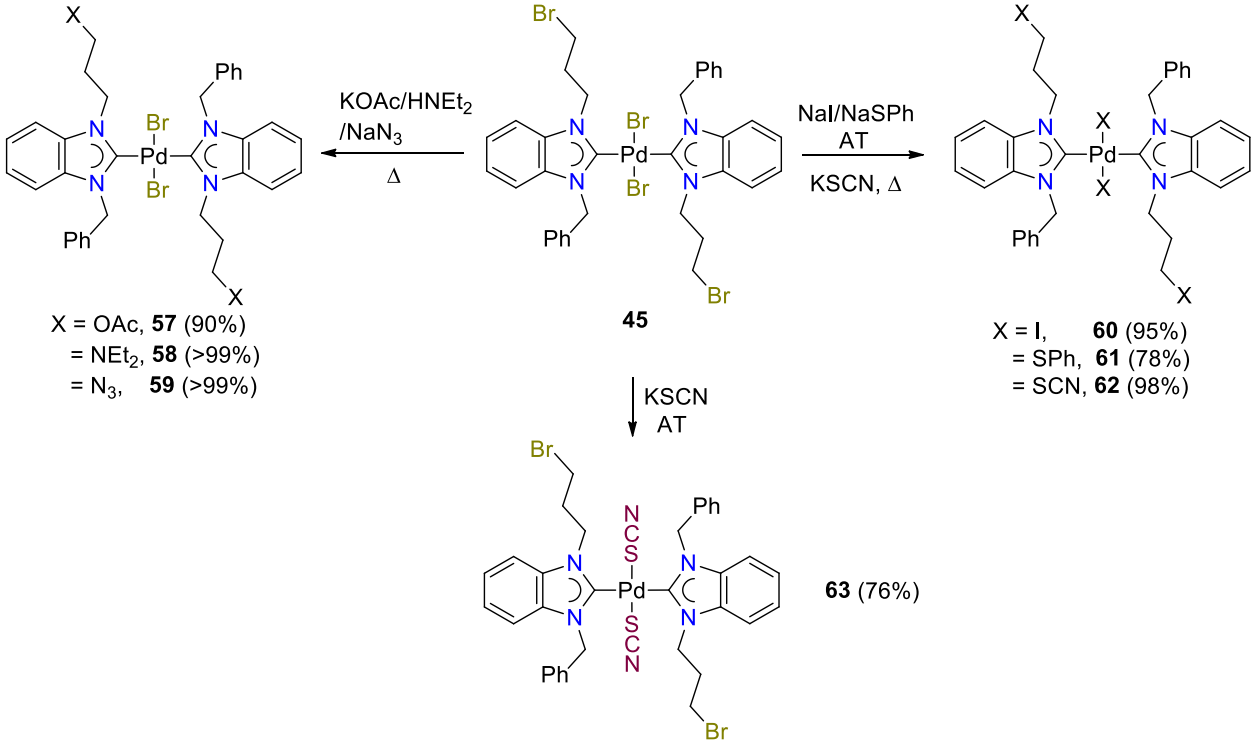

Scheme 3.11. First generation postmodifications of bis(NHC)-Pd(II) complex **45**.

The reactions with an excess (10 equiv) of KOAc, $HNEt_2$ or NaN_3 exclusively yielded complexes *trans*-[$PdBr_2(C_3X$-bimy$)_2$] (X = OAc, (**57**), NEt_2, (**58**), N_3, (**59**)) in almost quantitative yields showing selectivity for the nucleophilic substitution at the bromopropyl tethers. On the other hand, complexes of the type *trans*-[$PdX_2(C_3X$-bimy$)_2$] (X = I, (**60**), SPh, (**61**), SCN, (**62**)) were formed when excess KI, NaSPh and KSCN were used. This reactivity difference is ascribed to the soft nature of the palladium Lewis acid, which prefers binding of the softer iodide and sulphur containing ligands over bromido coordination. Reducing the amount of the nucleophiles to 2.2 equivalents with respect to parent complex **45** gave complicated mixtures of unreacted **45**,

partially exchanged complexes and fully substituted complexes. Among the three complexes **60**–**62**, only *trans*-[$Pd(SCN)_2(C_3SCN\text{-}bimy)_2$] was obtained by heating. The reaction at ambient temperature gave selectively complex [$Pd(SCN)_2(C_3Br\text{-}bimy)_2$] (**63**), where only ligand displacement took place.

Table 3.2. α-CH_2, $C_{carbene}$ NMR resonances and ESI mass signals of complexes **45**, [a] **46**, [b] **57**–**63**[a].

complex	X	coligand	δ (^{1}H)	δ ($^{13}C_{carbene}$)	main signals in ESI MS
45	Br	Br	3.63, 3.25	182.57, 182.49	843 $[M - Br]^+$
46	OH	Br	3.64, 3.34	181.17, 181.10	719 $[M - Br]^+$
57	OAc	Br	4.31, 3.99	182.58, 182.54	803 $[M - Br]^+$
58	NEt_2	Br	2.69, 2.39	182.53, 182.49	909 $[M]^+$
59	N_3	Br	3.60, 3.23	182.62, 182.58	769 $[M - Br]^+$
60	I	I	3.38, 3.03	181.84, 181.75	985 $[M - I]^+$
61	SPh	SPh	3.25, 3.02	191.07, 191.02	931 $[M - SPh]^+$
62	SCN	SCN	3.19, 2.79	180.82, 180.73	878 $[M + H + CH_3CN]^+$
63	Br	SCN	3.66, 3.35	181.02 (2 ×)[c]	822 $[M - SCN]^+$

[a] Measured in $CDCl_3$. [b] Measured in d_6-DMSO. [c] The carbene signals for the *trans-anti* and *trans-syn* rotamers are coincident.

Complexes **57**–**63** share similar NMR spectra with their parent complex **45** and the alcohol-functionalized counterpart **46**. Two sets of signals are generally observed for the *trans-anti* and *trans-syn* rotamers. Table 3.2 summarizes their α-CH_2 ^{1}H and $^{13}C_{carbene}$ NMR data. In accord with results obtained for the monocarbene series, an increase of the negative inductive (–*I*) effect in the order of SCN < SPh < I < N_3 < Br < OH < OAc was concluded on grounds of a gradual downfield shift of the α-CH_2 ^{1}H NMR signals. Complexes **45** and **57**–**59** have very similar $^{13}C_{carbene}$ resonances at ~182.5 ppm in $CDCl_3$ due to a similar coordination sphere, which is not affected by different functionalities five bonds away. The bigger difference in complex **46** (181.1 ppm) is a result of solvent effects arising from the d_6-DMSO solvent used. On the other

hand, displacement of the bromido ligands from the Pd(II) center leads to significant changes of the $^{13}C_{carbene}$ resonances compared to those observed for **45** as evidenced by values ranging from 180.7–191.0 ppm for complexes **60**–**63**, respectively. Complexes **62** and **63** have very close $^{13}C_{carbene}$ signals as they solely differ in the terminal functionality of the propyl arm.

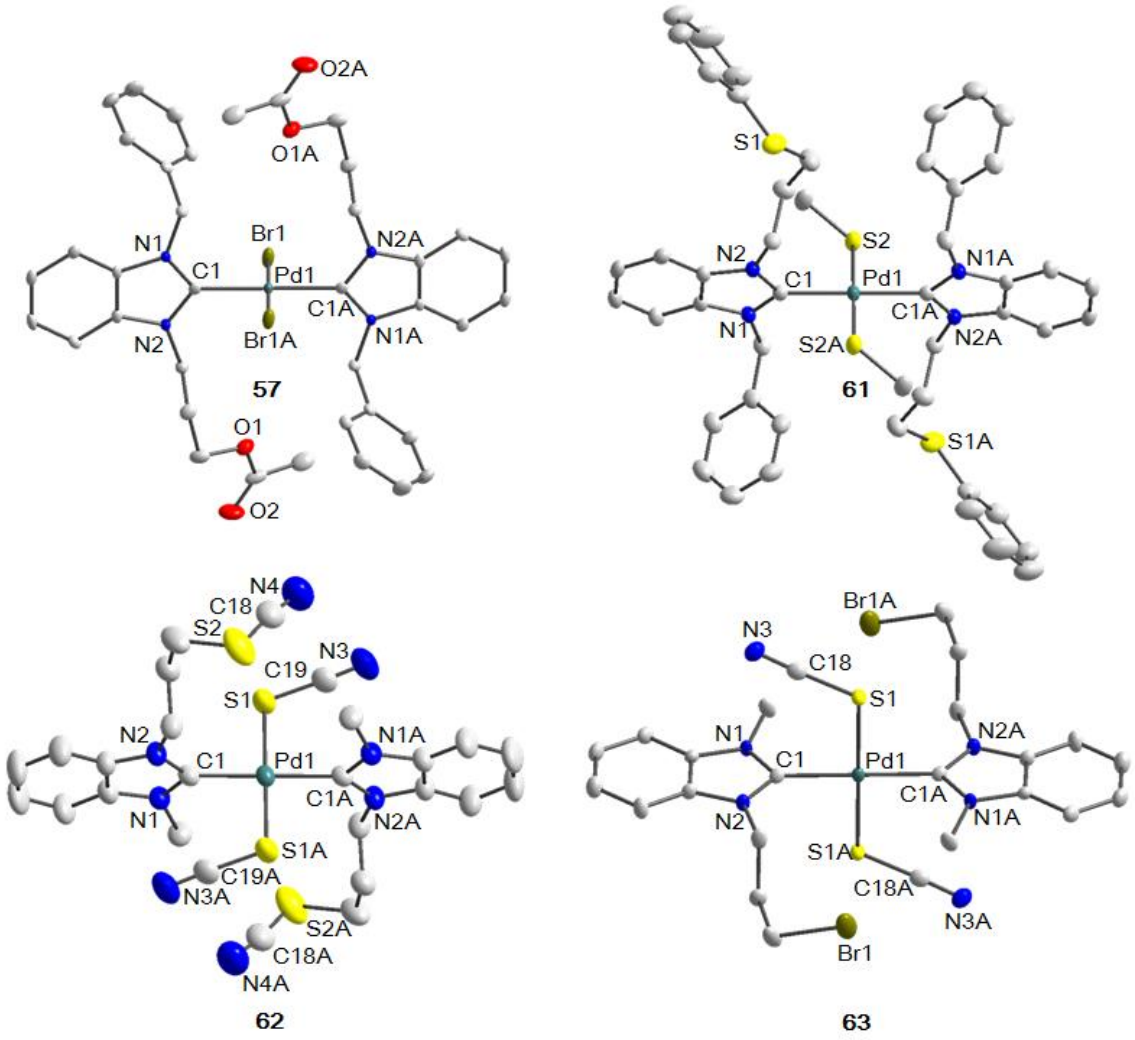

Figure 3.11. Molecular structures of **57**, **61**, **62** and **63** showing 50% probability ellipsoids; for the sake of clarity, solvent molecules, hydrogen atoms, phenyl rings of the coligands in **61** or the N-benzyl substituents in **62** and **63** are omitted. Selected bond length [Å] and bond angles [°]: **57**, Pd1–C1 2.020(3), Pd1–Br1 2.4359(3); C1–Pd1–Br1 92.49(8), C1–Pd1–Br1A 87.51(8); PdC_2Br_2/NHC dihedral angle 79.6°. **61**, Pd1–C1 2.027(2), Pd1–S2 2.3541(6); C1–Pd1–S2 87.15(7), C1–Pd1–S2A 92.85(7); PdC_2S_2/NHC dihedral angle 72.7°. **62**, Pd1–C1 2.016(4), Pd1–S1 2.3229(11); C1–Pd1–S1 87.27(11), C1–Pd1–S1A 92.73(11); PdC_2S_2/NHC dihedral angle 89.3°. **63**, Pd1–C1 2.024(4), Pd1–S1 2.3399(12); C1–Pd1–S1 92.46(13), C1–Pd1–S1A 87.54(13); PdC_2S_2/NHC dihedral angle 86.3°.

Formation of theses complexes is also supported by ESI-MS. Base peaks of $[M - Br]^+$ fragments for complexes **57** and **59** or the molecular ion $[M]^+$ for **58** are observed, while those for complexes **60** and **61** are assigned to $[M - X]^+$ fragments. Complexes **62** and **63** show weak palladium-containing isotopic pattern for $[M + H + CH_3CN]^+$ or $[M - SCN]^+$ fragments.

Single crystals of complexes **57** and **61**–**63** were obtained by slow evaporation of their saturated solutions in CH_2Cl_2/CH_3CN (**57**) or CH_2Cl_2 (**61**–**63**). Their molecular structures are depicted in Figure 3.11. All the five complexes crystallized as *trans-anti* rotamers with the palladium centers coordinated by two functionalized carbenes and two anionic coligands in square planar fashions. The Pd–$C_{carbene}$ bond distances fall in a narrow range from 2.020(3)–2.0353(15) Å.

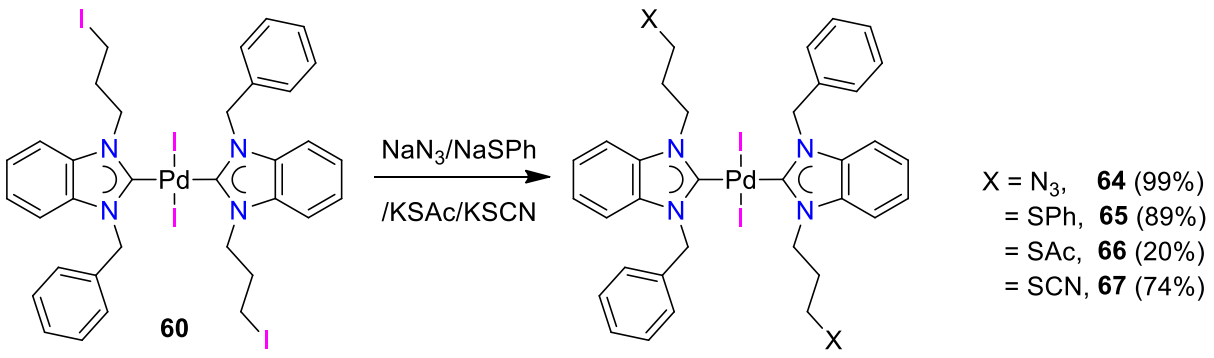

Scheme 3.12. Second generation postmodifications of bis(NHC)-Pd(II) complex **60**.

Second generation postmodifications of *trans*-$[PdI_2(C_3I\text{-bimy})_2]$ **(60)** were subsequently conducted. The softer iodido ligands in this complex are expected to form stronger Pd–I bonds in order to prevent the further ligand exchange reactions and therefore direct selectivity to substitutions at the iodo-propyl tether. Indeed complexes of the type *trans*-$[PdI_2(C_3X\text{-bimy})_2]$ (X = N_3, (**64**), SPh, (**65**), SAc, (**66**), SCN, (**67**)) were afforded in reactions with the respective

nucleophiles (Scheme 3.12). The low yield of complex **66** is attributed to hydrolysis of the thioester function by the wet solvent, but attempts to isolate defined hydrolysis products were to no avail.

All four complexes showed base peaks for the respective $[M - I]^+$ fragments in their ESI mass spectra indicating the successful reactions. Similar to all the other functionalized complexes, their formations are further discerned by their α-CH_2 ^{1}H NMR resonances in accord with the inductive effects of the newly introduced function, which are listed in Table 3.3. As expected, the $^{13}C_{carbene}$ resonances at ~181.7 ppm show little variations.

Table 3.3. α-CH_2, $C_{carbene}$ NMR resonances and ESI mass signals of complexes **60**, **64**–**67**[a]

Complex	X	δ (^{1}H)	δ ($^{13}C_{carbene}$)	Main signals in ESI Mass
60	I	3.38, 3.03	181.84, 181.75	985 $[M - I]^+$
64	N_3	3.59, 3.28	181.85, 181.82	815 $[M - I]^+$
65	SPh	3.12, 2.85	181.71, 181.66	951 $[M - I]^+$
66	SAc	3.12, 2.81	181.69, 181.61	881 $[M - I]^+$
67	SCN	3.19, 2.77	181.65, 181.53	847 $[M - I]^+$

[a]Measured in $CDCl_3$.

The solid state structure of *trans*-$[PdI_2(C_3SCN\text{-}bimy)_2]$ (**67**) was obtained by an X-ray diffraction study on single crystals obtained by slow evaporation of a saturated solution in $CHCl_3$/hexane. The structure depicted in Figure 3.12 confirms the successful and selective substitution of the iodopropyl arm. The Pd(II) center is coordinated by two iodido ligands and two SCN-functionalized-NHC ligands in the *trans-anti* configuration.

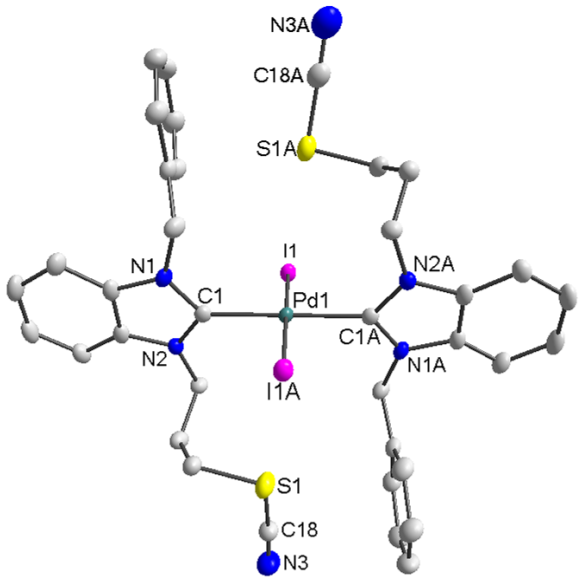

Figure 3.12. Molecular structure of **67** showing 50% probability ellipsoids; hydrogen atoms are omitted for clarity. Selected bond length [Å] and bond angles [°]: Pd1–C1 2.038(3), Pd1–I1 2.6043(3); C1–Pd1–I1 88.00(8), C1–Pd1–I1A 92.00(8); PdC_2I_2/NHC dihedral angle 76.8°.

Second generation postmodification was also conducted on the amino-functionalized-NHC complex *trans*-[$PdBr_2$(C_3NEt_2-bimy)$_2$] (**58**) by ethylating the two tertiary amino functions to afford the ammonium-functionalized complex *trans*-[$PdBr_2$(C_3NEt_3-bimy)$_2$]Br_2 (**68**) (Scheme 3.13). After the reaction mixture was heated overnight, complex **68** was collected as the precipitate. Minor amounts of undesired mono-alkylated side product can be washed off with CH_3CN.

The solubility of complex **68** decreases going from MeOH to CH_3CN and chlorinated solvents. It is insoluble in hexane, diethyl ether and water. Evidence of its formation can be found in its ESI spectrum, which shows a base peak at *m/z* 1047 attributed to the $[M - Br]^+$ fragment and a weaker signal at *m/z* 483 for the $[M - 2Br]^{2+}$ dication. Two sets of signals due to the *trans-anti* and *trans-syn* rotamers are still observed in its NMR spectra, while the *anti*:*syn* rotameric ratio increases from to 1.9 for the parent **58** to 4.5 in complex **68**. The increased preference for

the *anti* rotamer can be rationalized by the intramolecular electrostatic repulsion between the two positive charged ammonium groups only present in the *syn*-rotamer.

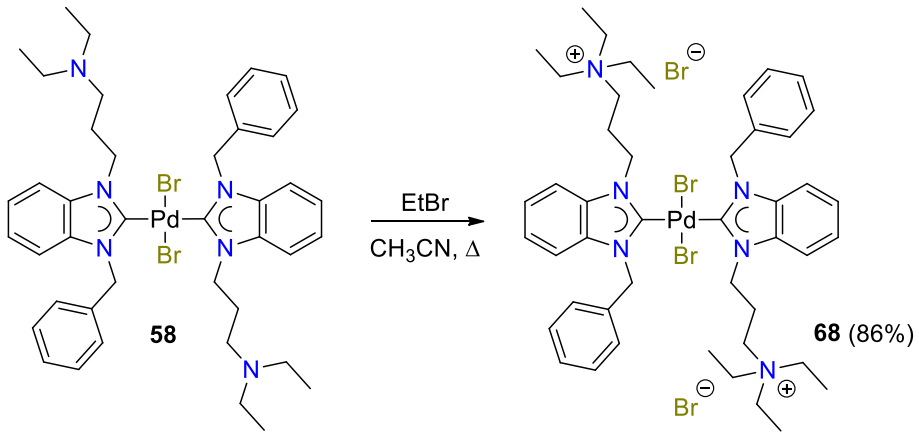

Scheme 3.13. Synthesis of propyl ammonium complex **68**.

Mizoroki-Heck Catalysis study. The addition of excess tetraalkylammonium salts to stabilize palladium catalysts in C-C coupling reactions to enhance reaction rates is known as Jeffery conditions.[17,85,86,87] Complex *trans*-[$PdBr_2(C_3NEt_3$-bimy$)_2]Br_2$ (**68**) can be regarded as a potential Pd-catalyst that is already decorated with two tetraalkylammonium moieties and two bromide counter anions. Therefore, the catalytic activity of complex **68** was evaluated and compared to that of its analogues *trans*-[$PdBr_2(C_3X$-bimy$)_2$] (X = Br, (**45**), OAc, (**57**), NEt_2, (**58**)) to discern any influences brought about by different functionalities. We were particularly interested to see if the tetraalkylammonium bromide tether would lead to any notable increased catalytic activity.

The double Mizoroki-Heck coupling of 1,4-dibromobenzene with *t*-butyl acrylate at 1 mol% catalyst loading was chosen as a standard test reaction. Under these conditions, complex **68** indeed displayed the best activity in forming the 1,4-phenylene-dicinnamate in a yield of 82%.

However, the yield is not as good as that with a [PdCl(IMes)(*N*,*N*-dimethylbenzylamine)] complex, where only 0.5 mol% was required to afford 81% product formation.[88] Among **45**, **57** and **58**, the amino-functionalized complex performed better than the ester analogue followed by the parent bromo-complex (Table 3.4, entries 1–4), which is understandable since the amine moiety is easily protonated to form an ammonium tether in the course of the catalytic reaction. As expected, addition of 1.5 equiv of tetrabutylammonium bromide (TBAB) to the reaction with **45** or **58** significantly improves the product yield from 56 and 76% to 92 and 93%, respectively, which is merely ~10% better than that of the reaction with pure **68** containing only catalytic amounts of a tethered ammonium salt. In comparison, additional TBAB improves the activity of **68** further giving a near-quantitative yield of 98%.

The reaction scope was extended to other polyhalogenated benzenes using complex **68** without additional TBAB. Good and comparable yields of approximately 84% were obtained for the all three isomers of dicinnamates (entries 4–6). Increasing the number of the bromo-substituents on the benzene ring to three and four allowed us to isolate the respective tri- and tetra-cinnamates (**69**) as major products (76% and 38%, entries 7 and 8). The yield of the tri-cinnamate is higher than that previously obtained using a $Pd(OAc)_2$/tri-*o*-tolylphophine catalytic system (62%).[89] Partially olefinated substrates were observed as minor by-products as well. In comparison, reaction with 1,2-dichlorobenzene only gave the monocinnamate as a major product in a low yield of 10% (entry 9). The yield of monocinnamate was improved to 23% from reaction with 1,2,4,5-tetrachlorobenzene (entry 10). In these more challenging cases, the addition of TBAB could only led to a small improvement of the yields of the major product (monocinnamate). Besides the benzene halides, bromoheterocycles were coupled with *tert*-butyl acrylate with good yields of up to 92% (entries 11 and 12).

Table 3.4. Mizoroki-Heck coupling reactions.[a]

entry	cat.	aryl halide	product	yield[b]
1	**45**	1,4-dibromobenzene	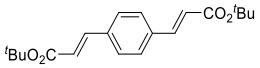	56%(92[c])
2	**57**	1,4-dibromobenzene	″	65%
3	**58**	1,4-dibromobenzene	″	76%(93[c])
4	**68**	1,4-dibromobenzene	″	82%(98[c])
5	**68**	1,2-dibromobenzene	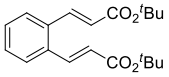	84%
6	**68**	1,3-dibromobenzene	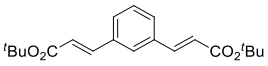	84%
7	**68**	1,3,5-tribromobenzene	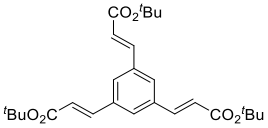	76%
8	**68**	1,2,4,5-tetrabromobenzene	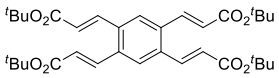	38%
9	**68**	1,2-dichlorobenzene	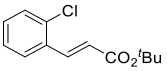	10% (18[c])
10	**68**	1,2,4,5-tetrachlorobenzene	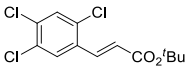	23%(36[c])
11	**68**	3-bromopyridine	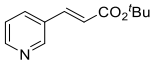	92%
12	**68**	2-bromothiophene	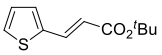	82%

[a]Reaction conditions: 1/n mmol of aryl halide (n = number of halide on aryl ring); 1.5 mmol of *tert*-butyl acrylate; 1.5 mmol of NaOAc; 3 mL of DMF; 0.01 mmol of precatalyst; 130 ℃, 20 h. [b]Isolated yields for an average of two runs. [c]With addition of 1.5 equiv of $[N(n\text{-}C_4H_9)_4]Br$.

A preliminary study was carried out to identify any active Pd(0) species derived from complex **68** by formate reduction. For this purpose, silver formate was added to **68**, and instant AgBr precipitation was seen indicating the successful anion metathesis to yield complex *trans*-$[PdBr_2(C_3NEt_3\text{-bimy})_2](HCO_2)_2$ (**70**). The presence of the HCO_2^- anion is corroborated by a downfield ^1H singlet at 8.61 ppm and a ^{13}C signal at 167.7 ppm. All other signals remain largely

unchanged upon metathesis. In addition, a base peak is observed at *m/z* 483 for the [M – $2HCO_2$]$^{2+}$ ion in the positive ESI mass spectrum.

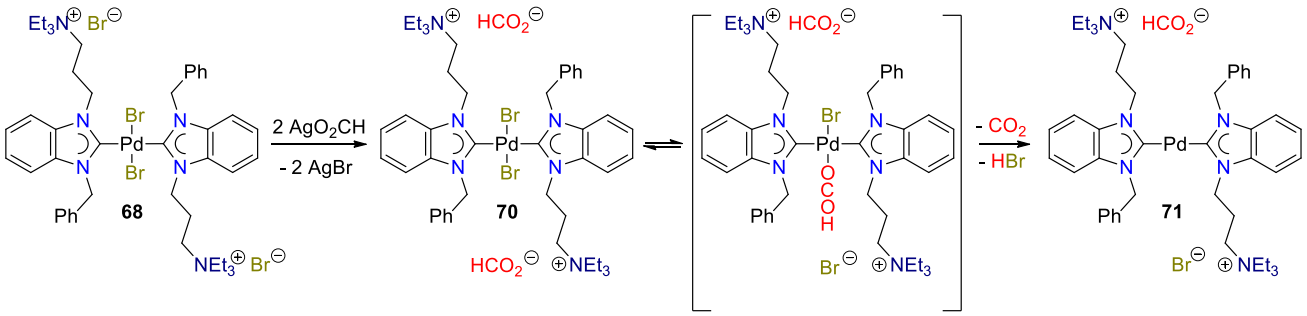

Scheme 3.14. Reduction of *trans*-[$PdBr_2$(C_3NEt_3-bimy)$_2$]Br_2 (**68**) to [Pd(C_3NEt_3-bimy)$_2$]X_2 (**71**).

Interestingly, the NMR sample of **70** showed a color change from grey to yellow on standing, and a small amount of Pd black was also observed. NMR analysis of this resulting yellow mixture showed enormous differences: (i) the ^{1}H NMR spectrum shows only one set of signals; (ii) the integral ratio of for the formate ^{1}H singlet at 8.61 ppm is reduced; (iii) the original two $^{13}C_{carbene}$ signals at 182.4 and 182.2 ppm for the rotamers of **70** have been replaced by a new and more downfield $^{13}C_{carbene}$ signal at 193.4 ppm. Both the color change and the spectroscopic differences suggest that Pd(0) species might be generated. In particular, the enhanced downfield shift of the carbene carbon is indicative of a more electron rich metal center in line with a reduction of Pd(II) to Pd(0).[90]

Scheme 3.14 displays a possible pathway, which is supposedly initiated by a ligand exchange between inner and outer sphere involving bromido and formato ligands. The resulting ionization isomer of **70** subsequently undergoes decarboxylation generating an intermediate hydrido species, which reductively eliminates HBr to give the respective Pd(0) species [Pd^0(C_3NEt_3-bimy)$_2$]X_2 (**71**, X = Br and HCO_2).[91] The absence of rotamers for **71** as indicated by

the NMR analysis is consistent to observations made for other d^{10} metal complexes, i.e. Ag(I), Au(I), with linearly coordinated bis(NHC) ligands.[92] Such bis(NHC)-Pd(0) complexes are only known with imidazoe-derived carbenes,[90] which were prepared by either metal vapor condensation or ligand exchange. Hence, complex **71** is the first example of a 14 electron Pd(0) complex coordinated by two benzimidazolin-2-ylidene ligands, which is generated by reduction of Pd(II) with fomate salt. It is noteworthy that the mechanism study is only preliminary, further research has to be done to comfirm that complex **71** is the real catalyst. Since the catalytic condition is rather forcing, further ligand dissociation and hetergeneization to Pd(0) nanoparticles as the active catalyst is one of the other possible paths.

4. Multi-metallic Complexes Bearing Dipropyl-pyridine-2,6-dicarboxamide bridged diNHC Ligands

Pyridine-2,6-dicarboxamide has been extensively explored as a pincer ligand towards a large library of transition metals such as Fe(III), Co(III), Ni(II), Cu(II), Cu(III), Ru (III), Pd(II), Pt(II), and Au(III).[93] Remarkably, this dianionic ligand has the ability to decrease the redox potential of metal center in high oxidation state and thereby stabilizes the resulting complexes. The combination of pyridine-2,6-dicarboxamide with carbene ligands will result in multidentate ligands, which have both coordination sites to hard and soft Lewis acid metals centers. This may help in the complexes preparation, and probably, direct self-assembling.

4.1 Synthesis and Characterization of Ligand Precursors

The dipropyl-pyridine-2,6-dicarboxamide bridged dibenzimidazolium salts with benzyl (**L_{Bn}**) and methyl (**L_{Me}**) N-substituents were prepared as summarized in Scheme 4.1. Pyridine 2,6-dicarboxylic acid chloride was reacted with 3-chloropropylamine, which was generated from its hydrochloride salt by reacting with triethylamine, to afford the bis(3-chloropropyl)pyridine-2,6-dicarboxamide (**K**) in a yield of 64%. Subsequent reaction with benzyl- or methyl-benzimidazole gave only trace amounts of the dicationic salts. Addition of NaI promoted the double alkylations. However, prolonged heating for 48 h was required to achieve satisfactory yields (> 80%) of the desired salts **L_{Bn}** and **L_{Me}**. The reaction was further optimized by using microwave irradiation, which shortened the reaction time extensively to 3 h, yet gave better yields of 98% and 89%, respectively. These two salts are well soluble in polar solvents such as CH_3CN, DMSO, and MeOH, poorly soluble in chlorinated solvents and not soluble in water.

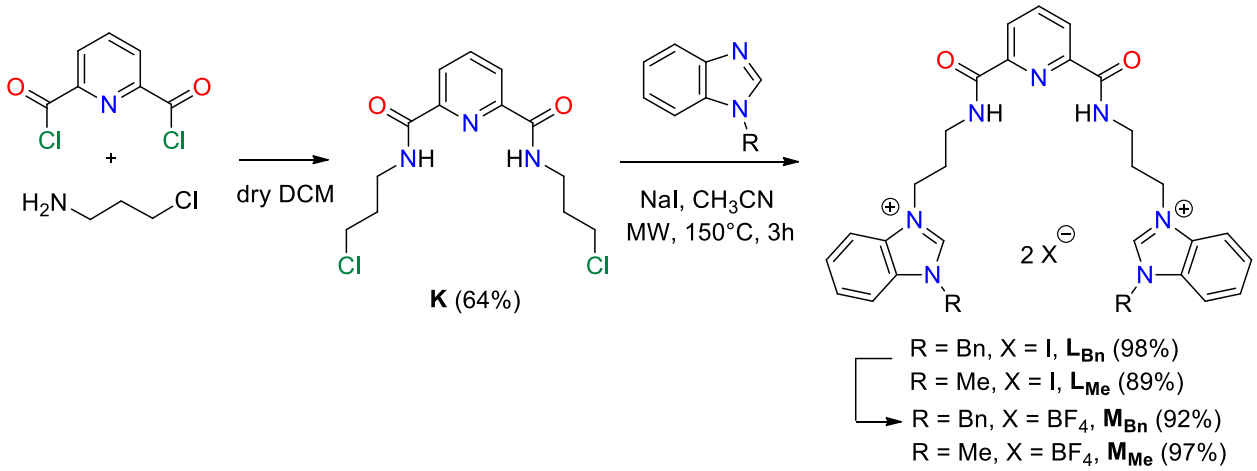

Scheme 4.1. Synthesis of dipropyl-pyridine-2,6-dicarboxamide bridged dibenzimidazolium ligand precursors

Anion metathesis with $AgBF_4$ smoothly gave the dipropyl-pyridine-2,6-dicarboxamide bridged dibenzimidazolium salts $\mathbf{M_{Bn}}$ and $\mathbf{M_{Me}}$. Compared with their iodide analogues these two white solid salts generally show better solubilities in organic solvents including DCM, CH_3CN, DMSO, and MeOH. In addition, the $\mathbf{M_{Me}}$ salt is sparingly soluble in H_2O. Formation of these four salts is supported by ESI-MS. For $\mathbf{L_{Bn}}$/$\mathbf{M_{Bn}}$, base peaks at *m/z* 790/750 assignable to $[M - I/BF_4]^+$ cations and weaker signals at *m/z* 332 attributed to $[M - 2I/BF_4]^{2+}$ dications are observed. The respective signals of salts $\mathbf{L_{Me}}$ and $\mathbf{M_{Me}}$ were found at *m/z* 638/598 and 256. Moreover, their ^{1}H NMR spectra show a downfield singlet in the range of 9.14–9.99 ppm characteristic for the acidic NCHN protons. The CONH protons resonate as triplets in the more upfield region of 8.54–9.40 ppm. Notably, after anion exchange from I^- to BF_4^-, both the NCHN and CONH protons shift upfield, suggesting weaker hydrogen bonding strengths with BF_4^-. The propyl chains in all cases appear as one triplet (NC$\mathbf{H}_2$) and two multiplets (NHC$\boldsymbol{H}_2$C$\boldsymbol{H}_2$) in the region of 2.28–4.62 ppm. The benzylic or the methyl protons on the other hand resonate as singlets at ~5.65 or ~4.00 ppm, respectively. The ^{13}C NMR resonances for the NCHN and CO carbon atoms are not much

affected by the different N-substituents or counter anions resonating at ~142.8 and ~164.9 ppm, respectively.

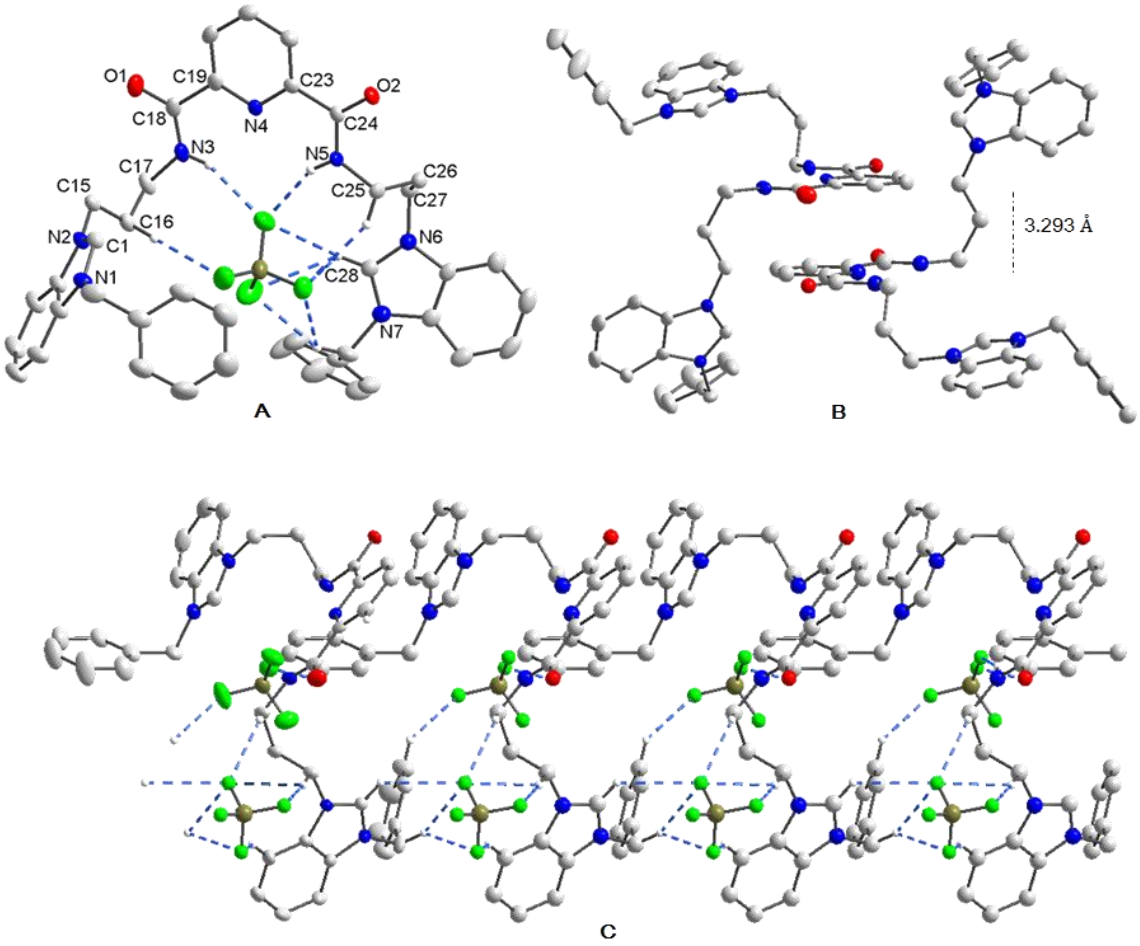

Figure 4.1. Molecular structure and perspective view of $\mathbf{M_{Bn}}$ showing 50% probability ellipsoids; solvent molecules and most hydrogen atoms are omitted for clarity. Selected bond lengths [Å] and bond angles [deg]: N1-C1 1.328(3), N2-C1 1.326(3), N6-C28 1.321(3), N7-C28 1.331(3), O1-C18 1.227(3), O2-C24 1.231(3), N4-C19 1.339(3), N4-C23 1.338(3); N1-C1-N2 110.6(2), N6-C28-N7 110.9(2), N3-C18-C19 114.5(2), N5-C24-C23 115.61(19), N19-N4-C23 117.4(2).

The identity of the $\mathbf{M_{Bn}}$ salt was further confirmed by X-ray diffraction of a single crystal obtained via slow evaporation of a saturated solution in $CHCl_3$. Figure 4.1 depicting its molecular structure shows the expected connectivity. The amide protons (N3–H and N5–H), one of the NCHN protons (C28–H) and several aliphatic protons cooperatively form hydrogen bonding

interactions with one BF_4^- anion, embedding it inside a cationic cage-like structure (A). The molecular salts are arranged into an infinite chain via intermolecular hydrogen bonds between the BF_4^- anions and the various C–H protons (C). Besides, offset face to face π···π interactions are noted between the two perfectly coplanar pyridine rings from the neighboring molecules with a separation of 3.293 Å (B).[94]

4.2 Synthesis and Characterization of Gold Complexes

4.2.1 Synthesis and Characterization of Metallocyclic NHC-Silver(I), Gold(I) and Gold(III) Complexes

The reactivity of the $\mathbf{M_{Bn}}$ or $\mathbf{M_{Me}}$ salts towards Ag_2O was attempted in CH_3CN (Scheme 4.2). The reaction mixture was heated to 60 ℃ to afford the respective [Ag(diNHC)]BF_4 complexes [diNHC = dipropyl-pyridine-2,6-dicarboxamide bridged dibenzimidazolin-2-ylidene with N-benzyl (**72$_{Bn}$**) or -methyl substituents (**72$_{Me}$**)]. Complex **72$_{Me}$** is less soluble in CH_3CN and precipitated out, whereas complex **72$_{Bn}$** has a better solubility and remained in solution. These two complexes are isolated as white solids exhibiting good stability when kept in the dark. However, their solutions in CH_3CN or DMSO show signs of decomposition and turn yellow after several days.[95] The occurrence of reaction is well evidenced by the disappearance of the characteristic downfield signal for the NCHN protons of the salt precursors in the ^{1}H NMR spectra. In addition, signal broadening appears for all the aliphatic protons upon metallocycle formation, which is apparently attributed to a rigid structure arising from dicarbene ligand coordination. As with many Ag NHC complexes, the carbene signal could not be resolved despite prolonged acquisition time.[96] Nevertheless, base peaks at *m*/*z* 768 or 618 owing to the respective

$[M - BF_4]^+$ fragments are found in their positive mode ESI mass spectra, supporting the formation of the desired complexes.

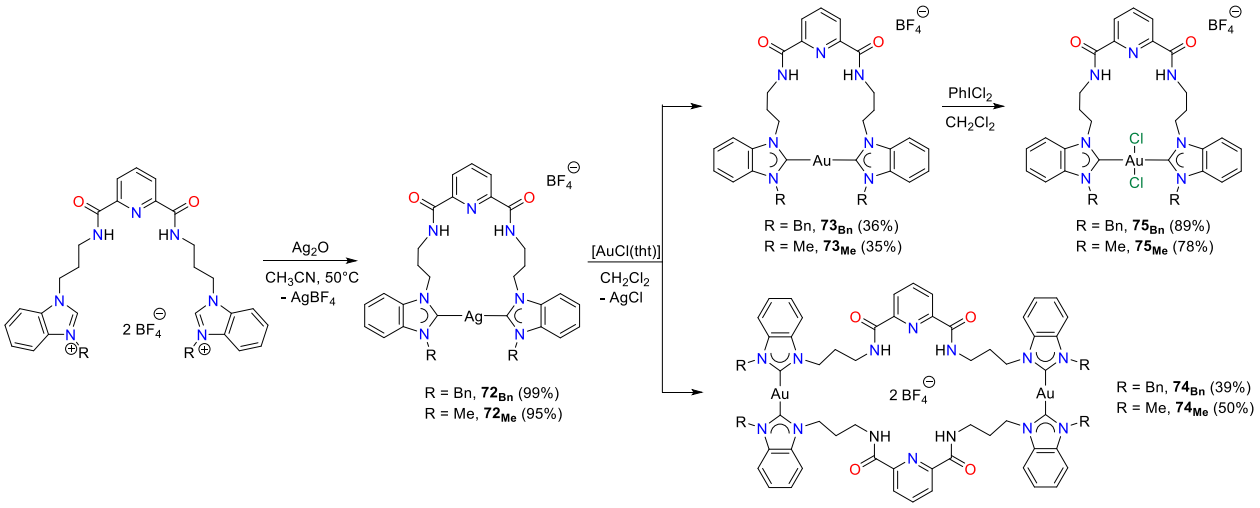

Scheme 4.2. Synthesis of silver and gold complexes.

The silver complexes $\mathbf{72_{Bn,Me}}$ were subsequently reacted with [AuCl(THT)] in CH_2Cl_2 in an attempt to synthesize the corresponding gold complexes.[15] Instant formation of AgCl precipitate indicated the successful transmetalation. The reaction was stopped after 4 h, and a product mixture of mononuclear complexes $[Au(diNHC)]BF_4$ (**73**) and dinuclear complexes $[Au(diNHC)]_2(BF_4)_2$ (**74**) was observed in both cases. Complexes $\mathbf{73_{Bn}}$ and $\mathbf{74_{Bn}}$ were separated by column chromatography using $CHCl_3/CH_3CN$ [7:2 (v/v)]. Unexpectedly, the dinuclear complex $\mathbf{74_{Bn}}$ eluted first followed by the mononuclear complex $\mathbf{73_{Bn}}$ with R_f values of 0.3 and 0.15, respectively. Complex $\mathbf{73_{Me}}$ and $\mathbf{74_{Me}}$, on the other hand, have very similar R_f values using varying solvent mixtures as mobile phase and could not be efficiently separated after column chromatography. Additional washing with CH_3CN allows for the separation of the two complexes, whereby the mononuclear complex $\mathbf{73_{Me}}$ dissolves, while the dinuclear complex $\mathbf{74_{Me}}$ remains insoluble. The two dinuclear complexes were isolated in slightly higher yields of 39/50% ($\mathbf{74_{Bn/Me}}$) compared to the mononuclear complexes, for which yields of 36/35% ($\mathbf{73_{Bn/Me}}$) were

obtained. All four complexes are white solids. The digold complexes are air stable both in solid state and solutions. In contrast, the monogold complexes show limited stability as optically evidenced by a color change from white to purple when stored in air.

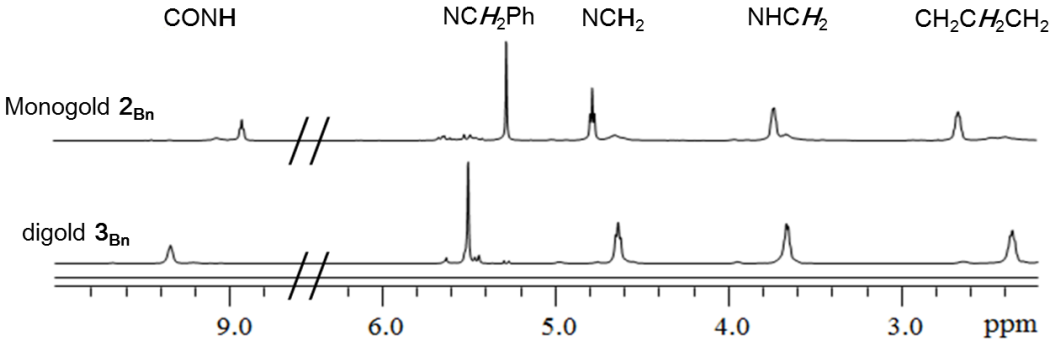

Figure 4.2. ^{1}H NMR spectra of monogold **73$_{Bn}$** and digold **74$_{Bn}$** complexes in the range of 2.2 to 10.0 ppm in $CDCl_3$.

In the NMR spectra of all four complexes, only one set of signals was observed indicating the dicarbene ligands are symmetrically bonded. The $^{13}C_{carbene}$ resonances are found at 190.8–191.9 ppm, which fall in the range typically observed for bis(NHC)-Au complexes.[97] The ^{1}H NMR spectra in the range of 2.2–10.0 ppm of complexes **73$_{Bn}$** and **74$_{Bn}$** are displayed in Figure 4.2. The CONH hydrogen signals of the digold complex **74$_{Bn}$** is significantly downfield shifted by 0.45 ppm compared to those in the monogold complex **73$_{Bn}$**, presumably due to stronger short contacts with the BF_4^- anions (*vide infra*). The NCH_2Ph and CH_2 protons, on the other hand, are resonating at higher field in the dinuclear complex **74$_{Bn}$**. Generally, the mononuclear and dinuclear complexes have similarly patterned NMR spectra. The ^{1}H NMR spectra of the complexes **73$_{Me}$** and **74$_{Me}$** are similar to their benzyl-substituted analogous and hence will not be discussed in detail.

The similarity of the NMR spectra and the identical weight percentage for carbon, hydrogen and nitrogen elements due to the same empirical formula of the respective mononuclear and dinuclear complex pairs make their differentiation using these methods difficult. Nevertheless, ESI MS spectrometry turns out to be a useful tool. Although respective complex pairs show their base peaks at same *m*/*z* values, 858 (**73**/**74**$_{\mathbf{Bn}}$) or 706 (**73**/**74**$_{\mathbf{Me}}$), respectively, the isotopic peak spacing of 0.5 observed for dinuclear complexes **74**$_{\mathbf{Bn/Me}}$ indicate doubly charged cations, which are assignable to their $[M - 2BF_4]^{2+}$ fragments (Figure 4.3).

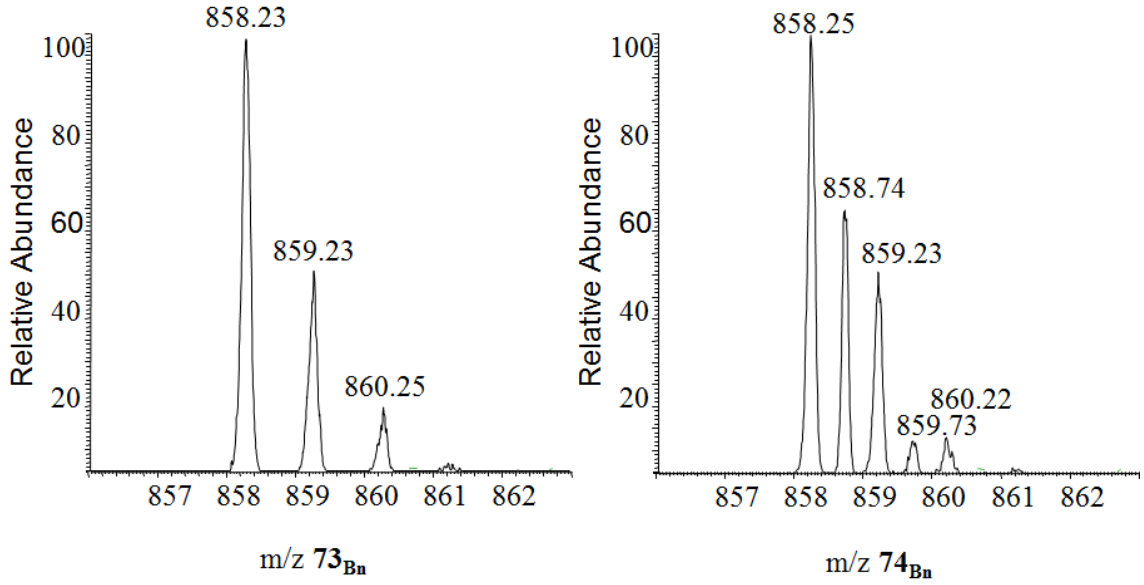

Figure 4.3. Isotopic pattern of the base peaks belonging to monogold **73**$_{\mathbf{Bn}}$ and digold **74**$_{\mathbf{Bn}}$ complexes in the respective positive ESI mass spectrum.

Single crystals of complex **73**$_{\mathbf{Me}}$ and **74**$_{\mathbf{Bn}}$ were obtained by diffusion of diethyl ether to the respective saturated solutions in CH_3CN. The solid state molecular structures determined by X-ray diffraction analysis are depicted in Figure 4.4 and 4.5, respectively. They confirm the expected nuclearity and compositions as found by ESI-MS. Surprisingly, the two almost coplanar NHC moieties (dihedral angle of 3.2°) of the bidentate ligand in **73**$_{\mathbf{Me}}$ are found in an *anti*-

arrangement, resulting in a twisted 18-membered metallocyle. Notably, this phenomenon was only observed in the solid state as solution NMR data show a symmetrical bonding mode of the ligand (*vide supra*). Hence, the unusually twisted geometry formed upon crystallization, is due to a better molecular packing in order to achieve a more dense structure. Additionally, offset face to face π···π interactions are noted between the two neighboring pyridine rings with a separation of 3.285 Å. Weak hydrogen bonding interactions are observed between the two CONH hydrogen atoms with one fluorine atom of the BF_4^- anion (omitted in Figure 4.4 for the sake of clarity). The Au–$C_{carbene}$ distances are 2.029(4) and 2.025(4) Å, which fall in the range of normal bis(NHC)-Au complexes.[97]

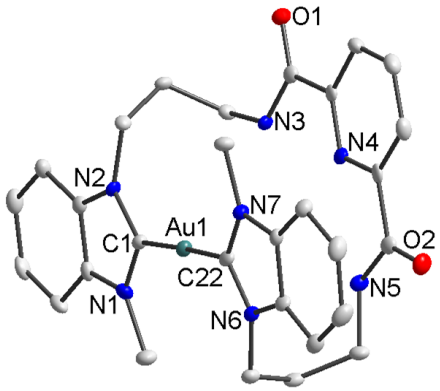

Figure 4.4. Molecular structure of **73$_{Me}$** showing 50% probability ellipsoids; BF_4^- anion and hydrogen atoms are omitted for clarity. Selected bond lengths [Å] and bond angles [deg]: Au1-C1 2.029(4), Au1-C22 2.025(4), C1-Au1-C22 177.72(13).

The cation in digold complex **74$_{Bn}$** has C2 symmetry with the rotational axis perpendicular to the average plane of the molecule and passing through the center. In comparison to what is observed for **73$_{Me}$**, the two NHC moieties (dihedral angle of 4.2°) coordinated to the same Au center in complex **74$_{Bn}$** are retained in a *syn*-arrangement in the solid state in line with the symmetrical ligand bonding also observed by solution NMR spectroscopy. The two N-substituents point towards opposite directions with respect to the NHC planes to relieve steric

hindrance. In addition, the Au–$C_{carbene}$ distances are 2.0420(1) and 2.0546(1) Å and longer than those in mononuclear complex **73_{Me}**. Numerous hydrogen bonding contacts are noted between the methylene and CONH hydrogen atoms with BF_4^- anions. As an interesting result, one BF_4^- anion sits right in the center of the 36-membered-metallocycle. This phenomenon provides hints for a potential application of this cationic molecule for anion recognition, which is an area gaining increasing interest in recent decades.[98]

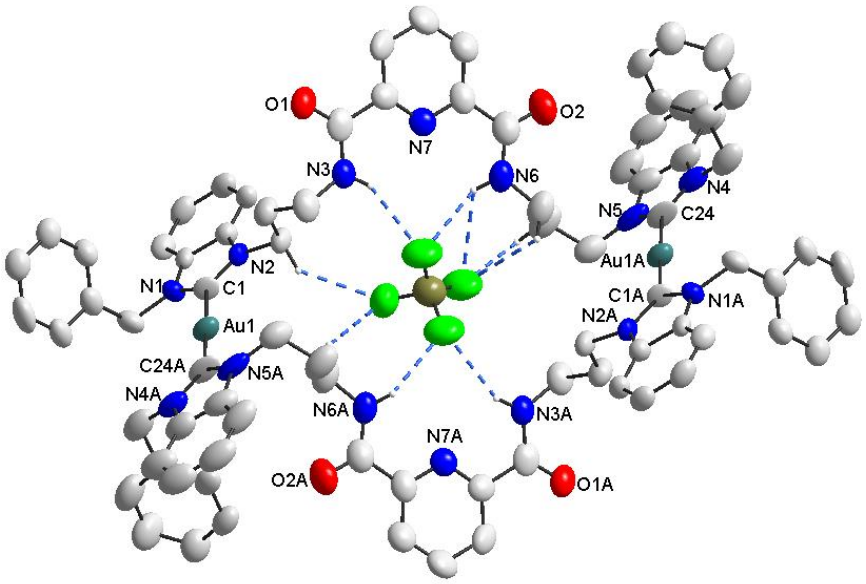

Figure 4.5. Molecular structure of **74_{Bn}** showing 50% probability ellipsoids; BF_4^- anion and hydrogen atoms are omitted for clarity unless referred in text. Selected bond lengths [Å] and bond angles [deg]: Au1-C1 2.042(9), Au1-C24 2.055(10), C1-Au1-C24A 178.6(5).

Oxidation of the monogold(I) complexes **$73_{Bn,Me}$** with $PhICl_2$[99] yielded the respective monogold(III) complexes **75_{Bn}** and **75_{Me}** as pale yellow powders (Scheme 4.2). In comparison to the parent complexes, their solubilities in common organic solvents have significantly decreased. In addition, their ^{1}H NMR spectra show even broader signals for the CONH and the propylene protons at room temperature, which did not sharpen at different temperatures (223–373 K). The

carbene resonances shifted to much higher field at ~163 ppm in line with the more Lewis acidic gold centers.[24e,95,100] The base peaks in ESI mass spectra at *m*/*z* 928 and 776, respectively, further corroborate the coordination of two additional chlorido ligands. Oxidation of the dinuclear complexes **74$_{Bn}$** and **74$_{Me}$** gave rise to insoluble compounds, which hamper the characterization and identification.

4.2.2 Synthesis and Characterization of a Macrocyclic Bimetallic Trinuclear [Au(I), Co(III)] Double Helical Complex

Complex **74$_{Bn}$** is a potential metallo-ligand with six donors capable of bis(pincer) coordination. After deprotonation, each N',N,N'-pincer includes one neutral nitrogen and two anionic amide nitrogen donors, which together are suitable for a hexa-coordination to a metal center. Cobalt(III) is known to favor octahedral coordination and can be largely stabilized by such ligands.[93d,93h,101] Hence, it was chosen to be studied.

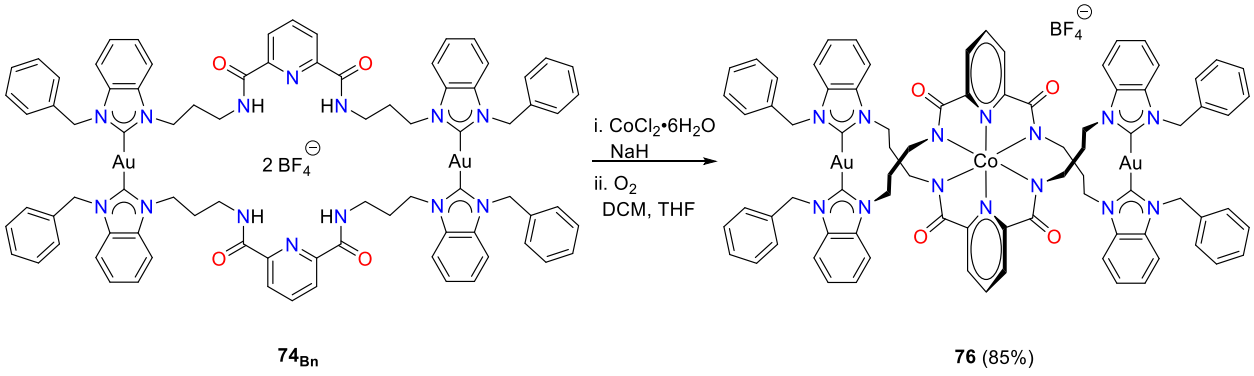

Scheme 4.3. Synthesis of mixed Au(I)/Co(III) complex **76**.

Complex **74$_{Bn}$** was reacted with $CoCl_2 \cdot 6H_2O$ in the presence of excess NaH under nitrogen gas (Scheme 4.3). A series of color changes from purple → pale blue → grey was

observed during the reaction. Exposure of the mixture to air afforded a finally brownish suspension. After simple filtration and washing with hexane, complex **76** was isolated as a brownish-yellow solid soluble in organic solvents such as $CHCl_3$, CH_2Cl_2, CH_3CN, DMSO, and MeOH, but insoluble in hexane, toluene and diethyl ether. Its formation was evidenced by a high-resolution ESI mass spectrum, in which a base peak at 1771.4702 assignable to the $[M - BF_4]^+$ (calcd: 1771.4675) with a peak spacing of one was found. The cation is balanced by one BF_4^- anion, which was also detected in the negative ESI mass spectrum. Magnetic susceptibility measurements of the resulting compound both in solid and solution states showed that complex **76** is diamagnetic in nature, indicating that the ground state of the Co^{3+} center is low-spin (Figure 4.6).

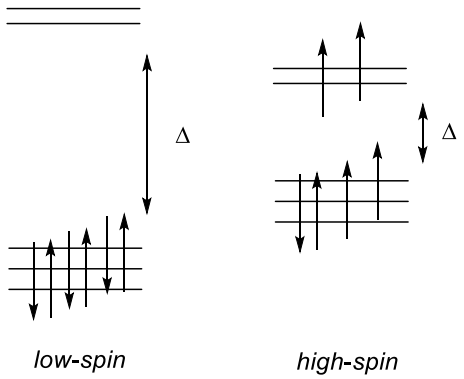

Figure 4.6. Possible spin states of d^6 metal complexes.

^1H NMR analysis of the resulting compound at room temperature afforded only multiple broad signals in line with its complicated helical structure. The multiple signals are possible due to diastereotopy of the methylene protons upon Co^{3+} coordination. Variable-temperature NMR (243–313 K) experiments were conducted; however, the resolution did not improve. In the ^{13}C NMR spectrum, the $^{13}C_{CO}$ resonance at 169.5 ppm is shifted to lower-field by 4.6 ppm in comparison to that of the complex precursor, which is in line with decreased electron density of

the amide moieties upon coordination to a Lewis acid. In contrast, the $^{13}C_{NCN}$ signal is observed at 190.1 ppm, which is shifted to higher field, probably due to the shielding effect exerted by the electron cloud of the cobalt ion.

The identity of complex **76** was unambiguously confirmed by X-ray diffraction analysis on single crystals obtained by slow evaporation of a saturated solution in CH_2Cl_2/toluene. As depicted in Figure 4.7, two metallo-bis(pincer) ligand strands interwined each other around the center Co^{3+} ion with a meridional configuration. As a result, the macrocyclic molecule forms a racemic double-stranded helix with loss of the C_2 symmetry found for its precursor $\mathbf{74_{Bn}}$ (only the *P*-form is shown in Figure 4.7).

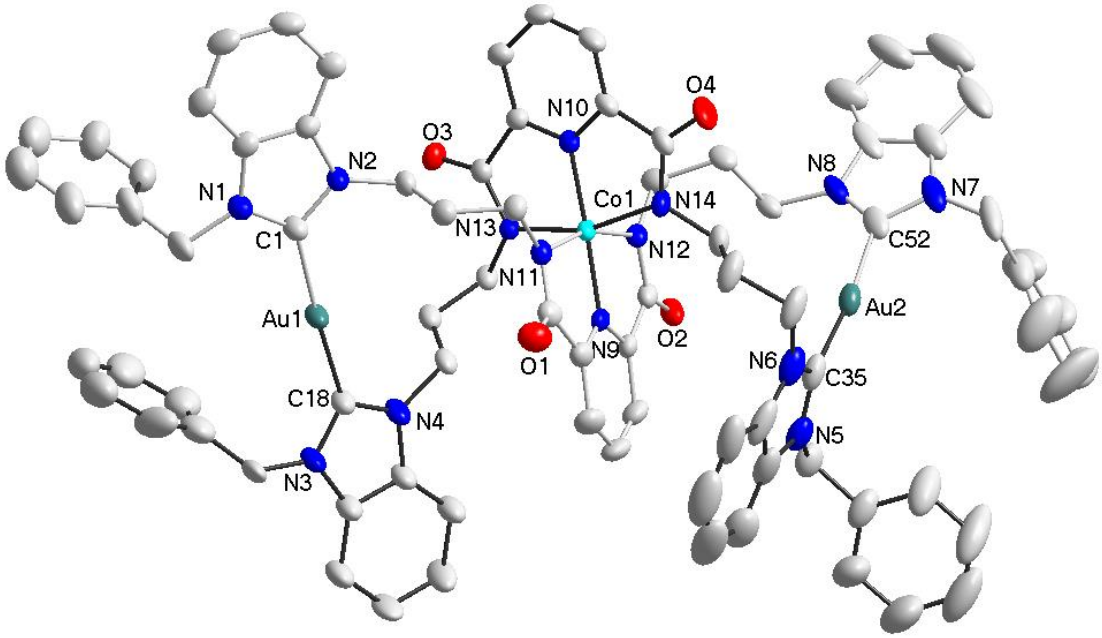

Figure 4.7. Molecular structure of *P*-**76** showing 50% probability ellipsoids; BF_4^- anion and hydrogen atoms are omitted for clarity. Selected bond lengths [Å] and bond angles [deg]: Au1-C1 2.013(6), Au1-C18 2.005(6), Au2-C35 2.013(8), Au2-C52 2.024(8), Co1-N9 1.862(5), Co1-N11 1.985(5), Co1-N12 1.949(5), Co1-N10 1.860(5), Co1-N13 1.974(5), Co1-N14 1.949(5), C1-Au1-C18 176.7 (3), C35-Au2-C52 173.6(3), N9-Co1-N10 176.5(2), N9-Co1-N11 81.6(2), N9-Co1-N12 81.6(2), N11-Co1-N12 163.1(2), N10-Co1-N13 81.7(2), N10-Co1-N14 81.4(2), N13-Co1-N14 162.5(2).

A closer inspection of the structure shows that the C2 symmetry found for complex **74$_{Bn}$** is lost upon Co coordination. Around the Co center, the bond distances of the four equatorial Co–N bonds [1.949(5)–1.985(5) Å] are significantly longer than the two axial ones [1.860(5) and 1.862(5) Å] with the differences beyond the 3σ limit. Moreover, the four equatorial Co–N bonds are tilted towards the respective pyridine rings with N–Co1–N angles measuring 163.1 ° and 162.5 °. For the two Au coordination spheres, the C–Au–C bond angles of 173.6 ° and 176.7 ° further deviate from perfect linearity. Strikingly, the two planes of the NHC coordinated to the Au2 center are almost perpendicular to each other. In contrast, those coordinated to Au1 are closer to co-planarity similar to those observed in complex **74$_{Bn}$**, but with an increased dihedral angle of 15.3 °.

4.3 Synthesis and Characterization of Palladium(II) complexes

In an attempt to extend the coordination chemistry of the pentadentate diNHC ligand to group 10 metals, the Ag complexes **72$_{Bn/Me}$** were reacted with [$PdCl_2(CH_3CN)_2$] in the presence of tetramethylammonium chloride to afford the respective Pd-diNHC complexes (Scheme 4.4).

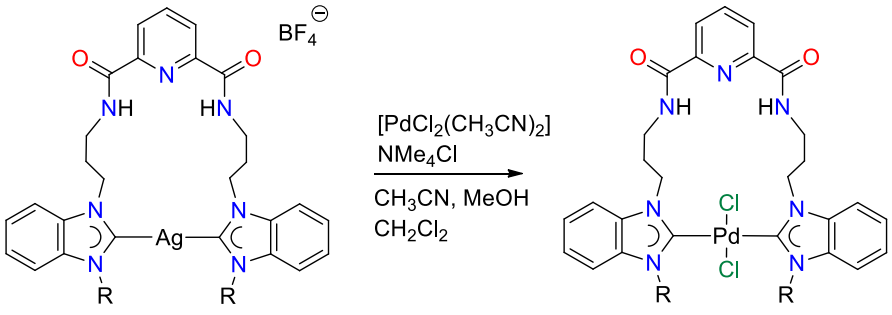

Scheme 4.4. Synthesis of *trans*-[$PdCl_2$(diNHC)] complexes **77$_{Bn/Me}$**.

Notably, only mononuclear complexes of the formula *trans*-[$PdCl_2$(diNHC)] (diNHC = dipropyl-pyridine-2,6-dicarboxamide bridged dibenzimidazolin-2-ylidene with N-benzyl (**77$_{Bn}$**) or -methyl substituents (**77$_{Me}$**)) were isolated as air-stable pale yellow solids. Generally, complex **77$_{Bn}$** has better solubilities in polar organic solvents such as chlorinated solvents, CH_3CN, and DMSO. Both of them are not soluble in less polar solvents including hexane, diethyl ether, and ethyl acetate. Formation of these complexes is supported by positive mode ESI-MS, which shows a base peak at *m*/*z* 803 and 650, respectively, due to the $[M - Cl]^+$ fragment of complex **77$_{Bn/Me}$**.

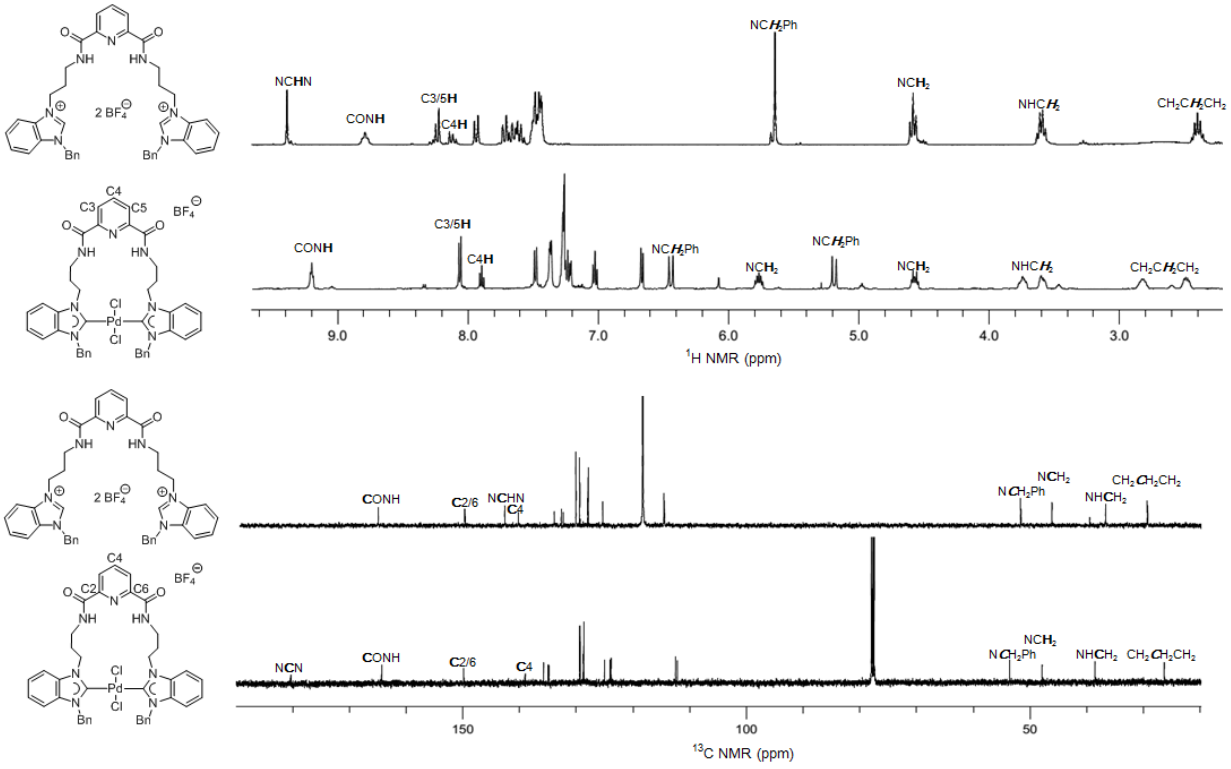

Figure 4.8. ^1H and ^{13}C NMR spectra of salt precursor **M$_{Bn}$** (CD_3CN) and *trans*-[$PdCl_2$(diNHC)] complex **77$_{Bn}$** ($CDCl_3$).

In the NMR spectra, only one set of signals were observed indicating a symmetrical bonding of the ligand in both cases. However, the CH_2 protons become diastereotopic owing to

the restricted rotational freedom arising from palladation. For complex **77$_{Bn}$**, eight signals are observed for the four chemically distinct CH_2 groups. The benzylic protons appear as two doublets at 6.44 and 5.19 ppm with geminal coupling constants of ^2J(H,H) = 15.1 Hz, while the propylene protons are resonating as six multiplets centered at 5.77, 4.57 (NCH_2), 3.73, 3.60 ($NHCH_2$) and 2.82, 2.49 ($CH_2CH_2CH_2$) ppm. Its carbene and carbonyl carbon atoms are observed at 180.3 and 164.3 ppm, respectively (Figure 4.8). Complex **77$_{Me}$** has a similar splitting pattern for the propylene protons, while the NCH_3 protons resonate as one singlet at 3.97 ppm. The chemical shifts of the carbene and carbonyl carbon atoms are found at 179.4 and 164.1 ppm, respectively. The signal for the CONH hydrogen atoms of both complexes remain as one triplet at 9.20 and 9.12 ppm, respectively.

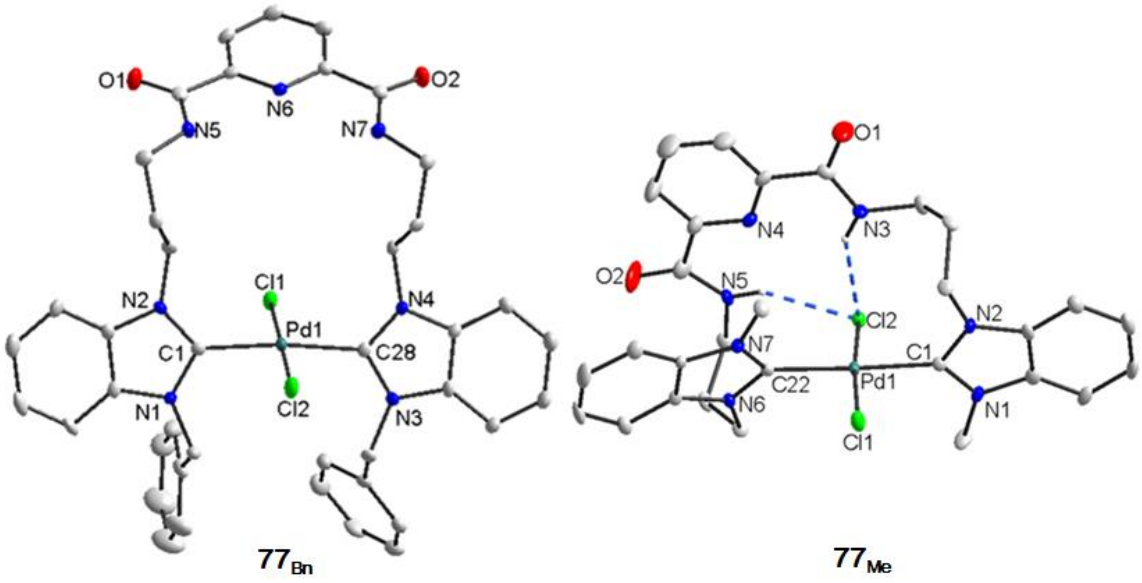

Figure 4.9. Molecular structures of **77$_{Bn}$** and **77$_{Me}$** showing 50% probability ellipsoids; most hydrogen atoms are omitted for clarity. Selected bond lengths [Å] and bond angles [deg]: **77$_{Bn}$**, Pd1-C1 2.037(3), Pd1-Cl1 2.3009(9), Pd1-C28 2.044(3), Pd1-Cl2 2.3295(9), C1-Pd1-Cl1 90.02(9), Cl1-Pd1-C28 91.04(9), C28-Pd1-Cl2 89.73(9), Cl2-Pd1-C1 89.31(9), C1-Pd1-C28 173.38(13), Cl1-Pd1-Cl2 178.84(3); PdC_2Cl_2/NHC(left, right) dihedral angle: 69.9, 63.2 °. **77$_{Me}$**, Pd1-C1 2.010(5), Pd1-Cl1 2.3069(13), Pd1-C22 2.059(5), Pd1-Cl2 2.3255(12), C1-Pd1-Cl1 89.09(14), Cl1-Pd1-C22 88.13(14), C22-Pd1-Cl2 96.73(14), Cl2-Pd1-C1 86.27(14), C1-Pd1-C22 175.0(2), Cl1-Pd1-Cl2 174.38(5); PdC_2Cl_2/NHC(left, right) dihedral angle: 65.6, 77.1 °.

Single crystals of complexes **77$_{Bn/Me}$** suitable for X-ray diffraction studies were obtained by either slow diffusion of diethyl ether into a solution in CH_3CN (**77$_{Bn}$**) or slow evaporation of a saturated solution in $CHCl_3$ (**77$_{Me}$**). Their molecular structures are depicted in Figure 4.9 with selected bond parameters. Both **77$_{Bn}$** and **77$_{Me}$** crystallize as mononuclear complexes, in which the palladium centers are coordinated by two chlorido ligands and the *trans*-spanning diNHC ligand in square planar modes. 18-membered metallocycles are formed as results. Similar to the gold(I) analogue, the metallocycle of complex **77$_{Me}$** is twisted due to the *anti*-arrangement of the two NHC moieties in the solid state. In contrast, the two NHC moieties in complex **77$_{Bn}$** remain *syn* to each other due to the steric congestions induced by the benzyl substituent. As consequences, the two NHC planes in complex **77$_{Bn}$** are closer to coplanarity with a dihedral angle of 6.7 °versus 14.5 °in complex **77$_{Me}$**. The two Pd–$C_{carbene}$ distances in complex **77$_{Bn}$** are essentially equal [2.037(3) and 2.044(3) Å], while they are slightly different in complex **77$_{Me}$** [2.059(5) and 2.010(5) Å]. Nevertheless, they all fall in the range of those typically observed for *trans*-[$PdCl_2(NHC)_2$] complexes.[102] Additionally, the molecules of complex **77$_{Bn}$** are paired up by intermolecular hydrogen bonding between CONH hydrogen atoms and chlorido ligands. In contrast, short intramolecular contacts between the closer spaced chlorido ligand and CONH protons are noted in complex **77$_{Me}$**.

The salt precursors showed different reactivities when triethylamine was added as a base (Scheme 4.5). Only the CONH groups were deprotonated, and subsequent addition of [$PdBr_2(CH_3CN)_2$] afforded yellow complexes [$PdCl(N^{'},N,N^{'})$]BF_4 (**78$_{Bn/Me}$**). These cationic complexes are not soluble in hexane, diethyl ether, and ethyl acetate, but readily soluble in the polar organic solvents including $CHCl_3$, CH_2Cl_2, CH_3CN and DMSO. Surprisingly, the methyl-substituted complex **78$_{Me}$** is soluble in MeOH and H_2O as well. In the positive mode ESI mass

spectra, base peaks due to the $[M - BF_4]^+$ fragments are observed at *m*/*z* 802 and 652, respectively, confirming the formation of these cationic complexes.

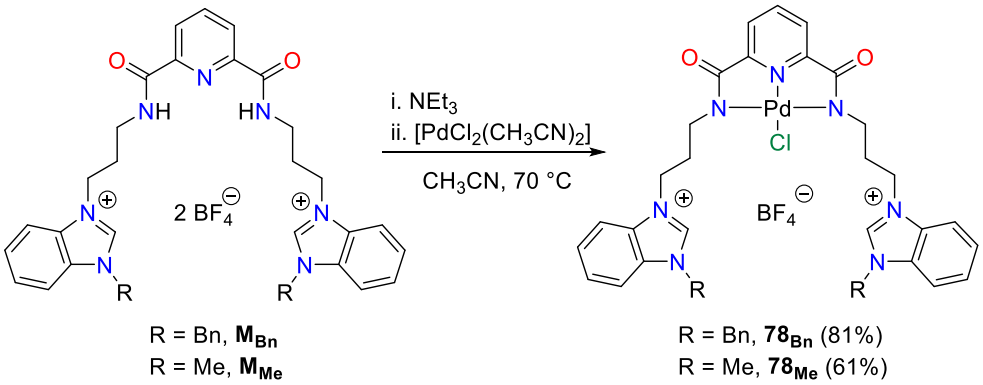

Scheme 4.5. Synthesis of pincer type $[PdCl(N^{\prime},N,N^{\prime})]BF_4$ complexes $\mathbf{7_{Bn/Me}}$.

NMR spectroscopic studies reveal significant downfield shifts of the ^{13}C carbonyl carbon signals ($\mathbf{M_{Bn/Me}}$: 164.9/164.8, $\mathbf{78_{Bn/Me}}$: 171.7 ppm for both) and the absences of the CONH protons, which were found in the salt precursors. These observations indicate the successful coordination of the $N^{\prime},N,N^{\prime}$ pincer moieties to the palladium centers (Figure 4.10). Not surprisingly, the acidic NCHN of the benzimidazolium moieties and methylene protons remain largely unchanged.

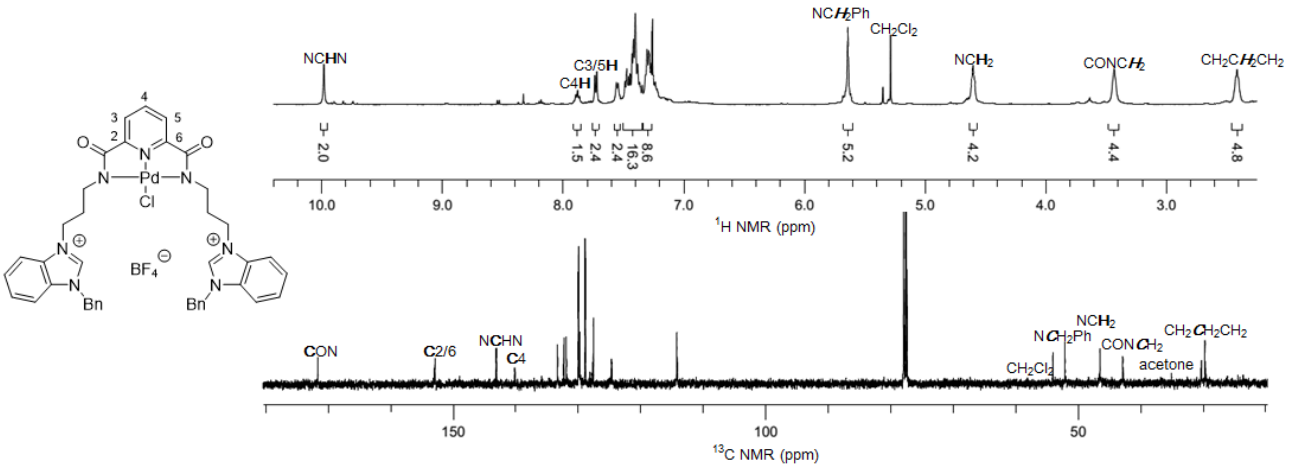

Figure 4.10. ^1H and ^{13}C NMR spectra of complex $\mathbf{78_{Bn}}$ $[PdCl(N^{\prime},N,N^{\prime})]BF_4$ ($CDCl_3$).

The identity of complex **78$_{Me}$** was also corroborated by X-ray diffraction analysis of a single crystal obtained via diffusion of diethyl ether to its solution in CH_3CN. The molecular structure depicted in Figure 4.11 confirms the coordination of the N',N,N' pincer to the Pd(II) center with two azolium moieties dangling. One chlorido ligand coordinates to the fourth site resulting in a square planar geometry. Similar to the observations made for the cobalt complex **76**, the two equatorial Pd–N bonds [2.042(2) and 2.036(2) Å] are significantly longer than the axial Pd–N bond [1.924(2) Å].

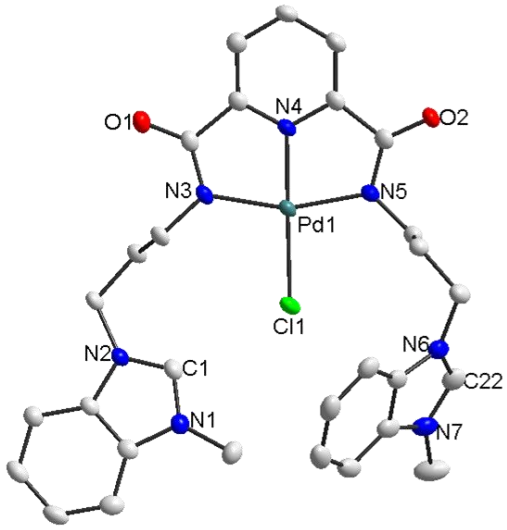

Figure 4.11. Molecular structure of **78$_{Me}$** showing 50% probability ellipsoids; hydrogen atoms, BF_4 anion and solvent molecules are omitted for clarity. Selected bond lengths [Å] and bond angles [deg]: Pd1-Cl1 2.3211(7), Pd1-N3 2.042(2), Pd1-N4 1.924(2), Pd1-N5 2.036(2), N3-Pd1-Cl1 100.68(7), Cl1-Pd1-N5 98.45(7), N5-Pd1-N4 80.56(9), N4-Pd1-N3 80.23(9), Cl1-Pd1-N4 177.92(7), N3-Pd1-N5 160.69(9).

Having successfully installed one Pd(II) to this potential pentadentate ligand either via carbene (**77**) or N',N,N' pincer coordination (**78**), attempts were made to introduce a second palladium metal by treating complexes **77$_{Bn}$** and **78$_{Bn}$** with $Pd(OAc)_2$ in the presence of excess tetramethylammonium chloride as a source for additional anionic ligands (Scheme 4.6). Surprisingly, both reactions gave a tetranuclear-complex **79** as a common product instead of the

expected symmetrical dinuclear complex. Complex **79** has two types of Pd(II) centers. One of them is coordinated by the N^,N,N^ pincer and its fourth coordination site is taken up by one NHC arm, resulting in the formation of an additional seven-membered-metallocycle as the driving force. The second Pd(II), on the other hand, is coordinated by the remaining NHC together with one terminal and two bridging chlorido ligands, giving rise to a tetranuclear species.

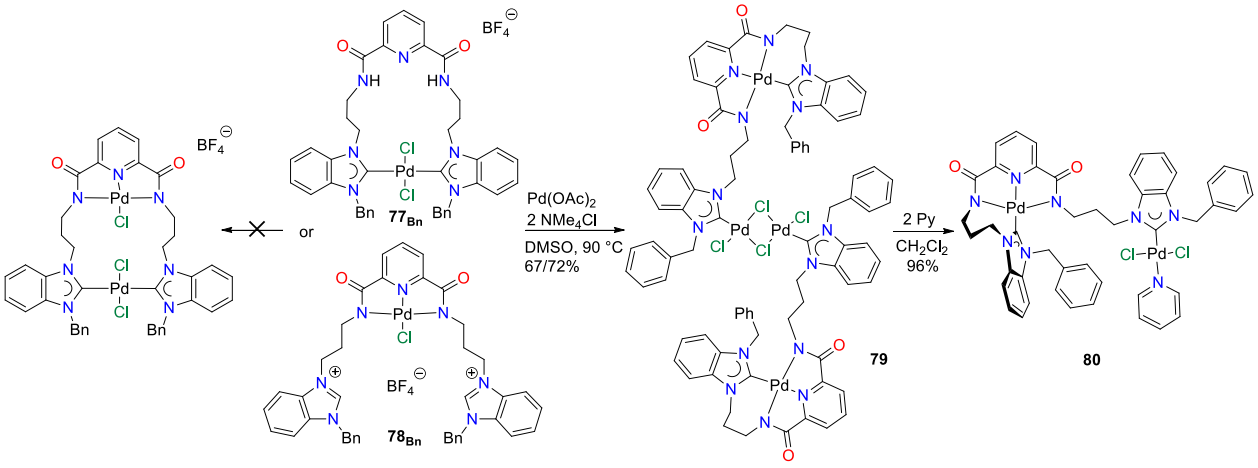

Scheme 4.6. Synthesis of tetranuclaer complex **79** and dipalladium pyridine adduct **80**.

Formation of the tetranuclear complex **79** was first proven by ESI-MS, which shows an isotopic envelope centered at *m*/*z* 1888 assignable to $[M + H]^+$. The ^{1}H NMR spectrum shows the disappearance of all acidic CONH and NCHN protons characteristic for their salt precursors. Two carbonyl carbon signals are observed at 173.0 and 171.7 ppm in the ^{13}C NMR spectrum with the two carbene carbon atoms resonating at 180.8 and 161.5 ppm. This suggests the coordination of both the N^,N,N^ pincer and NHC in an asymmetric mode, which is further corroborated by the signal doubling of all the other proton and carbon atoms of the ligand (Figure 4.12). Two CONC**H**$_2$ and three CH$_2$C***H***$_2$CH$_2$ proton signals are not resolved or coincide with solvent signals. The $^{13}C_{carbene}$ signal at 161.5 ppm is assigned to the carbene donors of the bridging dipalladium

unit by comparison with analogues signals of reported dimeric $[PdX_2(NHC)]_2$ complexes.[103] Such dimeric complexes are known to be readily cleaved by pyridines.[59c] Hence, formation of the "dimeric" tetrapalladium complex **79** was indirectly corroborated via isolation of a dipalladium pyridine adduct **80** as a result from reaction of **79** with pyridine (Scheme 4.6). The dipalladium complex **80** shows slightly better solubilities in common organic solvents. Characterizations with ESI-MS and elemental analysis confirm its formation. In addition, NMR spectroscopy shows additional pyridine signals and a prominent downfield shift of the second carbene carbon from 161.5 to 165.5 ppm (Table 4.1, *vide infra*).

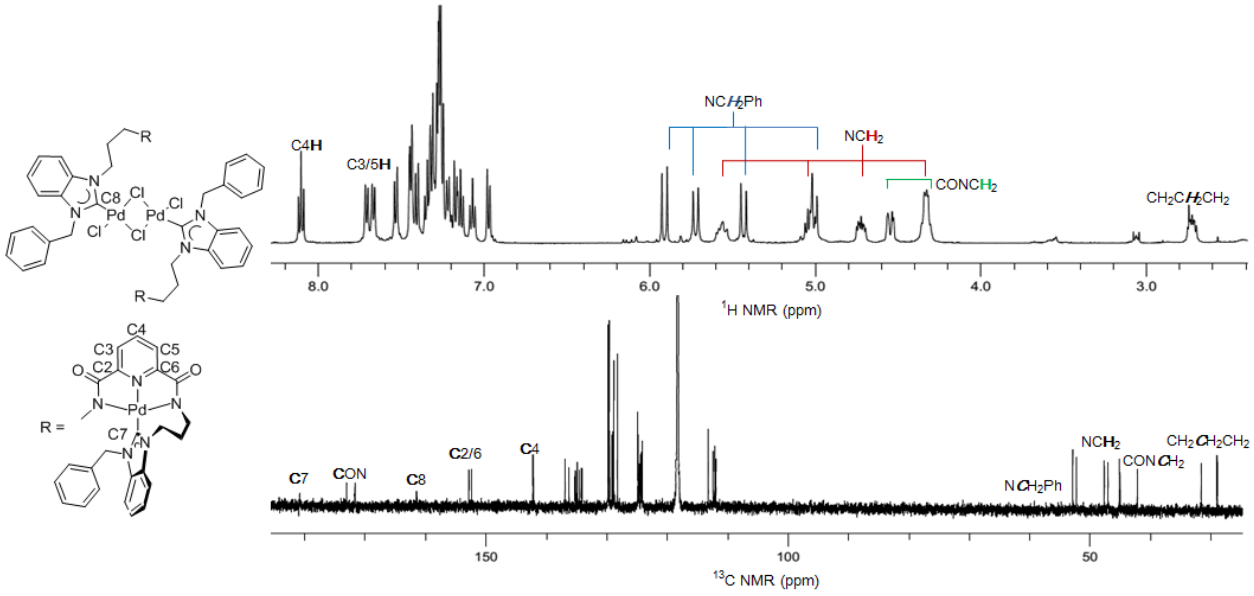

Figure 4.12. ^{1}H and ^{13}C NMR spectra of tetranuclar complex **79** (CD_3CN).

To study a possible pathway for the formation of the tetranuclear complex **79**, complex precursor $[PdCl(N',N,N')]BF_4$ (**78$_{Bn}$**) was treated with 0.6 equiv Ag_2O. The reaction proceeded smoothly at ambient temperature yielding complex **81**, in which one carbene was generated and replaced the chlorido ligand on the Pd(II) center, while the other azolium moiety remained intact and dangling (Scheme 4.7). A remarkable shift of base peak from *m*/*z* 802 to 766 in the positive

mode ESI mass spectrum was observed due to the loss of chlorido ligand upon cyclization. The unsymmetrical bonding of the ligand leads to signal doubling in NMR spectra. Expectedly, the ^{1}H NMR signals of the dangling benzimidazolium moiety resemble that of the precursor salt $\mathbf{M_{Bn}}$. In contrast, the cyclized unit gives rise to diasterotopic hydrogen signals as what observed for the tetranuclear complex **79**.

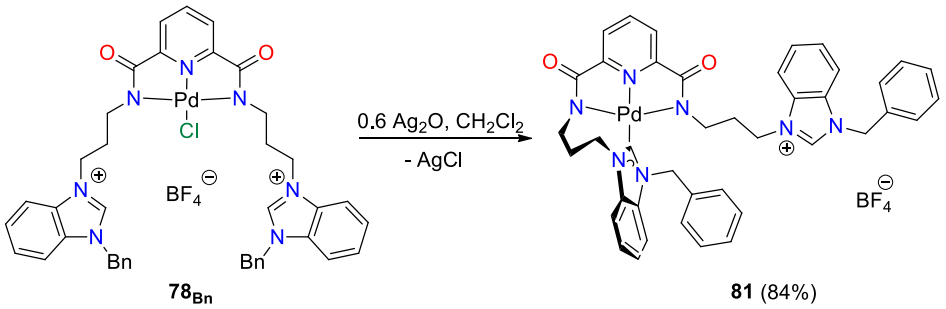

Scheme 4.7. Synthesis of complex **81**.

Complex **81** was then reacted with $Pd(OAc)_2$ and tetramethylammnoiun chloride. Indeed, the tetranuclear complex **79** was isolated again (Scheme 4.8). Hence, formation of the tetranuclear complex **79** from complex $\mathbf{78_{Bn}}$ is a two-step process involving a first carbene generation and pincer-Pd(II) coordination followed by a second carbene formation, Pd(II) coordination and subsequent dimerization.

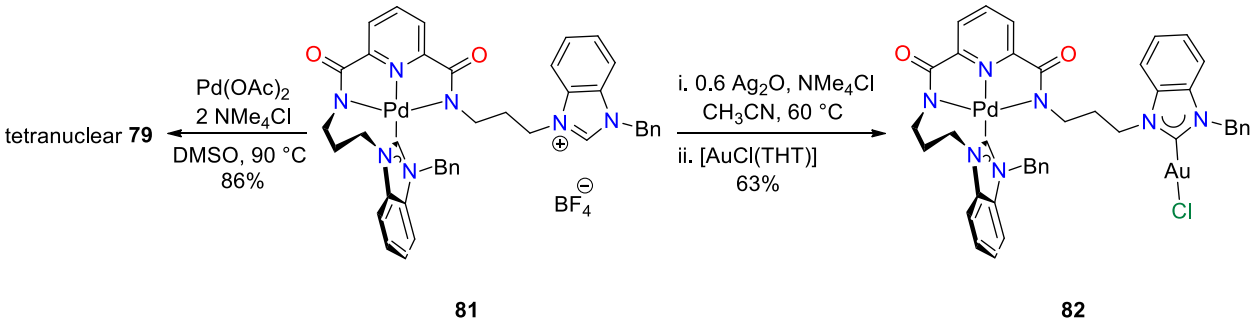

Scheme 4.8. Synthesis of tetranuclaer complexes **79** and hetero-bimetallic [Pd(II)/Au(I)] complex **82** from complex **81**.

Table 4.1. Selected NMR data of salts $\mathbf{M_{Bn/Me}}$, their Ag(I)-complexes $\mathbf{72_{Bn/Me}}$, and Pd(II)-complexes **77**–**82**.

complex	NC(***H***)N	CON(***H***)	N***C***(H)N	***C***ON(H)	***C***2, ***C***6
$\mathbf{M_{Bn}}$[a]	9.35	8.75	142.7	164.9	149.7
$\mathbf{M_{Me}}$[a]	9.14	8.54	142.9	164.8	149.5
$\mathbf{72_{Bn}}$[a]	-	8.57	-[d]	164.4	149.5
$\mathbf{72_{Me}}$[b]	-	9.02	-[d]	162.3	148.0
$\mathbf{77_{Bn}}$[c]	-	9.20	180.3	164.3	149.8
$\mathbf{77_{Me}}$[c]	-	9.12	179.4	164.1	149.3
$\mathbf{78_{Bn}}$[c]	9.98	-	143.1	171.7	152.9
$\mathbf{78_{Me}}$[a]	9.50	-	143.4	171.7	153.1
79[a]	-	-	180.8, 161.5	173.0, 171.7	152.8, 152.4
80[a]	-	-	180.9, 165.5	173.0, 171.6	152.7, 152.4
81[c]	9.67	-	179.4, 142.5	173.3, 171.7	152.3, 151.9
82[a]	-	-	180.7, 179.0	172.9, 171.8	152.6, 152.5

[a] Measured in CD_3CN. [b] Measured in d_6-DMSO. [c] Measured in $CDCl_3$. [d]The signals were not resolved despite of prolonged acquisition time.

The remaining benzimidazolium salt moiety in complex **81** could also offer access to hetero-bimetallic complexes. It was hence reacted with 0.6 equiv Ag_2O in the presence of 1 equiv tetramethylammonium chloride to afford the Ag NHC complex intermediate. Without isolation, the Ag NHC complex was directly used for the subsequent transmetalation to Au(I) by reacting with [AuCl(THT)] (Scheme 4.8).

The yellow hetero-bimetallic (palladium, gold) complex **82** was yielded with good solubilities in $CHCl_3$, CH_2Cl_2, CH_3CN, and DMSO. ESI-MS shows a base peak at 998 for the $[M + H]^+$ fragemnt. In comparison to the NMR spectra recorded for the complex precursor **81**, the ^1H NMR spectrum of complex **82** shows the absence of the NCHN acidic proton signal. Moreover,

the second set of the propylene protons become diasterotopic upon coordination to the gold(I) center.

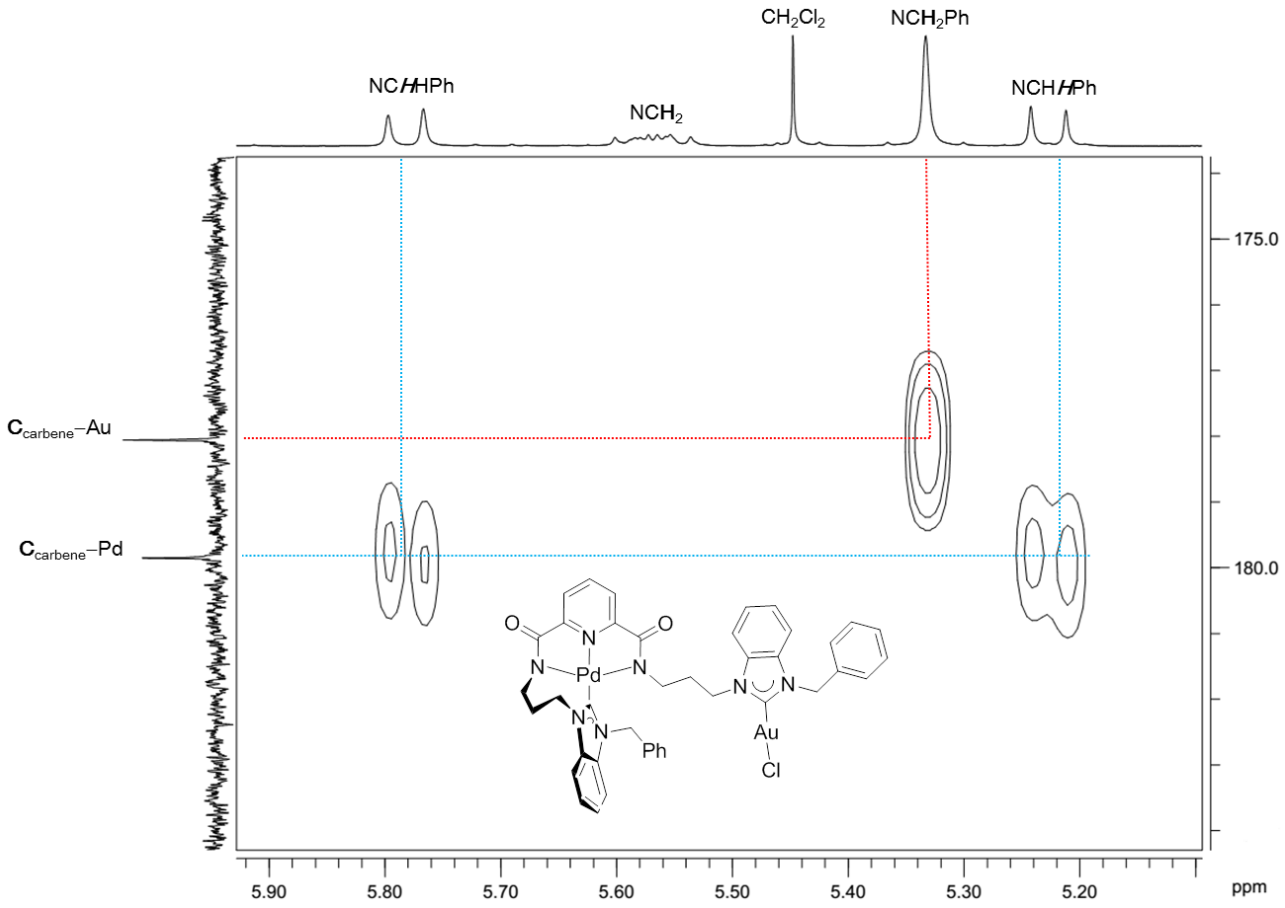

Figure 4.13. Section of the 2D $^{1}H,^{13}C$-HMBC NMR spectrum of complex **82**.

Notably, ^{13}C NMR spectrum of complex **82** in CD_3CN shows two downfield signals at 180.7 and 179.0 due to the two distinct carbene carbon atoms. The signal at 180.7 ppm can be readily assigned to the Pd–$C_{carbene}$ as it is similar to that observed in the tetranuclear complex **79** (180.8 ppm) or the pyridine cleaved complex **80** (180.9 ppm). The difference of 1.0 ppm compared to that of the precursor complex **81** (179.4 ppm, $CDCl_3$) is likely due to the different solvent effect. The new $^{13}C_{carbene}$ signal at 179.0 ppm is in the range typically reported for [AuCl(NHC)] (NHC = benzimidazolin-2-ylidene) complexes and hence was assigned to the

Au–$C_{carbene}$.[97b,104] The assignment was further corroborated by 2D $^{1}H,^{13}C$-HMBC spectroscopy, which shows correlation peaks of the 180.7 ppm signal to the two diasterotopic benzylic protons of Pd–NHC. In contrast, the benzylic protons of the Au–NHC remain as a singlet and a cross-peak correlating to the 179.0 ppm is observed (Figure 4.13).

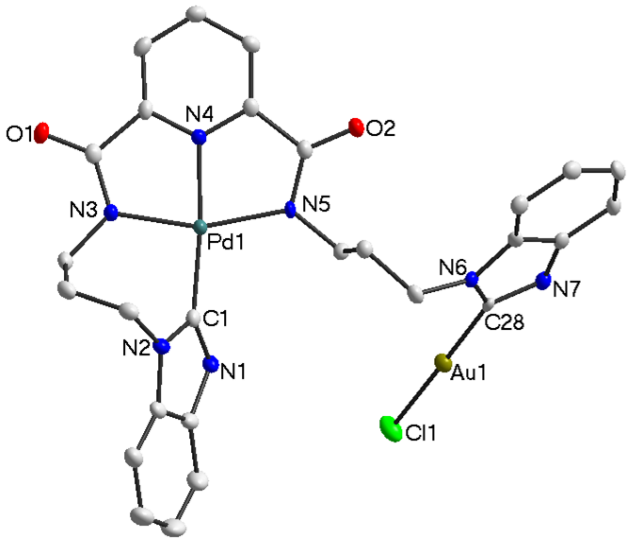

Figure 4.14. Molecular structure of **82** showing 50% probability ellipsoids; solvent molecules, hydrogen atoms and the benzyl substituents on N1 and N7 are omitted for clarity Selected bond lengths [Å] and bond angles [deg]: Pd1-C1 1.984(3), Pd1-N3 2.015(3), Pd1-N4 1.957(3), Pd1-N5 2.045(3), Au1-C28 1.975(3), Au1-Cl1 2.2679(3), C1-Pd1-N3 93.97(12), N3-Pd1-N4 80.80(11), N4-Pd1-N5 79.70(11), N5-Pd1-C1 105.55(12), N4-Pd1-C1 174.52(12), N3-Pd1-N5 160.46(11), C28-Au1-Cl1 179.05(10); $PdCN_3$/NHC dihedral angle: 55.3 °.

Single crystals suitable for X-ray diffraction analysis were obtained for complex **82** via diffusion of diethyl ether into a concentrated solution in CH_3CN. The determined structure confirms the expected connectivity (Figure 4.14). The palladium is coordinated by the N',N,N' pincer and one NHC in a square planar geometry. The dihedral angle between the PdCN4 coordination plane and the NHC plane is 55.3°. The gold, on the other hand, is coordinated by the second NHC and one chlorido ligand in a linear fashion.

5. Conclusion

This dissertation deals with synthesis, functionalization and application of transition metal (mainly palladium) complexes bearing benzannulated N-heterocyclic carbene ligands. The findings were presented in three chapters.

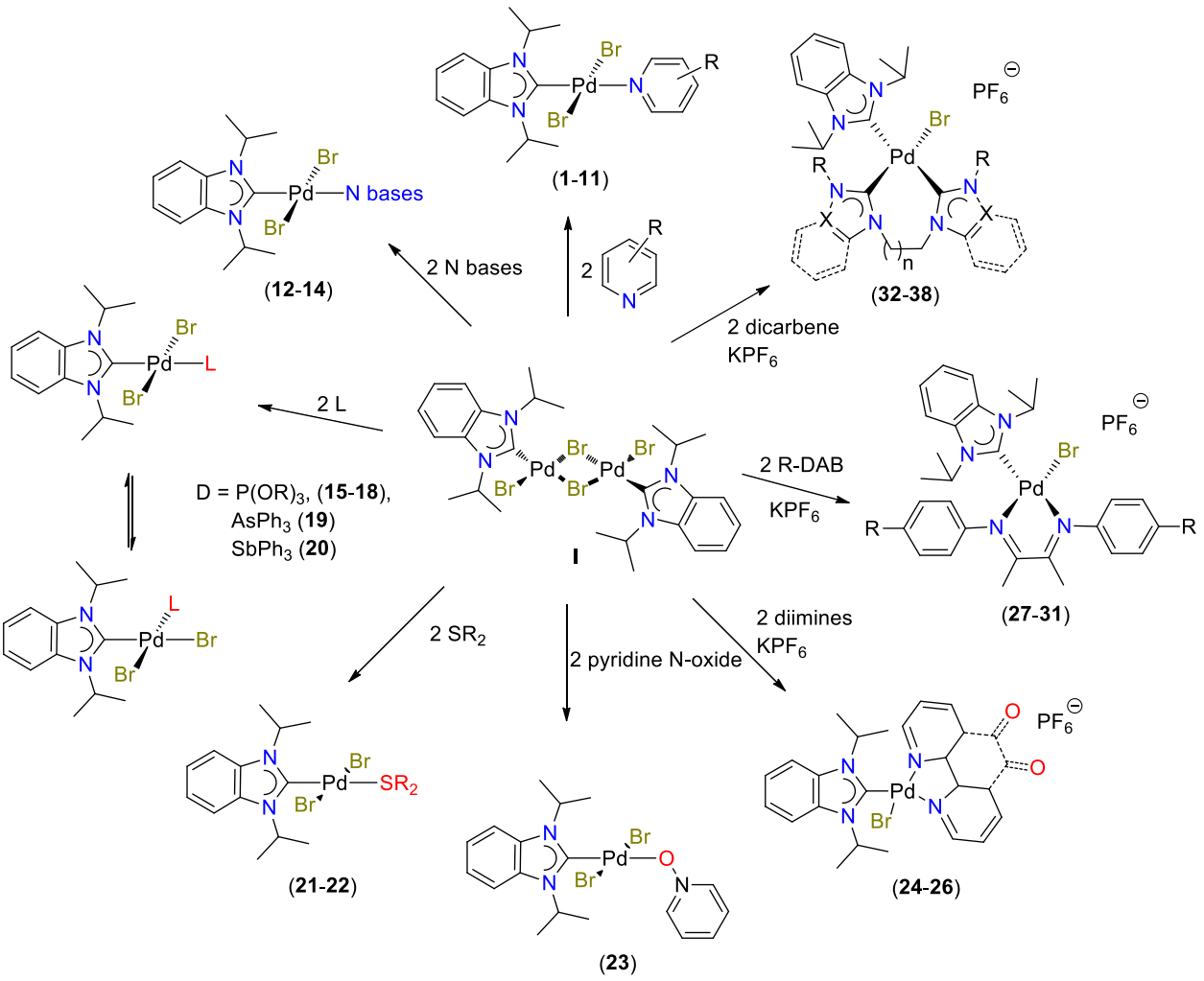

Scheme 5.1. $[PdBr_2(^iPr_2\text{-bimy})(L)]$ and $[PdBr(^iPr_2\text{-bimy})(L_2)]PF_6$ complexes.

Chapter 2 described the synthesis of complexes with the formula $[PdBr_2(^iPr_2\text{-bimy})(L)]$ (**1**–**23**) via bridge-cleavage reaction of the common complex precursor $[PdBr_2(^iPr_2\text{-bimy})]_2$ with

various monodentate ligands L. Based on the $^{13}C_{carbene}$ NMR resonances of the *trans*-[$PdBr_2$($^{i}Pr_2$-bimy)(L)] complexes, the electron donating abilities of the ligands L including substituted pyridines, other nitrogen bases, phosphites, triphenylarsine, thioethers and pyridine N-oxide were ranked. The study was also extended to bidentate ligands via the synthesis and characterization of 15 cationic complexes of the type [PdBr($^{i}Pr_2$-bimy)(L_2)]PF_6 (**24**–**38**) (L_2 = aromatic 1,2-diimines, diazabutadienes or methylene-, ethylene- and propylene-bridged di-N-heterocyclic carbenes) through similar bridge-cleavage reaction of [$PdBr_2$($^{i}Pr_2$-bimy)]$_2$. The $^{13}C_{carbene}$ NMR signals of the $^{i}Pr_2$-bimy reporter ligand in the chelate complexes reflect the net electron donating abilities of the L_2 ligands.

Notably, this method is sufficiently sensitive to detect subtle changes within the same type of ligands. Based on the data, it can be concluded that substituents (up to five bonds away) do influence the electronic properties of ligands in general including pyridines, phosphites, thioethers, diazabutadienes and diNHCs (N-substituents or linkers). In addition, the ligands backbones of diimines (benzannulated or carbonyl groups), NHCs (unsaturated, benzannulated, or heteroatom) have a significant influence on their donor strengths. These findings, although in some cases contradicting previous results obtained from carbonyl-based systems, are reasonable and able to reflect the influence of inductive and mesomeric effects more correctly.

Although most of the electron donating property was accurately determined, the difficulty in determining the donor strengths of very bulky ligands accurately represents one limitation of the ^{13}C NMR based method to be studied in future. In addition, the current study of bidentate ligands was only restricted to the symmetrical and neutral ligands. The exploration of asymmetrical or anionic types using this method is challenging at this stage, yet an interesting area for future research.

Chapter 3 introduced a new postmodification method to prepare mono- and bis-(functionalized-NHC) complexes (**47**–**52** and **57**–**67**), which was mainly realized via nucleophilic substitution reactions of the two parent complexes *trans*-[$PdBr_2(C_3Br$-bimy)(Py)] (**44**) and *trans*-[$PdBr_2(C_3Br$-bimy)$_2$] (**45**). Depending on the nature of the nucleophiles, competing co-ligand displacements also occurred in several cases. The resulting complexes could undergo further postmodifications. For example, third generation base-assisted hydrolysis of the mono-(thioester-functionalized) NHC complex **52** gave rise to a propyl-thiolato-bridged dinuclear complex **53**, which was subsequently oxidized by Oxone affording a sulfonate-functionalized NHC complex **54**. Moreover, second generation ethylation of the amino NHC complex **58** yielded a tetraalkylammonium-functionalized complex *trans*-[$PdBr_2(C_3NEt_3$-bimy)$_2$]Br_2 (**68**), which showed a positive effect in catalyzing the Mizoroki-Heck coupling reactions compared to its parent complexes.

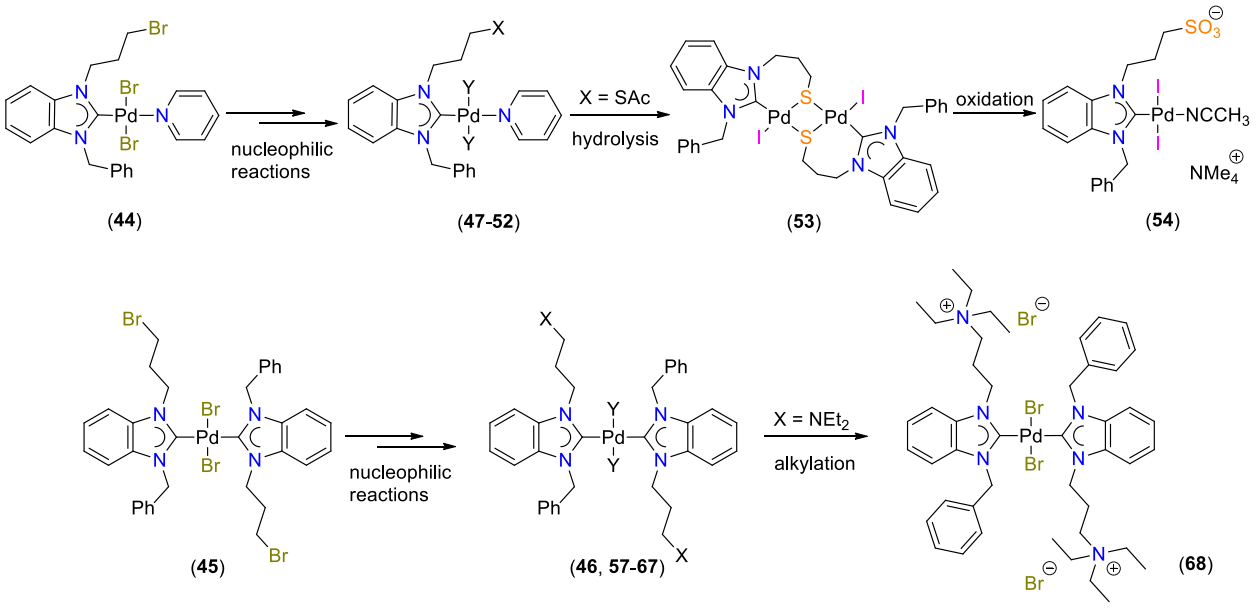

Scheme 5.2. Mono- and bis-(functionalized NHC) Pd(II) complexes.

Notably, the thioester or thiocyanate functionalized NHC complexes are not accessible via the traditional way due to the incompatibilities with coordination conditions. Moreover, the new synthetic approach to the sulfonate NHC complex proved necessary as it is feasible to synthesize analogous complex with a xylenyl linker, which is also not obtainable via prefunctionalization due to the unavailability of the corresponding sultone precursor. All these highlight the importance of the current postmodification protocol, which not only complements the traditional methodology, but also provides functionalized NHC compounds that are otherwise not accessible.

Further research employing different types of postmodification reactions is needed to increase the modularity and diversity of this approach. For instance, copper catalyzed azide–alkyne cycloaddition (Click) reactions of the azido–NHC complexes to form triazole NHC-complexes, or their Staudinger reduction to form NHC complexes bearing a primary amino group can be considered. Moreover, the SCN-functionalized NHC complexes could be hydrolyzed to a thiocarbamate in the Riemschneider thiocarbamate synthesis. It is also feasible that such a strategy could be useful in the anchoring of NHC based complexes on various solid supports for immobilization and use in heterogeneous catalysis. In addition, extension of this approach to other heterocycles and haloalkyl/aryl spacers as well as to other metal centers is conceivable to extend its generality and applicability.

Chapter 4 presented the application of benzimidazolin-2-ylidenes functionalized with a dipropyl-pyridine-2,6-dicarboxamide bridge, as building blocks in metallosupramolecular chemistry. The silver dicarbene complexes $\mathbf{72_{Bn/Me}}$ were obtained by reacting the dibenzimidazolium salts $\mathbf{M_{Bn/Me}}$ with Ag_2O. Transmetalation to gold(I) afforded two metallocyclic monogold and digold complexes with same empirical formula. The di-Au(I)

complex could be further deprotonated at the amide groups and in the presence of $CoCl_2 \cdot 6H_2O$, affording a bimetallic gold-cobalt trinuclear complex **76** with a double-stranded helicate architecture.

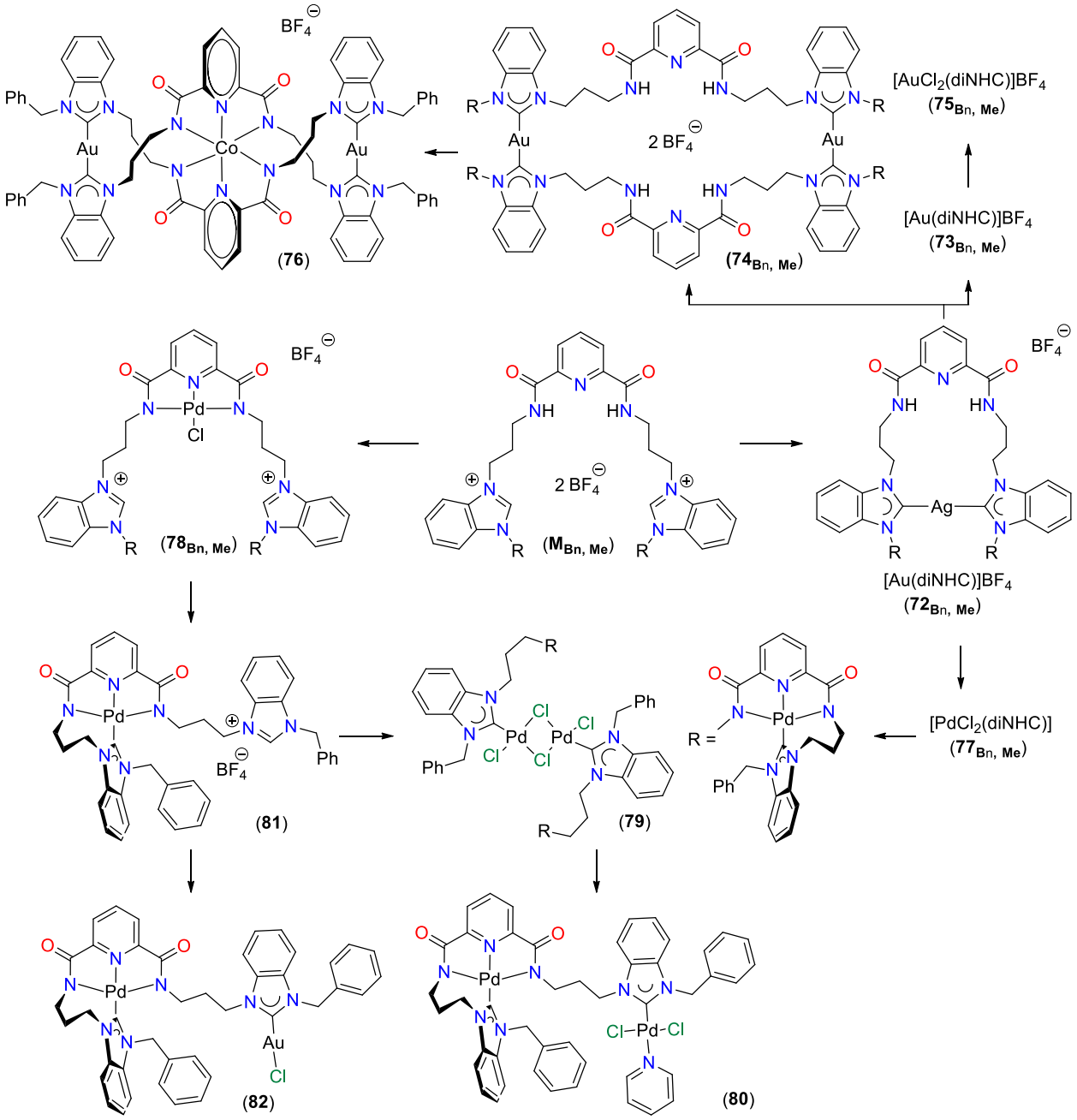

Scheme 5.3. Complexes bearing dipropyl-pyridine-2,6-dicarboxamide bridged dibenzimidazolin-2-ylidene ligands.

The silver intermediates **72$_{Bn/Me}$** could also react with palladium, giving only the mono-Pd(II) complexes **77$_{Bn/Me}$**. Deprotonation of complex **77$_{Bn}$** with $Pd(OAc)_2$ afforded an unexpected tetra-palladium complex **79**. This complex was also obtainable via reacting $Pd(OAc)_2$ with a $[PdCl(N^{'},N,N^{'})]BF_4$ complex **78$_{Bn}$**, which in turn was prepared by palladation of the dipropylpyridine-2,6-dicarboxamide bridged dibenzimidazolium salts **M$_{Bn}$** in the presence of NEt_3 base. Formation of **79** from **78$_{Bn}$** proved to be a two-step process as evidenced by the isolation of the intermediate complex **81**, which could also serve as a complex precursor to the hetero-bimetallic palladium-gold complex **82**.

The coordination chemistry of the dipropyl-pyridine-2,6-dicarboxamide bridged dibenzimidazolin-2-ylidene ligand described here is preliminary. Future investigation may be extended to other metals such as Fe, Ru, Ir, Cu and Ni. The versatile coordination geometries of different metal centers may lead to more diverse architectures. In addition, applications of the resulting complexes will be worth exploring. For instance, the phenomenon that one BF_4^- anion sits right in the center of the 36-membered-metallocycle in the solid state structure of complex **74$_{Bn}$** provided hints for a potential future exploration of such molecules for anion recognition. In addition, the multimetallic complexes may show cooperative effects in catalysis, or the hetero-multimetallic complexes may be employed in catalyzing tandem reactions.

6. Experimental Section

General considerations

Unless otherwise noted all operations were performed without taking precautions to exclude air and moisture. All solvents and chemicals were used as received without any further treatment if not noted otherwise. ^{1}H, ^{13}C, ^{19}F, and ^{31}P NMR spectra were recorded on a Bruker ACF 300 spectrometer or a Bruker AMX 500 spectrometer. The chemical shift (δ) were internally referenced to the residual solvent signals relative to tetramethylsilane (^{1}H and ^{13}C), or externally to CF_3CO_2H (^{19}F) and 85% H_3PO_4 (^{31}P). ESI mass spectra were measured using a Finnigan LCQ spectrometer. Elemental analyses were performed on an Elementar Vario Micro Cube elemental analyzer at the Department of Chemistry, National University of Singapore.

Complex $[PdBr_2(^{i}Pr_2\text{-bimy})]_2$ (**I**) was prepared according to literature.[58] $[PdBr_2(CH_3CN)_2]$ was prepared by stirring $PdBr_2$ in CH_3CN at 50 ℃ for 3 h. Fresh NaSPh was prepared via reaction of HSPh and NaOH (molar ratio, 1:1.2) in degassed EtOH.

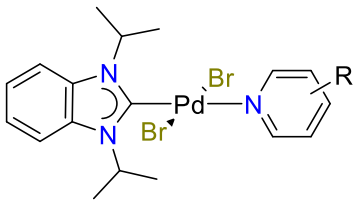

***trans*-[PdBr$_2$(^{i}Pr$_2$-bimy)(R-Py)]** (**1**–**11**). The suitable pyridine (0.10 mmol) was added to the solution of complex **I** (47 mg, 0.05 mmol) in CH_2Cl_2 (15 mL) and stirred for 2 h. The volatile was removed under reduced pressure and the residue washed with small amount of diethyl ether to give the product as yellow solids.

R = 3-F, (**1**). Yield: 55 mg, 0.10 mmol, 97%. ^{1}H NMR (500 MHz, $CDCl_3$): δ 9.12 (t, 1 H, Py–H), 9.02 (d, 1 H, Py–H), 7.58 (dd, 2 H, Ar–H), 7.55–7.52 (m, 1 H, Py–H), 7.39–7.35 (m, 1 H, Py–H), 7.22 (dd, 2 H, Ar–H), 6.30 (m, ^{3}J(H,H) = 7.0 Hz, 2 H, NCH), 1.79 (d, ^{3}J(H,H) = 7.0 Hz,

12 H, CH_3). $^{13}C\{^1H\}$ NMR (125.77 MHz, $CDCl_3$): 159.8 (d, ^1J(C,F) = 253.9 Hz, Py–C), 158.6 ($C_{carbene}$), 149.6 (d, ^3J(C,F) = 4.6 Hz, Py–C), 142.5 (d, ^2J(C,F) = 30.2 Hz, Py–C), 134.1 (Ar–C), 125.8 (d, ^2J(C,F) = 12.8 Hz), 125.7, 123.0, 113.3 (Ar–C), 55.3 (NCH), 21.2 (CH_3). $^{19}F\{^1H\}$ NMR (282.38 MHz, $CDCl_3$): –46.3 (F). Anal. Calcd for $C_{18}H_{22}Br_2FN_3Pd$: C, 38.22; H, 3.92; N, 7.43. Found: C, 38.36; H, 3.67; N, 7.38. MS (ESI): *m/z* 469 $[M – Py + H]^+$.

R = 3-Cl, (**2**). Yield: 58 mg, 0.10 mmol, >99%. ^1H NMR (500 MHz, $CDCl_3$): δ 9.18 (d, 1 H, Py–H), 9.07 (d, 1 H, Py–H), 7.77–7.76 (m, 1 H, Py–H), 7.59 (dd, 2 H, Ar–H), 7.33–7.30 (m, 1 H, Py–H), 7.22 (dd, 2 H, Ar–H), 6.30 (m, ^3J(H,H) = 7.0 Hz, 2 H, NCH), 1.79 (d, ^3J(H,H) = 7.0 Hz, 12 H, CH_3). $^{13}C\{^1H\}$ NMR (125.77 MHz, $CDCl_3$): δ 158.7 ($C_{carbene}$), 152.4, 151.4, 138.6, 134.1, 133.3, 125.5, 123.0, 113.3 (Ar–C), 55.3 (NCH), 21.2 (CH_3). Anal. Calcd for $C_{18}H_{22}Br_2ClN_3Pd$: C, 37.14; H, 3.81; N, 7.22. Found: C, 37.31; H, 3.80; N, 7.22. MS (ESI): *m/z* 469 $[M – Py + H]^+$.

R = 3-Br, (**3**). Yield: 60 mg, 0.1 mmol, 96%. ^1H NMR (500 MHz, $CDCl_3$): δ 9.26 (d, 1 H, Py–H), 9.11 (m, 1 H, Py–H), 7.93–7.91 (m, 1 H, Py–H), 7.59 (dd, 2 H, Ar–H), 7.28–7.25 (m, 1 H, Py–H), 7.22 (dd, 2 H, Ar–H), 6.29 (m, ^3J(H,H) = 7.0 Hz, 2 H, NCH), 1.79 (d, ^3J(H,H) = 7.0 Hz, 12 H, CH_3). $^{13}C\{^1H\}$ NMR (125.77 MHz, $CDCl_3$): 158.6 ($C_{carbene}$), 154.4, 151.7, 141.5, 134.1, 125.9, 123.0, 121.3, 113.3 (Ar–C), 55.3 (NCH), 21.2 (CH_3). Anal. Calcd for $C_{18}H_{22}Br_3N_3Pd$: C, 34.51; H, 3.54; N, 6.71. Found: C, 34.75; H, 3.35; N, 6.75. MS (ESI): *m/z* 469 $[M – Py + H]^+$.

R = 3-I, (**4**). Yield: 45 mg, 0.07 mmol, 67%. ^1H NMR (500 MHz, $CDCl_3$): δ 9.36 (s, 1 H, Py–H), 9.12 (d, 1 H, Py–H), 8.09 (d, 1 H, Py–H), 7.59 (dd, 2 H, Ar–H), 7.22 (dd, 2 H, Ar–H), 7.16–7.13 (m, 1 H, Py–H), 6.29 (m, ^3J(H,H) = 7.0 Hz, 2 H, NCH), 1.79 (d, ^3J(H,H) = 7.0 Hz, 12 H, CH_3). $^{13}C\{^1H\}$ NMR (125.77 MHz, $CDCl_3$): 159.0 (Ar–C), 158.7 ($C_{carbene}$), 152.0, 147.0, 134.1, 126.3, 123.0, 113.3, 92.9 (Ar–C), 55.3 (NCH), 21.2 (CH_3). Anal. Calcd for

$C_{18}H_{22}Br_2IN_3Pd$: C, 32.10; H, 3.29; N, 6.24. Found: C, 32.23; H, 3.21; N, 6.27. MS (ESI): *m/z* 469 $[M - Py + H]^+$.

R = 3-OH, (**5**). Yield: 58 mg, 0.10 mmol, >99%. ^{1}H NMR (500 MHz, $CDCl_3$): δ 8.63 (d, 1 H, Py–H), 8.54 (d, 1 H, Py–H), 7.59 (dd, 2 H, Ar–H), 7.23 (dd, 2 H, Ar–H), 7.18–7.15 (m, 1 H, Py–H), 7.09–7.06 (m, 1 H, Py–H), 6.32 (m, ^3J(H,H) = 7.0 Hz, 2 H, NCH), 1.80 (d, ^3J(H,H) = 7.0 Hz, 12 H, CH_3). $^{13}C\{^1H\}$ NMR (125.77 MHz, $CDCl_3$): δ 159.6 ($C_{carbene}$), 153.6, 145.1, 141.9, 134.2, 125.27, 125.25, 123.0, 113.3 (Ar–C), 55.3 (NCH), 21.3 (CH_3). Anal. Calcd for $C_{18}H_{23}Br_2N_3OPd$: C, 38.36; H, 4.11; N, 7.46. Found: C, 38.52; H, 3.90; N, 7.37. MS (ESI): *m/z* 525 $[M - Br + CH_3CN]^+$.

R = 3-Ph, (**6**). Yield: 62 mg, 0.10 mmol, 99%. ^{1}H NMR (500 MHz, $CDCl_3$): δ 9.39 (d, 1 H, Py–H), 9.12 (dd, 1 H, Py–H), 7.95 (d, 1 H, Py–H), 7.62–7.59 (m, 4 H, Ar–H & Py–H), 7.49 (t, 2 H, Ar–H), 7.44–7.41 (m, 2 H, Ar–H), 7.21 (dd, 2 H, Ar–H), 6.37 (m, ^3J(H,H) = 7.0 Hz, 2 H, NCH), 1.81 (d, ^3J(H,H) = 7.0 Hz, 12 H, CH_3). $^{13}C\{^1H\}$ NMR (125.77 MHz, $CDCl_3$): δ 159.8 ($C_{carbene}$), 152.0, 151.7, 138.4, 137.1, 136.8, 134.1, 129.8, 129.3, 127.9, 124.9, 122.9, 113.2 (Ar–C), 55.2 (NCH), 21.2 (CH_3). Anal. Calcd for $C_{24}H_{27}Br_2N_3Pd$: C, 46.22; H, 4.36; N, 6.74. Found: C, 45.99; H, 4.02; N, 6.60. MS (ESI): *m/z* 697 $[M + CH_3CN + MeOH + H]^+$.

R = 4-Cl, (**7**). Yield: 47 mg, 0.08 mmol, 80%. ^{1}H NMR (500 MHz, $CDCl_3$): δ 9.08 (d, 2 H, Py–H), 7.58 (dd, 2 H, Ar–H), 7.36 (d, 2 H, Py–H), 7.21 (dd, 2 H, Ar–H), 6.29 (m, ^3J(H,H) = 7.0 Hz, 2 H, NCH), 1.78 (d, ^3J(H,H) = 7.0 Hz, 12 H, CH_3). $^{13}C\{^1H\}$ NMR (125.77 MHz, $CDCl_3$): δ 158.98 ($C_{carbene}$), 154.1, 147.2, 134.1, 125.6, 122.9, 113.2 (Ar–C), 55.2 (NCH), 21.2 (CH_3). Anal. Calcd for $C_{18}H_{22}Br_2ClN_3Pd$: C, 37.14; H, 3.81; N, 7.22. Found: C, 37.21; H, 3.72; N, 7.14. MS (ESI): *m/z* 469 $[M - Py + H]^+$.

R = 4-Br, (**8**). Yield: 56 mg, 0.09 mmol, 89%. ^{1}H NMR (500 MHz, $CDCl_3$): δ 8.94 (d, 2 H, Py–H), 7.58 (dd, 2 H, Ar–H), 7.53 (d, 2 H, Py–H), 7.21 (dd, 2 H, Ar–H), 6.29 (m, ^{3}J(H,H) = 7.0 Hz, 2 H, NCH), 1.78 (d, ^{3}J(H,H) = 7.0 Hz, 12 H, CH_3). $^{13}C\{^{1}H\}$ NMR (125.77 MHz, $CDCl_3$): δ 159.03 ($C_{carbene}$), 153.9, 136.1, 134.1, 128.7, 123.0, 113.3 (Ar–C), 55.2 (NCH), 21.2 (CH_3). Anal. Calcd for $C_{18}H_{22}Br_3N_3Pd$: C, 34.51; H, 3.54; N, 6.71. Found: C, 34.52; H, 3.59; N, 6.27 (the best result obtained). ^{1}H and ^{13}C NMR spectra are attached in the appendix. MS (ESI): *m/z* 469 $[M - Py + H]^+$.

R = 4-I, (**9**). Yield: 47 mg, 0.07 mmol, 70%. ^{1}H NMR (500 MHz, $CDCl_3$): δ 8.79 (d, 2 H, Py–H), 7.73 (d, 2 H, Py–H), 7.58 (dd, 2 H, Ar–H), 7.21 (dd, 2 H, Ar–H), 6.28 (m, ^{3}J(H,H) = 7.0 Hz, 2 H, NCH), 1.78 (d, ^{3}J(H,H) = 7.0 Hz, 12 H, CH_3). $^{13}C\{^{1}H\}$ NMR (125.77 MHz, $CDCl_3$): δ 159.2 ($C_{carbene}$), 153.3, 134.7, 134.1, 123.0, 113.3, 109.0 (Ar–C), 55.2 (NCH), 21.2 (CH_3). Anal. Calcd for $C_{18}H_{22}Br_2IN_3Pd$: C, 32.10; H, 3.29; N, 6.24. Found: C, 32.48; H, 3.25; N, 6.14. MS (ESI): *m/z* 469 $[M - Py + H]^+$.

R = 4-OH, (**10**). Yield: 58 mg, 0.10 mmol, >99%. ^{1}H NMR (500 MHz, $CDCl_3$): δ 8.59 (d, 2 H, Py–H), 7.59 (dd, 2 H, Ar–H), 7.21 (dd, 2 H, Ar–H), 6.67 (d, 2 H, Py–H), 6.32 (m, ^{3}J(H,H) = 7.0 Hz, 2 H, NCH), 1.79 (d, ^{3}J(H,H) = 7.0 Hz, 12 H, CH_3). $^{13}C\{^{1}H\}$ NMR (125.77 MHz, $CDCl_3$): δ 165.1 (Ar–C), 160.2 ($C_{carbene}$), 153.8, 134.2, 123.0, 113.3, 113.1 (Ar–C), 55.2 (NCH), 21.3 (CH_3). Anal. Calcd for $C_{18}H_{23}Br_2N_3OPd$: C, 38.36; H, 4.11; N, 7.46. Found: C, 38.56; H, 3.76; N, 7.59. MS (ESI): *m/z* 525 $[M - Br + CH_3CN]^+$.

R = 4-Ph, (**11**). Yield: 54 mg, 0.09 mmol, 87%. ^{1}H NMR (500 MHz, $CDCl_3$): δ 9.16 (d, 2 H, Py–H), 7.63–7.60 (m, 4 H, Ar–H), 7.56–7.55 (d, 2 H, Py–H), 7.49–7.48 (m, 3 H, Ar–H), 7.22 (br–s, 2 H, Ar–H), 6.38 (m, ^{3}J(H,H) = 7.0 Hz, 2 H, NCH), 1.81 (d, ^{3}J(H,H) = 7.0 Hz, 12 H, CH_3). $^{13}C\{^{1}H\}$ NMR (125.77 MHz, $CDCl_3$): δ 160.2 ($C_{carbene}$), 153.4, 150.8, 137.3, 134.1, 130.5, 129.9,

127.7, 122.9, 122.8, 113.2 (Ar–C), 55.2 (NCH), 21.2 (CH_3). Anal. Calcd for $C_{24}H_{27}Br_2N_3Pd$: C, 46.22; H, 4.36; N, 6.74. Found: C, 46.60; H, 3.99; N, 6.72. MS (ESI): *m/z* 697 [M + CH_3CN + MeOH + H]$^+$.

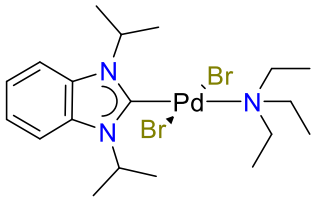

***trans*-[PdBr$_2$(^{i}Pr$_2$-bimy)(TEA)]** (**12**). 2.5 equiv of triethylamine (TEA) (35 μL, 0.25 mmol) was added to the suspension of **I** (47 mg, 0.05 mmol) in CH_2Cl_2 (20 mL) and stirred overnight. The volatiles were removed in vacuo, affording the product as a yellow powder (57 mg, 0.10 mmol, >99%). ^{1}H NMR (300 MHz, $CDCl_3$): δ 7.52 (dd, 2 H, Ar–H), 7.15 (dd, 2 H, Ar–H), 6.22 (m, ^3J(H,H) = 7.1 Hz, 2 H, NCH), 3.03 (m, ^3J(H,H) = 7.1 Hz, 6 H, NCH_2), 1.74 (d, ^3J(H,H) = 7.1 Hz, 12 H, CH_3), 1.34 (t, ^3J(H,H) = 7.1 Hz, 9 H, CH_2CH_3). ^{13}C{^{1}H} NMR (75.48 MHz, $CDCl_3$): 158.0 ($C_{carbene}$), 134.0, 122.6, 113.0 (Ar–C), 54.7 (NCH), 48.9 (NCH_2), 20.9 (CH_3), 10.8 (NCH_2CH_3). Anal. Calcd for $C_{19}H_{33}Br_2N_3Pd$: C, 40.06; H, 5.84; N, 7.38. Found: C, 38.71; H, 5.79; N, 7.06 (the best result obtained). ^{1}H and ^{13}C NMR spectra are attached in the appendix. MS (ESI): *m/z* 469 [M – TEA + H]$^+$.

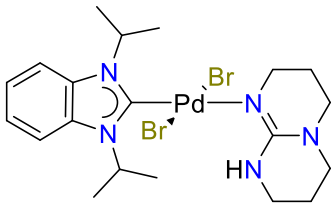

***trans*-[PdBr$_2$(^{i}Pr$_2$-bimy)(TBD)]** (**13**). Compound 1,5,7-Triazabicyclo[4.4.0]dec-5-ene (TBD) (14 mg, 0.10 mmol) was added to the suspension of dimer **I** (47 mg, 0.05 mmol) in CH_2Cl_2 (20 mL) and stirred for 1 h. Solvent was removed under reduced pressure. The residue was washed with hexane (3 × 10 mL) and dried in vacuo, affording the product as a yellow powder (61 mg, 0.10 mmol, >99%). ^{1}H NMR (300 MHz, $CDCl_3$): δ 7.50 (dd, 2 H, Ar–H), 7.13 (dd, 2 H, Ar–H), 6.27 (m, ^3J(H,H) = 7.1 Hz, 2 H, NCH), 3.49 (t, ^3J(H,H) = 5.6 Hz, 2 H,

TBD–CH_2), 3.26 (t, ^3J(H,H) = 5.8 Hz, 2 H, TBD–CH_2), 3.10–3.05 (m, 4 H, TBD–CH_2), 1.90 (m, 4 H, TBD–CH_2), 1.74 (d, ^3J(H,H) = 7.1 Hz, 12 H, CH_3). $^{13}C\{^1H\}$ NMR (75.48 MHz, $CDCl_3$): 165.8 ($C_{carbene}$), 152.4 (C=N), 134.0, 122.5, 113.0 (Ar–C), 54.8 (NCH), 48.4, 48.0, 46.8, 40.1, 23.9, 22.8 (TBD–C), 21.4 (CH_3). Anal. Calcd for $C_{20}H_{31}Br_2N_5Pd$: C, 39.53; H, 5.14; N, 11.52. Found: C, 39.86; H, 5.08; N, 11.31. MS (ESI): *m/z* 528 $[M - Br]^+$.

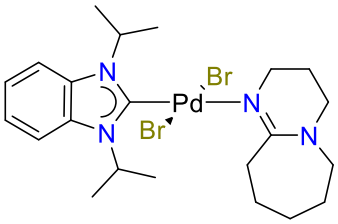

***trans*-[PdBr$_2$(^{i}Pr$_2$-bimy)(DBU)]** (**14**). Complex **14** was prepared in analogy to complex **13** from 1,8-diazabicyclo[5.4.0]undec-7-ene (DBU) (15 µL, 0.10 mmol) and dimer **I** (47 mg, 0.05 mmol). Yield: 62 mg, 0.10 mmol, >99%. ^{1}H NMR (500 MHz, $CDCl_3$): δ 7.52 (dd, 2 H, Ar–H), 7.16 (dd, 2 H, Ar–H), 6.31 (br–s, 2 H, NCH), 3.56 (t, ^3J(H,H) = 5.5 Hz, 2 H, DBU–CH_2), 3.40–3.38 (m, 2 H, DBU–CH_2), 3.27–3.26 (m, 2 H, DBU–CH_2), 3.23 (t, ^3J(H,H) = 6.0 Hz, 2 H, DBU–CH_2), 1.98 (m, 2 H, DBU–CH_2), 1.89 (m, 2 H, DBU–CH_2), 1.77 (d, ^3J(H,H) = 7.0 Hz, 12 H, CH_3), 1.72 (m, 2 H, DBU–CH_2), 1.60 (br–s, 2 H, DBU–CH_2). $^{13}C\{^1H\}$ NMR (125.77 MHz, $CDCl_3$): 166.3 ($C_{carbene}$), 163.9 (C=N), 134.1, 122.6, 113.0 (Ar–C), 54.9 (NCH), 54.1, 48.5, 47.6, 38.7, 30.0, 28.6, 25.0, 23.1 (DBU–C), 21.4 (CH_3). Anal. Calcd for $C_{22}H_{34}Br_2N_4Pd$: C, 42.57; H, 5.52; N, 9.03. Found: C, 42.26; H, 5.21; N, 8.98. MS (ESI): *m/z* 582 $[M - Br + CH_3CN]^+$.

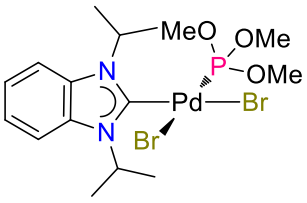

***cis*-[PdBr$_2$(^{i}Pr$_2$-bimy){P(OMe)$_3$}]** (*cis*-**15**). Complex **I** (24 mg, 0.03 mmol) and trimethylphosphite (6 µL, 0.05 mmol) were dissolved in $CDCl_3$ (0.6 mL) for direct NMR analysis. ^{1}H NMR (300 MHz, $CDCl_3$): δ 7.61 (dd, 2 H, Ar–H), 7.28 (dd, 2 H, Ar–H), 5.79 (m, ^3J(H,H) = 7.0 Hz, 2 H, NCH), 3.83 (d, ^3J(P,H) = 13 Hz, 6 H, OCH_3), 3.77 (d, ^3J(P,H) = 13 Hz, 3 H, OCH_3), 1.74 (d, ^3J(H,H) = 7.0 Hz, 6

H, NCH(CH_3)$_2$), 1.66 (d, ^3J(H,H) = 7.0 Hz, 6 H, NCH(CH_3)$_2$). ^{13}C{^{1}H} NMR (75.48 MHz, $CDCl_3$): 170.8 (d, ^2J(C,P) = 21.4 Hz, $C_{carbene}$), 133.8, 123.5, 113.7 (Ar–C), 55.2 (br–s, NCH), 55.0 (d, ^2J(P,C) = 5.5 Hz, OCH_3), 73.4 (d, ^2J(P,C) = 4.4 Hz, OCH_3), 21.0, 20.9 (NCH(CH_3)$_2$). ^{31}P{^{1}H} NMR (121.49 MHz, $CDCl_3$): 101.0 (P). Anal. Calcd for $C_{16}H_{27}Br_2N_2O_3PPd$: C, 32.43; H, 4.59; N, 4.73. Found: C, 32.56; H, 5.02; N, 4.45. MS (ESI): *m/z* 545 $[M - Br + MeOH]^+$.

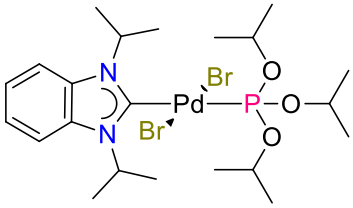

***trans*-[PdBr$_2$(^{i}Pr$_2$-bimy){P(O^{i}Pr)$_3$}]** (*trans*-**16**). ^{13}C-labeled complex **I** (9.4 mg, 0.01 mmol) and triisopropylphosphite (5 µL, 0.02 mmol) were dissolved in $CDCl_3$ (0.6 mL) for direct NMR spectroscopic analysis. ^{1}H NMR (300 MHz, $CDCl_3$): δ 7.56 (dd, 2 H, Ar–H), 7.21 (dd, 2 H, Ar–H), 5.91 (m, ^3J(C,H) = 4.3 Hz, ^3J(H,H) = 7.1 Hz, 2 H, NCH), 5.15 (m, ^3J(P,H) = 8.6 Hz, ^3J(H,H) = 6.1 Hz, 3 H, OCH), 1.77 (d, ^3J(H,H) = 7.1 Hz, 12 H, NCH(CH_3)$_2$), 1.42 (d, ^3J(H,H) = 6.1 Hz, 18 H, OCH(CH_3)$_2$). ^{13}C{^{1}H} NMR (75.48 MHz, $CDCl_3$): 175.3 (d, ^2J(C,P) = 287.1 Hz, $C_{carbene}$). ^{31}P{^{1}H} NMR (121 MHz, $CDCl_3$): 113.4 (d, ^2J(C,P) = 287.1 Hz, P).

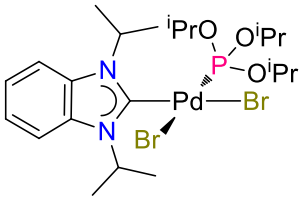

***cis*-[PdBr$_2$(^{i}Pr$_2$-bimy){P(O^{i}Pr)$_3$}]** (*cis*-**16**). Complex **I** (47 mg, 0.05 mmol) and triisopropylphosphite (25 µL, 0.10 mmol) were dissolved in CH_2Cl_2 (10 mL) and stirred for 0.5 h. The solvent was removed under reduced pressure and the residue was washed with diethyl ether to give the off-white product (57 mg, 0.08 mmol, 84%). ^{1}H NMR (500 MHz, $CDCl_3$): δ 7.58 (dd, 2 H, Ar–H), 7.23 (dd, 2 H, Ar–H), 5.82 (m, ^3J(H,H) = 7.0 Hz, 2 H, NCH), 5.15 (br–m, 3 H, OCH), 1.71 (d, ^3J(H,H) = 7.0 Hz, 6 H, NCH(CH_3)$_2$), 1.69 (d, ^3J(H,H) = 7.0 Hz, 6 H, NCH(CH_3)$_2$), 1.19 (d, ^3J(H,H) = 6.3 Hz, 18 H, OCH(CH_3)$_2$). ^{13}C{^{1}H} NMR (125.77 MHz, $CDCl_3$): 172.0 (d, ^2J(C,P) = 22.9 Hz, $C_{carbene}$), 133.8,

123.3, 113.4 (Ar–C), 73.4 (d, ^{2}J(P,C) = 4.6 Hz, OCH), 55.1 (d, ^{4}J(P,C) = 1.8 Hz, NCH), 24.5 (d, ^{3}J(P,C) = 4.6 Hz, OCH(CH_3)$_2$), 21.3, 21.1 (NCH(CH_3)$_2$). $^{31}P\{^{1}H\}$ NMR (202.45 MHz, $CDCl_3$): 90.4 (P). Anal. Calcd for $C_{22}H_{39}Br_2N_2O_3PPd$: C, 39.04; H, 5.81; N, 4.14. Found: C, 39.06; H, 5.40; N, 4.08. MS (ESI): *m/z* 628 $[M - Br + MeOH]^+$.

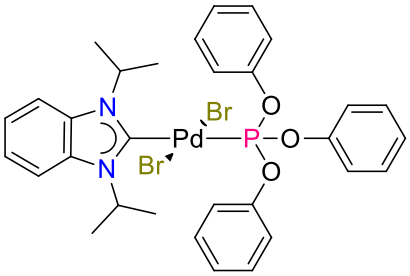

***trans*-[PdBr$_2$(^{i}Pr$_2$-bimy){P(OPh)$_3$}]** (*trans*-**17**). Complex **I** (24 mg, 0.03 mmol) and triphenylphosphite (13 µL, 0.05 mmol) were dissolved in $CDCl_3$ (0.6 mL) for direct NMR analysis. ^{1}H NMR (300 MHz, $CDCl_3$): δ 7.50–7.30 (m, 11 H, Ar–H), 7.25–7.14 (m, 8 H, Ar–H), 5.21 (m, ^{3}J(H,H) = 7.2 Hz, 2 H, NCH), 1.51 (d, ^{3}J(H,H) = 7.2 Hz, 12 H, CH_3). $^{13}C\{^{1}H\}$ NMR (75.48 MHz, $CDCl_3$): 171.7 (d, ^{2}J(C,P) = 289.8 Hz, $C_{carbene}$), 151.8 (d, ^{2}J(C,P) = 5.5 Hz, Ar–C), 134.0 (d, ^{4}J(C,P) = 9.3 Hz, Ar–C), 130.2, 125.7, 123.0 (Ar–C), 122.2 (d, ^{3}J(C,P) = 6.0 Hz, Ar–C), 113.5 (Ar–C), 54.6 (NCH), 21.3 (CH_3). $^{31}P\{^{1}H\}$ NMR (202.45 MHz, $CDCl_3$): 102.3 (P).

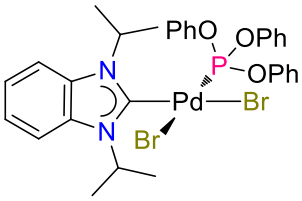

***cis*-[PdBr$_2$(^{i}Pr$_2$-bimy){P(OPh)$_3$}]** (*cis*-**17**). Complex **I** (47 mg, 0.05 mmol) and triphenylphosphite (26 µL, 0.10 mmol) were suspended in MeOH (10 mL) and stirred overnight. The off-white solid product was isolated by filtration and further dried in vacuo. Yield: 72 mg, 0.09 mmol, 93%. ^{1}H NMR (500 MHz, $CDCl_3$): δ 7.55 (d, 2 H, Ar–H), 7.34–7.29 (m, 11 H, Ar–H), 7.27–7.22 (m, 6 H, Ar–H), 5.32 (m, ^{3}J(H,H) = 7.0 Hz, 2 H, NCH), 1.57 (d, ^{3}J(H,H) = 7.0 Hz, 6 H, CH_3), 1.14 (d, ^{3}J(H,H) = 7.0 Hz, 6 H, CH_3). $^{13}C\{^{1}H\}$ NMR (125.77 MHz, $CDCl_3$): 169.3 (d, ^{2}J(C,P) = 22.9 Hz, $C_{carbene}$), 151.1 (d, ^{2}J(C,P) = 8.3 Hz, Ar–C), 133.9, 130.8, 126.7, 123.6 (Ar–C), 122.0 (d, ^{3}J(C,P) = 4.6 Hz,

Ar–C), 113.8 (Ar–C), 55.6 (NCH), 20.9, 20.8 (CH_3). $^{31}P\{^1H\}$ NMR (202.45 MHz, $CDCl_3$): 86.3 (P). Anal. Calcd for $C_{31}H_{33}Br_2N_2O_3PPd$: C, 47.81; H, 4.27; N, 3.60. Found: C, 48.13; H, 4.46; N, 3.90. MS (ESI): *m/z* 740 $[M - Br + CH_3CN]^+$.

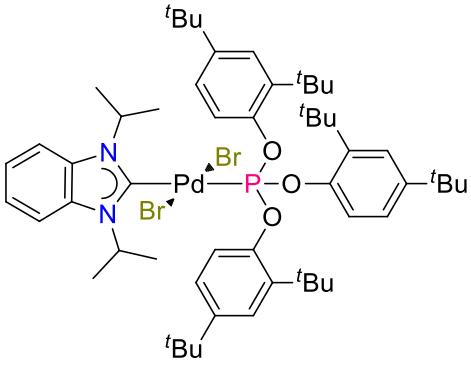

***trans*-[PdBr$_2$(^{i}Pr$_2$-bimy){P(O-2,4-^{t}Bu-Ph)$_3$}]** (**18**). This complex was synthesized by reacting complex **I** (47 mg, 0.05 mmol) and tris(2,4-di-*tert*-butyltriphenyl)phosphite (65 mg, 0.10 mmol) for 30 min in CH_2Cl_2 before dried in vacuum. Yield: 120 mg, 0.01 mmol, >99%. ^1H NMR (500 MHz, $CDCl_3$): δ 8.09 (dd, 3 H, Ar–H), 7.53 (dd, 2 H, Ar–H), 7.44 (d, 3 H, Ar–H), 7.22–7.20 (m, 5 H, Ar–H), 5.66 (m, ^3J(H,H) = 7.0 Hz, 2 H, NCH), 1.62 (s, 27 H, C(CH_3)$_3$), 1.59 (d, ^3J(H,H) = 7.0 Hz, 12 H, CH_3), 1.35 (s, 27 H, C(CH_3)$_3$). $^{13}C\{^1H\}$ NMR (125.77 MHz, $CDCl_3$): 171.5 (d, ^2J(C,P) = 289.6 Hz, $C_{carbene}$), 149.3 (d, ^2J(C,P) = 3.7 Hz, Ar–C), 146.8 (Ar–C), 139.5 (d, ^3J(C,P) = 5.5 Hz, Ar–C), 134.1 (d, ^4J(C,P) = 9.2 Hz, Ar–C), 125.5, 123.4, 122.9 (Ar–C), 120.1 (d, ^3J(C,P) = 11.9 Hz, Ar–C), 113.4 (Ar–C), 54.7 (NCH), 36.0, 35.2 (*C*(CH_3)$_3$), 32.3, 31.5 (C(*C*H_3)$_3$), 21.2 (CH_3). $^{31}P\{^1H\}$ NMR (202.45 MHz, $CDCl_3$): 103.6 (P). Anal. Calcd for $C_{55}H_{81}Br_2N_2O_3PPd$: C, 59.22; H, 7.32; N, 2.51. Found: C, 59.48; H, 7.12; N, 2.16. MS (ESI): *m/z* 1075 $[M - Br + CH_3CN]^+$.

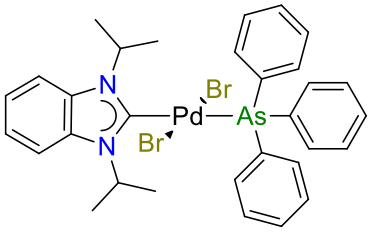

***trans*-[PdBr$_2$(^{i}Pr$_2$-bimy)(AsPh$_3$)]** (*trans*-**19**). Complex **I** (24 mg, 0.03 mmol) and triphenylarsine (15 mg, 0.05 mmol) were dissolved in $CDCl_3$ (0.6 mL) for direct NMR measurement. ^1H NMR (500 MHz, $CDCl_3$): δ 7.69–7.68 (m, 6 H, Ar–H), 7.59 (dd, 2

H, Ar–H), 7.44–7.39 (m, 9 H, Ar–H), 7.22 (dd, 2 H, Ar–H), 6.15 (m, ^{3}J(H,H) = 7.1 Hz, 2 H, NCH), 1.79 (d, ^{3}J(H,H) = 7.1 Hz, 12 H, CH_3). $^{13}C\{^{1}H\}$ NMR (125.77 MHz, $CDCl_3$): 169.2 ($C_{carbene}$), 135.2, 134.3, 133.5, 130.5, 129.2, 123.0, 113.5 (Ar–C), 55.1 (NCH), 21.5 (CH_3).

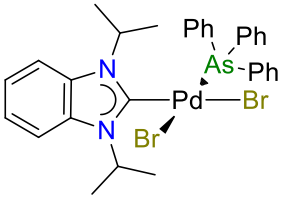

***cis*-[PdBr$_2$(^{i}Pr$_2$-bimy)(AsPh$_3$)]** (*cis*-**19**). The upper complex was left in $CDCl_3$ for 6 d to isomerize to this complex as major product. ^{1}H NMR (500 MHz, $CDCl_3$): δ 7.47 (dd, 2 H, Ar–H), 7.38 (t, ^{3}J(H,H) = 7.3 Hz, 4 H, Ar–H), 7.33–7.27 (m, 5 H, Ar–H), 7.25–7.19 (m, 8 H, Ar–H), 5.90 (m, ^{3}J(H,H) = 7.0 Hz, 2 H, NCH), 1.66 (d, ^{3}J(H,H) = 7.0 Hz, 6 H, CH_3), 0.89 (d, ^{3}J(H,H) = 7.0 Hz, 6 H, CH_3). $^{13}C\{^{1}H\}$ NMR (125.77 MHz, $CDCl_3$): 169.3 ($C_{carbene}$), 135.2, 134.1, 132.7, 131.3, 129.7 (2 ×), 113.4 (Ar–C), 55.4 (NCH), 21.6, 19.9 (CH_3). Anal. Calcd for $C_{31}H_{33}AsBr_2N_2Pd$: C, 48.06; H, 4.29; N, 3.62. Found: C, 48.42; H, 4.16; N, 3.80. MS (ESI): *m/z* 736 $[M - Br + CH_3CN]^+$.

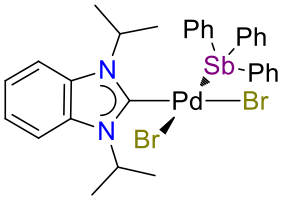

***cis*-[PdBr$_2$(^{i}Pr$_2$-bimy)(SbPh$_3$)]** (**20**). Complex **I** (24 mg, 0.03 mmol) and triphenylantimony (18 mg, 0.05 mmol) were dissolved in $CDCl_3$ (0.6 mL) for direct NMR measurement. ^{1}H NMR (500 MHz, $CDCl_3$): δ 7.49 (dd, 2 H, Ar–H), 7.36 (ps–t, 3 H, Ar–H), 7.31 (ps–d, 6 H, Ar–H), 7.25 (dd, 2 H, Ar–H), 7.20 (ps–t, 6 H, Ar–H), 5.88 (m, ^{3}J(H,H) = 7.0 Hz, 2 H, NCH), 1.66 (d, ^{3}J(H,H) = 7.0 Hz, 6 H, CH_3), 1.04 (d, ^{3}J(H,H) = 7.0 Hz, 6 H, CH_3). $^{13}C\{^{1}H\}$ NMR (125.77 MHz, $CDCl_3$): 167.5 ($C_{carbene}$), 136.1, 134.4, 131.4, 130.1, 129.9, 123.5, 113.3 (Ar–C), 55.3 (NCH), 21.4, 20.2 (CH_3). Anal. Calcd for $C_{31}H_{33}Br_2N_2PdSb$: C, 45.32; H, 4.05; N, 3.41. Found: C, 45.25; H, 3.99; N, 3.44. MS (ESI): *m/z* 782 $[M - Br + CH_3CN]^+$.

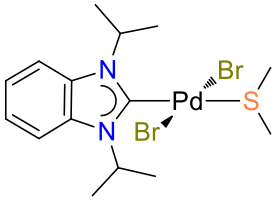

***trans*-[PdBr$_2$(^{i}Pr$_2$-bimy)(SMe$_2$)]** (**21**). Complex **21** was prepared in analogy to the pyridine complexes as a yellow solid from the reaction of dimethyl sulfide (8 µL, 0.10 mmol) and complex **I** (47 mg, 0.05 mmol) in CH_2Cl_2 (10 mL). Yield: 53 mg, 0.10 mmol, >99%. ^{1}H NMR (500 MHz, $CDCl_3$): δ 7.58 (dd, 2 H, Ar–H), 7.12 (dd, 2 H, Ar–H), 6.04 (m, ^3J(H,H) = 7.0 Hz, 2 H, NCH), 2.47 (s, 6 H, SCH_3), 1.74 (d, ^3J(H,H) = 7.0 Hz, 12 H, CH_3). ^{13}C{^{1}H} NMR (125.77 MHz, $CDCl_3$): 163.5 ($C_{carbene}$), 134.1, 123.1, 113.4 (Ar–C), 55.2 (NCH), 21.8 (SCH_3), 21.3 (CH_3). Anal. Calcd for $C_{15}H_{24}Br_2N_2PdS$: C, 33.95; H, 4.56; N, 5.28. Found: C, 33.86; H, 4.08; N, 5.66 (the best result obtained). ^{1}H and ^{13}C NMR spectra are attached in the appendix. MS (ESI): *m/z* 572 $[M + CH_3CN + H]^+$.

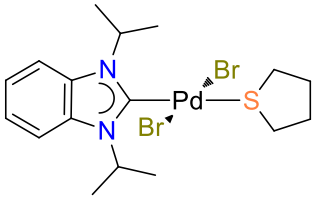

***trans*-[PdBr$_2$(^{i}Pr$_2$-bimy)(THT)]** (**22**). Complex **22** was also prepared in analogy to the pyridine complexes as a yellow solid from the reaction of tetrahydrothiophene (THT) (9 µL, 0.10 mmol) and complex **I** (47 mg, 0.05 mmol) in CH_2Cl_2 (10 mL). Yield: 56 mg, 0.10 mmol, >99%. ^{1}H NMR (500 MHz, $CDCl_3$): δ 7.56 (dd, 2 H, Ar–H), 7.20 (dd, 2 H, Ar–H), 6.04 (m, ^3J(H,H) = 6.9 Hz, 2 H, NCH), 3.30 (br–s, 4 H, SCH_2), 2.07 (br–s, 4 H, CH_2), 1.74 (d, ^3J(H,H) = 6.9 Hz, 12 H, CH_3). ^{13}C{^{1}H} NMR (125.77 MHz, $CDCl_3$): 163.6 ($C_{carbene}$), 134.1, 123.0, 113.3 (Ar–C), 55.1 (NCH), 36.4 (SCH_2), 30.8 (CH_2), 21.3 (CH_3). Anal. Calcd for $C_{17}H_{26}Br_2N_2PdS$: C, 36.68; H, 4.71; N, 5.03. Found: C, 36.66; H, 4.64; N, 5.14. MS (ESI): *m/z* 518 $[M – Br + CH_3CN]^+$.

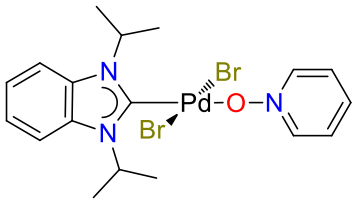

***trans*-[PdBr$_2$(^{i}Pr$_2$-bimy)(PNO)]** (**23**). Complex **I** (47 mg, 0.10 mmol) and pyridine N-oxide (24 mg, 0.25 mmol) were heated in $CHCl_3$ (20 mL) at 70°C overnight. The resulting solution was

concentrated to 3 mL before diethyl ether (20 mL) was added. The orange precipitate was collected and dried as the product (101 mg, 0.18 mmol, 90%). ^{1}H NMR (300 MHz, $CDCl_3$): δ 8.59 (br–s, 2 H, Ar–H), 7.51 (dd, 2 H, Ar–H), 7.45 (br–s, 3 H, Ar–H), 7.15 (dd, 2 H, Ar–H), 6.38 (m, ^{3}J(H,H) = 7.1 Hz, 2 H, NCH), 1.72 (d, ^{3}J(H,H) = 7.1 Hz, 12 H, CH_3). ^{13}C{^{1}H} NMR (75.48 MHz, $CDCl_3$): 155.7 ($C_{carbene}$), 142.4, 133.9, 126.5 (2 ×), 122.8, 113.0 (Ar–C), 55.2 (NCH), 21.1 (CH_3). Anal. Calcd for $C_{18}H_{23}Br_2N_3OPd$: C, 38.36; H, 4.11; N, 7.46. Found: C, 38.17; H, 4.16; N, 7.24. MS (ESI): *m/z* 525 $[M - Br + CH_3CN]^+$.

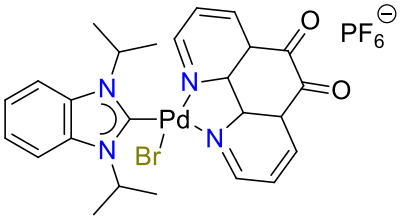

[PdBr(^{i}Pr$_2$-bimy)(phen-dione)]PF$_6$ (24). Complex **I** (94 mg, 0.10 mmol) was suspended in CH_2Cl_2 (10 mL) and solutions of 1,10-penanthroline-5,6-dione (43 mg, 0.20 mmol) in CH_2Cl_2 (3 mL) and KPF_6 (200 mg, 1.00 mmol) in acetone (5 mL) were added stepwise. The reaction mixture was stirred overnight, and the all volatiles were removed under reduced pressure. The residue was washed with H_2O (3 × 10 mL) and diethyl ether (5 × 10 mL) before it was dried in vacuo to give the product as a yellow solid (126 mg, 0.17 mmol, 85%). ^{1}H NMR (500 MHz, CD_3CN): δ 9.50 (d, 1 H, Ar–H), 8.78–8.72 (m, 2 H, Ar–H), 8.02–8.00 (m, 2 H, Ar–H), 7.91 (dd, 2 H, Ar–H), 7.71–7.68 (m, 1 H, Ar–H), 7.45 (dd, 2 H, Ar–H), 6.07 (m, ^{3}J(H,H) = 7 Hz, 2 H, NCH), 1.76 (d, ^{3}J(H,H) = 7 Hz, 6 H, CH_3), 1.68 (d, ^{3}J(H,H) = 7 Hz, 6 H, CH_3). ^{13}C{^{1}H} NMR (125.77 MHz, CD_3CN): 175.6, 175.5 (CO), 159.8 ($C_{carbene}$), 157.1, 156.7, 155.8, 155.4, 140.8, 140.7, 134.5, 131.0, 130.4, 130.3, 130.2, 124.9, 114.6 (Ar–C), 55.9 (NCH), 21.4, 20.9 (CH_3). ^{31}P{^{1}H} NMR (202.45 MHz, CD_3CN): –143.3 (m, ^{1}J(P,F) = 708 Hz, PF_6). ^{19}F{^{1}H} NMR (282.38 MHz, CD_3CN): 3.4 (d, ^{1}J(P,F) = 708 Hz, PF_6). Anal. Calcd for $C_{25}H_{24}BrF_6N_4O_2PPd$: C, 40.37; H, 3.25; N, 7.53. Found: C, 40.08; H, 3.65; N, 8.10 (best result obtained after multiple

trials). ^{1}H and ^{13}C NMR spectra are attached in the appendix. (ESI): *m/z* 631 [M – PF_6 + MeOH]$^{+}$. The ^{13}C-labeled complex was obtained though the same procedure starting from the ^{13}C-labeled complex **I**. $^{13}C\{^{1}H\}$ NMR (125.77 MHz, $CDCl_3$): δ 160.0 ($C_{carbene}$). MS (ESI): *m/z* 632 [M – PF_6 + MeOH]$^{+}$.

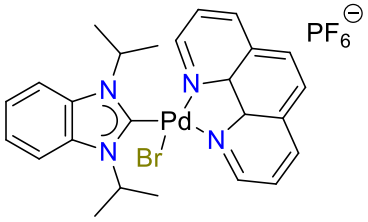

[PdBr(*i*Pr$_2$-bimy)(phen)]PF_6 (**25**). Complex **I** (94 mg, 0.10 mmol) was suspended in CH_2Cl_2 (10 mL) and solutions of phenanthroline (36 mg, 0.20 mmol) in CH_2Cl_2 (3 mL) and KPF_6 (200 mg, 1.00 mmol) in acetone (5 mL) were added stepwise. The reaction mixture was stirred overnight, and all volatiles were removed under reduced pressure. CH_2Cl_2 (30 mL) was added to the residue and the suspension was filtered. The solvent of the filtrate was removed under vacuum, giving the crude product as a yellow solid. The product was further purified by recrystallization from chloroform/hexane. Yield: 138 mg, 0.19 mmol, 96%. ^{1}H NMR (500 MHz, $CDCl_3$): δ 9.65 (d, 1 H, Ar–H), 8.85–8.83 (m, 1 H, Ar–H), 8.77–8.75 (m, 1 H, Ar–H), 8.18 (d, 2 H, Ar–H), 8.02–7.97 (m, 3 H, Ar–H), 7.77 (dd, 2 H, Ar–H), 7.43 (dd, 2 H, Ar–H), 6.11 (m, ^{3}J(H,H) = 7 Hz, 2 H, NCH), 1.82 (d, ^{3}J(H,H) = 7 Hz, 6 H, CH_3), 1.72 (d, ^{3}J(H,H) = 7 Hz, 6 H, CH_3). $^{13}C\{^{1}H\}$ NMR (125.77 MHz, $CDCl_3$): 161.4 ($C_{carbene}$), 151.9, 151.6, 147.8, 147.1, 141.9, 140.7, 134.3, 132.2, 131.4, 128.9 (2 ×), 127.7, 126.6, 124.7, 114.1 (Ar–C), 55.9 (NCH), 22.1, 21.6 (CH_3). $^{31}P\{^{1}H\}$ NMR (202.45 MHz, $CDCl_3$): –144.1 (m, ^{1}J(P,F) = 712 Hz, PF_6). $^{19}F\{^{1}H\}$ NMR (282.38 MHz, $CDCl_3$): 2.5 (d, ^{1}J(P,F) = 712 Hz, PF_6). Anal. Calcd for $C_{25}H_{28}BrF_6N_4PPd$: C, 41.95; H, 3.94; N, 7.83. Found: C, 41.81; H, 3.66; N, 7.73. MS (ESI): *m/z* 569 [M – PF_6]$^{+}$.

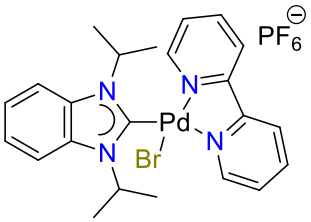

[PdBr(*i*Pr$_2$-bimy)(bipy)]PF$_6$ (**26**). Complex **26** was prepared in analogy to **25** from **I** (47 mg, 0.05 mmol), 2,2'-bipyridine (16 mg, 0.10 mmol) and KPF_6 (100 mg, 0.50 mmol). Yield: 63 mg, 0.09 mmol, 91%. ^{1}H NMR (500 MHz, d_6-DMSO): δ 9.23 (d, 1 H, Ar–H), 8.74–8.70 (m, 2 H, Ar–H), 8.45–8.38 (m, 2 H, Ar–H), 8.06 (dd, 2 H, Ar–H), 7.92–7.88 (m, 2 H, Ar–H), 7.61 (t, 1 H, Ar–H), 7.45 (dd, 2 H, Ar–H), 6.03 (m, ^3J(H,H) = 7 Hz, 2 H, NCH), 1.71 (d, ^3J(H,H) = 7 Hz, 6 H, CH_3), 1.64 (d, ^3J(H,H) = 7 Hz, 6 H, CH_3). ^{13}C{^{1}H} NMR (125.77 MHz, d_6-DMSO): 161.4 ($C_{carbene}$), 156.5, 155.4, 152.3, 149.9, 141.61, 141.55, 133.0, 128.5, 127.8, 124.5, 123.8, 123.6, 113.6 (Ar–C), 54.2 (NCH), 20.6, 20.1 (CH_3). ^{31}P{^{1}H} NMR (202.45 MHz, d_6-DMSO): –143.0 (m, ^1J(P,F) = 711 Hz, PF_6). ^{19}F{^{1}H} NMR (282.38 MHz, d_6-DMSO): 5.8 (d, ^1J(P,F) = 711 Hz, PF_6). Anal. Calcd for $C_{23}H_{26}BrF_6N_4PPd$: C, 40.05; H, 3.80; N, 8.12. Found: C, 40.08; H, 3.65; N, 8.10. MS (ESI): *m/z* 545 [M – PF_6]$^+$. The ^{13}C-labeled complex was obtained by the same procedure starting from the ^{13}C-labeled complex **I**. ^{13}C{^{1}H} NMR (125.77 MHz, $CDCl_3$): δ 162.7 ($C_{carbene}$). MS (ESI): *m/z* 546 [M – PF_6]$^+$.

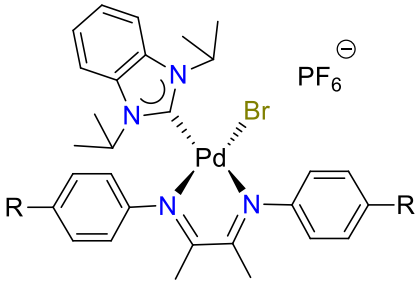

[PdBr(*i*Pr$_2$-bimy)(R-DAB)]PF$_6$ (**27**–**31**). Complexes **27**–**31** were prepared in analogy to **25** from **I** (94 mg, 0.10 mmol), the respective diimine R-DAB (0.20 mmol) and KPF_6 (200 mg, 1.00 mmol).

R = Br, (**27**). This complex was further purified by column chromatography (SiO_2, EA/hexane: 1/2). Yield: 74 mg, 0.08 mmol, 40%. ^{1}H NMR (500 MHz, $CDCl_3$): δ 7.60 (d, 2 H, Ar–H), 7.51 (dd, 2 H, Ar–H), 7.36 (d, 2 H, Ar–H), 7.21 (dd, 2 H, Ar–H), 7.12–7.08 (m, 4 H, Ar–H), 5.83 (m, ^3J(H,H) = 7 Hz, 2 H, NCH), 2.31 (s, 3 H, CH_3), 2.25 (s, 3 H, CH_3), 1.66 (d,

^{3}J(H,H) = 7 Hz, 6 H, CH(CH_3)$_2$), 1.62 (d, ^{3}J(H,H) = 7 Hz, 6 H, CH(CH_3)$_2$). ^{13}C{^{1}H} NMR (125.77 MHz, $CDCl_3$): 182.7, 179.9 (C=N), 160.5 ($C_{carbene}$), 147.1, 144.7, 133.7, 133.4, 132.7, 124.7, 123.9, 123.7, 122.8, 122.2, 113.8 (Ar–C), 55.5 (NCH), 22.2, 21.7 (CH(*C*H_3)$_2$), 21.5, 21.4 (CH_3). ^{31}P{^{1}H} NMR (202.45 MHz, $CDCl_3$): –143.8 (m, ^{1}J(P,F) = 713 Hz, PF_6). ^{19}F{^{1}H} NMR (282.38 MHz, $CDCl_3$): 4.1 (d, ^{1}J(P,F) = 713 Hz, PF_6). Anal. Calcd for $C_{29}H_{32}Br_3F_6N_4PPd$: C, 37.55; H, 3.48; N, 6.04. Found: C, 38.84; H, 3.48; N, 6.57 (best result obtained after multiple trials). ^{1}H and ^{13}C NMR spectra are attached in the appendix. MS (ESI): *m/z* 783 $[M - PF_6]^+$.

R = H, (**28**). Yield: 151 mg, 0.20 mmol, 98%. ^{1}H NMR (500 MHz, $CDCl_3$): δ 7.46 (dd, 2 H, Ar–H), 7.41 (t, 2 H, Ar–H), 7.23 (d, 5 H, Ar–H), 7.19–7.14 (m, 4 H, Ar–H), 7.03 (t, 1 H, Ar–H), 5.90 (m, ^{3}J(H,H) = 7 Hz, 2 H, NCH), 2.27 (s, 3 H, CH_3), 2.24 (s, 3 H, CH_3), 1.66 (d, ^{3}J(H,H) = 7 Hz, 6 H, CH(CH_3)$_2$), 1.59 (d, ^{3}J(H,H) = 7 Hz, 6 H, CH(CH_3)$_2$). ^{13}C{^{1}H} NMR (125.77 MHz, $CDCl_3$): 182.5, 179.7 (C=N), 162.2 ($C_{carbene}$), 148.3, 146.2, 133.6, 130.0, 129.3, 128.8, 128.0, 123.5, 122.9, 122.0, 113.6 (Ar–C), 55.3 (NCH), 22.0, 21.5 (CH(*C*H_3)$_2$), 21.3, 21.2 (CH_3). ^{31}P{^{1}H} NMR (202.45 MHz, $CDCl_3$): –143.7 (m, ^{1}J(P,F) = 713 Hz, PF_6). ^{19}F{^{1}H} NMR (282.38 MHz, $CDCl_3$): 4.2 (d, ^{1}J(P,F) = 713 Hz, PF_6). Anal. Calcd for $C_{29}H_{34}BrF_6N_4PPd$: C, 45.24; H, 4.45; N, 7.28. Found: C, 45.34; H, 4.61; N, 7.33. MS (ESI): *m/z* 625 $[M - PF_6]^+$.

R = Me, (**29**). Yield: 152 mg, 0.19 mmol, 95%. ^{1}H NMR (500 MHz, $CDCl_3$): δ 7.48 (dd, 2 H, Ar–H), 7.20 (ps–d, 2 H, Ar–H), 7.16 (dd, 2 H, Ar–H), 7.10–7.08 (m, 4 H, Ar–H), 6.97 (ps–d, 2 H, Ar–H), 5.89 (m, ^{3}J(H,H) = 7 Hz, 2 H, NCH), 2.32 (s, 3 H, $NCCH_3$), 2.27 (s, 3 H, $NCCH_3$), 2.23 (s, 3 H, CH_3), 2.12 (s, 3 H, CH_3), 1.65 (d, ^{3}J(H,H) =7 Hz, 6 H, CH(CH_3)$_2$), 1.61 (d, ^{3}J(H,H) = 7 Hz, 6 H, CH(CH_3)$_2$). ^{13}C{^{1}H} NMR (125.77 MHz, $CDCl_3$): 182.4, 179.7 (C=N), 162.6 ($C_{carbene}$), 146.0, 143.8, 138.9, 137.7, 133.6, 130.5, 129.8, 123.5, 122.8, 121.9, 113.7 (Ar–C), 55.3 (NCH), 22.0 (CH(*C*H_3)$_2$), 21.8, 21.54 (NC*C*H_3), 21.47 (CH(*C*H_3)$_2$), 21.3, 21.1

(CH_3). $^{31}P\{^1H\}$ NMR (202.45 MHz, $CDCl_3$): –143.7 (m, ^1J(P,F) = 713 Hz, PF_6). $^{19}F\{^1H\}$ NMR (282.38 MHz, $CDCl_3$): 4.0 (d, ^1J(P,F) = 713 Hz, PF_6). Anal. Calcd for $C_{31}H_{38}BrF_6N_4PPd$: C, 46.66; H, 4.80; N, 7.02. Found: C, 46.74; H, 4.61; N, 7.33. MS (ESI): *m/z* 653 $[M - PF_6]^+$.

R = OMe, (**30**). Yield: 156 mg, 0.19 mmol, 94%. ^1H NMR (500 MHz, $CDCl_3$): δ 7.48 (dd, 2 H, Ar–H), 7.17–7.13 (m, 6 H, Ar–H), 6.91 (d, 2 H, Ar–H), 6.66 (d, 2 H, Ar–H), 5.91 (m, ^3J(H,H) = 7 Hz, 2 H, NCH), 3.74 (s, 3 H, OCH_3), 3.61 (s, 3 H, OCH_3), 2.28 (s, 3 H, CH_3), 2.24 (s, 3 H, CH_3), 1.65 (d, ^3J(H,H) = 7 Hz, 6 H, $CH(CH_3)_2$), 1.61 (d, ^3J(H,H) = 7 Hz, 6 H, $CH(CH_3)_2$). $^{13}C\{^1H\}$ NMR (125.77 MHz, $CDCl_3$): 182.5, 179.8 (C=N), 162.8 ($C_{carbene}$), 159.6, 159.1, 141.5, 139.5, 133.6, 124.5, 123.6, 123.5, 115.0, 114.4, 113.7 (Ar–C), 56.2, 56.1 (OCH_3), 55.3 (NCH), 22.0, 21.5 ($CH(CH_3)_2$), 21.4, 21.2 (CH_3). $^{31}P\{^1H\}$ NMR (202.45 MHz, $CDCl_3$): –143.7 (m, ^1J(P,F) = 713 Hz, PF_6). $^{19}F\{^1H\}$ NMR (282.38 MHz, $CDCl_3$): 4.0 (d, ^1J(P,F) = 713 Hz, PF_6). Anal. Calcd for $C_{31}H_{38}BrF_6N_4O_2PPd$: C, 44.86; H, 4.61; N, 6.75. Found: C, 44.80; H, 4.58; N, 6.47. MS (ESI): *m/z* 685 $[M - PF_6]^+$.

R = ^{t}Bu, (**31**). Yield: 152 mg, 0.17 mmol, 86%.^1H NMR (500 MHz, $CDCl_3$): δ 7.46–7.42 (m, 4 H, Ar–H), 7.16–7.13 (m, 4 H, Ar–H), 7.10 (s, 4 H, Ar–H), 5.87 (m, ^3J(H,H) = 7 Hz, 2 H, NCH), 2.31 (s, 3 H, CH_3), 2.29 (s, 3 H, CH_3), 1.68 (d, ^3J(H,H) = 7 Hz, 6 H, $CH(CH_3)_2$), 1.57 (d, ^3J(H,H) = 7 Hz, 6 H, $CH(CH_3)_2$), 1.28 (s, 9 H, $C(CH_3)_3$), 0.98 (s, 9 H, $C(CH_3)_3$). $^{13}C\{^1H\}$ NMR (125.77 MHz, $CDCl_3$): 181.9, 179.7 (C=N), 163.4 ($C_{carbene}$), 151.9, 150.8, 145.5, 143.7, 133.6, 126.6, 126.1, 123.4, 122.5, 121.9, 113.5 (Ar–C), 55.3 (NCH), 35.3, 35.1 ($C(CH_3)_3$), 32.0, 31.5 ($C(CH_3)_3$), 22.0, 21.8 ($CH(CH_3)_2$), 21.4, 21.2 (CH_3). $^{31}P\{^1H\}$ NMR (202.45 MHz, $CDCl_3$): –143.7 (m, ^1J(P,F) = 713 Hz, PF_6). $^{19}F\{^1H\}$ NMR (282.38 MHz, $CDCl_3$): 4.0 (d, ^1J(P,F) = 713 Hz, PF_6). Anal. Calcd for $C_{37}H_{50}BrF_6N_4PPd$: C, 50.38; H, 5.71; N, 6.35. Found: C, 50.63; H, 5.60; N, 6.57. MS (ESI): *m/z* 737 $[M - PF_6]^+$.

[PdBr(^{i}Pr$_2$-bimy)(diNHC)]PF$_6$ (**32**–**36**). The dicarbene precusor salts (0.20 mmol) and silver oxide (47 mg, 0.20 mmol) were stirred in MeOH (10 mL) and CH_2Cl_2 (5 mL) at ambient temperature for three hours. To the resulting suspension was slowly dropped in the solution of complex **II** in CH_3CN. KPF_6 (200 mg, 1.00 mmol) was then added to the suspension and the mixture was stirred overnight. Solvent was removed under reduced pressure, 50 mL of CH_2Cl_2 was added to the residue and the suspension was filtered. The filtrate was concentrated to 5 mL and added to diethyl ether (50 mL). The precipitate was collected and dried to give the products as off-white solids.

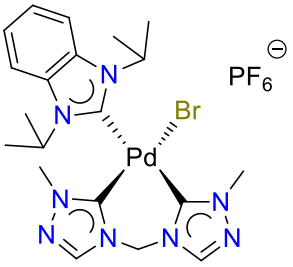

Dicarbene = A, (**32**). Yield: 93 mg, 0.13 mmol, 65%. ^{1}H NMR (500 MHz, $CDCl_3$, 243K): δ 9.47 (s, 1 H, Ar–H), 9.07 (s, 1 H, Ar–H), 8.48 (d, ^{2}J(H,H) = 13 Hz, 1 H, NC*H*HN), 7.69 (d, 1 H, Ar–H), 7.57 (d, 1 H, Ar–H), 7.32–7.26 (m, 2 H, Ar–H), 6.29 (d, ^{2}J(H,H) = 13 Hz, 1 H, NCH*H*N), 5.79 (m, ^{3}J(H,H) = 7 Hz, 1 H, NCH), 5.14 (m, ^{3}J(H,H) = 7 Hz, 1 H, NCH), 4.24 (s, 3 H, NCH_3), 3.38 (s, 3 H, NCH_3), 1.83–1.81 (m, 6 H, CH(CH_3)$_2$), 1.57 (d, ^{3}J(H,H) = 7 Hz, 3 H, CH(CH_3)$_2$), 1.18 (d, ^{3}J(H,H) = 7 Hz, 3 H, CH(CH_3)$_2$). ^{13}C{^{1}H} NMR (125.77 MHz, $CDCl_3$): 177.1 ($C_{carbene\text{-}probe}$), 170.5 ($C_{carbene\text{-}\textit{trans}}$), 163.8 ($C_{carbene\text{-}\textit{cis}}$), 143.7, 142.1, 134.0, 124.0, 114.2 (Ar–C), 59.6 (NCH_2N), 55.7 (br–s, NCH), 41.9, 40.3 (NCH_3), 21.7 (br–s, CH(*C*H_3)$_2$). ^{31}P{^{1}H} NMR (202.45 MHz, $CDCl_3$): –143.7 (m, ^{1}J(P,F) = 714 Hz, PF_6). ^{19}F{^{1}H} NMR (282.38 MHz, $CDCl_3$): 4.5 (d, ^{1}J(F,P) = 714 Hz, PF_6). Anal. Calcd for $C_{20}H_{28}BrF_6N_8PPd$: C, 33.75; H, 3.97; N, 15.74. Found: C, 33.40; H, 3.78; N, 15.34. MS (ESI): *m/z* 567 $[M - PF_6]^+$.

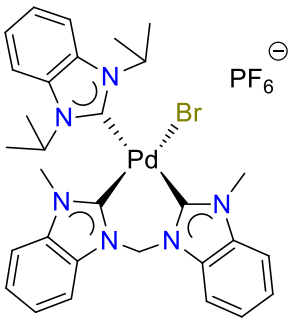

Dicarbene = B, (**33**). Yield: 126 mg, 0.16 mmol, 78%. ^{1}H NMR (500 MHz, $CDCl_3$): δ 8.04 (d, 1 H, Ar–H), 7.85 (d, 1 H, Ar–H), 7.74 (d, 1 H, Ar–H), 7.56 (d, 1 H, Ar–H), 7.44–7.40 (m, 2 H, Ar–H), 7.37–7.28 (m, 6 H, Ar–H), 7.05 (d, ^{2}J(H,H) = 14 Hz, 1 H, NC*H*HN), 6.68 (d, ^{2}J(H,H) = 14 Hz, 1 H, NCH*H*N), 6.02 (m, ^{3}J(H,H) = 7 Hz, 1 H, NCH), 5.41 (m, ^{3}J(H,H) = 7 Hz, 1 H, NCH), 4.27 (s, 3 H, NCH_3), 3.60 (s, 3 H, NCH_3), 1.97–1.93 (m, 6 H, $CH(CH_3)_2$), 1.62 (d, ^{3}J(H,H) = 7 Hz, 3 H, $CH(CH_3)_2$), 1.03 (d, ^{3}J(H,H) = 7 Hz, 3 H, $CH(CH_3)_2$). $^{13}C\{^{1}H\}$ NMR (125.77 MHz, $CDCl_3$): 179.1 ($C_{carbene\text{-}trans}$), 178.7 ($C_{carbene\text{-}probe}$), 172.2 ($C_{carbene\text{-}cis}$), 135.2, 134.2, 133.9, 133.8, 133.3, 133.2, 126.4, 125.9, 125.7, 125.2, 124.00, 123.97, 114.3, 114.1, 112.2, 111.8, 111.6, 111.2 (Ar–C), 57.8 (NCH_2N), 55.7, 55.5 (NCH), 36.9, 35.4 (NCH_3), 22.4, 21.8, 21.2, 20.7 ($CH(CH_3)_2$). 2D HMBC NMR spectrum is attached in Figure S7 (*vide infra*). $^{31}P\{^{1}H\}$ NMR (121.49 MHz, $CDCl_3$): –143.5 (m, ^{1}J(P,F) = 712 Hz, PF_6). $^{19}F\{^{1}H\}$ NMR (282.38 MHz, $CDCl_3$): 3.9 (d, ^{1}J(F,P) = 712 Hz, PF_6). Anal. Calcd for $C_{30}H_{34}BrF_6N_6PPd$: C, 44.49; H, 4.23; N, 10.38. Found: C, 44.21; H, 4.20; N, 9.99. MS (ESI): *m/z* 665 $[M - PF_6]^+$.

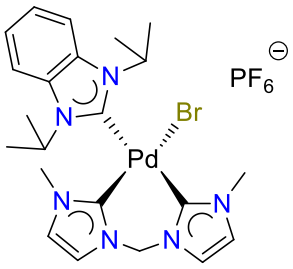

Dicarbene = C, (**34**). Yield: 135 mg, 0.19 mmol, 95%. ^{1}H NMR (500 MHz, $CDCl_3$): δ 7.68 (d, 1 H, Ar–H), 7.57 (d, 1 H, Ar–H), 7.45 (d, 1 H, Ar–H), 7.36 (d, 1 H, Ar–H), 7.30–7.26 (m, 2 H, Ar–H), 6.95–6.94 (m, 2 H, Ar–H), 6.27 (s, 2 H, NCH_2N), 5.90 (m, ^{3}J(H,H) = 7 Hz, 1 H, NCH), 5.25 (m, ^{3}J(H,H) = 7 Hz, 1 H, NCH), 4.05 (s, 3 H, NCH_3), 3.23 (s, 3 H, NCH_3), 1.87 (d, ^{3}J(H,H) = 7 Hz, 3 H, $CH(CH_3)_2$), 1.81 (d, ^{3}J(H,H) = 7 Hz, 3 H, $CH(CH_3)_2$), 1.56 (d, ^{3}J(H,H) = 7 Hz, 3 H, $CH(CH_3)_2$), 1.17 (d, ^{3}J(H,H) = 7 Hz, 3 H, $CH(CH_3)_2$). $^{13}C\{^{1}H\}$ NMR (125.77 MHz, $CDCl_3$): 179.9 ($C_{carbene\text{-}probe}$), 168.6 ($C_{carbene\text{-}trans}$), 161.1 ($C_{carbene\text{-}cis}$), 134.0, 133.6, 123.8, 123.7, 123.3,

123.0, 121.9 (2 ×), 114.1, 114.0 (Ar–C), 63.4 (NCH_2N), 55.4, 55.2 (NCH), 39.7, 38.3 (NCH_3), 22.2, 21.7, 21.3, 20.6 ($CH(CH_3)_2$). $^{31}P\{^1H\}$ NMR (202.45 MHz, $CDCl_3$): –143.6 (m, ^1J(F,P) = 713 Hz, PF_6). $^{19}F\{^1H\}$ NMR (282.38 MHz, $CDCl_3$): 4.4 (d, ^1J(F,P) = 713 Hz, PF_6). Anal. Calcd for $C_{22}H_{30}BrF_6N_6PPd$: C, 37.23; H, 4.26; N, 11.84. Found: C, 36.87; H, 3.96; N, 11.66. MS (ESI): *m/z* 565 $[M - PF_6]^+$.

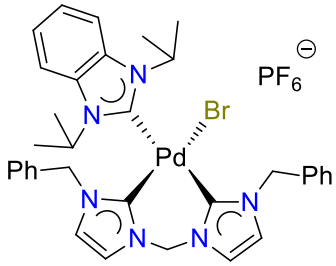

Dicarbene = D, (**35**). Yield: 156 mg, 0.18 mmol, 90%. ^1H NMR (500 MHz, $CDCl_3$): δ 7.60 (d, 1 H, Ar–H), 7.57–7.56 (m, 2 H, Ar–H), 7.49 (d, 1 H, Ar–H), 7.34–7.33 (m, 5 H, Ar–H), 7.28 (t, 2 H, Ar–H), 7.19 (t, 1 H, Ar–H), 7.09 (t, 2 H, Ar–H), 6.99 (ps–d, 1 H, Ar–H), 6.68–6.67 (m, 3 H, Ar–H), 6.45–6.37 (m, 2 H, NCH_2N), 6.19 (d, ^2J(H,H) = 15 Hz, 1 H, NC*H*HPh), 5.51 (m, ^3J(H,H) = 7 Hz, 1 H, NCH), 5.42 (d, ^2J(H,H) = 15 Hz, 1 H, NCH*H*Ph), 5.39 (m, ^3J(H,H) = 7 Hz, 1 H, NCH), 4.71 (d, ^2J(H,H) = 15 Hz, 1 H, NC*H*HPh), 4.43 (d, ^2J(H,H) = 15 Hz, 1 H, NCH*H*Ph), 1.79 (d, ^3J(H,H) = 7 Hz, 3 H, CH_3), 1.63 (d, ^3J(H,H) = 7 Hz, 3 H, CH_3), 1.44 (d, ^3J(H,H) = 7 Hz, 3 H, CH_3), 1.27 (d, ^3J(H,H) = 7 Hz, 3 H, CH_3). $^{13}C\{^1H\}$ NMR (125.77 MHz, $CDCl_3$): 179.51 ($C_{carbene\text{-}probe}$), 169.0 ($C_{carbene\text{-}\textit{trans}}$), 161.3 ($C_{carbene\text{-}\textit{cis}}$), 137.4, 134.0, 133.8, 129.8, 129.6, 129.4, 128.8, 128.7, 128.3, 124.3, 123.8, 123.3, 122.0, 121.2, 113.9 (Ar–C), 63.8 (NCH_2N), 55.5, 55.0, 54.4, 54.1 (NCH and NCH_2Ph), 22.2, 21.3, 21.2, 20.7 (CH_3). $^{31}P\{^1H\}$ NMR (202.45 MHz, $CDCl_3$): –143.4 (m, ^1J(F,P) = 712 Hz, PF_6). $^{19}F\{^1H\}$ NMR (282.38 MHz, $CDCl_3$): 4.2 (d,^1J(F,P) = 712 Hz, PF_6). Anal. Calcd for $C_{34}H_{38}BrF_6N_6PPd$: C, 47.37; H, 4.44; N, 9.75. Found: C, 47.97; H, 4.54; N, 9.63 (best result obtained after multiple trials). ^1H and ^{13}C NMR spectra are attached in the appendix. MS (ESI): *m/z* 717 $[M - PF_6]^+$.

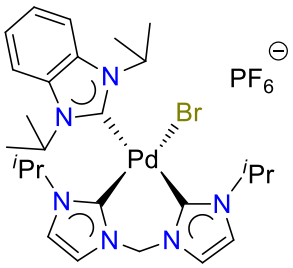

Dicarbene = E, (**36**). Yield: 95 mg, 0.12 mmol, 62%. ^{1}H NMR (500 MHz, $CDCl_3$): δ 7.73 (d, 1 H, Ar–H), 7.68 (d, 1 H, Ar–H), 7.57–7.55 (m, 2 H, Ar–H), 7.31–7.27 (m, 2 H, Ar–H), 7.02–7.00 (m, 2 H, Ar–H), 6.51 (d, ^{2}J(H,H) = 13 Hz, 1 H, NC*H*HN), 6.26 (d, ^{2}J(H,H) = 13 Hz, 1 H, NCH*H*N), 5.83 (m, ^{3}J(H,H) = 7 Hz, 1 H, NCH), 5.53 (m, ^{3}J(H,H) = 7 Hz, 1 H, NCH), 5.44 (m, ^{3}J(H,H) = 7 Hz, 1 H, NCH), 4.31 (m, ^{3}J(H,H) = 7 Hz, 1 H, NCH), 1.90 (d, ^{3}J(H,H) = 7 Hz, 3 H, CH_3), 1.84 (d, ^{3}J(H,H) = 7 Hz, 3 H, CH_3), 1.62 (d, ^{3}J(H,H) = 7 Hz, 3 H, CH_3), 1.57 (d, ^{3}J(H,H) = 7 Hz, 3 H, CH_3), 1.42 (d, ^{3}J(H,H) = 7 Hz, 3 H, CH_3), 1.32 (d, ^{3}J(H,H) = 7 Hz, 3 H, CH_3), 1.17 (d, ^{3}J(H,H) = 7 Hz, 3 H, CH_3), 0.61 (d, ^{3}J(H,H) = 7 Hz, 3 H, CH_3). ^{13}C{^{1}H} NMR (125.77 MHz, $CDCl_3$): 180.0 ($C_{carbene\text{-}probe}$), 167.2 ($C_{carbene\text{-}\textit{trans}}$), 159.9 ($C_{carbene\text{-}\textit{cis}}$), 134.0, 133.6, 124.7, 123.9 (2 ×), 122.8, 118.4, 117.6, 114.0, 113.9 (Ar–C), 63.4 (NCH_2N), 55.5, 55.2, 53.45, 53.39 (NCH), 25.0, 24.1, 23.7, 22.4, 21.9, 21.4, 21.3, 20.4 (CH_3). ^{31}P{^{1}H} NMR (202.45 MHz, $CDCl_3$): –143.5 (m, ^{1}J(F,P) = 712 Hz, PF_6). ^{19}F{^{1}H} NMR (282.38 MHz, $CDCl_3$): 4.2 (d, ^{1}J(F,P) = 712 Hz, PF_6). Anal. Calcd for $C_{26}H_{38}BrF_6N_6PPd$: C, 40.77; H, 5.00; N, 10.97. Found: C, 40.54; H, 4.85; N, 10.61. MS (ESI): m/z 621 $[M - PF_6]^+$.

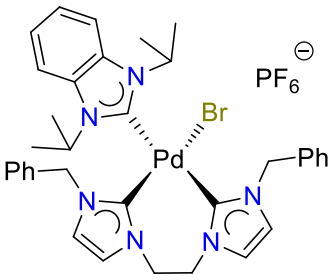

Dicarbene = F, (**37**). This complex could be obtained in analogy to the previous complexes (method 1) with further purification using colum chromatography (DCM/MeOH: 40/1) in low yield (14 mg, 0.02 mmol, 8%). The yield was increased by using a different protocol (method 2): complex **III** (121 mg, 0.20 mmol), 1,3-diisopropylbenzimidazolium salt (57 mg, 0.20 mmol), K_2CO_3 (34 mg, 0.24 mmol) and KPF_6 (200 mg, 1.00 mmol) were mixed in DMSO (10 mL) and heated at 90 ℃ overnight. The solvent was removed by vacum distillation.

The resulting residue was suspended in CH_2Cl_2 (30 mL) and then extracted with H_2O (4 × 20 mL). Drying of the organic phase over Na_2SO_4 followed by removal of the solvent in vacuo afforded an orange solid. The solid was washed with $CHCl_3$ (20 mL) to give the off white product. Yield: 98 mg, 0.11 mmol, 56%.^{1}H NMR (500 MHz, CD_3CN): δ 7.73 (d, 1 H, Ar–H), 7.51 (d, 1 H, Ar–H), 7.44 (t, 2 H, Ar–H), 7.39 (d, 1 H, Ar–H), 7.35 (d, 1 H, Ar–H), 7.30 (t, 1 H, Ar–H), 7.27 (ps–d, 1 H, Ar–H), 7.24–7.20 (m, 2 H, Ar–H), 7.07 (d, 2 H, Ar–H), 7.01 (t, 1 H, Ar–H), 6.80 (t, 2 H, Ar–H), 6.76 (d, 1 H, Ar–H), 6.33 (d, ^2J(H,H) = 16 Hz, 1 H, NC*H*HPh), 6.27 (d, 2 H, Ar–H), 6.05–5.98 (m, 1 H, NC*H*HCH$_2$), 5.58 (m, ^3J(H,H) = 7 Hz, 1 H, NCH), 5.45 (d, ^2J(H,H) = 16 Hz, 1 H, NCH*H*Ph), 5.41 (m, ^3J(H,H) = 7 Hz, 1 H, NCH), 4.82–4.76 (m, 2 H, NC*H*HPh and NCH*H*CH$_2$), 4.54–4.48 (m, 3 H, NCH*H*Ph and NCH$_2$C*H*$_2$), 1.69–1.66 (m, 6 H, CH_3), 1.29 (d, ^3J(H,H) = 7 Hz, 3 H, CH_3), 1.13 (d, ^3J(H,H) = 7 Hz, 3 H, CH_3). ^{13}C{^{1}H} NMR (125.77 MHz, CD_3CN): 180.4 ($C_{carbene\text{-}probe}$), 166.1 ($C_{carbene\text{-}\textit{trans}}$), 161.4 ($C_{carbene\text{-}\textit{cis}}$), 138.9, 135.6, 134.3, 133.6, 130.2, 129.4, 129.1, 128.8, 127.6, 127.3, 125.1, 124.6, 124.5, 124.01, 123.96, 123.0, 114.32, 114.28 (Ar–C), 55.5, 55.4, 55.3, 54.1 (NCH and NCH_2Ph), 49.7, 47.8 (NCH_2), 21.8, 21.0, 20.3, 20.2 (CH_3). ^{31}P{^{1}H} NMR (202.45 MHz, CD_3CN): –144.0 (m, ^1J(F,P) = 708 Hz, PF_6). ^{19}F{^{1}H} NMR (282.38 MHz, CDCl3): 3.4 (d, ^1J(F,P) = 708 Hz, PF_6). Anal. Calcd for $C_{35}H_{40}BrF_6N_6PPd$: C, 47.99; H, 4.60; N, 9.59. Found: C, 47.91; H, 4.31; N, 9.78. MS (ESI): *m/z* 731 $[M - PF_6]^+$. The ^{13}C-labeled complex was obtained though the same procedure starting from the C2 ^{13}C-labeled 1,3-diisopropylbenzimidazolium salt. ^{13}C{^{1}H} NMR (125.77 MHz, $CDCl_3$): δ 179.54 ($C_{carbene\text{-}probe}$). MS (ESI): *m/z* 732 $[M - PF_6]^+$.

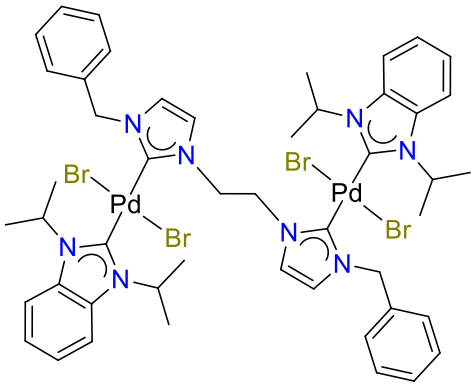

Ethylene bridged dipalladium complex (**39**). Yield: 44 mg, 0.03 mmol, 34%. ^{1}H NMR (500 MHz, $CDCl_3$): δ 7.60–7.58 (m, 2 H, Ar–H), 7.55–7.53 (m, 2 H, Ar–H), 7.50 (ps–d, 4 H, Ar–H), 7.40 (t, 4 H, Ar–H), 7.34 (t, 2 H, Ar–H), 7.22–7.20 (m, 4 H, Ar–H), 7.19 (d, 2 H, Ar–H), 6.56 (d, 2 H, Ar–H), 6.19 (m, ^{3}J(H,H) = 7 Hz, 2 H, NCH), 6.06 (m, ^{3}J(H,H) = 7 Hz, 2 H, NCH), 5.80 (s, 4 H, NCH_2Ph), 5.48 (s, 4 H, NCH_2), 1.89 (d, ^{3}J(H,H) = 7 Hz, 12 H, CH_3), 1.67 (d, ^{3}J(H,H) = 7 Hz, 12 H, CH_3). ^{13}C{^{1}H} NMR (125.77 MHz, $CDCl_3$): 178.8 ($C_{carbene\text{-}benz}$), 170.7 ($C_{carbene\text{-}imi}$), 136.8, 134.3, 134.2, 129.5, 128.9, 128.8, 124.8, 122.7 (2 ×), 120.8, 113.32, 113.30 (Ar–C), 55.3, 54.7, 54.5 (NCH, NCH_2Ph), 51.4 (NCH_2), 21.9, 21.6 (CH_3). Anal. Calcd for $C_{48}H_{58}Br_4N_8Pd_2$: C, 45.06; H, 4.57; N, 8.76. Found: C, 44.79; H, 4.48; N, 8.64. MS (ESI): *m/z* 1199 $[M - Br]^+$.

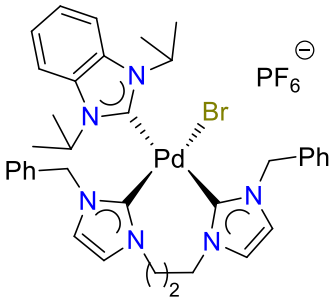

Dicarbene = G, (**38**). Method 1, yield: 32 mg, 0.04 mmol, 18%; or Method 2 from complex **IV** (62 mg, 0.10 mmol), 1,3-diisopropylbenzimidazolium salt (28 mg, 0.10 mmol), potassium carbonate (17 mg, 0.12 mmol) and KPF_6 (200 mg, 1.00 mmol). Yield: 76 mg, 0.09 mmol, 85%. ^{1}H NMR (500 MHz, CD_3CN): δ 7.78 (d, 1 H, Ar–H), 7.61 (d, 1 H, Ar–H), 7.40–7.38 (m, 3 H, Ar–H), 7.31 (t, 1 H, Ar–H), 7.25 (t, 1 H, Ar–H), 7.21–7.19 (m, 3 H, Ar–H), 7.14 (d, 1 H, Ar–H), 7.11 (d, 1 H, Ar–H), 6.94 (t, 2 H, Ar–H), 6.87 (d, 1 H, Ar–H), 6.74 (d, 1 H, Ar–H), 6.31 (d, 2 H, Ar–H), 6.01 (m, ^{3}J(H,H) = 7 Hz, 1 H, NCH), 5.90 (d, ^{2}J(H,H) = 15 Hz, 1 H, NC*H*HPh), 5.87 (m, ^{3}J(H,H) = 7 Hz, 1 H, NCH), 5.28 (d, ^{2}J(H,H) = 15 Hz, 1 H, NCH*H*Ph), 5.13 (t, ^{3}J(H,H) = 12 Hz, 1 H, NCH_2), 5.08 (d, ^{2}J(H,H) = 15

Hz, 1 H, NC*H*HPh), 4.94 (t, ^{3}J(H,H) = 12 Hz, 1 H, NCH_2), 4.66 (d, ^{2}J(H,H) = 15 Hz, 1 H, NCH*H*Ph), 4.60–4.56 (m, 1 H, NCH_2), 4.46–4.42 (m, 1 H, NCH_2), 2.48 (br–s, 1 H, CH_2), 2.10 (br–s, 1 H, CH_2), 1.76 (d, ^{3}J(H,H) = 7 Hz, 3 H, CH_3), 1.66 (d, ^{3}J(H,H) = 7 Hz, 3 H, CH_3), 1.48 (d, ^{3}J(H,H) = 7 Hz, 3 H, CH_3), 1.44 (d, ^{3}J(H,H) = 7 Hz, 3 H, CH_3). $^{13}C\{^{1}H\}$ NMR (125.77 MHz, CD_3CN): 181.1 ($C_{carbene\text{-}probe}$), 168.9 ($C_{carbene\text{-}\textit{trans}}$), 162.3 ($C_{carbene\text{-}\textit{cis}}$), 137.3, 136.5, 134.5, 133.7, 130.0 (2 ×), 129.6, 129.3, 129.2, 128.8, 127.4, 126.2, 124.6, 123.9, 123.1, 122.9, 114.5, 114.4 (Ar–C), 55.6, 55.5, 54.7, 54.2, 53.6, 53.2 (NCH_2Ph, NCH_2 and NCH), 30.3 (CH_2), 21.9, 21.0, 20.7, 20.5 (CH_3). $^{31}P\{^{1}H\}$ NMR (202.45 MHz, CD_3CN): –143.1 (m, ^{1}J(F,P) = 708 Hz, PF_6). $^{19}F\{^{1}H\}$ NMR (282.38 MHz, $CDCl_3$): 3.4 (d, ^{1}J(F,P) = 708 Hz, PF_6). Anal. Calcd for $C_{36}H_{42}BrF_6N_6PPd$: C, 48.58; H, 4.76; N, 9.44. Found: C, 48.50; H, 4.67; N, 9.56. MS (ESI): *m/z* 745 $[M - PF_6]^+$. The ^{13}C-labeled complex was obtained though the same procedure starting from C2 ^{13}C-labeled 1,3-diisopropylbenzimidazolium salt. $^{13}C\{^{1}H\}$ NMR (125.77 MHz, $CDCl_3$): δ 180.3 ($C_{carbene\text{-}probe}$). MS (ESI): *m/z* 746 $[M - PF_6]^+$.

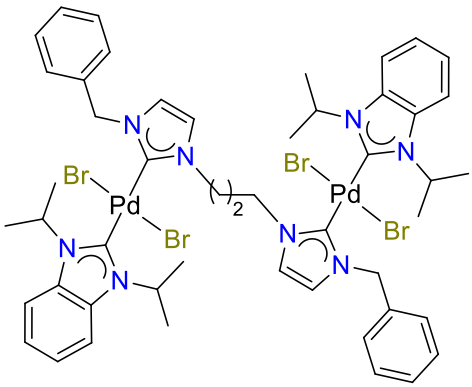

Propylene bridged dipalladium complex (**40**). Yield: 93 mg, 0.07 mmol, 72%. ^{1}H NMR (500 MHz, $CDCl_3$): δ 7.58–7.56 (m, 2 H, Ar–H), 7.53–7.52 (m, 6 H, Ar–H), 7.40 (t, 4 H, Ar–H), 7.35 (t, 2 H, Ar–H), 7.21–7.17 (m, 4 H, Ar–H), 7.15 (d, 2 H, Ar–H), 6.52 (d, 2 H, Ar–H), 6.23 (m, ^{3}J(H,H) = 7 Hz, 2 H, NCH), 6.07 (m, ^{3}J(H,H) = 7 Hz, 2 H, NCH), 5.76 (s, 4 H, NCH_2Ph), 4.76 (t, ^{3}J(H,H) = 7 Hz, 4 H, NCH_2), 3.34 (m, ^{3}J(H,H) = 7 Hz, 2 H, CH_2), 1.84 (d, ^{3}J(H,H) = 7 Hz, 12 H, CH_3), 1.68 (d, ^{3}J(H,H) = 7 Hz, 12 H, CH_3). $^{13}C\{^{1}H\}$ NMR (125.77 MHz, $CDCl_3$): 179.1 ($C_{carbene\text{-}benz}$), 170.4 ($C_{carbene\text{-}imi}$), 136.9, 134.2, 129.5, 129.2,

128.8, 123.0, 122.7, 121.2, 113.2 (Ar–C), 55.3, 54.6, 54.5 (NCH, NCH_2Ph), 49.7 (NCH_2), 32.1 (CH_2), 21.8, 21.6 (CH_3). Anal. Calcd for $C_{49}H_{60}Br_4N_8Pd_2$: C, 45.50; H, 4.68; N, 8.66. Found: C, 45.52; H, 4.36; N, 9.01. MS (ESI): *m/z* 1213 $[M - Br]^+$.

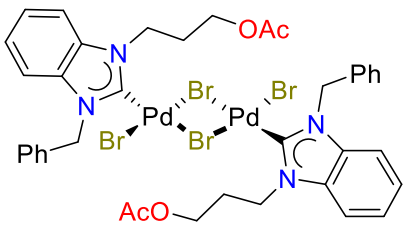

$[PdBr_2(C_3OAc\text{-}bimy)]_2$ (41). Salt **H** (820 mg, 2 mmol), $Pd(OAc)_2$ (449 mg, 2 mmol) and NaBr (823 mg, 8 mmol) were mixed in DMSO (10 mL) and stirred at 90 °C for 24 h. The solvent of the mixture was removed by vacuum distillation, and CH_2Cl_2 (50 mL) was added. The suspension was filtered over Celite and the filtrate was concentrated to 2 mL, which was subjected to column chromatography using a mixture of ethyl acetate and hexane as eluent, giving the product as a red solid (437 mg, 0.38 mmol, 38%). ^{1}H NMR (300 MHz, $CDCl_3$): δ 7.51 (ps–d, 4 H, Ar–H), 7.42–7.30 (m, 10 H, Ar–H), 7.15 (t, 2 H, Ar–H), 7.08 (ps–d, 2 H, Ar–H), 6.19 (s, 4 H, NCH_2Ph), 5.00 (t, ^3J(H,H) = 7.2 Hz, 4 H, NCH_2), 4.26 (br–s, 4 H, CH_2OCOCH_3), 2.63 (br–s, 4 H, $CH_2CH_2CH_2$), 2.10 (s, 6 H, $COCH_3$). $^{13}C\{^1H\}$ NMR (75.48 MHz, $CDCl_3$): δ 171.6 (CO), 160.6 ($C_{carbene}$), 135.4, 134.9, 134.8, 129.7, 129.1, 128.6, 124.5, 112.6, 110.0 (Ar–C, 1 × coincident), 62.2 (CH_2OCOCH_3), 54.4 (NCH_2Ph), 46.5 (NCH_2), 29.3 (CH_2OCOCH_3), 21.7 ($CH_2CH_2CH_2$). IR (KBr pellet) $\tilde{\nu}$ = 1738 cm^{-1} (s, C=O). Anal. Calcd for $C_{38}H_{40}Br_4N_4Pd_2$: C, 39.71; H, 3.51; N, 4.88. Found: C, 40.00; H, 3.45; N, 4.89. MS (ESI): *m/z* 682 $[M/2 + Pd + H]^+$.

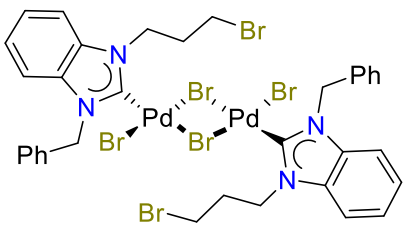

$[PdBr_2(C_3Br\text{-}bimy)]_2$ (42). A mixture of Ag_2O (232 mg, 1 mmol) and salt **H** (820 mg, 2 mmol) was suspended in CH_2Cl_2 (30 mL) and stirred at ambient temperature for 3 h shielded

from light. The resulting mixture was filtered into a solution of [$PdBr_2(CH_3CN)_2$] ($PdBr_2$, 533 mg, 2 mmol) in CH_3CN (30 mL). The reaction mixture was stirred for 20 h and filtered through a sintered funnel. The solvent of the filtrate was removed under vacuum to give a red brown residue, which was suspended and stirred in diethyl ether (100 mL) overnight. The resulting suspension was filtered through a sintered funnel and washed with diethyl ether (10 mL × 3). Drying the residue in vacuo afforded the product as red brown powders (1.0 g, 0.86 mmol, 86%). ^{1}H NMR (500 MHz, d_6-DMSO): δ 7.77 (d, 2 H, Ar–H), 7.60 (d, 4 H, Ar–H), 7.38–7.29 (m, 8 H, Ar–H), 7.24 (m, 4 H, Ar–H), 6.07 (s, 4 H, NCH_2Ph), 4.94 (t, ^3J(H,H) = 7.4 Hz, 4 H, NCH_2), 3.76 (t, ^3J(H,H) = 6.4 Hz, 4 H, CH_2Br), 2.69 (m, ^3J(H,H) = 7.2 Hz, 4 H, $CH_2CH_2CH_2$). $^{13}C\{^1H\}$ NMR (125.77 MHz, d_6-DMSO): δ 135.0, 134.1, 133.3, 128.5, 128.0, 123.5, 123.4, 111.6, 110.9 (Ar–C, 1 × coincident), 52.2 (NCH_2Ph). 46.6 (NCH_2), 31.7 (CH_2Br), 31.5 ($CH_2CH_2CH_2$), the $C_{carbene}$ signal could not be detected. Anal. Calcd for $C_{34}H_{34}Br_6N_4Pd_2$: C, 34.29; H, 2.88; N, 4.70. Found: C, 34.63; H, 2.87; N, 4.64. MS (ESI): *m/z* 329 $[L + H]^+$.

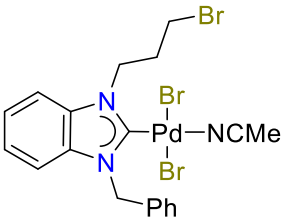

***trans*-[$PdBr_2(C_3Br$-bimy$)(CH_3CN)$] (43).** A suspension of complex **42** (120 mg, 0.10 mmol) in CH_3CN (20 mL) was stirred at 80 °C overnight. The reaction mixture was filtered over Celite and removal of the solvent from the filtrate in vacuo afforded the product as a yellow powder (57 mg, 0.09 mmol, 90%). ^{1}H NMR (300 MHz, CD_3CN): δ 7.61 (d, 1 H, Ar–H), 7.54–7.51 (m, 2 H, Ar–H), 7.34–7.30 (m, 4 H, Ar–H), 7.20–7.14 (m, 2 H, Ar–H), 6.06 (s, 2 H, NCH_2Ph), 4.93 (t, ^3J(H,H) = 7.4 Hz, 2 H, NCH_2), 3.65 (t, ^3J(H,H) = 6.4 Hz, 2 H, CH_2Br), 2.76 (m, ^3J(H,H) = 7.4 Hz, 2 H, $CH_2CH_2CH_2$), 1.95 (s, $NCCH_3$, correct integration was not obtained due to ligand exchange with the solvent). $^{13}C\{^1H\}$ NMR (75.48 MHz, CD_3CN): δ 161.8 ($C_{carbene}$), 136.0, 135.5, 134.7,

129.5, 129.05, 124.6, 124.5 (Ar–C, 1 × coincident), 118.3 (CN), 112.5, 111.7 (Ar–C), 53.8 (NCH_2Ph), 47.8 (NCH_2), 32.8 (CH_2Br), 31.8 ($CH_2CH_2CH_2$). Anal. Calcd for $C_{19}H_{20}Br_3N_3Pd$: C, 35.85; H, 3.17; N, 6.60. Found: C, 35.78; H, 2.98; N, 6.63. MS (ESI): *m/z* 558 $[M - Br]^+$.

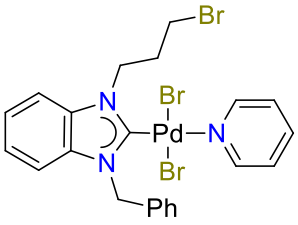

***trans*-[PdBr$_2$(C$_3$Br-bimy)(Py)]** (**44**). Pyridine (88.6 µL, 1.1 mmol) was added to the suspension of complex **42** (596 mg, 0.5 mmol) in CH_2Cl_2 (25 mL) and stirred at ambient temperature for 2 h. The solvent was removed under reduced pressure, and the residue was washed with diethyl ether to give a yellow solid product (277 mg, 0.4 mmol, 82%). ^{1}H NMR (500 MHz, $CDCl_3$): δ 9.05 (d, 2 H, py–H), 7.76 (t, 1 H, py–H), 7.58 (ps–d, 2 H, py–H), 7.54 (d, 1 H, Ar–H), 7.38–7.30 (m, 5 H, Ar–H), 7.25 (t, 1 H, Ar–H), 7.11 (t, 1 H, Ar–H), 7.05 (ps–d, 1 H, Ar–H), 6.17 (s, 2 H, NCH_2Ph), 5.07 (t, ^3J(H,H) = 7.2 Hz, 2 H, NCH_2), 3.67 (t, ^3J(H,H) = 5.9 Hz, 2 H, CH_2Br), 2.93 (m, ^3J(H,H) = 6.5 Hz, 2 H, $CH_2CH_2CH_2$). ^{13}C{^{1}H} NMR (125.77 MHz, $CDCl_3$): δ 164.6 ($C_{carbene}$), 153.3, 138.7, 135.8, 135.5, 135.0, 129.5, 128.9, 128.8, 125.3, 124.0, 123.9, 112.3, 111.0 (Ar–C), 54.5 (NCH_2Ph), 47.4 (NCH_2), 32.7 (CH_2Br), 31.8 ($CH_2CH_2CH_2$). Anal. Calc for $C_{22}H_{22}Br_3N_3Pd$: C, 39.17; H, 3.29; N, 6.23. Found: C, 39.60; H, 3.43; N, 6.53. MS (ESI): *m/z* 594 $[M - Br]^+$.

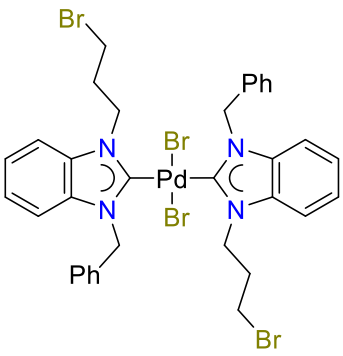

***trans*-[PdBr$_2$(C$_3$Br-bimy)$_2$]** (**45**). A mixture of Ag_2O (232 mg, 1.00 mmol) and salt **H** (410 mg, 2.00 mmol) were suspended in CH_2Cl_2 (60 mL) and stirred at ambient temperature for 3 h shielded from light. A solution of $[PdBr_2(CH_3CN)_2]$ ($PdBr_2$, 266 mg, 1.00 mmol) in CH_3CN (200 mL) was added. The reaction mixture was stirred for

20 h, and the resulting suspension was filtered through a sintered funnel. Removal of the solvent under vacuum yielded the product as a pale-yellow powder. Yields and *syn*:*anti* ratios: 922 mg, 1.00 mmol, >99%, 1:2.2. ^{1}H NMR (300 MHz, $CDCl_3$): δ 7.62 (d, 5 H, Ar–H), 7.56 (d, 2 H, Ar–H), 7.49 (d, 3 H, Ar–H), 7.42–7.33 (m, 11 H, Ar–H), 7.23 (m, 8 H, Ar–H), 7.17–7.12 (m, 7 H, Ar–H), ***syn***: 5.95 (s, 4 H, NCH_2Ph), 5.05 (t, ^{3}J(H,H) = 7.0 Hz, 4 H, NCH_2), 3.63 (t, ^{3}J(H,H) = 6.0 Hz, 4 H, CH_2Br), 2.96 (m, ^{3}J(H,H) = 6.5 Hz, 4 H, $CH_2CH_2CH_2$), ***anti***: 6.18 (s, 4 H, NCH_2Ph), 4.92 (t, ^{3}J(H,H) = 7.2 Hz, 4 H, NCH_2), 3.25 (t, ^{3}J(H,H) = 6.0 Hz, 4 H, CH_2Br), 2.73 (m, ^{3}J(H,H) = 6.5 Hz, 4 H, $CH_2CH_2CH_2$). ^{13}C{^{1}H} NMR (75.47 MHz, $CDCl_3$): δ 182.6, 182.5 ($C_{carbene}$), 135.9, 135.8, 135.6, 135.5, 135.1, 134.9, 129.6, 129.3, 128.8, 128.5, 128.3, 123.9, 123.8, 112.1, 112.0, 111.1, 111.0 (Ar–C, 3 × coincident), 53.7, 53.3 (NCH_2Ph), 47.1 (2 × NCH_2), 33.5, 33.2 (CH_2Br), 31.7, 31.2 ($CH_2CH_2CH_2$). Anal. Calcd for $C_{34}H_{34}Br_4N_4Pd$: C, 44.16; H, 3.71; N, 6.06. Found: C, 44.12; H, 3.60; N, 6.12. MS (ESI): *m/z* 843 $[M - Br]^+$.

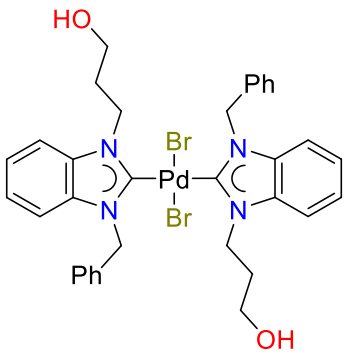

trans*-[PdBr$_2$(C$_3$OH-bimy)$_2$]** (**46**). Complex **45** was suspended in d_6-DMSO (0.6 mL) and heated to 110°C for one day before NMR. *syn*:*anti* ratios: 1:1.4. ^{1}H NMR (400 MHz, d_6-DMSO): δ 7.74 (d, 5 H, Ar–H), 7.67 (d, 2 H, Ar–H), 7.60–7.58 (m, 4 H, Ar–H), 7.37–7.29 (m, 14 H, Ar–H), 7.25–7.21 (m, 11 H, Ar–H), ***syn: 6.15 (s, 4 H, NCH_2Ph), 4.82 (t, ^{3}J(H,H) = 7.6 Hz, 4 H, NCH_2), 3.34 (t, ^{3}J(H,H) = 6.0 Hz, 4 H, CH_2O), 2.23 (m, 4 H, ^{3}J(H,H) = 6.8 Hz, $CH_2CH_2CH_2$), ***anti***: 6.00 (s, 4 H, NCH_2Ph), 4.93 (t, ^{3}J(H,H) = 7.2 Hz, 4 H, NCH_2), 3.64 (t, ^{3}J(H,H) = 6.0 Hz, 4 H, CH_2O), 2.36 (m, ^{3}J(H,H) = 6.7 Hz, 4 H, $CH_2CH_2CH_2$), the OH signals are found at 4.62 (t, ^{3}J(H,H) = 4.9 Hz, 2 H, OH). ^{13}C{^{1}H} NMR (100.62 MHz, d_6-DMSO): δ 181.2, 181.1 ($C_{carbene}$), 135.84, 135.76, 134.3, 134.2, 133.5, 133.3, 128.5, 128.3, 128.0,

127.8, 127.7, 123.1, 123.00, 122.97, 111.5, 111.4, 111.0, 110.9 (Ar–C, 2 × coincident), 58.1, 57.8 (CH_2O), 51.7, 51.5 (NCH_2Ph), 44.91, 44.86 (NCH_2), 32.7, 32.5 ($CH_2CH_2CH_2$). Anal. Calc. for $C_{34}H_{36}Br_2N_4O_2Pd$: C, 51.12; H, 4.54; N, 7.01. Found: C, 51.38; H, 4.26; N, 6.95. MS (ESI): *m/z* 719 $[M - Br]^+$.

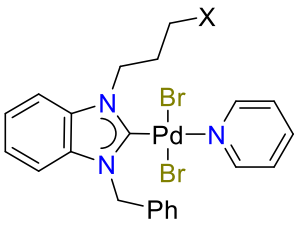

***trans*-[PdBr$_2$(C$_3$X-bimy)$_2$]** (**47–48**). Complex **44** (67 mg, 0.10 mmol) and KOAc (25 mg, 0.25 mmol) or NaN_3 (85 mg, 0.13 mmol) were mixed in CH_3CN (20 mL) and refluxed overnight. CH_2Cl_2 (30 mL) was added after the solvent was removed. The resulting suspension was filtered over Celite and the solvent removed under reduced pressure, giving the product as red brown (**47**) or yellow (**48**) powders.

X = OAc, (**47**). Yield: 59 mg, 0.90 mmol, 90%. ^{1}H NMR (300 MHz, $CDCl_3$): δ 9.04 (dd, 2 H, py–H), 7.76 (t, 1 H, py–H), 7.57 (ps–d, 2 H, py–H), 7.40 (d, 1 H, Ar–H), 7.38–7.31 (m, 5 H, Ar–H), 7.23 (t, 1 H, Ar–H), 7.10 (t, 1 H, Ar–H), 7.04 (ps–d, 1 H, Ar–H), 6.16 (s, 2 H, NCH_2Ph), 4.99 (t, ^3J(H,H) = 7.6 Hz, 2 H, NCH_2), 4.31 (t, ^3J(H,H) = 5.9 Hz, 2 H, CH_2OCOCH_3), 2.68 (m, ^3J(H,H) = 7.3 Hz, 2 H, $CH_2CH_2CH_2$), 2.09 (s, 3 H, CH_3). ^{13}C{^{1}H} NMR (75.48 MHz, $CDCl_3$): δ 171.5 (C=O), 164.3 ($C_{carbene}$), 153.2, 138.7, 135.6, 135.4, 134.9, 129.5, 128.8, 128.7, 125.2, 123.9. 123.8, 112.3, 110.7 (Ar–C), 62.5 (CH_2OCOCH_3), 54.3 (NCH_2Ph), 46.3 (NCH_2), 29.0 (CH_2OCOCH_3), 21.6 ($CH_2CH_2CH_2$). Anal. Calcd for $C_{24}H_{25}Br_2N_3O_2Pd$: C, 44.10; H, 3.85; N, 6.43. Found: C, 44.58; H, 3.49; N, 6.30 (best result obtained). ^{1}H and ^{13}C NMR spectra are attached in the appendix. MS (ESI): *m/z* 573 $[M - Br]^+$.

X = N_3, (**48**). Yield: 64 mg, 0.10 mmol, >99%. ^{1}H NMR (500 MHz, $CDCl_3$): δ 9.04 (d, 2 H, py–H), 7.76 (t, 1 H, py–H), 7.58 (ps–d, 2 H, py–H), 7.46 (d, 1 H, Ar–H), 7.38–7.30 (m, 5 H, Ar–H), 7.25 (t, 1 H, Ar–H), 7.11 (t, 1 H, Ar–H), 7.05 (ps–d, 1 H, Ar–H), 6.17 (s, 2 H, NCH_2Ph), 4.98 (t, ^3J(H,H) = 7.3 Hz, 2 H, NCH_2), 3.60 (t, ^3J(H,H) = 6.2 Hz, 2 H, CH_2N_3), 2.61 (m, ^3J(H,H) = 6.7 Hz, 2 H, $CH_2CH_2CH_2$). ^{13}C{^{1}H} NMR (125.77 MHz, $CDCl_3$): δ 164.4 ($C_{carbene}$), 153.2, 138.7, 135.7, 135.4, 134.9, 129.5, 128.9, 128.7, 125.3, 124.0, 123.9, 112.3, 110.8 (Ar–C), 54.4 (NCH_2Ph), 49.3 (NCH_2), 46.2 (CH_2N_3), 29.2 ($CH_2CH_2CH_2$). Anal. Calcd for $C_{22}H_{22}Br_2N_6Pd$: C, 41.50; H, 3.48; N, 13.20. Found: C, 41.76 ;H, 3.74; N, 13.52. MS (ESI): *m/z* 557 $[M - Br]^+$.

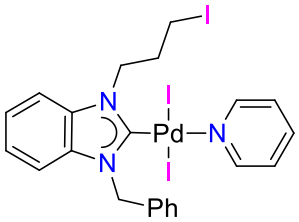

***trans*-[$PdI_2(C_3I$-bimy)(Py)]** (**49**). NaI (1.5 g, 10 mmol) was added into the solution of complex **44** (675 mg, 1 mmol) in acetone and stirred at ambient temperature for 4 h. The solvent of the suspension was removed in vacuo before CH_2Cl_2 (20 mL) was added. The resulting red orange suspension was filtered over Celite, and the solvent of the filtrate was removed under reduced pressure to give the product as an orange powder (775 mg, 0.95 mmol, 95%). ^{1}H NMR (500 MHz, $CDCl_3$): δ 9.07 (d, 2 H, py–H), 7.74 (t, 1 H, py–H), 7.58 (ps–d, 2 H, py–H), 7.52 (d, 1 H, Ar–H), 7.38–7.31 (m, 5 H, Ar–H), 7.23 (t, 1 H, Ar–H), 7.08 (t, 1 H, Ar–H), 6.95 (ps–d, 1 H, Ar–H), 6.05 (s, 2 H, NCH_2Ph), 4.94 (t, ^3J(H,H) = 7.5 Hz, 2 H, NCH_2), 3.43 (t, ^3J(H,H) = 6.2 Hz, 2 H, CH_2I), 2.86 (m, ^3J(H,H) = 7.3 Hz, 2 H, $CH_2CH_2CH_2$). ^{13}C{^{1}H} NMR (125.77 MHz, $CDCl_3$): δ 163.3 ($C_{carbene}$), 154.6, 138.4, 135.9, 135.3, 135.2, 129.4, 129.0, 128.9, 125.2, 123.8, 123.7, 112.4, 111.0 (Ar–C), 55.4 (NCH_2Ph), 50.3 (NCH_2), 32.3 (CH_2I), 4.0 ($CH_2CH_2CH_2$). Anal. Calcd for $C_{22}H_{22}I_3N_3Pd$: C, 32.40; H, 2.72; N, 5.15. Found: C, 32.84; H, 2.98; N, 5.69 (best result obtained). ^{1}H and ^{13}C NMR spectra are attached in the appendix.. MS (ESI): *m/z* 687 $[M - I]^+$.

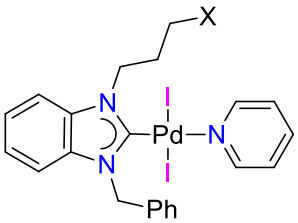

***trans*-[PdI$_2$(C$_3$X-bimy)(Py)]** (**50–52**). Complex **49** (159 mg, 0.20 mmol) and NaN_3 or KSCN or KSAc (13/19/24 mg, 0.20 mmol) were stirred in CH_3CN (20 mL) overnight at 90 °C. The suspension was filtered over Celite, and the solvent of the filtrate was removed under reduced pressure, affording a red-orange solid. After washing with H_2O (3 × 5 mL), CH_2Cl_2 (50 mL) was added. The resulting suspension was filtered over Celite, and the filtrate was dried in vacuo giving the product as red-orange (**50**) or orange (**51**) or brown (**52**) solids.

X = N$_3$, (**50**). Yield: 144 mg, 0.20 mmol, 98%. ^{1}H NMR (500 MHz, $CDCl_3$): δ 9.05 (d, 2 H, py–H), 7.73 (t, 1 H, py–H), 7.59 (ps–d, 2 H, py–H), 7.46 (d, 1 H, Ar–H), 7.39–7.31 (m, 5 H, Ar–H), 7.24 (t, 1 H, Ar–H), 7.08 (t, 1 H, Ar–H), 6.96 (ps–d, 1 H, Ar–H), 6.06 (s, 2 H, NCH_2Ph), 4.90 (t, ^3J(H,H) = 7.5 Hz, 2 H, NCH_2), 3.60 (t, ^3J(H,H) = 6.1 Hz, 2 H, CH_2N_3), 2.63 (m, ^3J(H,H) = 7.0 Hz, 2 H, $CH_2CH_2CH_2$). ^{13}C{^{1}H} NMR (125.77 MHz, $CDCl_3$): δ 163.0 ($C_{carbene}$), 154.4, 138.4, 135.8, 135.2, 135.1, 129.4, 128.9, 128.8, 125.2, 123.8, 123.7, 112.4, 110.7 (Ar–C), 55.3 (NCH_2Ph), 49.4 (NCH_2), 47.0 (CH_2N_3), 28.5 ($CH_2CH_2CH_2$). Anal. Calcd for $C_{22}H_{22}I_2N_6Pd$: C, 36.16; H, 3.03; N, 11.50. Found: C, 36.32; H, 2.94; N 11.13. MS (ESI): *m/z* 249 $[L - N_3]^+$.

X = SCN, (**51**). Yield: 135 mg, 0.18 mmol, 90%. ^{1}H NMR (500 MHz, $CDCl_3$): δ 9.04 (d, 2 H, py–H), 7.76 (t, 1 H, py–H), 7.56 (ps–d, 2 H, py–H), 7.45 (d, 1 H, Ar–H), 7.38–7.34 (m, 5 H, Ar–H), 7.26 (t, 1 H, Ar–H), 7.11 (t, 1H, Ar–H), 6.98 (d, 1 H, Ar–H), 6.06 (s, 2 H, NCH_2Ph), 5.01 (t, ^3J(H,H) = 6.8 Hz, 2 H, NCH_2), 3.28 (t, ^3J(H,H) = 6.5 Hz, 2 H, CH_2SCN), 2.89 (m, ^3J(H,H) = 6.7 Hz, 2 H, $CH_2CH_2CH_2$). ^{13}C{^{1}H} NMR (125.77 MHz, $CDCl_3$): δ 163.9 ($C_{carbene}$), 154.6, 138.5, 135.7, 135.5, 135.1, 129.5, 129.0, 125.3, 124.1, 124.0, 112.7 (Ar–C, 1 × coincident), 112.4 (SCN), 110.7 (Ar–C), 55.6 (NCH_2Ph). 47.7 (NCH_2), 32.5 (CH_2SCN), 28.9 ($CH_2CH_2CH_2$). Anal.

Calcd for $C_{23}H_{22}I_2N_4PdS$: C, 36.99; H, 2.97; N, 7.50. Found: C, 36.77; H, 3.26; N, 7.96. MS (ESI): *m/z* 719 $[M - SCN + MeOH]^+$.

X = SAc, (**52**). Yield: 99 mg, 0.13 mmol, 65%. ^{1}H NMR (500 MHz, $CDCl_3$): δ 9.06 (d, 2 H, py–H), 7.74 (t, 1 H, py–H), 7.56 (ps–d, 2 H, py–H), 7.48 (d, 1 H, Ar–H), 7.37–7.34 (m, 5 H, Ar–H), 7.22 (t, 1 H, Ar–H), 7.06 (t, 1 H, Ar–H), 6.93 (ps–d, 1 H, Ar–H), 6.03 (s, 2 H, NCH_2Ph), 4.85 (t, ^3J(H,H) = 7.8 Hz, 2 H, NCH_2), 3.14 (t, ^3J(H,H) = 6.9 Hz, 2 H, CH_2SCOCH_3), 2.62 (m, ^3J(H,H) = 7.7 Hz, 2 H, $CH_2CH_2CH_2$), 2.38 (s, 3 H, $SCOCH_3$). ^{13}C{^{1}H} NMR (125.77 MHz, $CDCl_3$): δ 196.0 (C=O), 162.9 ($C_{carbene}$), 154.5, 138.4, 135.7, 135.2, 129.4, 128.9, 128.8, 125.2, 123.7, 123.6, 112.4, 110.8 (Ar–C, 1 × coincident), 55.2 (NCH_2Ph), 48.7 (NCH_2), 31.4 (SCH_2), 28.9 ($SCOCH_3$), 27.3 ($CH_2CH_2CH_2$). Anal. Calcd for $C_{24}H_{25}I_2N_3OPdS$: C, 37.74; H, 3.30; N, 5.50. Found: C, 37.49; H, 3.28; N, 5.26. MS (ESI): *m/z*763 $[M - I]^+$.

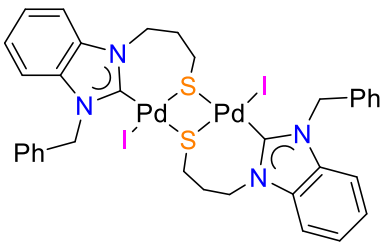

Propyl thiolato bridged complex (**53**). Sodium hydroxide (10 mg, 0.25 mmol) in methanol (6 mL) was added to the solution of complex **52** (140 mg, 0.17 mmol) in CH_2Cl_2 (10 mL) and stirred overnight. The solvent of the mixture was removed, and CH_2Cl_2 (20 mL) was added. The resulting suspension was filtered through Celite, and removal of the solvent of the filtrate gave the product as an orange powder (73 mg, 0.07 mmol, 82%). ^{1}H NMR (500 MHz, $CDCl_3$): δ 7.49 (ps–d, 3 H, Ar–H), 7.39 (ps–d, 3 H, Ar–H), 7.33 (t, 4 H, Ar–H), 7.30–7.24 (m, 6 H, Ar–H), 7.18 (t, 2 H, Ar–H), 6.37 (d, ^2J(H, H) = 15.8 Hz, 2 H, NC*H*HPh), 6.25 (m, 2 H, NC*H*H), 5.32 (d, ^2J(H, H) = 15.8 Hz, 2 H, NCH*H*Ph), 4.65 (m, 2 H, NCH*H*), 3.10–3.00 (m, 4 H, SCH_2), 2.25 (m, 2 H, CH_2CHHCH_2), 1.72 (m, 2 H, CH_2CHHCH_2). ^{13}C{^{1}H} NMR (125.77

MHz, $CDCl_3$): δ 174.8 ($C_{carbene}$), 136.0, 135.5, 134.0, 129.5, 128.9, 128.5, 124.3, 124.1, 112.4, 110.7 (Ar–C), 54.0 (NCH_2Ph). 43.9(NCH_2), 27.1 (SCH_2), 27.0 ($CH_2CH_2CH_2$). Anal. Calcd for $C_{34}H_{34}I_2N_4Pd_2S_2$: C, 39.67; H, 3.33; N, 5.44. Found: C, 39.98; H, 3.56; N, 5.22. MS (ESI): *m/z* 903 $[M - I]^+$.

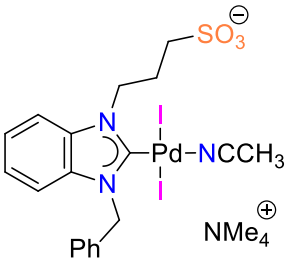

***trans*-[PdI$_2$(C$_3$SO$_3$-bimy)(CH$_3$CN)](NMe$_4$) (54)**. Complex **53** (103 mg, 0.10 mmol), Oxone (20 mg, 0.30 mmol) and NMe_4I (101 mg, 0.50 mmol) in DMF (10 mL) and H_2O (4 mL) were stirred at ambient temperature overnight. After the solvent was removed, the resulting solid was triturated with CH_3CN (3 × 10 mL) and the suspension filtered. The solvent of the filtrate was removed and the residue was washed with H_2O (3 × 3 mL) and redissolved in CH_3CN (20 mL). Removal of the solvent gave the product as a yellow powder. A second batch was obtained by removing the solvent of the aqueous solution, washing the residue with little H_2O (3 × 1 mL), and recrystallization in CH_3CN (5 mL) (137 mg, 0.17 mmol, 85%). ^{1}H NMR (500 MHz, CD_3CN): δ 7.68 (d, 1 H, Ar–H), 7.49 (br–s, 2 H, Ar–H), 7.31 (br–s, 3 H, Ar–H), 7.23 (t, 1 H, Ar–H), 7.08 (t, 1 H, Ar–H), 6.99 (d, 1 H, Ar–H), 5.90 (s, 2 H, NCH_2Ph), 4.84 (br–s, 2 H, NCH_2), 3.08 (s, 12 H, NMe_4), 2.65 (br–s, 2 H, CH_2SO_3), 2.56 (br–s, 2 H, $CH_2CH_2CH_2$), 1.96 (s, CH_3CN, correct integration is not possible due to ligand exchange with the solvent). ^{13}C{^{1}H} NMR (125.77 MHz, CD_3CN): 159.9 (NCN), 135.7, 135.6, 135.1, 129.4, 129.1, 129.0, 124.5, 124.2 (Ar–C), 118.1 (CN), 112.4, 112.0 (Ar–C), 56.2 (t, ^1J(C,N) = 3.7 Hz, NMe_4), 54.6 (NCH_2Ph), 49.4 (CH_2SO_3), 48.9 (NCH_2), 24.6 ($CH_2CH_2CH_2$), 1.32 (m, CH_3CN, assignment is tentative due to overlap with solvent signals). Anal. Calcd for $C_{23}H_{32}I_2N_4O_3PdS$: C, 34.32; H, 4.01; N, 6.96. Found: C, 33.99; H, 3.83; N, 7.12. MS (ESI): *m/z* 74 $[NMe_4]^+$, 689 $[M - NMe_4 - CH_3CN]^-$.

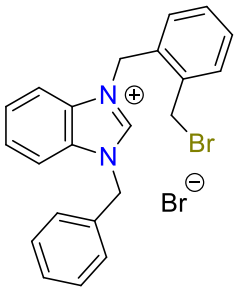

Salt I. α,α'-dibromo-*o*-xylene (5.3 g, 20 mmol) and 1-benzylbenzimidazole (208 mg, 1 mmol) were dissolved in toluene (50 mL) and stirred at 50 ℃ overnight, resulting in a suspension. The white solid was collected by centrifuging and washed with toluene (3 × 10 mL) and diethyl ether (3 × 10 mL). The solid was redissolved in CH_2Cl_2 and filtered. Slow evaporation of the filtrate gives the product as a white crystalline solid (179 mg, 0.38 mmol, 38%). ^{1}H NMR (500 MHz, $CDCl_3$): δ 11.44 (s, 1 H, NCHN), 7.58 (d, 1 H, Ar–H), 7.54–7.42 (m, 5 H, Ar–H), 7.35–7.28 (m, 6 H, Ar–H), 7.18 (d, 1 H, Ar–H), 6.11 (s, 2 H, NCH_2Ph), 5.82 (s, 2 H, NCH_2Ph), 4.70 (s, 2 H, CH_2Br). $^{13}C\{^1H\}$ NMR (125.77 MHz, $CDCl_3$): 144.0 (NCHN), 136.9, 133.1, 132.33, 132.25, 131.9, 131.7, 130.4, 129.9, 129.83, 129.76, 129.0, 128.9, 127.83, 127.82, 114.6, 114.5 (Ar–C), 52.4, 49.6 (NCH_2Ph), 32.0 (CH_2Br). MS (ESI): *m/z* 391 $[M - Br]^+$.

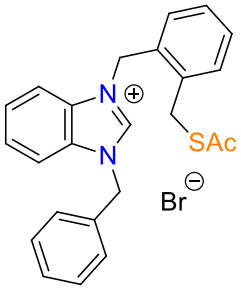

Salt J. A mixture of salt **I** (63 mg, 0.13 mmol) and KSAc (18 mg, 0.16 mmol) in CH_3CN (20 mL) was stirred overnight. The solvent of the mixture was removed in vacuo before CH_2Cl_2 (30 mL) was added. The resulting suspension was filtered and dried under reduced pressure to afford the product as off-white oil (50 mg, 0.11 mmol, 83%). ^{1}H NMR (300 MHz, $CDCl_3$): δ 11.15 (s, 1 H, NCHN), 7.64–7.61 (m, 1 H, Ar–H), 7.50–7.39 (m, 5 H, Ar–H), 7.32–7.11 (m, 7 H, Ar–H), 5.92 (s, 2 H, NCH_2Ph), 5.85 (s, 2 H, NCH_2Ph), 4.18 (s, 2 H, CH_2S), 2.13 (s, 3 H, CH_3). $^{13}C\{^1H\}$ NMR (75.47 MHz, $CDCl_3$): 195.1 (CO), 143.6 (NCHN), 136.3, 133.2, 132.0, 131.81, 131.79, 131.0, 130.1, 129.7, 129.6, 129.4, 129.1, 129.0, 127.8, 127.7, 114.5, 114.3 (Ar–C), 52.1, 49.5 (NCH_2Ph), 31.2 (CH_2S), 30.8 (CH_3). MS (ESI): *m/z* 387 $[M - Br]^+$.

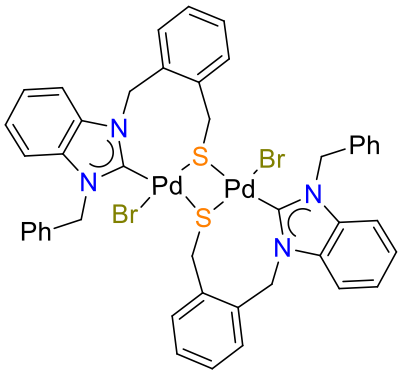

Xylenyl-thiolato-bridged complex (**55**). A mixture of salt **J** (472 mg, 1.0 mmol) and $Pd(OAc)_2$ (224 mg, 1.0 mmol) in DMSO (5 mL) was stirred at 80 ℃ overnight. The resulting suspension was filtered, and the yellow solid was washed with H_2O (3 × 20 mL) and dried to give the products (403 mg, 0.38 mmol, 76%). ^{1}H NMR (500 MHz, $CDCl_3$): δ 7.59 (d, 2 H, Ar–H), 7.43–7.39 (m, 4 H, Ar–H), 7.35–7.32 (m, 8 H, Ar–H), 7.22–7.09 (m, 12 H, Ar–H and NC*H*HPh), 7.07–7.06 (m, 2 H, Ar–H), 6.96–6.88 (m, 2 H, NC*H*H), 5.32 (d, 2 H, NCH*H*Ph), 4.91–4.81 (m, 2 H, NCH*H*), 4.39 (d, ^2J(H,H) = 15.1 Hz, 1 H, NC*H*HS), 4.22 (d, ^2J(H,H) = 15.1 Hz, 1 H, NC*H*HS), 2.63 (d, ^2J(H,H) = 15.1 Hz, 2 H, NCH*H*S). Anal. Calcd for $C_{44}H_{38}Br_2N_4Pd_2S_2 \cdot H_2O$: C, 49.04; H, 3.74; N, 5.20. Found: C, 48.72; H, 3.48; N, 5.05. MS (ESI): *m/z* 979 $[M - Br]^+$. The ^{13}C NMR spectrum could not be obtained due to poor solubility.

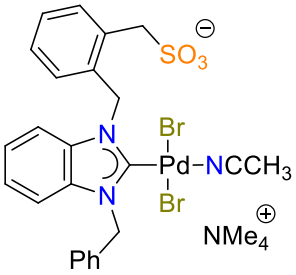

Xylenyl-sulfonate complex (**56**). This complex was prepared in analogy to complex **54** from complex **55** (212 mg, 0.2 mmol), Oxone (39 mg, 0.6 mmol) and NMe_4Br (154 mg, 1.0 mmol). Yield: 207 mg, 0.3 mmol, 74%. ^{1}H NMR (500 MHz, CD_3CN): δ 7.59 (d, 2 H, Ar–H), 7.41–7.33 (m, 4 H, Ar–H), 7.22 (t, 1 H, Ar–H), 7.17–7.11 (m, 4 H, Ar–H), 7.04 (t, 1 H, Ar–H), 6.86 (d, 1 H, Ar–H), 6.41 (s, 2 H, NCH_2Ph), 6.13 (s, 2 H, NCH_2Ph), 4.17 (s, 2 H, CH_2SO_3), 3.06 (s, 12 H, NMe_4) 1.96 (s, CH_3CN, correct integration is not possible due to ligand exchange with the solvent). ^{13}C{^{1}H} NMR (125.77 MHz, CD_3CN): 162.6 (NCN), 136.1, 135.4, 135.2, 134.9, 133.5, 133.2, 129.6, 129.03, 128.96, 128.2, 128.0, 127.8, 124.5, 124.4 (Ar–C), 118.1 (CN), 113.1, 112.4 (Ar–C), 56.1 (t, ^1J(C,N) = 3.7 Hz, NMe_4), 55.5, 53.8 (NCH_2Ph), 51.0 (CH_2SO_3), 1.32 (m,

CH_3CN, assignment is tentative due to overlap with solvent signals). Anal. Calcd for $C_{28}H_{34}Br_2N_4O_3PdS$: C, 43.51; H, 4.43; N, 7.25. Found: C, 43.23; H, 4.49; N, 7.24. MS (ESI): *m/z* 74 $[NMe_4]^+$, 659 $[M - NMe_4 - CH_3CN]^-$.

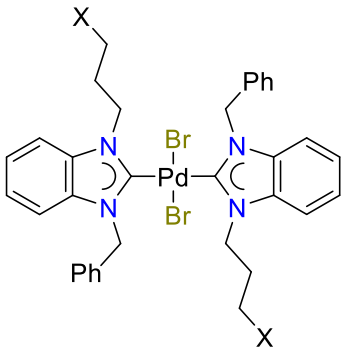

***trans*-[PdBr$_2$(C$_3$X-bimy)$_2$]** (**57**–**59**). A mixture of **45** (93 mg, 0.10 mmol) and KOAc or NaN_3 (98/65 mg, 1.00 mmol) was suspended in CH_3CN (20 mL) and heated to reflux at 85°C for one day. The resulting product was dried under reduced pressure followed by addition of CH_2Cl_2 (30 mL). The resulting yellow suspension was filtered over Celite and the solvent of the filtrate was removed in vacuo, affording complexes **57** and **59** as yellow solids. Complex **58** was obtained via the reaction complex **45** (186 mg, 0.20 mmol) and diethylamine (0.20 mL, 2.00 mmol), which were dissolved in $CHCl_3$ (15 mL) and reflux at 70°C for one day. The resulting orange liquid was dried under reduced pressure and washed with H_2O (3 × 5 mL) to give a brown solid.

X = OAC, (**57**). Yield and *syn*:*anti* ratio: 79 mg, 0.09 mmol, 90%, 1:1.5. ^{1}H NMR (500 MHz, $CDCl_3$): δ 7.66 (d, 5 H, Ar–H), 7.42–7.31 (m, 15 H, Ar–H), 7.22 (m, 9 H, Ar–H), 7.12–7.11 (m, 7 H, Ar–H), ***syn***: 5.95 (s, 4 H, NCH_2Ph), 4.98 (t, ^3J(H,H) = 7.3 Hz, 4 H, NCH_2), 4.31 (t, ^3J(H,H) = 6.0 Hz, 4 H, CH_2O), 2.74 (m, 4 H, ^3J(H,H) = 6.5 Hz, $CH_2CH_2CH_2$), 2.12 (s, 6 H, CH_3), ***anti***: 6.17 (s, 4 H, NCH_2Ph), 4.85 (t, ^3J(H,H) = 7.5 Hz, 4 H, NCH_2), 3.99 (t, ^3J(H,H) = 6.0 Hz, 4 H, CH_2O), 2.53 (m, ^3J(H,H) = 6.8 Hz, 4 H, $CH_2CH_2CH_2$), 1.96 (s, 6 H, CH_3). ^{13}C{^{1}H} NMR (125.77 MHz, $CDCl_3$): δ 182.6, 182.5 ($C_{carbene}$), 171.5, 171.4 (CO), 135.9, 135.8, 135.54, 135.49, 135.0, 134.8, 129.5, 129.3, 128.8, 128.42, 128.35, 126.2, 126.1, 123.72, 123.71, 123.69, 112.2, 112.0, 110.74, 110.69 (Ar–C), 62.6, 62.4 (CH_2O), 53.6, 53.3 (NCH_2Ph), 45.8 (2 × NCH_2), 29.7,

29.5 ($CH_2CH_2CH_2$), 21.6, 21.4 (CH_3). Anal. Calcd for $C_{38}H_{40}Br_2N_4O_4Pd$: C, 51.69; H, 4.57; N, 6.35. Found: C, 51.76; H, 4.18; N, 6.15. MS (ESI): *m/z* 803 $[M - Br]^+$.

X = NEt$_2$, (**58**). Yield and *syn*:*anti* ratio: 182 mg, 0.20 mmol, >99%, 1:1.9. ^{1}H NMR (500 MHz, $CDCl_3$): δ 7.66 (d, 5 H, Ar–H), 7.50 (d, 1 H, Ar–H), 7.42 (d, 5 H, Ar–H), 7.37 (t, 6 H, Ar–H), 7.31 (t, 3 H, Ar–H), 7.21–7.20 (m, 8 H, Ar–H), 7.10–7.06 (m, 8 H, Ar–H), ***syn***: 5.96 (s, 4 H, NCH_2Ph), 4.94 (t, ^3J(H,H) = 7.4 Hz, 4 H, NCH_2CH_2), 2.69 (t, ^3J(H,H) = 6.9 Hz, 4 H, $CH_2NCH_2CH_3$), 2.62 (m, ^3J(H,H) = 7.1 Hz, 8 H, $CH_2NCH_2CH_3$), 2.50 (m, ^3J(H,H) = 7.2 Hz, 4 H, $CH_2CH_2CH_2$), 1.07 (t, ^3J(H,H) = 7.1 Hz, 12 H, CH_3), ***anti***: 6.18 (s, 4 H, NCH_2Ph), 4.82 (t, ^3J(H,H) = 7.6 Hz, 4 H, NCH_2CH_2), 2.41–2.39 (m, 12 H, $CH_2NCH_2CH_3$ and $CH_2NCH_2CH_3$), 2.31 (m, ^3J(H,H) = 7.2 Hz, 4 H, $CH_2CH_2CH_2$), 0.91 (t, ^3J(H,H) = 7.2 Hz, 12 H, CH_3). $^{13}C\{^1H\}$ NMR (125.77 MHz, $CDCl_3$): δ 182.53, 182.49 ($C_{carbene}$), 136.17, 136.15, 135.7, 135.6, 135.1, 134.9, 129.5, 129.4, 129.2, 128.7, 128.6, 128.5, 128.38, 123.37, 123.5, 123.4, 112.1, 111.9, 111.4, 111.2 (Ar–C), 53.8, 53.3 (NCH_2Ph), 51.2, 50.9, 47.4, 47.3, 47.2 (2 ×) (NCH_2), 28.3, 28.1 ($CH_2CH_2CH_2$), 12.2, 12.1 (CH_3). Anal. Calcd for $C_{42}H_{54}Br_2N_6Pd$: C, 55.49; H, 5.99; N, 9.24. Found: C, 55.11; H, 5.98; N, 8.93. MS (ESI): *m/z* 909 $[M]^+$.

X = N$_3$, (**59**). Yield and *syn*:*anti* ratio: 85 mg, 0.10 mmol, >99%, 1:2.1. ^{1}H NMR (500 MHz, $CDCl_3$): δ 7.64 (d, 4 H, Ar–H), 7.47 (d, 2 H, Ar–H), 7.40 (ps–t, 10 H, Ar–H), 7.34 (ps–t, 3 H, Ar–H), 7.28–7.21 (m, 9 H, Ar–H), 7.13–7.12 (m, 8 H, Ar–H), ***syn***: 5.95 (s, 4 H, NCH_2Ph), 4.98 (t, ^3J(H,H) = 7.1 Hz, 4 H, NCH_2), 3.60 (t, ^3J(H,H) = 6.0 Hz, 4 H, CH_2N_3), 2.62 (m, ^3J(H,H) = 6.4 Hz, 4 H, $CH_2CH_2CH_2$), ***anti***: 6.19 (s, 4 H, NCH_2Ph), 4.83 (t, ^3J(H,H) = 7.3 Hz, 4 H, NCH_2), 3.23 (t, ^3J(H,H) = 6.1 Hz, 4 H, CH_2N_3), 2.40 (m, ^3J(H,H) = 6.5 Hz, 4 H, $CH_2CH_2CH_2$). $^{13}C\{^1H\}$

NMR (125.77 MHz, $CDCl_3$): δ 182.62, 182.58 ($C_{carbene}$), 136.0, 135.9, 135.53, 135.46, 135.1, 134.9, 129.6, 129.3, 128.8, 128.5, 128.35, 128.33, 123.89, 123.88, 123.80, 112.2, 112.1, 111.0, 110.9 (Ar–C, 2 × coincident), 53.7, 53.3 (NCH_2Ph), 49.5, 49.3 (CH_2N_3), 46.0, 45.9 (NCH_2), 29.9, 29.7 ($CH_2CH_2CH_2$). Anal. Calcd for $C_{34}H_{34}Br_2N_{10}Pd$: C, 48.10; H, 4.04; N, 16.50. Found: C, 48.06; H, 3.45; N, 15.80 (best result obtained). ^1H and ^{13}C NMR spectra are attached in the appendix. MS (ESI): *m/z* 769 $[M - Br]^+$.

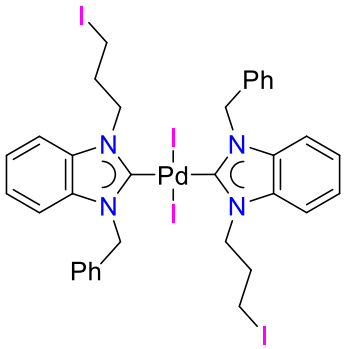

trans*-[PdI$_2$(C$_3$I-bimy)$_2$]** (**60**). A solution of NaI (0.30 g, 2.00 mmol) in acetone (50 mL) was added to a suspension of complex **45** (93 mg, 0.10 mmol) in CH_2Cl_2 (20 mL) and stirred overnight. The solvent of the suspension was removed in vacuo, and 100 mL of CH_2Cl_2 was added. The resulting yellow suspension was filtered over Celite, and the solvent removed under reduced pressure to give the products as yellow powders. Yield and *syn*:*anti* ratio: 106 mg, 0.10 mmol, 95%, 1:1.2. ^1H NMR (500 MHz, $CDCl_3$): δ 7.59–7.55 (m, 6 H, Ar–H), 7.48 (d, 2 H, Ar–H), 7.38 (t, 8 H, Ar–H), 7.34 (d, 2 H, Ar–H), 7.24 (m, 10 H, Ar–H), 7.14–7.09 (m, 4 H, Ar–H), 7.03 (t, 4 H, Ar–H), ***syn: 5.85 (s, 4 H, NCH_2Ph), 4.89 (t, ^3J(H,H) = 7.3 Hz, 4 H, NCH_2), 3.38 (t, ^3J(H,H) = 6.4 Hz, 4 H, CH_2I), 2.89 (m, ^3J(H,H) = 7.2 Hz, 4 H, $CH_2CH_2CH_2$), ***anti***: 6.06 (s, 4 H, NCH_2Ph), 4.78 (t, ^3J(H,H) = 7.5 Hz, 4 H, NCH_2), 3.03 (t, ^3J(H,H) = 6.3 Hz, 4 H, CH_2I), 2.68 (m, ^3J(H,H) = 7.4 Hz, 4 H, $CH_2CH_2CH_2$). $^{13}C\{^1H\}$ NMR (125.77 MHz, $CDCl_3$): δ 181.8, 181.7 ($C_{carbene}$), 136.0, 135.9, 135.57, 135.56, 135.4, 129.6, 129.3, 128.8, 128.58, 128.56, 128.54, 123.72, 123.68, 112.3, 112.2, 111.1, 111.0 (Ar–C, 3 × coincident), 54.7, 54.2 (NCH_2Ph), 49.9 (2 × CH_2I), 33.2, 32.8 (NCH_2), 3.84, 3.20

($CH_2CH_2CH_2$). Anal. Calcd for $C_{34}H_{34}I_4N_4Pd$: C, 36.70; H, 3.08; N, 5.04. Found: C, 36.49; H, 3.43; N, 4.98. MS (ESI): *m/z* 985 $[M - I]^+$.

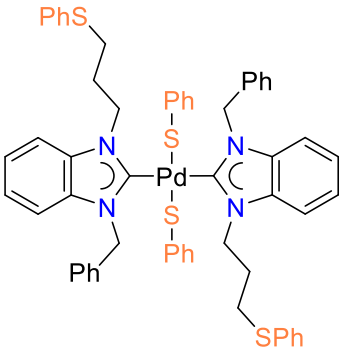

trans*-[Pd(SPh)$_2$(C$_3$SPh-bimy)$_2$]** (**61**). Complex **45** (93 mg, 0.10 mmol) and freshly made NaSPh (132 mg, 1.00 mmol) were suspended in degassed THF (30 mL) and stirred overnight. The suspension was dried under reduced pressure and CH_2Cl_2 (50 mL) was added. The liquid was collected by filtration, concentrated to 5 mL, and subjected to colum chromatography (SiO_2, ethyl acetate:hexane = 1:8). The products were collected as bright yellow solids. Yield and *syn*:*anti* ratio: 81 mg, 0.08 mmol, 78%, 1:1.5. ^{1}H NMR (500 MHz, $CDCl_3$): δ 7.77 (d, 4 H, Ar–H), 7.59 (d, 3 H, Ar–H), 7.52 (t, 1 H, Ar–H), 7.47 (d, 2 H, Ar–H), 7.43–7.38 (m, 5 H, Ar–H), 7.33–7.26 (m, 22 H, Ar–H), 7.19 (t, 6 H, Ar–H), 7.11–7.06 (m, 7 H, Ar–H), 7.01 (t, 4 H, Ar–H), 6.96 (d, 4 H, Ar–H), 6.91 (d, 5 H, Ar–H), 6.86 (d, 2 H, Ar–H), 6.60–6.53 (m, 4 H, Ar–H), 6.46–6.42 (m, 7 H, Ar–H), ***syn: 5.72 (s, 4 H, NCH_2Ph), 4.93 (t, ^3J(H,H) = 7.5 Hz, 4 H, NCH_2), 3.25 (t, ^3J(H,H) = 6.6 Hz, 4 H, CH_2S), 2.69 (m, ^3J(H,H) = 7.2 Hz, 4 H, $CH_2CH_2CH_2$), ***anti***: 5.98 (s, 4 H, NCH_2Ph), 4.71 (t, ^3J(H,H) = 7.7 Hz, 4 H, NCH_2), 3.02 (t, ^3J(H,H) = 6.6 Hz, 4 H, CH_2S), 2.56 (m, ^3J(H,H) = 7.4 Hz, 4 H, $CH_2CH_2CH_2$). ^{13}C{^{1}H} NMR (125.77 MHz, CDCl3): δ 191.1, 191.0 ($C_{carbene}$), 145.1, 145.0, 136.9, 136.8, 136.5, 135.8, 135.5, 135.4, 135.1, 135.02, 134.96, 130.0, 129.9, 129.7, 129.6, 129.4, 129.3, 129.0, 128.9, 128.7, 128.6, 128.5, 127.5, 127.4, 126.8, 126.7, 124.02, 123.96, 123.03, 122.98, 122.95, 111.8, 111.7, 110.6 (Ar–C, 2 × coincident), 53.8, 53.4 (NCH_2Ph), 47.8 (2 × NCH_2), 32.2, 31.9 (CH_2S), 29.5, 29.4 ($CH_2CH_2CH_2$). Anal. Calcd for $C_{58}H_{54}N_4PdS_4$: C, 66.87; H, 5.23; N, 5.38. Found: C, 66.50; H, 5.09; N, 5.32. MS (ESI): *m/z* 931 $[M - SPh]^+$.

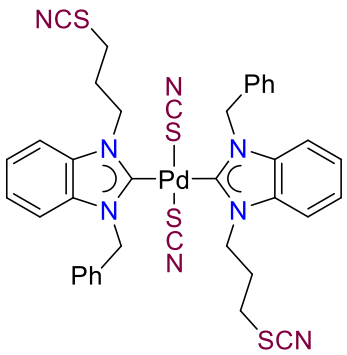

trans*-[Pd(SCN)$_2$(C$_3$SCN-bimy)$_2$] (62)**. Complex **45** (93 mg, 0.10 mmol) and KSCN (98 mg, 1.00 mmol) were suspended in CH_3CN (30 mL) and refluxed overnight. The resulting yellow suspension was dried in vacuo before CH_2Cl_2 (20 mL) was added. The suspension was then filtered and dried to give the pure products as pale yellow solids. Yield and *syn*:*anti* ratio: 82 mg, 0.10 mmol, 98%, 1:1.9. ^{1}H NMR (500 MHz, $CDCl_3$): δ 7.54 (d, 2 H, Ar–H), 7.50 (d, 2 H, Ar–H), 7.47–7.40 (m, 12 H, Ar–H), 7.35–7.31 (m, 4 H, Ar–H), 7.29–7.28 (m, 6 H, Ar–H), 7.23–7.17 (m, 10 H, Ar–H), ***syn: 5.89 (s, 4 H, NCH_2Ph), 5.03 (t, ^3J(H,H) = 6.9 Hz, 4 H, NCH_2), 3.19 (t, ^3J(H,H) = 6.8 Hz, 4 H, CH_2SCN), 2.88 (m, ^3J(H,H) = 6.9 Hz, 4 H, $CH_2CH_2CH_2$), ***anti***: 6.21 (s, 4 H, NCH_2Ph), 4.90 (t, ^3J(H,H) = 6.9 Hz, 4 H, NCH_2), 2.79 (t, 4 H, ^3J(H,H) = 6.7 Hz, CH_2SCN), 2.60 (m, ^3J(H,H) = 6.8 Hz, 4 H, $CH_2CH_2CH_2$). ^{13}C{^{1}H} NMR (125.77 MHz, $CDCl_3$): δ 180.8, 180.7 ($C_{carbene}$), 136.0, 135.90, 135.88, 135.8, 135.1, 135.0, 130.0, 129.63, 129.60, 129.2, 128.9, 127.5, 127.4, 124.99, 124.95 124.91 (Ar–C), 120.5, 120.4 (PdSCN), 112.7, 112.5 (Ar–C), 112.4, 112.3 (CH_2SCN), 112.1, 111.2 (Ar–C), 53.4, 53.1 (NCH_2Ph), 47.0, 46.7 (NCH_2), 31.8, 31.3 (CH_2SCN), 30.6, 30.0 ($CH_2CH_2CH_2$). Anal. Calcd for $C_{38}H_{34}N_8PdS_4$: C, 54.50; H, 4.09; N, 13.38. Found: C, 54.41; H, 4.39; N, 12.92 (best result obtained). ^{1}H and ^{13}C NMR spectra are attached in the appendix. MS (ESI): *m/z* 878 [M + H + CH_3CN]$^+$.

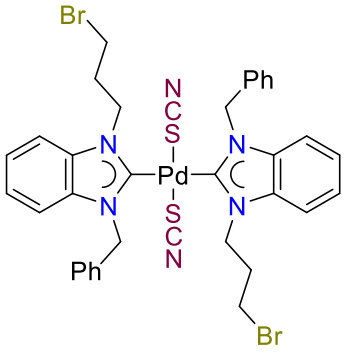

***trans*-[Pd(SCN)$_2$(C$_3$Br-bimy)$_2$] (63)**. Complex **45** (93 mg, 0.10 mmol) and KSCN (98 mg, 1.00 mmol) were suspended in THF (30 mL) and stirred overnight. The resulting yellow suspension was filtered before the filtrate was dried in vacuo and CH_2Cl_2 (20 mL)

was added. The CH_2Cl_2 layer was collected by filtration and left slow evaporation to afford the products as yellow crystals. Yield and *syn*:*anti* ratio: 67 mg, 0.08 mmol, 76%, 1:2.6. ^{1}H NMR (500 MHz, $CDCl_3$): δ 7.63 (d, 1 H, Ar–H), 7.55 (d, 3 H, Ar–H), 7.47–7.41 (m, 12 H, Ar–H), 7.39–7.37 (m, 4 H, Ar–H), 7.32–7.28 (m, 8 H, Ar–H), 7.17 (t, 5 H, Ar–H), 7.13 (d, 3 H, Ar–H), ***syn***: 5.88 (s, 4 H, NCH_2Ph), 5.02 (t, ^3J(H,H) = 7.2 Hz, 4 H, NCH_2), 3.66 (t, 4 H, ^3J(H,H) = 5.9 Hz, CH_2Br), 2.88 (m, ^3J(H,H) = 6.5 Hz, 4 H, $CH_2CH_2CH_2$), ***anti***: 6.19 (s, 4 H, NCH_2Ph), 4.89 (t, ^3J(H,H) = 7.4 Hz, 4 H, NCH_2), 3.35 (t, ^3J(H,H) = 5.8 Hz, 4 H, CH_2Br), 2.67 (m, ^3J(H,H) = 6.7 Hz, 4 H, $CH_2CH_2CH_2$). ^{13}C{^{1}H} NMR (125.77 MHz, $CDCl_3$): δ 181.0 (2 × $C_{carbene}$), 136.4, 136.3, 136.0, 135.8, 135.3, 135.2, 129.8, 129.71, 129.65, 129.1, 128.9, 128.1, 127.8, 127.7, 124.69, 124.67 (Ar–C), 120.64, 120.61 (PdSCN), 112.7, 112.3, 111.5, 111.3 (Ar–C), 53.7, 53.1 (NCH_2Ph), 47.5 (2 × NCH_2), 33.5, 33.1 (CH_2Br), 31.4, 30.9 ($CH_2CH_2CH_2$). Anal. Calcd for $C_{36}H_{34}Br_2N_6PdS_2$: C, 49.08; H, 3.89; N, 9.54. Found: C, 49.06; H, 4.17; N, 9.47. MS (ESI): *m/z* 822 $[M - SCN]^+$.

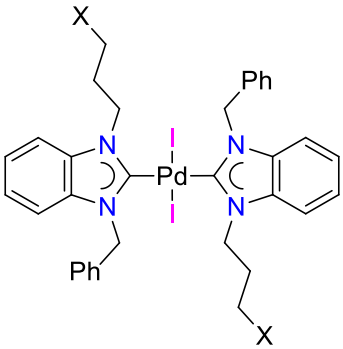

***trans*-[PdI$_2$(C$_3$X-bimy)$_2$]** (**64–67**). Complex **60** (56 mg, 0.05 mmol) and NaN_3 (33 mg, 0.50 mmol) or NaSPh (18 mg, 0.14 mmol) or KSAc (21 mg, 0.19 mmol) or KSCN (15 mg, 0.15 mmol) were suspended in CH_3CN (20 mL) and stirred overnight. The solvent of the suspension was removed in vacuo, and CH_2Cl_2 (50 mL) of was added. The resulting yellow suspension was filtered over Celite and the solvent removed under reduced pressure to give the products as yellow powders.

X = N$_3$, (**64**). Yield and *syn*:*anti* ratio: 42 mg, 0.05 mmol, 99%, 1:1.7. ^{1}H NMR (500 MHz, $CDCl_3$): δ 7.62 (d, 4 H, Ar–H), 7.47 (d, 2 H, Ar–H), 7.42–7.38 (m, 10 H, Ar–H), 7.36–7.33 (m, 2

H, Ar–H), 7.28–7.22 (m, 9 H, Ar–H), 7.14–7.09 (m, 4 H, Ar–H), 7.04 (t, 4 H, Ar–H), 6.99 (s, 1 H, Ar–H), ***syn***: 5.87 (s, 4 H, NCH_2Ph), 4.89 (t, ^3J(H,H) = 7.3 Hz, 4 H, NCH_2), 3.59 (t, ^3J(H,H) = 6.1 Hz, 4 H, CH_2N_3), 2.61 (m, ^3J(H,H) = 7.2 Hz, 4 H, $CH_2CH_2CH_2$), ***anti***: 6.09 (s, 4 H, NCH_2Ph), 4.77 (t, ^3J(H,H) = 7.5 Hz, 4 H, NCH_2), 3.28 (t, ^3J(H,H) = 6.2 Hz, 4 H, CH_2N_3), 2.42 (m, ^3J(H,H) = 7.3 Hz, 4 H, $CH_2CH_2CH_2$). $^{13}C\{^1H\}$ NMR (125.77 MHz, $CDCl_3$): δ 181.9, 181.8 ($C_{carbene}$), 135.95, 135.87, 135.64, 135.59, 135.5, 135.3, 129.5, 129.3, 128.8, 128.6, 128.5, 126.2, 123.7, 123.64, 123.60, 112.3, 112.2 110.9, 110.8 (Ar–C, 2 × coincident), 54.5, 54.2 (NCH_2Ph), 49.6, 49.3 (CH_2N_3), 46.6, 46.4 (NCH_2), 29.2, 29.0 ($CH_2CH_2CH_2$). Anal. Calcd for $C_{34}H_{34}I_2N_{10}Pd$: C, 43.31; H, 3.65; N, 14.85. Found: C, 43.64; H, 3.81; N, 12.89 (best result obtained). ^1H and ^{13}C NMR spectra are attached in the appendix. MS (ESI): *m/z* 815 $[M - I]^+$.

X = SPh, (**65**). Yield and *syn*:*anti* ratio: 48 mg, 0.44 mmol, 89%, 1:1.3. ^1H NMR (500 MHz, $CDCl_3$): δ 7.60 (d, 4 H, Ar–H), 7.51 (d, 1 H, Ar–H), 7.42–7.29 (m, 22 H, Ar–H), 7.26–7.21 (m, 15 H, Ar–H), 7.20–7.15 (m, 6 H, Ar–H), 7.10–7.06 (m, 4 H, Ar–H), 7.02–7.00 (m, 4 H, Ar–H), ***syn***: 5.86 (s, 4 H, NCH_2Ph), 4.93 (t, ^3J(H,H) = 7.4 Hz, 4 H, NCH_2), 3.12 (t, 4 H, ^3J(H,H) = 6.6 Hz, CH_2S), 2.65 (m, ^3J(H,H) = 7.2 Hz, 4 H, $CH_2CH_2CH_2$), ***anti***: 6.08 (s, 4 H, NCH_2Ph), 4.83 (t, ^3J(H,H) = 7.5 Hz, 4 H, NCH_2), 2.85 (t, ^3J(H,H) = 6.5 Hz, 4 H, CH_2S), 2.49 (m, ^3J(H,H) = 7.3 Hz, 4 H, $CH_2CH_2CH_2$). $^{13}C\{^1H\}$ NMR (125.77 MHz, $CDCl_3$): δ 181.71, 181.66 ($C_{carbene}$), 136.4, 136.3, 135.9, 135.8, 135.7, 135.5, 135.3, 130.4, 130.1, 129.8, 129.7, 129.6, 129.5, 129.3, 128.7, 128.59, 128.57, 128.5, 128.1, 127.0, 126.8, 123.52, 123.47, 123.45, 112.2, 112.0, 111.04, 110.96 (Ar–C), 54.6, 54.1 (NCH_2Ph), 48.0, 47.9 (NCH_2), 32.0, 31.5 (CH_2S), 28.8, 28.5 ($CH_2CH_2CH_2$). Anal. Calcd for $C_{46}H_{44}I_2N_4PdS_2$: C, 51.29; H, 4.12; N, 5.20. Found: C, 51.68; H, 4.58; N, 4.66

(best result obtained). ^{1}H and ^{13}C NMR spectra are attached in the appendix. MS (ESI): *m/z* 951 $[M - I]^+$.

X = SAc, (**66**). Yield and *syn*:*anti* ratio: 10 mg, 0.01 mmol, 20%, 1:1.1. ^{1}H NMR (500 MHz, $CDCl_3$): δ 7.63 (d, 4 H, Ar–H), 7.44 (d, 2 H, Ar–H), 7.39–7.36 (m, 12 H, Ar–H), 7.33 (d, 2 H, Ar–H), 7.24–7.20 (m, 8 H, Ar–H), 7.12–7.07 (m, 4 H, Ar–H), 7.01 (t, 4 H, Ar–H), ***syn***: 5.85 (s, 4 H, NCH_2Ph), 4.86 (t, ^{3}J(H,H) = 7.5 Hz, 4 H, NCH_2), 3.12 (t, ^{3}J(H,H) = 7.1 Hz, 4 H, CH_2S), 2.64, (m, ^{3}J(H,H) = 7.4 Hz, 4 H, $CH_2CH_2CH_2$), 2.40 (s, 6 H, CH_3), ***anti***: 6.09 (s, 4 H, NCH_2Ph), 4.72 (t, ^{3}J(H,H) = 7.7 Hz, 4 H, NCH_2), 2.81 (t, ^{3}J(H,H) = 6.9 Hz, 4 H, CH_2S), 2.44 (m, ^{3}J(H,H) = 7.4 Hz, 4 H, $CH_2CH_2CH_2$), 2.16 (s, 6 H, CH_3). $^{13}C\{^{1}H\}$ NMR (125.77 MHz, $CDCl_3$): δ 196.2, 196.1 (CO), 181.7, 181.6 ($C_{carbene}$), 135.9, 135.8, 135.7, 135.6, 135.4, 129.5, 129.3, 128.79, 128.77, 128.63, 128.61, 128.5, 123.61, 123.56, 123.5, 112.4, 112.3, 112.2, 111.0, 110.9 (Ar–C), 54.7, 54.2 (NCH_2Ph), 48.3, 48.2 (NCH_2), 31.4, 31.1 (CH_2S), 29.8, 29.4 ($CH_2CH_2CH_2$), 27.4, 27.1 (CH_3). Anal. Calcd for $C_{38}H_{40}I_2N_4O_2PdS_2$: C, 45.23; H, 4.00; N, 5.35. Found: C, 45.48; H, 3.87; N, 5.59. MS (ESI): *m/z* 881 $[M - I]^+$.

X = SCN, (**67**). Yield and *syn*:*anti* ratio: 36 mg, 0.04 mmol, 74%, 1:1.8. ^{1}H NMR (500 MHz, $CDCl_3$): δ 7.52 (d, 5 H, Ar–H), 7.48 (d, 2 H, Ar–H), 7.44–7.35 (m, 8 H, Ar–H), 7.32–7.22 (m, 12 H, Ar–H), 7.15 (t, 5 H, Ar–H), 7.06 (ps–d, 4 H, Ar–H), ***syn***: 5.84 (s, 4 H, NCH_2Ph), 4.97 (t, ^{3}J(H,H) = 6.8 Hz, 4 H, NCH_2), 3.19 (t, ^{3}J(H,H) = 6.8 Hz, 4 H, CH_2SCN), 2.91 (m, ^{3}J(H,H) = 6.8 Hz, 4 H, $CH_2CH_2CH_2$), ***anti***: 6.10 (s, 4 H, NCH_2Ph), 4.86 (t, ^{3}J(H,H) = 6.8 Hz, 4 H, NCH_2), 2.77 (t, ^{3}J(H,H) = 6.6 Hz, 4 H, CH_2SCN), 2.63 (m, ^{3}J(H,H) = 6.7 Hz, 4 H, $CH_2CH_2CH_2$). $^{13}C\{^{1}H\}$ NMR (125.77 MHz, $CDCl_3$): δ 181.6, 181.5 ($C_{carbene}$), 135.7, 135.54, 135.48, 135.3, 129.7, 129.3,

129.0, 128.6, 128.4, 128.1, 124.10, 124.06, 124.0, 112.5 (Ar–C), 112.40, 112.38 (SCN), 110.9 (Ar–C, 5 × coincident), 54.5, 54.1 (NCH_2Ph), 47.2, 47.1 (NCH_2), 32.1, 31.6 (CH_2SCN), 29.6, 29.0 ($CH_2CH_2CH_2$). Anal. Calcd for $C_{36}H_{34}I_2N_6PdS_2$: C, 44.35; H, 3.51; N, 8.62. Found: C, 44.59, H, 3.63; N, 8.32. MS (ESI): *m/z* 847 $[M - I]^+$.

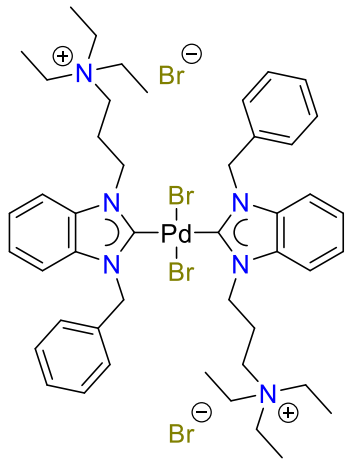

trans*-[PdBr$_2$(C$_3$NEt$_3$-bimy)$_2$]Br$_2$ (68)**. Complex **58** (1.20 g, 1.30 mmol) was dissolved in ethyl bromide (15 mL, 200 mmol) in a sealed Schlenk tube and stirred overnight at 70 ℃. The precipitate was collected by filtration and washed with CH_3CN (3 × 5 mL) to give the product as off-white solid (1.20 g, 1.10 mmol, 86%) in a *syn*:*anti* ratio of 1:4.5. ^{1}H NMR (500 MHz, d_6-DMSO): δ 7.98 (d, 1 H, Ar–H), 7.91 (d, 3 H, Ar–H), 7.60 (d, 6 H, Ar–H), 7.55 (d, 2 H, Ar–H),7.42–7.32 (m, 15 H, Ar–H), 7.26 (ps–d, 7 H, Ar–H), 7.21 (ps–d, 2 H, Ar–H), ***syn: 6.05 (s, 4 H, NCH_2Ph), 5.02 (t, ^3J(H,H) = 6.7 Hz, 4 H, NCH_2CH_2), 3.53 (t, ^3J(H,H) = 7.3 Hz, 4 H, $CH_2CH_2N^+$), 3.30 (m, ^3J(H,H) = 6.7 Hz, 12 H, $N^+CH_2CH_3$), 2.62 (br–m, 4 H, $CH_2CH_2CH_2$), 1.15 (t, ^3J(H,H) = 7.1 Hz, 18 H, CH_3), ***anti***: 6.25 (s, 4 H, NCH_2Ph), 4.97 (t, ^3J(H,H) = 6.7 Hz, 4 H, NCH_2CH_2), 3.20 (t, ^3J(H,H) = 7.5 Hz, 4 H, $CH_2CH_2N^+$), 3.00 (m, ^3J(H,H) = 7.0 Hz, 12 H, $N^+CH_2CH_3$), 2.36 (br–m, 4 H, $CH_2CH_2CH_2$), 0.96 (t, ^3J(H,H) = 7.1 Hz, 18 H, CH_3). ^{13}C{^{1}H} NMR (125.77 MHz, d_6-DMSO): δ 180.7, 180.5 ($C_{carbene}$), 135.7, 135.4, 134.0, 133.9, 133.7, 133.3, 128.5, 128.3, 127.90, 127.87, 127.7, 123.6, 123.5, 111.9, 111.7, 111.6, 111.4 (Ar–C, 3 × coincident), 53.7 (2 × NCH_2Ph), 52.3, 52.1 (2 ×), 51.8 (N^+CH_2), 44.7 (2 × NCH_2), 21.7 (2 × $CH_2CH_2CH_2$), 7.3, 7.0 (CH_3). Anal. Calcd for $C_{46}H_{64}Br_4N_6Pd$: C, 49.02; H, 5.72; N, 7.46. Found:

C, 49.41; H, 5.48; N, 6.99 (best result obtained). ^{1}H and ^{13}C NMR spectra are attached in the appendix. MS (ESI): *m/z* 483 $[M - 2Br]^{2+}$, 1047 $[M - Br]^{+}$.

General procedure for the Mizoroki-Heck cross-couplings. In a typical run, a reaction tube was charged with a mixture of aryl halide (1 mmol for monohalides. 0.5 mmol for dihalides, 0.33 mmol for trihalides and 0.25 mmol for tetrahalides), NaOAc (1.5 equiv per halide present), *tert*-butyl acrylate (1.5 equiv per halide present), catalyst (1 mol% per halide present) and DMF (3 mL). The reaction was stirred and heated at 130 ℃ for 20 h. After the mixture was cooled to ambient temperature, dichloromethane (5 mL) was added. The organic layer was then washed with water (5 × 10 mL) and dried over Na_2SO_4. The solvent was reduced and the residue was subjected to column chromatography (hexane/ethyl acetate).

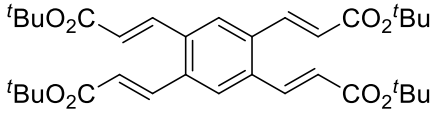

1,2,4,5-tetra-^{t}butylcinnamates (**69**). ^{1}H NMR (500 MHz, $CDCl_3$): δ 7.86 (d, ^{3}J(H,H) = 15.8 Hz, 4 H, CH), 7.70 (s, 2 H, Ar–H), 6.32 (d, ^{3}J(H,H) = 15.8 Hz, 4 H, CH), 1.53 (s, 36 H, CH_3). ^{13}C{^{1}H} NMR (125.77 MHz, $CDCl_3$): δ 166.0 (CO), 139.8, 136.1, 127.3, 125.5 (Ar–C and CH=CH), 81.7 ($C(CH_3)_3$), 28.9 (CH_3). Anal. Calcd for $C_{34}H_{46}O_8$: C, 70.08; H, 7.96. Found: C,70.00, H, 8.11. MS (ESI): *m/z* 663 $[M + K + CH_3CN]^{+}$.

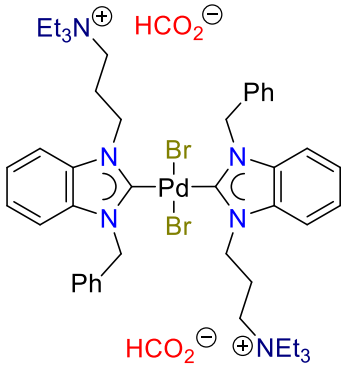

***trans*-[PdBr$_2$(C$_3$NEt$_3$-bimy)$_2$](HCO$_2$)$_2$** (**70**). Complex **68** (48 mg, 0.04 mmol) and silver formate (13 mg, 0.09 mmol) were mixed in CH_2Cl_2/MeOH (10/5 mL). The mixture was stirred for 2 h before the precipitate was filtered off through Celite. Removal of the solvent gave an off-white solid which was dissolved in CD_3CN for NMR.

The *syn*:*anti* ratio is 1:2.9. ^{1}H NMR (300 MHz, CD_3CN): δ 8.60 (s, 2 H, $HCOO^-$), 7.81 (d, 1 H, Ar–H), 7.74 (d, 3 H, Ar–H), 7.55–7.53 (m, 6 H, Ar–H), 7.48–7.45 (m, 2 H, Ar–H), 7.39–7.30 (m, 15 H, Ar–H), 7.24–7.18 (m, 9 H, Ar–H), ***syn***: 6.02 (s, 4 H, NCH_2Ph), 5.08 (t, ^{3}J(H,H) = 6.7 Hz, 4 H, NCH_2CH_2), 3.58 (m, 4 H, $CH_2CH_2N^+$), 1.14 (t, ^{3}J(H,H) = 7.2 Hz, 18 H, CH_3), the $N^+CH_2CH_3$ protons are overlapped with $CH_2CH_2N^+$ protons of the *anti*-isomer at 3.26–3.16 (m, 20 H), the $CH_2CH_2CH_2$ protons are overlapped with the water signal at 2.69 ppm, ***anti***: 6.25 (s, 4 H, NCH_2Ph), 4.98 (t, ^{3}J(H,H) = 6.3 Hz, 4 H, NCH_2CH_2), 2.93 (m, ^{3}J(H,H) = 7.5 Hz, 12 H, $N^+CH_2CH_3$), 2.37 (m, 4 H, $CH_2CH_2CH_2$), 0.94 (t, ^{3}J(H,H) = 7.2 Hz, 18 H, CH_3). $^{13}C\{^{1}H\}$ NMR (75.48 MHz, CD_3CN): δ 182.4, 182.2 ($C_{carbene}$), 167.7 ($HCOO^-$), 137.3, 136.7, 135.4, 134.8, 129.7, 129.6, 129.5, 129.1, 128.9, 128.8, 128.6, 128.5, 124.8, 124.6, 124.2, 124.1, 112.7, 112.24, 112.15, 111.9 (Ar–C), 55.34, 55.25 (NCH_2Ph), 53.6 (2 ×), 53.34, 53.27 (N^+CH_2), 46.1, 45.8 (NCH_2), 22.99, 22.90 ($CH_2CH_2CH_2$), 7.8, 7.7 (CH_3). MS (ESI): *m/z* 483 $[M - 2Br]^{2+}$.

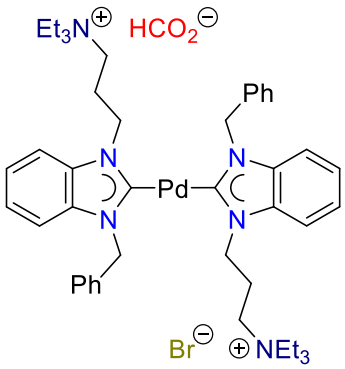

$[Pd^0(C_3NEt_3\text{-bimy})_2]X_2$ (**71**, X = Br and HCO_2). Complex **70** was left in CD_3CN for 2 h to convert to this complex. ^{1}H NMR (500 MHz, CD_3CN): δ 8.62 (s, 1 H, $HCOO^-$), 7.76 (d, 2 H, Ar–H), 7.53 (br–s, 4 H, Ar–H), 7.34–7.33 (m, 7 H, Ar–H), 7.28–7.22 (m, 5 H, Ar–H), 6.05 (s, 4 H, NCH_2Ph), 5.84 (br–s, 4 H, NCH_2CH_2), 3.32 (br–s, 4 H, $CH_2CH_2N^+$), 3.03 (m, ^{3}J(H,H) = 7.0 Hz, 12 H, $N^+CH_2CH_3$), 2.41 (br–s, 4 H, $CH_2CH_2CH_2$), 0.94 (t, ^{3}J(H,H) = 6.8 Hz, 18 H, CH_3). $^{13}C\{^{1}H\}$ NMR (125.77 MHz, CD_3CN): δ 193.4 ($C_{carbene}$), 167.7 ($HCOO^-$), 137.4, 135.4, 135.1, 129.6, 128.9, 128.6, 124.2, 124.1, 112.2, 111.9 (Ar–C), 55.3 (NCH_2Ph), 53.7, 53.3 (N^+CH_2), 46.2 (NCH_2), 23.1 ($CH_2CH_2CH_2$), 7.8 (CH_3). MS (ESI): *m/z* 429 $[M + MeOH + H_2O]^{2+}$.

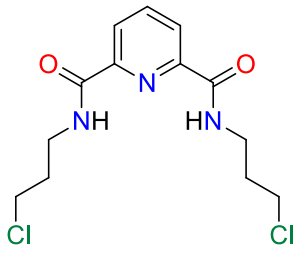

Compound K. A mixture of 2-chloropropylamine hydrochloride (780 mg, 6 mmol) and NEt_3 (1.35 mL) in dry CH_2Cl_2 (30 mL) was stirred for 1 h to give the free amine. Compound pyridine 2,6-dicarboxylic acid chloride (600 mg, 2.9 mmol) was added to this solution, and the reaction mixture was stirred at room temperature for 8 h. The solvent was evaporated before H_2O was added. The aqueous layer was extracted with $CHCl_3$ (3 × 50 mL), and the combined organic phases was dried over anhydrous Na_2SO4 and concentrated in vacuo. The resulting crude solid was purified by column chromatography (SiO_2, hexane/ethyl acetate: 1/1) to give **K** as a white solid (590 mg, 1.9 mmol, 64%). ^{1}H NMR (500 MHz, $CDCl_3$): δ 8.36–8.34 (ps–d, 2 H, Py–H), 8.17 (br–s, 2 H, CONH), 8.06–8.01 (ps–t, 1 H, Py–H), 3.66 (m, 8 H, NHC*H*$_2$ and CH_2Cl), 2.13 (m, 4 H, CH_2). ^{13}C{^{1}H} NMR (125.77 MHz, $CDCl_3$): δ 164.5 (CO), 149.3, 139.8, 125.7 (Py–C), 43.7 (CH_2Cl), 38.1 ($NHCH_2$), 32.6 (CH_2). Anal. Calcd for $C_{13}H_{17}Cl_2N_3O_2$: C, 49.07; H, 5.38; N, 13.21. Found: C, 49.31; H, 5.29; N, 12.98. MS (ESI): *m/z* 318 $[M]^+$.

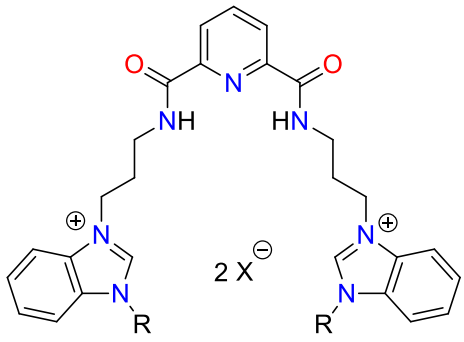

Salt L_{Bn}. To the solution of compound **K** (159 mg, 0.5 mmol) in CH_3CN (30 mL), 1-benzylbenzimidazole (260 mg, 1.25 mmol) and NaI (750 mg, 5 mmol) was added. After the mixture was applied with microwave for 3 h at 150 °C, the solvent was removed under reduced pressure and CH_2Cl_2 (100 mL) was added. The resulting suspension was filtered through Celite. Solvent of the filtrate was dried off in vacuo. Ethyl acetate (3 × 20 mL) was added to wash the residue, giving the product as a pale yellow powder (450 mg, 0.49 mmol, 98%). ^{1}H NMR (500 MHz, DMSO-d_6): δ 9.99 (s, 2 H, NCHN), 9.40 (t, ^3J(H,H) = 6.1 Hz, 2 H, NH), 8.19 (ps–s, 3 H, Py–H),

8.11 (d, 2 H, Ar–H), 7.92 (d, 2 H, Ar–H), 7.67–7.60 (m, 4 H, Ar–H), 7.52 (ps–d, 4 H, Ar–H), 7.43–7.36 (m, 6 H, Ar–H), 5.76 (s, 4 H, NCH_2Ph), 4.62 (t, ^3J(H,H) = 7.0 Hz, 4 H, NCH_2), 3.51 (m, ^3J(H,H) = 6.4 Hz, 4 H, $NHCH_2$), 2.31 (m, ^3J(H,H) = 6.9 Hz, 4 H, $CH_2CH_2CH_2$). $^{13}C\{^1H\}$ NMR (125.77 MHz, DMSO-d_6): δ 163.4 (CO), 148.4 (C2/6), 142.6 (NCHN), 139.5 (C4), 133.9, 131.2, 130.9, 129.0, 128.7, 128.3, 126.7, 126.6 (Ar–C), 124.3 (C3/5), 113.9, 113.8 (Ar–C), 49.9 (NCH_2Ph), 45.0 (NCH_2), 35.9 ($NHCH_2$), 28.9 ($CH_2CH_2CH_2$). Anal. Calcd for $C_{41}H_{41}I_2N_7O_2$: C, 53.66; H, 4.50; N, 10.68. Found: C, 53.68; H, 4.88; N. 10.59 MS (ESI): *m/z* 332 $[M - 2\ I]^{2+}$, 790 $[M - I]^+$.

Salt L_{Me}. This salt was prepared in analogy to **L_{Bn}** from 0.5 mmol of compound **K** with 1-methylbenzimidazole (165 mg, 1.25 mmol) and NaI (750 mg, 5 mmol). Yield: 341 mg, 0.45 mmol, 89%. ^{1}H NMR (500 MHz, DMSO-d_6): δ 9.77 (s, 2 H, NCHN), 9.29 (t, ^3J(H,H) = 5.9 Hz, 2 H, NH), 8.17 (br–s, 3 H, Py–H), 8.09 (ps–t, 2 H, Ar–H), 7.97 (ps–t, 2 H, Ar–H), 7.66 (ps–t, 4 H, Ar–H), 4.60 (t, ^3J(H,H) = 6.5 Hz, 4 H, NCH_2), 4.06 (s, 6 H, NCH_3), 3.50 (m, ^3J(H,H) = 6.0 Hz, 4 H, $NHCH_2$), 2.28 (br–m, 4 H, $CH_2CH_2CH_2$). $^{13}C\{^1H\}$ NMR (125.77 MHz, DMSO-d_6): δ 163.3 (CO), 148.3 (C2/6), 142.8 (NCHN), 139.5 (C4), 131.8, 130.8, 126.4 (Ar–C, two are coincident), 124.2 (C3/5), 113.53, 113.47 (Ar–C), 44.8 (NCH_2), 36.0 (NCH_3), 33.2 ($NHCH_2$), 28.8 ($CH_2CH_2CH_2$). Anal. Calcd for $C_{29}H_{33}I_2N_7O_2$: C, 45.51; H, 4.35; N, 12.81. Found: C, 45.82; H, 4.37; N, 12.45. MS (ESI): *m/z* 256 $[M - 2\ I]^{2+}$, 638 $[M - I]^+$.

Salt M_{Bn}. Salt **L_{Bn}** (890 mg, 0.97 mmol) was mixed with $AgBF_4$ (380 mg, 1.95 mmol) in CH_3CN and stirred for 3 h. The precipitation was removed by filtering through Celite. The filtrate was dried in vacuo to afford the product as white powders (747 mg, 0.89 mmol, 92%). ^{1}H NMR (300 MHz, CD_3CN): δ 9.35 (s, 2 H, NCHN), 8.75 (t, ^3J(H,H) = 5.9 Hz, 2 H, NH), 8.20 (ps–d, 2 H, C3/5–H), 8.08 (ps–t, 1 H, C4–H), 7.90 (d, 2 H, Ar–H), 7.69–7.53 (m, 6 H, Ar–H), 7.46–7.39 (m,

10 H, Ar–H), 5.60 (s, 4 H, NCH_2Ph), 4.54 (t, ^3J(H,H) = 6.8 Hz, 4 H, NCH_2), 3.56 (m, ^3J(H,H) = 6.3 Hz, 4 H, $NHCH_2$), 2.36 (m, ^3J(H,H) = 6.5 Hz, 4 H, $CH_2CH_2CH_2$). $^{13}C\{^1H\}$ NMR (75.48 MHz, CD_3CN): δ 164.9 (CO), 149.7 (C2/6), 142.7 (NCHN), 140.2 (C4), 140.0, 132.7, 132.4, 130.2, 130.1, 129.5, 128.0 (Ar–C, two are coincident), 125.4 (C3/5), 114.7, 114.6 (Ar–C), 51.7 (NCH_2Ph), 46.3 (NCH_2), 36.8 ($NHCH_2$), 29.4 ($CH_2CH_2CH_2$). ^{19}F NMR (282.38 MHz, CD_3CN): δ -74.82, -74.87 (s, BF_4). Anal. Calcd for $C_{41}H_{41}B_2F_8N_7O_2$: C, 58.80; H, 4.93; N, 11.71. Found: C, 58.36; H, 4.64; N, 11.68. MS (ESI): *m/z* 332 $[M - 2\ BF_4]^{2+}$, 750 $[M - BF_4]^+$.

Salt $\mathbf{M_{Me}}$. This salt was prepared in analogy to $\mathbf{M_{Bn}}$ from $\mathbf{L_{Me}}$ (742 mg, 0.97 mmol) and $AgBF_4$ (380 mg, 1.95 mmol). Yield: 645 mg, 0.94 mmol, 97%. ^1H NMR (500 MHz, CD_3CN): 9.14 (s, 2 H, NCHN), 8.54 (t, ^3J(H,H) = 5.6 Hz, 2 H, NH), 8.16 (ps–d, 2 H, C3/5–H), 8.05 (ps–t, 1 H, C4–H), 7.87–7.85 (m, 2 H, Ar–H), 7.74–7.73 (m, 2 H, Ar–H), 7.61–7.58 (m, 4 H, Ar–H), 4.52 (t, ^3J(H,H) = 6.8 Hz, 4 H, NCH_2), 4.00 (s, 6 H, NCH_3), 3.54 (m, ^3J(H,H) = 6.3 Hz, 4 H, $NHCH_2$), 2.33 (m, ^3J(H,H) = 6.5 Hz, 4 H, $CH_2CH_2CH_2$). $^{13}C\{^1H\}$ NMR (125.77 MHz, CD_3CN): δ 164.8 (CO), 149.5 (C2/6), 142.9 (NCHN), 140.3 (C4), 133.2, 132.2, 127.83, 127.79 (Ar–C), 125.4 (C3/5), 114.3, 114.1 (Ar–C), 46.2 (NCH_2), 37.0 (NCH_3), 34.1 ($NHCH_2$), 29.4 ($CH_2CH_2CH_2$). ^{19}F NMR (282.38 MHz, CD_3CN): δ -74.87, -74.93 (s, BF_4). Anal. Calcd for $C_{29}H_{33}B_2F_8N_7O_2$: C, 50.83; H, 4.85; N, 14.31. Found: C, 50.97; H, 4.78; N, 14.28. MS (ESI): *m/z* 256 $[M - 2\ BF_4]^{2+}$, 598 $[M - BF_4]^+$.

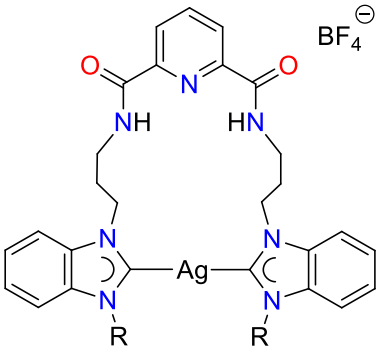

Silver(I) dicarbene complex $\mathbf{72_{Bn}}$. A mixture of salt $\mathbf{M_{Bn}}$ (84 mg, 0.10 mmol) was dissolved in CH_3CN (20 mL) before Ag_2O (28 mg, 0.12 mmol) was added. The mixture was heated at 60 °C with stirring for 5 h. The resulting suspension was dried in vacuo

before 100 mL of CH_2Cl_2 was added and filtered. The filtrate was consequently extracted with water (5 × 100 mL) and fried over Na_2SO_4. After the solvent was removed under reduced pressure, the white solid obtained was the product (86 mg, 0.10 mmol, 99%). ^{1}H NMR (500 MHz, CD_3CN): δ 8.57 (br–s, 2 H, NH), 7.73 (br–s, 2 H, C3/5), 7.60 (br–s, 3 H, C4–H and Ar–H), 7.40 (ps–t, 4 H, Ar–H), 7.34 (ps–t, 2 H, Ar–H), 7.22–7.19 (m, 6 H, Ar–H), 7.15 (m, 4 H, Ar–H), 5.30 (br–s, 4 H, NCH_2Ph), 4.45 (br–s, 4 H, NCH_2), 3.47 (br–s, 4 H, $NHCH_2$), 2.20 (m, $CH_2CH_2CH_2$, correct integration is not obtained due to overlapping with H_2O signal). ^{13}C{^{1}H} NMR (75.48 MHz, CD_3CN): δ 164.4 (CO), 149.5 (C2/6), 139.8 (C4), 136.9, 134.7, 134.5, 129.9, 129.2, 128.4, 125.29, 125.26 (Ar–C), 124.8 (C3/5), 113.0 (Ar–C, two are coincident), 53.0 (NCH_2Ph), 48.6 (NCH_2), 37.7 ($NHCH_2$), 30.3 (br–s, $CH_2CH_2CH_2$), the carbene signal was not obtained despite prolonged measuring. ^{19}F NMR (282.38 MHz, CD_3CN): δ -74.83, -74.89 (s, BF_4). Anal. Calcd for $C_{41}H_{39}AgBF_4N_7O_2$: C, 57.50; H, 4.59; N, 11.45. Found: C, 57.67; H, 4.35; N, 11.38. MS (ESI): *m/z* 768 $[M - BF_4]^+$.

Silver(I) dicarbene complex 72_{Me}. This complex was obtained in analogy to $\mathbf{72_{Bn}}$ from $\mathbf{M_{Me}}$ (69 mg, 0.10 mmol) and Ag_2O (28 mg, 0.12 mmol). Yield: 67 mg, 0.10 mmol, 95%. ^{1}H NMR (500 MHz, DMSO-d_6): δ 9.02 (br–s, 2 H, NH), 8.04 (t, 1 H, C4–H), 7.90 (d, 2 H, C3/5–H), 7.83 (d, 2 H, Ar–H), 7.53 (d, 2 H, Ar–H), 7.48–7.41 (m, 4 H, Ar–H), 4.75 (br–s, 4 H, NCH_2), 3.71 (s, 6 H, NCH_3), 3.44 (br–s, 4 H, $NHCH_2$), 2.47 (br–s, 4 H, $CH_2CH_2CH_2$). ^{13}C{^{1}H} NMR (125.77 MHz, DMSO-d_6): δ 162.3 (CO), 148.0 (C2/6), 139.3 (C4), 133.8, 133.2, 123.95, 123.92 (Ar–C), 123.4 (C3/5), 112.3, 111.6 (Ar–C), 47.2 (NCH_2), 36.8 (NCH_3), 35.1 ($NHCH_2$), 27.3 ($CH_2CH_2CH_2$), the carbene signal was not obtained despite prolonged measuring. ^{19}F NMR (282.38 MHz, DMSO-d_6): δ -72.25, -72.30 (s, BF_4). Anal. Calcd for $C_{29}H_{31}AgBF_4N_7O_2$: C, 49.46; H, 4.44; N, 13.92. Found: C, 49.32; H, 4.48; N, 13.98. MS (ESI): *m/z* 618 $[M - BF_4]^+$.

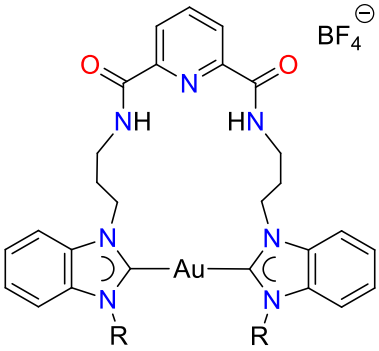

Monogold(I) dicarbene complex 73$_{Bn}$. A solution of [AuCl(THT)] (40 mg, 0.12 mmol) in CH_2Cl_2 (10 mL) was slowly added to the solution of complex **72$_{Bn}$** (106 mg, 0.12 mmol) in CH_2Cl_2 (20 mL). The mixture was kept stirring for 4 h before the precipitation was removed by centrifuging. The liquid was concentrated to 3 mL and subjected to column chromatography (SiO_2, $CH_3CN/CHCl_3$, 2:7). Yield of mononuclear complex **73$_{Bn}$**: 42 mg, 0.04 mmol, 36%. ^{1}H NMR (500 MHz, $CDCl_3$): δ 8.89 (t, ^3J(H,H) = 5.2 Hz, 2 H, NH), 7.99 (ps–d, 2 H, C3/5–H), 7.90 (ps–t, 2 H, C4–H), 7.60 (d, 2 H, Ar–H), 7.43 (t, 2 H, Ar–H), 7.31 (t, 2 H, Ar–H), 7.22–7.21 (m, 6 H, Ar–H), 7.12–7.10 (m, 6 H, Ar–H), 5.24 (s, 4 H, NCH_2Ph), 4.74 (t, ^3J(H,H) = 6.6 Hz, 4 H, NCH_2), 3.69 (br–s, 4 H, $NHCH_2$), 2.63 (m, ^3J(H,H) = 5.1 Hz, 4 H, $CH_2CH_2CH_2$). ^{13}C{^{1}H} NMR (125.77 MHz, $CDCl_3$): δ 191.7 ($C_{carbene}$), 164.0 (CO), 149.4 (C2/6), 139.1 (C4), 135.5, 134.2, 133.9, 129.7, 129.1, 127.5, 125.7 (Ar–C, two are coincident), 124.5 (C3/5), 113.0, 112.5 (Ar–C), 52.6 (NCH_2Ph), 48.2 (NCH_2), 37.6 ($NHCH_2$), 28.1 ($CH_2CH_2CH_2$). ^{19}F NMR (282.38 MHz, $CDCl_3$): δ -74.50, -74.56 (s, BF_4). Anal. Calcd for $C_{41}H_{39}AuBF_4N_7O_2$: C, 52.08; H, 4.16; N, 10.37. Found: C, 52.02; H, 3.84; N, 10.53. MS (ESI): *m/z* 858 $[M - BF_4]^+$.

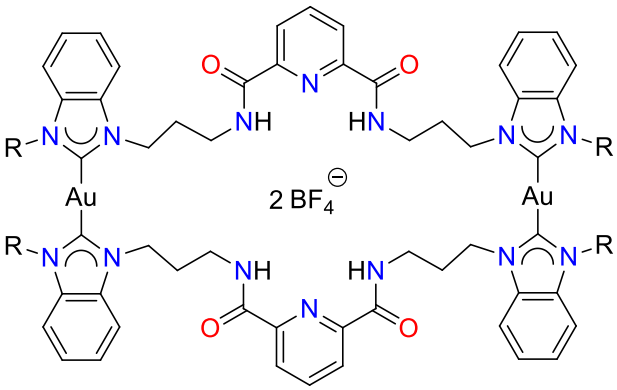

Digold(I) tetracarbene complex 74$_{Bn}$. This complex was isolated in the yield of 46 mg, 0.02 mmol, 39%. ^{1}H NMR (500 MHz, $CDCl_3$): δ 9.34 (br–s, 4 H, NH), 7.80 (ps–d, 4 H, C3/5–H), 7.47 (ps–d, 4 H, C4–H and Ar–H),

7.39 (m, 4 H, Ar–H), 7.34 (m, 10 H, Ar–H), 7.22 (m, 12 H, Ar–H), 7.15 (m, 8 H, Ar–H), 5.49 (s, 8 H, NCH_2Ph), 4.63 (t, ^3J(H,H) = 7.1 Hz, 8 H, NCH_2), 3.65 (m, ^3J(H,H) = 5.6 Hz, 8 H, $NHCH_2$), 2.34 (m, ^3J(H,H) = 6.2 Hz, 8 H, $CH_2CH_2CH_2$). $^{13}C\{^1H\}$ NMR (125.77 MHz, $CDCl_3$): δ 191.1 ($C_{carbene}$), 164.9 (CO), 149.3 (C2/6), 138.3 (C4), 135.6, 133.9, 133.7, 129.7, 129.1, 127.5, 125.8, 125.7 (Ar–C), 124.5 (C3/5), 112.7, 112.6 (Ar–C), 52.7 (NCH_2Ph), 47.8 (NCH_2), 37.7 ($NHCH_2$), 30.5 ($CH_2CH_2CH_2$). ^{19}F NMR (282.38 MHz, CD_3CN): δ -74.96, -74.98 (s, BF_4). Anal. Calcd for $C_{82}H_{78}Au_2B_2F_8N_{14}O_4$: C, 52.08; H, 4.16; N, 10.37. Found: C, 52.24; H, 4.25; N, 10.55. MS (ESI): *m/z* 858 $[M - 2\ BF_4]^{2+}$.

Monogold(I) dicarbene complexes $\mathbf{73_{Me}}$. Complexes $\mathbf{73_{Me}}$ and $\mathbf{74_{Me}}$ were synthesized in analogy to the previous complexes but purified by column chromatography (SiO_2, CH_2Cl_2/MeOH, 30:1). They were further separated by washing with CH_3CN. Complex $\mathbf{73_{Me}}$ was collected from the CH_3CN phase and dried as a white powder (35 mg, 0.04 mmol, 35%). ^1H NMR (500 MHz, CD_3CN): δ 8.20 (t, ^3J(H,H) = 5.4 Hz, 2 H, NH), 7.95 (t , 1 H, C3/5–H), 7.82 (ps–d, 2 H, C4–H), 7.71 (d, 2 H, Ar–H), 7.47–7.41 (m, 4 H, Ar–H), 7.38 (ps–d, 2 H, Ar–H), 4.75 (t, ^3J(H,H) = 6.2 Hz, 4 H, NCH_2), 3.65 (s, 6 H, NCH_3), 3.39 (m, ^3J(H,H) = 5.5 Hz, 4 H, $NHCH_2$), 2.54 (m, ^3J(H,H) = 5.8 Hz, 4 H, $CH_2CH_2CH_2$). $^{13}C\{^1H\}$ NMR (125.77 MHz, $CDCl_3$): δ 191.9 ($C_{carbene}$), 163.5 (CO), 149.2 (C2/6), 140.4 (C4), 134.9, 134.1, 125.71, 125.68 (Ar–C), 124.7 (C3/5), 113.3, 112.7 (Ar–C), 48.1 (NCH_2), 37.9 (NCH_3), 35.4 ($NHCH_2$), 27.4 ($CH_2CH_2CH_2$). ^{19}F NMR (282.38 MHz, CD_3CN): δ -75.40, -75.41 (BF_4). Anal. Calcd for $C_{29}H_{31}AuBF_4N_7O_2$: C, 43.90; H, 3.94; N, 12.36. Found: C, 44.02; H, 3.84; N, 12.53. MS (ESI): *m/z* 706 $[M - BF_4]^+$.

Digold(I) tetracarbene complex 74_{Me}. This dinuclear complex was collected from the solid phase as a white powder (49 mg, 0.03 mmol, 50%). ^{1}H NMR (500 MHz, CD_2Cl_2): δ 9.02 (br–s, 4 H, NH), 7.79 (d, 4 H, C3/5–H), 7.47–7.44 (m, 14 H, C4–H and Ar–H), 7.37 (t, 4 H, Ar–H), 4.57 (t, ^{3}J(H,H) = 7.6 Hz, 8 H, NCH_2), 4.02 (s, 12 H, NCH_3), 3.57 (m, ^{3}J(H,H) = 6.1 Hz, 8 H, $NHCH_2$), 2.27 (m, ^{3}J(H,H) = 6.9 Hz, 8 H, $CH_2CH_2CH_2$). ^{13}C{^{1}H} NMR (125.77 MHz, CD_2Cl_2): δ 190.8 ($C_{carbene}$), 164.2 (CO), 148.9 (C2/6), 138.3 (C4), 134.2, 133.2, 125.25, 125.22 (Ar–C), 124.2 (C3/5), 111.9, 111.8 (Ar–C), 47.0 (NCH_2), 37.3 (NCH_3), 35.3 ($NHCH_2$), 30.3 ($CH_2CH_2CH_2$). ^{19}F NMR (282.38 MHz, CD_2Cl_2): δ -75.34, -75.40 (BF_4). Anal. Calcd for $C_{58}H_{62}Au_2B_2F_8N_{14}O_4$: C, 43.90; H, 3.94; N, 12.36. Found: C, 44.24; H, 4.25; N, 12.55. MS (ESI): *m/z* 706 $[M - 2\ BF_4]^{2+}$.

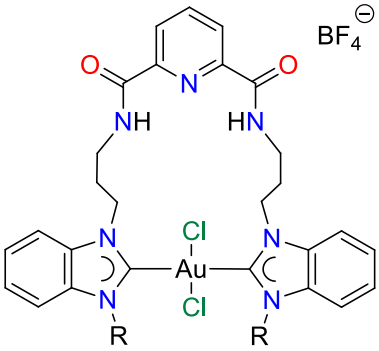

Monogold(III) dicarbene complexes 75_{Bn}. Complex $\mathbf{73_{Bn}}$ (95 mg 0.10 mmol) and $PhICl_2$ (33 mg, 0.12 mmol) were dissolved in CH_2Cl_2 (10 mL) and stirred for 24 h shielded from light. The solvent was then removed under vaccum, and the residue was washed with diethyl ether to give the product as pale yellow solid (90 mg, 0.09 mmol, 89%). ^{1}H NMR (300 MHz, $CDCl_3$): δ 9.35 (br–s, 2 H, NH), 8.25 (ps–d, 2 H, C3/5–H), 7.96 (t, 1 H, C4–H), 7.72 (ps–d, 2 H, Ar–H), 7.49 (t, 2 H, Ar–H), 7.35 (t, 2 H, Ar–H), 7.20 (m, 8 H, Ar–H), 6.93 (ps–d, 4 H, Ar–H), 5.46 (s, 4 H, NCH_2Ph), 4.99 (br–s, 4 H, NCH_2), 3.92 (br–s, 4 H, $NHCH_2$), 2.64 (br–s, 4 H, $CH_2CH_2CH_2$). ^{13}C{^{1}H} NMR (75.48 MHz, $CDCl_3$): δ 165.4 (CO), 163.4 ($C_{carbene}$), 149.6 (C2/6), 139.2 (C4), 134.8, 134.3, 133.4, 129.9, 129.4, 126.9, 126.7 (Ar–C, two are coincident), 125.1 (C3/5), 114.1, 113.4 (Ar–C), 52.0 (NCH_2Ph), 49.1 (NCH_2), 37.0 ($NHCH_2$), 28.8 ($CH_2CH_2CH_2$). ^{19}F NMR (282.38 MHz, $CDCl_3$): δ -73.58, -73.63

(BF_4). Anal. Calcd for $C_{41}H_{39}AuBCl_2F_4N_7O_2$: C, 48.45; H, 3.87; N, 9.65. Found: C, 48.22; H, 3.84; N, 10.03. MS (ESI): *m/z* 928 $[M - BF_4]^+$.

Monogold(III) dicarbene complexes 75_{Me}. This complex was prepared in analogy to complex $\mathbf{75_{Bn}}$ from complex $\mathbf{73_{Me}}$ (79 mg 0.10 mmol) and $PhICl_2$ (33 mg, 0.12 mmol). Yield: 67 mg, 0.08 mmol, 78%. ^{1}H NMR (500 MHz, $CDCl_3$ with several drops of MeOD): δ 10.4 (br–s, the integral was not correct due to fast exchange with the MeOD solvent, NH), 8.21 (ps–d, 2 H, C3/5–H), 7.94 (t, 1 H, C4–H), 7.74 (ps–d, 2 H, Ar–H), 7.59 (br–s, 1 H, Ar–H), 7.53 (m, 5 H, Ar–H), 4.96 (br–s, 4 H, NCH_2), 4.22 (s, 6 H, NCH_3), 3.85 (br–s, 4 H, $NHCH_2$), 2.61 (br–s, 4 H, $CH_2CH_2CH_2$). ^{13}C{^{1}H} NMR (125.77 MHz, $CDCl_3$ and several drops of MeOD): δ 165.8 (CO), 162.4 ($C_{carbene}$), 149.6 (C2/6), 139.2 (C4), 135.3, 133.9, 126.6 (Ar–C, two are coincident), 125.2 (C3/5), 113.8, 112.3 (Ar–C), 49.1 (NCH_2), 37.0 (NCH_3), 35.0 ($NHCH_2$), 28.8 ($CH_2CH_2CH_2$). ^{19}F NMR (282.38 MHz, $CDCl_3$ several drops of MeOD): δ -74.67, -74.73 (BF_4). Anal. Calcd for $C_{29}H_{31}AuBCl_2F_4N_7O_2$: C, 40.30; H, 3.62; N, 11.34. Found: C, 40.12; H, 3.84; N, 11.43. MS (ESI): *m/z* 776 $[M - BF_4]^+$.

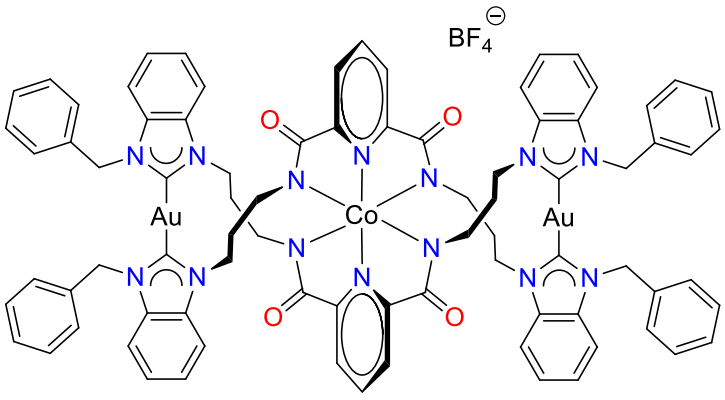

Gold(I), Gold(I) and Cobalt(III) trinuclear tetracarbene complexes 76. $Co(II)Cl_2\ 6H_2O$ (71 mg, 0.30 mmol) and 30 equivalents of NaH (360 mg, 9.00 mmol, 60% dispersion in mineral oil) were stirred in dry THF for 0.5 h before addition of complex $\mathbf{74_{Bn}}$ (567 mg, 0.30 mmol) in dry CH_2Cl_2 solution. After stirring the reaction mixture for 3 h under N_2, the mixture was stirring in air for 0.5 h. The

volatile was removed in vacuo before CH_2Cl_2 was added to dissolve the product. The CH_2Cl_2 phase was extracted with H_2O (5 × 10 mL) and dried over Na_2SO_4 to give the crude product. The residue was washed with hexane (5 × 10 mL) and dissolved in CH_2Cl_2 and toluene. Slow evaporation afforded the product as yellow solids (474 mg, 0.25 mmol, 85%). ^{1}H NMR (500 MHz, $CDCl_3$, 243-313 K) spectrum only showed broad siganls. $^{13}C\{^1H\}$ NMR (100.82 MHz, $CDCl_3$): δ 190.1 ($C_{carbene}$), 169.5 (CO), 157.2 (C2/6), 138.5 (C4), 135.5, 133.9, 133.7, 129.8, 129.7, 128.9, 127.9, 126.0 (Ar–C), 123.2 (C3/5), 113.4, 112.2 (Ar–C), 52.9 (N*C*H_2Ph), 49.3 (NCH_2), 43.4 (CON*C*H_2), 31.7 (CH_2*C*H_2CH_2). ^{19}F NMR (282.38 MHz, $CDCl_3$): δ -74.89, -74.95 (s, BF_4). Anal. Calcd for $C_{82}H_{74}Au_2BCoF_4N_{14}O_4$: C, 52.97; H, 4.01; N, 10.55. Found: C, 52.67; H, 4.34; N, 10.39. HRMS (ESI): *m/z* 1771.4702 (calcd for $[M - BF_4]^+$ 1771.4675).

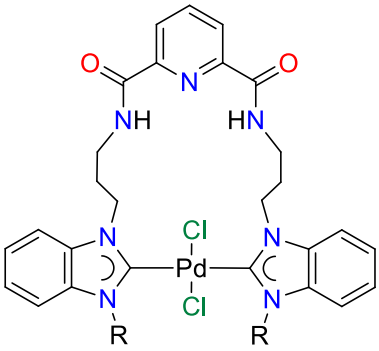

Palladium(II) dicarbene complex 77_{Bn}. A solution of $[PdCl_2(CH_3CN)_2]$ ($PdCl_2$: 18 mg, 0.10 mmol) in CH_3CN (20 mL) and tetramethylammonium chloride (15 mg, 0.14 mmol) in MeOH (2 mL) was slowly added to a solution of complex $\mathbf{72_{Bn}}$ (86 mg, 0.10 mmol) in CH_2Cl_2 (10 mL). The mixture was kept stirring overnight before the precipitation was filtered off through Celite. The filtrate was concentrated to 3 mL, which was subjected to column chromatography (SiO_2, hexane/ethyl acetate: 1/5) to obtain the product as a pale yellow solid (53 mg, 0.06 mmol, 63%). ^{1}H NMR (500 MHz, $CDCl_3$): δ 9.20 (t, ^3J(H,H) = 5.3 Hz, 2 H, CONH), 8.06 (d, 2 H, C3/5–H), 7.89 (t, 1 H, C4–H), 7.48 (d, 2 H, Ar–H), 7.37 (t, 4 H, Ar–H), 7.27–7.21 (m, 9 H, Ar–H), 7.02 (t, 2 H, Ar–H), 6.67 (d, 1 H, Ar–H), 6.44 (d, ^2J(H, H) = 15.1 Hz, 2 H, NC*H*HPh), 5.77 (m, 2 H, NCH_2), 5.19 (d, ^2J(H, H) = 15.1 Hz, 2 H, NCH*H*Ph), 4.57 (m, 2 H, NCH_2), 3.73 (m, 2 H, NHCH_2), 3.60 (m, 2 H,

NHCH_2), 2.82 (m, 4 H, $CH_2CH_2CH_2$), 2.49 (m, 4 H, $CH_2CH_2CH_2$). $^{13}C\{^1H\}$ NMR (125.77 MHz, $CDCl_3$): δ 180.3 ($C_{carbene}$), 164.3 (CO), 149.8 (C2/6), 139.0 (C4), 135.7, 134.9, 134.8, 129.3, 128.71, 128.68 (Ar–C), 125.0 (C3/5), 124.8, 123.8, 112.5, 112.2 (Ar–C), 53.6 (NCH_2Ph), 47.8 (NCH_2), 38.5 ($NHCH_2$), 26.3 ($CH_2CH_2CH_2$). Anal. Calcd for $C_{41}H_{39}Cl_2N_7O_2Pd$: C, 58.69; H, 4.68; N, 11.68. Found: C, 58.70; H, 5.01; N, 11.86. MS (ESI): *m/z* 803 $[M-Cl]^+$.

Palladium(II) dicarbene complex 77_{Me}. This complex was prepared in analogy to **77_{Bn}** from $PdCl_2$ (18 mg, 0.10 mmol), tetramethylammonium chloride (15 mg, 0.14 mmol) and complex **72_{Me}** (70 mg, 0.10 mmol). It was purified by column chromatography (SiO_2, CH_2Cl_2/MeOH: 40/1). Yield: 36 mg, 0.05 mmol, 52%. ^1H NMR (500 MHz, $CDCl_3$): δ 9.12 (t, ^3J(H,H) = 5.8 Hz, 2 H, CONH), 7.95 (d, 2 H, C3/5–H), 7.82 (t, 1 H, C4–H), 7.49 (d, 2 H, Ar–H), 7.30–7.27 (m, 2 H, Ar–H), 7.23 (t, 2 H, Ar–H), 7.06 (d, 2 H, Ar–H), 5.81–5.75 (m, 2 H, NCH_2), 4.61–4.56 (m, 2 H, NCH_2), 3.97 (s, 6 H, NCH_3), 3.77–3.70 (m, 2 H, NHCH_2), 3.51–3.48 (m, 2 H, NHCH_2), 2.84–2.80 (m, 4 H, $CH_2CH_2CH_2$), 2.40–2.37 (m, 4 H, $CH_2CH_2CH_2$). $^{13}C\{^1H\}$ NMR (125.77 MHz, $CDCl_3$): δ 179.4 ($C_{carbene}$), 164.1 (CO), 149.3 (C2/6), 138.9 (C4), 135.6, 134.1, (Ar–C), 124.6 (C3/5), 123.9, 112.7, 112.6 (Ar–C, two are coincident), 47.3 (NCH_2), 38.1 ($NHCH_2$), 34.9 (NCH_3), 26.0 ($CH_2CH_2CH_2$). Anal. Calcd for $C_{29}H_{31}Cl_2N_7O_2Pd$: C, 50.71; H, 4.55; N, 14.27. Found: C, 50.34; H, 4.17; N, 13.95. MS (ESI): *m/z* 650 $[M-Cl]^+$.

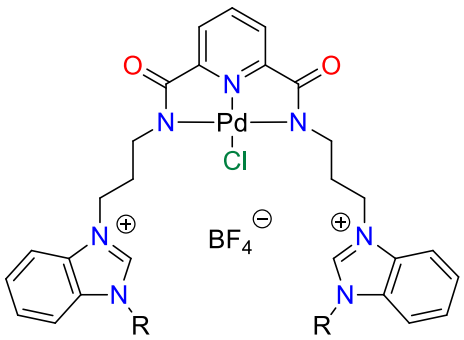

Palladium(II) (N',N,N')-pincer complex 78_{Bn}. Salt precusor **M_{Bn}** (84 mg, 0.10 mmol) was mixed with NEt_3 (30 µL, 0.22 mmol) in CH_3CN (10 mL) and stirred for 15 min at 70 °C. $[PdCl_2(CH_3CN)_2]$ ($PdCl_2$: 18 mg, 0.10 mmol) was added, and the mixture was kept stirring for 2 h at 70

°C. The resulting mixture was filtered and dried in vacuo. The residue was dissolved in CH_2Cl_2 (20 mL) and extracted with H_2O (5 × 20 mL). The organic layer was collected and dried over Na_2SO_4 to give the product as yellow solid (72 mg, 0.08 mmol, 81%). ^{1}H NMR (500 MHz, $CDCl_3$): δ 9.98 (s, 2 H, NCHN), 7.88 (t, 1 H, C4–H), 7.73 (d, 2 H, C3/5–H), 7.55 (d, 2 H, Ar–H), 7.47 (d, 2 H, Ar–H), 7.43–7.38 (m, 8 H, Ar–H), 7.31–7.27 (m, 6 H, Ar–H), 5.64 (s, 4 H, NCH_2Ph), 4.60 (br–s, 4 H, NCH_2), 3.43 (br–s, 4 H, $CONCH_2$), 2.42 (br–s, 4 H, $CH_2C\mathit{H}_2CH_2$). ^{13}C{^{1}H} NMR (125.77 MHz, $CDCl_3$): δ 171.7 (CO), 152.9 (C2/6), 143.1 (NCHN), 140.2 (C4), 133.3, 132.3, 131.9, 130.0, 129.8, 128.9, 127.6 (Ar–C, two are coincident), 124.7 (C3/5), 114.3, 114.2 (Ar–C), 52.1 (NCH_2Ph), 46.5 (NCH_2), 42.9 ($CON\mathit{C}H_2$), 29.7 ($CH_2\mathit{C}H_2CH_2$). ^{19}F NMR (282.38 MHz, $CDCl_3$): δ -74.44, -74.50 (BF_4). Anal. Calcd for $C_{41}H_{39}BClF_4N_7O_2Pd$: C, 55.30; H, 4.41; N, 11.01. Found: C, 55.32; H, 4.56; N, 11.06. MS (ESI): *m/z* 802 $[M - BF_4]^+$.

Palladium(II) (N',N,N')-pincer complex $\mathbf{78_{Me}}$. This complex was prepared in analogy to $\mathbf{78_{Bn}}$ from $\mathbf{M_{Me}}$ (68 mg, 0.10 mmol), NEt_3 (30 µL, 0.22 mmol) and $[PdCl_2(CH_3CN)_2]$ ($PdCl_2$: 18 mg, 0.10 mmol). However, $\mathbf{78_{Me}}$ is soluble in H_2O, which hampers the removal of the $HNEt_3Cl$ salt. Corresponding signals were observed in its ^{1}H and ^{13}C NMR spectra. The crude product yield is 45 mg, 0.06 mmol, 61%. ^{1}H NMR (500 MHz, CD_3CN): δ 9.50 (s, 2 H, NCHN), 7.99 (t, 1 H, C4–H), 7.88 (d, 2 H, C3/5–H), 7.69 (d, 2 H, Ar–H), 7.57 (m, 4 H, Ar–H), 7.48 (d, 2 H, Ar–H), 4.47 (t, ^3J(H,H) = 6.0 Hz, 4 H, NCH_2), 3.99 (s, 6 H, NCH_3), 4.00 (br–s, 4 H, $CONCH_2$), 2.29 (m, ^3J(H,H) = 6.0 Hz, 4 H, $CH_2C\mathit{H}_2CH_2$). ^{13}C{^{1}H} NMR (125.77 MHz, CD_3CN): δ 171.7 (CO), 153.1 (C2/6), 143.4 (NCHN), 141.0 (C4), 133.2, 132.4, 127.6, 127.5 (Ar–C), 124.6 (C3/5), 114.6, 113.8 (Ar–C), 46.6 (NCH_2), 43.0 ($CON\mathit{C}H_2$), 34.1 (NCH_3), 29.8 ($CH_2\mathit{C}H_2CH_2$). ^{19}F NMR (282.38 MHz, CD_3CN): δ -74.86, -74.95 (BF_4). ^{1}H and ^{13}C NMR spectra are attached in the appendix. MS (ESI): *m/z* 652 $[M - BF_4]^+$.

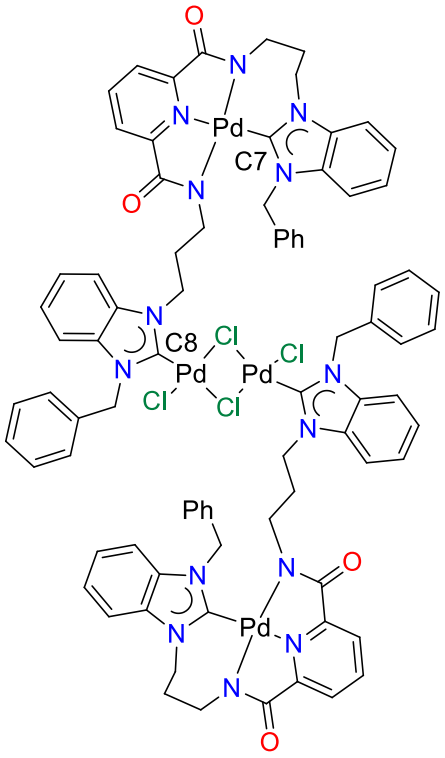

Tetrapalladium(II) tetracarbene complex 79. This complex could be obtained via reacting (A): **77$_{Bn}$** (84 mg, 0.10 mmol), (B) **78$_{Bn}$** (89 mg, 0.10 mmol) or (C) **81** (85 mg, 0.10 mmol) with $Pd(OAc)_2$ (86 mg, 0.10 mmol) in the presence of tetramethylammonium chloride (33 mg, 0.30 mmol) in DMSO (10 mL) at 90 ℃ overnight. A common workup procedure was used to purify the product. After the solvent was removed by vacuum distillation, the residue was dissolved in CH_2Cl_2 (30 mL) and then extracted with H_2O (5 × 20 mL). The organic layer was combined and dried over $NaSO_4$. After concentrated to 5 mL, the filtrate was subjected to Colum chromatography (SiO_2, CH_2Cl_2/MeOH: 20/1) to yield the product as yellow solids (Yields obtained from method A/B/C: 63/68/81 mg, 0.03/0.04/0.04 mmol, 67/72/86%). ^{1}H NMR (500 MHz, CD_3CN): δ 8.11 (t, 2 H, C4–H), 7.71 (d, 2 H, C3–H), 7.67 (d, 2 H, C5–H), 7.53 (d, 2 H, Ar–H), 7.45–7.39 (m, 6 H, Ar–H), 7.36–7.20 (m, 20 H, Ar–H), 7.18–7.13 (m, 4 H, Ar–H), 7.07 (t, 2 H, Ar–H), 6.97 (d, 2 H, Ar–H), 5.91 (d, ^2J(H, H) = 15.8 Hz, 2 H, NC*H*HPh), 5.72 (d, ^2J(H, H) = 15.8 Hz, 2 H, NC*H*HPh), 5.60–5.54 (m, 2 H, NCH_2), 5.43 (d, ^2J(H, H) = 16.4 Hz, 2 H, NCH*H*Ph), 5.06–4.97 (m, 4 H, NCH*H*Ph and NCH_2), 4.75–4.70 (m, 2 H, NCH_2), 4.57–4.53 (m, 2 H, $CONCH_2$), 4.35–4.30 (m, 4 H, NCH_2 and $CONCH_2$), 2.74–2.69 (m, 2 H, $CH_2CH_2CH_2$), two $CONCH_2$ and three $CH_2CH_2CH_2$ were not resolved or coincide with solvent signals. $^{13}C\{^1H\}$ NMR (125.77 MHz, CD_3CN): δ 180.8 ($C7_{carbene}$), 173.0, 171.7 (CO), 161.5 ($C8_{carbene}$), 152.8, 152.4 (C2 and C6), 142.2 (C4), 136.9, 136.2, 135.2, 134.9, 134.5, 134.1, 129.8, 129.6, 129.1, 129.0, 128.8, 128.3, 124.8, 124.7, 124.4, 124.3, 124.2, 113.2, 112.4, 112.1, 111.9 (Ar–C and C3,

C5, two are coincident), 52.9, 52.3 (NCH_2Ph), 47.7, 47.1 (NCH_2), 45.1, 42.2 ($CONCH_2$), 31.6, 29.0 ($CH_2CH_2CH_2$). Anal. Calcd for $C_{82}H_{74}Cl_4N_{14}O_4Pd_4$: C, 52.19; H, 3.95; N, 10.39. Found: C, 52.38; H, 4.30; N, 10.01. MS (ESI): *m/z* 975 $[M/2 + H + MeOH]^+$, 1888 $[M + H]^+$.

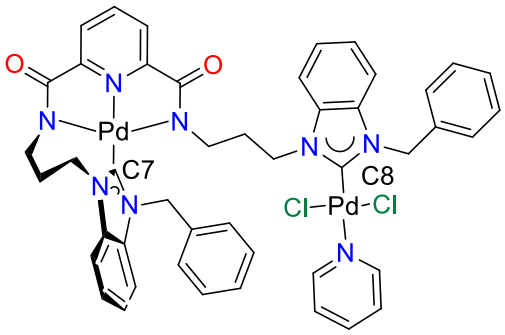

Dipalladium dicarbene pyridine complex 80. This complex was obtained by reacting the tetranuclear complex **79** (44 mg, 0.02 mmol) with pyridine (18 µL, 0.22 mmol) in CH_2Cl_2 (10 mL) for 2 h. The reaction was dried and the residue washed with diethyl ether to afford the product as a yellow solid (46 mg, 0.04 mmol, 96%). ^{1}H NMR (500 MHz, CD_3CN): δ 8.70 (d, 2 H, Py–H), 8.07 (t, 1 H, C4–H), 7.85 (t, 1 H, Py–H), 7.69 (d, 2 H, C3–H), 7.64 (d, 2 H, C5–H), 7.53–7.50 (m, 3 H, Ar–H), 7.44 (d, 2 H, Py–H), 7.37–7.17 (m, 13 H, Ar–H), 7.09 (t, 1 H, Ar–H), 7.03 (d, 1 H, Ar–H), 6.03 (d, ^2J(H, H) = 15.8 Hz, 1 H, NC*H*HPh), 5.80 (d, ^2J(H, H) = 15.8 Hz, 1 H, NC*H*HPh), 5.66 (d, ^2J(H, H) = 15.8 Hz, 1 H, NCH*H*Ph), 5.53–5.46 (m, 1 H, NC*H*H), 5.18 (d, ^2J(H, H) = 15.8 Hz, 1 H, NCH*H*Ph), 5.14–5.08 (m, 1 H, NCH*H*), 4.85–4.79 (m, 1 H, NC*H*H), 4.53–4.49 (m, 1 H, $CONCH_2$), 4.41–4.35 (m, 1 H, NCH*H*), 4.32–4.28 (m, 1 H, $CONCH_2$), 2.87–2.81 (m, 1 H, $CH_2CH_2CH_2$), 2.35–2.29 (m, 1 H, $CH_2CH_2CH_2$), 1.77–1.72 (m, 1 H, $CH_2CH_2CH_2$), two $CONCH_2$ and one $CH_2CH_2CH_2$ were not resolved or coincide with solvent signals. ^{13}C{^{1}H} NMR (125.77 MHz, CD_3CN): δ 180.9 ($C7_{carbene\text{-}cyclized}$), 173.0, 171.6 (CO), 165.5 ($C8_{carbene}$), 152.7, 152.4 (C2 and C6), 151.7 (Py–C), 142.2 (C4), 139.7 (Py–C), 137.0, 136.7, 135.2, 135.1, 134.6, 134.5, 129.8, 129.6, 129.09, 129.06, 129.00, 128.3, 125.8, 124.82, 124.76, 124.73, 124.23, 124.20, 124.1, 113.2, 112.3, 112.1, 111.8 (Ar–C, Py–C, C3 and C5), 52.9, 52.4 (NCH_2Ph), 47.8, 47.0 (NCH_2), 45.1, 42.1 ($CONCH_2$), 31.8, 29.0 ($CH_2CH_2CH_2$). Anal. Calcd

for $C_{46}H_{42}Cl_2N_8O_2Pd_2$: C, 54.03; H, 4.14; N, 10.96. Found: C, 53.93; H, 4.38; N, 11.05. MS (ESI): *m/z* 976 $[M - Py + MeOH + H]^+$.

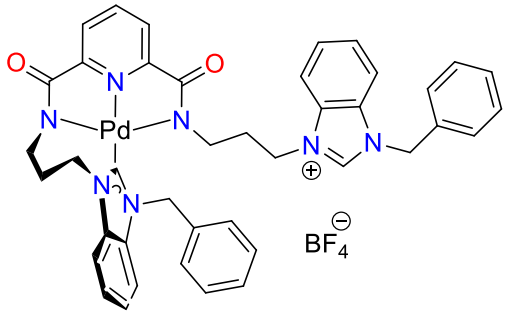

Palladium monocarbene complex 81. This complex was obtained by reacting complex **78$_{Bn}$** (89 mg, 0.10 mmol) with Ag_2O (14 mg, 0.06 mmol) in CH_2Cl_2 (30 mL) overnight. The resulting suspension was filtered to afford the product as yellow solid (72 mg, 0.08 mmol, 84%). ^{1}H NMR (500 MHz, $CDCl_3$): δ 9.67 (s, 1 H, NCHN), 8.03 (t, 2 H, C4–H), 7.81 (d, 2 H, C3–H), 7.76 (d, 2 H, C5–H), 7.52–7.45 (m, 4 H, Ar–H), 7.42 (d, 2 H, Ar–H), 7.38 (t, 4 H, Ar–H), 7.33–7.28 (m, 6 H, Ar–H), 7.24–7.20 (m, 2 H, Ar–H), 5.94 (d, ^2J(H, H) = 15.1 Hz, 2 H, NC*H*HPh), 5.62 (d, ^2J(H, H) = 15.1 Hz, 2 H, NCH*H*Ph), 5.59–5.53 (m, 2 H, NCH_2), 5.51 (s, 2 H, NCH_2Ph), 4.63–4.59 (m, 1 H, $CONCH_2$), 4.51–4.44 (m, 3 H, NCH_2 and $CONCH_2$), 4.02–3.96 (m, 2 H, NCH_2), 2.99–2.94 (m, 1 H, $CH_2CH_2CH_2$), 2.02–1.95 (m, 2 H, $CH_2CH_2CH_2$), two $CONCH_2$ and one $CH_2CH_2CH_2$ proton were not resolved or coincide with solvent signals.. ^{13}C{^{1}H} NMR (125.77 MHz, $CDCl_3$): δ 179.4 ($C_{carbene}$), 173.3, 171.7 (CO), 152.3, 151.9 (C2 and C6), 142.5 (NCHN), 141.5 (C4), 135.9, 134.8, 134.6, 133.1, 132.2, 131.8, 130.05, 129.95, 129.90, 129.7, 129.0, 128.8, 128.1, 127.8, 125.1, 124.83, 124.79, 124.4, 114.3, 114.2, 113.4, 111.1 (Ar–C, C3 and C5), 52.5, 52.0 (NCH_2Ph), 46.3, 45.8 (NCH_2), 44.4, 42.2 ($CONCH_2$), 30.4, 28.9 ($CH_2CH_2CH_2$). ^{19}F NMR (282.38 MHz, $CDCl_3$): δ -74.58, -74.59 (s, BF_4). Anal. Calcd for $C_{41}H_{38}BF_4N_7O_2Pd$: C, 57.66; H, 4.48; N, 11.48. Found: C, 57.38; H, 4.34; N, 11.09. MS (ESI): *m/z* 766 $[M - BF_4]^+$.

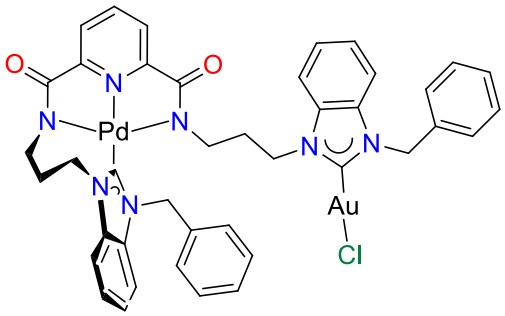

Palladium(II) and gold(I) hetero-bimetallic dicarbene complex 82. Complex **81** (85 mg, 0.10 mmol) was reacted with Ag_2O (14 mg, 0.06 mmol) in the presence of tetramethylammonium chloride (16 mg, 0.15 mmol) in CH_2Cl_2 (20 mL) and MeOH (2 mL) for 5 h. The resulting suspension was filtered into a solution of [AuCl(THT)] (32 mg, 0.10 mmol) in CH_2Cl_2 (5 mL) through Celite. The combined mixture was stirred for 5 h before the solvent was removed in vacuo. Washing the residue with H_2O (3 × 10 mL) gave the crude product, which was then subjected to column chromatography (SiO_2, CH_2Cl_2/MeOH : 30/1) to afford the product as a yellow solid (63 mg, 0.06 mmol, 63%). ^{1}H NMR (500 MHz, CD_3CN): δ 8.06 (t, 1 H, C4–H), 7.68–7.65 (t, 2 H, C3– and C5–H), 7.54 (d, 1 H, Ar–H), 7.48 (d, 1 H, Ar–H), 7.35–7.33 (m, 3 H, Ar–H), 7.27–7.19 (m, 13 H, Ar–H), 5.77 (d, ^2J(H, H) = 15.2 Hz, 1 H, NC*H*HPh), 5.58–5.52 (m, 1 H, NCH_2), 5.31 (s, 2 H, NCH_2Ph), 5.21 (d, ^2J(H, H) = 15.2 Hz, 1 H, NCH*H*Ph), 4.55–4.49 (m, 2 H, NCH_2), 4.39–4.29 (m, 2 H, NCH_2 and $CONCH_2$), 4.25–4.17 (m, 1 H, $CONCH_2$), 2.78–2.72 (m, 1 H, $CH_2CH_2CH_2$), two $CONCH_2$ and three $CH_2CH_2CH_2$ protons were not resolved or coincide with solvent signals.. ^{13}C{^{1}H} NMR (125.77 MHz, CD_3CN): δ 180.7 (Pd–$C_{carbene}$), 179.0 (Au–$C_{carbene}$), 172.9, 171.8 (CO), 152.6, 152.5 (C2 and C6), 142.2 (C4), 136.8, 136.6, 135.2, 134.7, 134.0, 133.5, 129.8, 129.18, 139.15, 128.4, 128.2, 125.4, 125.3, 125.0, 124.9, 124.8, 124.5, 113.3, 112.9, 112.8, 112.1 (Ar–C, C3 and C5, two are coincident), 52.7, 52.3 (NCH_2Ph), 47.8, 45.7 (NCH_2), 44.8, 42.1 ($CONCH_2$), 32.6, 28.9 ($CH_2CH_2CH_2$). Anal. Calcd for $C_{41}H_{37}AuClN_7O_2Pd$: C, 49.31; H, 3.73; N, 9.82. Found: C, 49.69; H, 4.02; N, 9.88. MS (ESI): *m/z* 998 $[M + H]^+$.

X-ray Diffraction Studies

X-ray data were collected with a Bruker AXS SMART APEX diffractometer, using Mo-K_α radiation with the SMART suite of Programs.[105] Data were processed and corrected for Lorentz and polarization effects with SAINT,[106] and for absorption effect with SADABS.[107] Structural solution and refinement were carried out with the SHELXTL suite of programs.[108] The structure was solved by direct methods to locate the heavy atoms, followed by difference maps for the light, non-hydrogen atoms. All non-hydrogen atoms were generally given anisotropic displacement parameters in the final model. All H-atoms were put at calculated positions. A summary of the most important crystallographic data is provided in the following section (see Selected X-ray Crystallographic Data), and individual CIF files are provided in the enclosed CD.

7. Selected Crystallographic Data

	13	***cis*-15** CH_2Cl_2	***cis*-16** $CHCl_3$	***cis*-17** $2CHCl_3$
formula	$C_{20}H_{31}Br_2N_5Pd$	$C_{16}H_{27}Br_2N_2O_3PPd\ CH_2Cl_2$	$C_{22}H_{39}Br_2N_2O_3PPd\ CHCl_3$	$C_{31}H_{33}Br_2N_2O_3PPd\ 2CHCl_3$
fw	607.72	677.51	796.11	1017.52
color, habit	orange, block	colourless, rod	colourless, block	colourless, rod
cryst size [mm]	0.60×0.44×0.10	0.54×0.10×0.08	0.70×0.60×0.40	0.16×0.24×0.40
temp [K]	223(2)	223(2)	223(2)	100(2)
crystsyst	orthorhombic	triclinic	monoclinic	monoclinic
space group	*P*bca	*P*-1	*P*2(1)/c	*P*2(1)/n
a[Å]	9.5113(4)	10.7930(9)	15.6417(8)	9.5178(8)
b [Å]	17.3866(7)	11.3295(10)	11.2303(5)	29.221(2)
c [Å]	28.6770(12)	12.8900(10)	19.3568(9)	14.4122(12)
α [deg]	90.00	65.134(2)	90.00	90.00
β [deg]	90.00	67.128(2)	97.7740(10)	93.881(2)
γ [deg]	90.00	82.651(2)	90.00	90.00
V [Å^3]	4742.3(3)	1316.43(19)	3369.0(3)	3999.2(6)
Z	8	2	4	4
D_c [g cm^{-3}]	1.702	1.709	1.570	1.690
radiation used	Mo Kα	Mo Kα	Mo Kα	Mo Kα
μ [mm^{-1}]	4.168	4.022	3.233	2.938
θ range [deg]	2.34–27.49	1.88–25.00	2.10–27.50	2.26–27.50
no. of unique data	31797	7783	23353	28805
max., min. transmn	0.6806, 0.1888	0.7391, 0.2200	0.3579, 0.2106	0.6523, 0.5313
final R indices	R_1 = 0.0497,	R_1 = 0.0551	R1 = 0.0391,	R1 = 0.0453,
[$I > 2\sigma(I)$]	wR_2 = 0.1062	wR_2 = 0.1401	wR2 = 0.0933	wR2 = 0.1059
R indices (all data)	R_1 = 0.0706,	R_1 = 0.0739	R1 = 0.0555,	R1 = 0.0652,
	wR_2 = 0.1140	wR_2 = 0.1568	wR2 = 0.0991	wR2 = 0.1133
goodness-of-fit	1.062	1.018	1.038	1.042
peak/hole [e Å^{-3}]	1.373/–1.796	0.920/–1.013	0.820/–0.572	1.081/-0.901

Continued…

	***cis*-19**	***cis*-20**	**22**	**23** $CHCl_3$
formula	$C_{31}H_{33}AsBr_2N_2Pd$	$C_{31}H_{33}Br_2N_2PdSb$	$C_{17}H_{26}Br_2N_2PdS$	$C_{18}H_{23}Br_2N_3OPd \cdot CHCl_3$
fw	774.73	821.56	556.68	682.98
color, habit	colourless, block	colourless, block	yellow, block	yellow, block
cryst size [mm]	0.208×0.098×0.088	0.293×0.258×0.080	0.31×0.25×0.21	0.25×0.31×0.31
temp [K]	100(2)	100(2)	100(2)	100(2)
crystsyst	monoclinic	monoclinic	monoclinic	monoclinic
space group	*P*21/n	*P*21/c	*P*2(1)/c	*P*21/n
a[Å]	10.5639(5)	10.3243(4)	12.7531(7)	10.2308(6)
b [Å]	17.5659(11)	14.7594(5)	9.9648(6)	17.7001(9)
c [Å]	16.5458(10)	20.3602(6)	16.0437(9)	13.5874(7)
α [deg]	90.00	90.00	90.00	90.00
β [deg]	93.981(2)	97.7730(12)	105.1420(10)	93.122(2)
γ [deg]	90.00	90.00	90.00	90.00
V [Å^3]	3062.9(3)	3073.99(18)	1968.08(19)	2456.8(2)
Z	4	4	4	4
D_c [g cm^{-3}]	1.680	1.775	1.879	1.846
radiation used	Mo Kα	Mo Kα	Mo Kα	Mo Kα
μ [mm^{-1}]	4.309	4.085	5.110	4.350
θ range [deg]	2.219–27.50	2.422–27.50	2.43–27.49	2.30–27.50
no. of unique data	103804	54062	13499	43049
max., min. transmn	0.7457, 0.6393	0.74, 0.53	0.5629, 0.4175	0.7457, 0.5143
final R indices	R_1 = 0.0228,	R_1 = 0.0299,	R1 = 0.0292,	R1 = 0.0240,
[$I > 2\sigma(I)$]	wR_2 = 0.0468	wR_2 = 0.0694	wR2 = 0.0682	wR2 = 0.0545
R indices (all data)	R_1 = 0.0327,	R_1 = 0.0466,	R1 = 0.0351,	R1 = 0.0293,
	wR_2 = 0.0494	wR_2 = 0.0745	wR2 = 0.0707	wR2 = 0.0564
goodness-of-fit	1.039	1.056	1.036	1.034
peak/hole [e Å^{-3}]	0.657/–0.586	1.096/–0.959	0.887/–0.737	0.660/-0.689

Continued…

	25·$CHCl_3$	**30**·$0.25H_2O$	**32**·$0.25H_2O$	**34**·$0.5CH_2Cl_2$
formula	$C_{25}H_{26}BrF_6N_4PPd·CHCl_3$	$C_{31}H_{38}BrF_6N_4O_2PPd·0.25H_2O$	$C_{20}H_{28}BrF_6N_8PPd·0.25H_2O$	$C_{22}H_{30}BrF_6N_6PPd·0.5CH_2Cl_2$
fw	833.15	835.77	715.78	752.27
color, habit	yellow, block	orange, block	colourless, block	colourless, block
cryst size [mm]	0.54×0.27×0.20	0.40×0.24×0.12	0.41×0.34×0.23	0.33×0.24×0.20
temp [K]	100(2)	100(2)	100(2)	293(2)
crystsyst	monoclinic	hexagonal	monoclinic	triclinic
space group	*P*2(1)/n	*P*6(5)	*P*2(1)/c	*P*-1
a[Å]	13.328(4)	13.0939(6)	18.5875(12)	13.372(12)
b [Å]	10.822(3)	13.0939(6)	9.1218(6)	14.825(13)
c [Å]	23.586(7)	34.369(3)	17.7695(11)	16.378(15)
α [deg]	90.00	90.00	90.00	112.263(17)
β [deg]	98.947(7)	90.00	116.2570(9)	99.074(18)
γ [deg]	90.00	120.00	90.00	98.184(18)
V [$Å^3$]	3360.6(16)	5103.1(6)	2702.0(3)	2894(5)
Z	4	6	4	2
D_c [g cm^{-3}]	1.647	1.632	1.760	1.727
radiation used	Mo Kα	Mo Kα	Mo Kα	Mo Kα
μ [mm^{-1}]	2.084	1.836	2.293	2.233
θ range [deg]	1.75–25.00	1.80–27.50	2.29–27.50	1.84–27.50
no. of unique data	18764	36526	19473	37912
max., min.transmn	0.6807, 0.3991	0.8098, 0.5271	0.5633, 0.4503	0.6637, 0.5262
final R indices [$I > 2\sigma(I)$]	R_1 = 0.0693, wR_2 = 0.1977	R_1 = 0.0320 wR_2 = 0.0652	R_1 = 0.0244, wR_2 = 0.0585	R_1 = 0.0449, wR_2 = 0.1180
R indices (all data)	R_1 = 0.0853, wR_2 = 0.2106	R_1 = 0.0390 wR_2 = 0.0681	R_1 = 0.0272, wR_2 = 0.0595	R_1 = 0.0566, wR_2 = 0.1240
goodness-of-fit	1.045	1.014	1.036	1.065
peak/hole [e $Å^{-3}$]	1.323/–0.975	0.543/–0.290	0.871/–0.352	2.645/–0.678

Continued…

	37·CH_3CN	**38**·$CHCl_3$	**40**	**41**
formula	$C_{35}H_{40}BrF_6N_6PPd·CH_3CN$	$C_{36}H_{42}BrF_6N_6PPd·CHCl_3$	$C_{49}H_{60}Br_4N_8Pd_2$	$C_{38}H_{40}Br_4N_4O_4Pd_2$
fw	917.06	1009.40	1293.49	1149.18
color, habit	colourless, block	colourless, block	yellow, thin plate	orange, plate
cryst size [mm]	0.47×0.19×0.12	0.19×0.13×0.07	0.56×0.26×0.04	0.28 x 0.14 x 0.06
temp [K]	100(2)	100(2)	100(2)	223(2)
crystsyst	triclinic	triclinic	monoclinic	monoclinic
space group	*P*-1	*P*-1	*P*21/c	*P*2(1)/c
a[Å]	9.0847(6)	9.6249(10)	8.5313(5)	9.0803(8)
b [Å]	11.6841(8)	11.6858(12)	18.2138(11)	21.2409(19)
c [Å]	18.3327(12)	18.6008(18)	32.4597(19)	10.8280(10)
α [deg]	95.0090(10)	94.5110(16)	90.00	90.00
β [deg]	98.1710(9)	102.3250(16)	91.9650(10)	90.902(2)
γ [deg]	92.6440(9)	99.6380(17)	90.00	90.00
V [$Å^3$]	1915.5(2)	2000.8(4)	5040.9(5)	2088.2(3)
Z	2	2	4	2
D_c [g cm^{-3}]	1.590	1.675	1.704	1.828
radiation used	Mo Kα	Mo Kα	Mo Kα	Mo Kα
μ [mm^{-1}]	1.636	1.768	3.926	4.730
θ range [deg]	1.99–27.50	1.13–26.37	1.68–27.50	1.92–27.49
no. of unique data	25415	24411	66154	14436
max., min. transmn	0.5629, 0.4760	0.8863, 0.7300	0.5633, 0.3623	0.7645, 0.3509
final R indices	R_1 = 0.0328,	R_1 = 0.0466,	R_1 = 0.0380,	R_1 = 0.0541,
[$I > 2\sigma(I)$]	wR_2 = 0.0887	wR_2 = 0.1072	wR_2 = 0.0879	wR_2 = 0.1314
R indices (all data)	R_1 = 0.0362,	R_1 = 0.0625,	R_1 = 0.0487,	R_1 = 0.0823,
	wR_2 = 0.0905	wR_2 = 0.1190	wR_2 = 0.0919	wR_2 = 0.1432
goodness-of-fit	1.075	1.076	1.053	1.006
peak/hole [e $Å^{-3}$]	0.816/–1.313	0.909/–1.209	1.775/–0.544	1.774/–0.771

Continued…

	41	**45**	**49** $CHCl_3$	**51** $CHCl_3$
formula	$C_{19}H_{20}Br_3N_3Pd$	$C_{34}H_{34}Br_4N_4Pd$	$C_{22}H_{22}I_3N_3Pd\ CH_2Cl_2$	$C_{23}H_{22}I_2N_4PdS\ CHCl_3$
fw	636.51	924.69	934.89	866.07
color, habit	yellow, block	yellow, block	orange, block	orange, thin plate
cryst size [mm]	0.60 x 0.24 x 0.20	0.50×0.42×0.26	0.40 x 0.16 x 0.14	0.44 x 0.20 x 0.10
temp [K]	223(2)	100(2)	100(2)	100(2)
crystsyst	monoclinic	monoclinic	triclinic	triclinic
space group	*P*2(1)/n	*P*2(1)/n	P–1	P1
a[Å]	7.8905(9)	10.5266(13)	8.1776(9)	8.339(5)
b [Å]	12.5212(14)	8.2026(10)	9.2817(11)	8.954(5)
c [Å]	21.373(2)	19.370(2)	20.433(2)	11.504(7)
α [deg]	90.00	90.00	82.449(2)	94.540(11)
β [deg]	90.503(3)	96.087(3)	88.771(2)	103.912(11)
γ [deg]	90.00	90.00	66.713(2)	116.140(10)
V [$Å^3$]	2111.5(4)	1663.1(3)	1411.4(3)	731.4(7)
Z	4	2	2	1
D_c [g cm^{-3}]	2.002	1.847	2.200	1.966
radiation used	Mo Kα	Mo Kα	Mo Kα	Mo Kα
μ [mm^{-1}]	6.564	5.394	4.240	3.111
θ range [deg]	1.88–27.47	2.11–27.49	2.01–27.50	1.87–27.45
no. of unique data	14614	11359	18736	9659
max., min. transmn	0.4915, 0.1529	0.3345, 0.1734	0.5883, 0.2818	0.4305, 0.3455
final R indices	R_1 = 0.0369	R_1 = 0.0393,	R1 = 0.0275,	R1 = 0.0345,
[$I > 2\sigma(I)$]	wR_2 = 0.0875	wR_2 = 0.1072	wR2 = 0.0661	wR2 = 0.0856
R indices (all data)	R_1 = 0.0512,	R_1 = 0.0469,	R1 = 0.0302,	R1 = 0.0360,
	wR_2 = 0.0927	wR_2 = 0.1110	wR2 = 0.0674	wR2 = 0.0866
goodness-of-fit	1.014	1.049	1.055	1.027
peak/hole [e $Å^{-3}$]	0.624/–1.047	1.489/–1.234	1.218/–0.825	1.540/–0.931

Continued…

	53 ·2$CHCl_3$	**55** 0.5$CHCl_3$ ·O (from H_2O)	**56**	**57** ·2CH_3CN
formula	$C_{34}H_{34}I_2N_4Pd_2S_2$ ·$C_2H_2Cl_6$	$C_{44}H_{38}Br_2N_4Pd_2S_2$ ·0.5$CHCl_3$ ·O	$C_{28}H_{34}Br_2N_4O_3PdS$	$C_{38}H_{40}Br_2N_4O_4Pd$ ·2CH_3CN
fw	1268.11	1135.21	772.87	965.07
color, habit	yellow, thin plate	orange, block	colourless, plate	colourless, rod
cryst size [mm]	0.46 x 0.24 x 0.04	0.20 x 0.14 x 0.14	0.46 x0.23 x0.12	0.37×0.13×0.07
temp [K]	100(2)	293(2)	100(2)	100(2)
crystsyst	monoclinic	tetragonal	orthorhombic	monoclinic
space group	*P*2(1)/n	*P*4(3)2(1)2	*P*2(1)2(1)2(1)	*P*2(1)/n
a[Å]	12.340(5)	18.5291(16)	7.529(3)	8.4490(4)
b [Å]	28.317(12)	18.5291 (16)	10.949(5)	23.3113(12)
c [Å]	13.650(6)	14.087(2)	36.970(15)	10.4417(4)
α [deg]	90.00	90.00	90.00	90.00
β [deg]	113.731(9)	90.00	90.00	94.643(2)
γ [deg]	90.00	90.00	90.00	90.00
V [$Å^3$]	4366(3)	4836.4(12)	3048(2)	2049.82(16)
Z	4	4	4	2
D_c [g cm^{-3}]	1.929	1.559	1.684	1.564
radiation used	Mo Kα	Mo Kα	Mo Kα	Mo Kα
μ [mm^{-1}]	2.732	2.601	3.335	2.451
θ range [deg]	1.78–27.50	1.82–27.49	1.94–27.50	2.14–28.35
no. of unique data	29974	63459	22225	20988
max., min. transmn	0.8986, 0.3663	0.6468, 0.5092	0.7457, 0.4883	0.7457, 0.6185
final R indices	R_1 = 0.0706,	R_1 = 0.0483,	R1 = 0.0360,	R_1 = 0.0387
[$I > 2\sigma(I)$]	wR_2 = 0.1479	wR_2 = 0.1425	wR2 = 0.0817	wR_2 = 0.0735
R indices (all data)	R_1 = 0.1003,	R_1 = 0.0581,	R1 = 0.0405,	R_1 = 0.0661
	wR_2 = 0.1587	wR_2 = 0.1501	wR2 = 0.0835	wR_2 = 0.0801
goodness-of-fit	1.127	1.073	1.041	1.033
peak/hole [e $Å^{-3}$]	2.625 /–1.897	1.408/–0.525	0.839/–0.458	0.613/–1.002

Continued…

	61	**62**	**63**	**67**
formula	$C_{58}H_{54}N_4PdS_4$	$C_{38}H_{34}N_8PdS_4$	$C_{36}H_{22}Br_2N_6PdS_2$	$C_{36}H_{34}I_2N_6PdS_2$
fw	1041.69	837.37	868.93	975.01
color, habit	orange, block	yellow, block	pale-yellow, block	yellow, block
cryst size [mm]	0.36×0.20×0.10	0.54×0.34×0.14	0.14×0.12×0.04	0.40×0.40×0.40
temp [K]	100(2)	223(2)	100(2)	100(2)
crystsyst	triclinic	monoclinic	monoclinic	monoclinic
space group	*P*-1	*P*2(1)/n	*C*2/c	*P*2(1)/n
a[Å]	10.6360(9)	10.9426(8)	25.707(3)	7.8570(10)
b [Å]	11.3645(9)	9.6095(7)	9.3604(12)	20.915(3)
c [Å]	11.4680(10)	18.7276(14)	16.538(2)	11.3480(15)
α [deg]	76.226(2)	90.00	90.00	90.00
β [deg]	66.087(2)	103.262(2)	116.555(4)	109.728(3)
γ [deg]	76.168(2)	90.00	90.00	90.00
V [Å^3]	1214.77(18)	1916.7(2)	3559.7 (8)	1755.3(4)
Z	1	2	4	2
D_c [g cm^{-3}]	1.424	1.451	1.621	1.845
radiation used	Mo Kα	Mo Kα	Mo Kα	Mo Kα
μ [mm^{-1}]	0.598	0.741	2.918	2.442
θ range [deg]	1.87–27.49	1.98–27.50	2.35–27.50	1.95–27.50
no. of unique data	16132	13088	25486	12380
max., min. transmn	0.7456, 0.6211	0.9033, 0.6903	0.7457, 0.6576	0.7673, 0.6022
final R indices	R1 = 0.0398,	R_1 = 0.0564,	R1 = 0.0501,	R_1 = 0.0294,
[$I > 2\sigma(I)$]	wR2 = 0.1038	wR_2 = 0.1302	wR2 = 0.1304	wR_2 = 0.0725
R indices (all data)	R1 = 0.0444,	R_1 = 0.0694,	R1 = 0.0693,	R_1 = 0.0306,
	wR2 = 0.1079	wR_2 = 0.1367	wR2 = 0.1404	wR_2 = 0.0731
goodness-of-fit	1.076	1.130	1.047	1.141
peak/hole [e Å^{-3}]	0.902/–0.514	1.127/–0.674	1.902/–1.902	1.284/–0.457

Continued…

	$\mathbf{M}_{\mathbf{Bn}}\cdot(CH_3)_2CO$	$\mathbf{73}_{\mathbf{Me}}$	$\mathbf{74}_{\mathbf{Bn}}\cdot 0.5H_2O$	$\mathbf{76}\cdot 0.25CH_2Cl_2$
formula	$C_{41}H_{41}B_2F_8N_7O_2\cdot(CH_3)_2CO$	$C_{29}H_{31}AuBF_4N_7O_2$	$C_{82}H_{78}Au_2B_2F_8N_{14}O_4\cdot 0.5H_2O$	$C_{82}H_{74}Au_2BCoF_4N_{14}O_4\cdot 0.25CH_2Cl_2$
fw	895.51	793.38	1908.14	1883.45
color, habit	colourless, block	colourless, plate	colourless, needle	yellow, block
cryst size [mm]	0.34×0.24×0.15	0.36×0.26×0.10	0.13×0.10×0.06	0.36×0.26×0.10
temp [K]	100(2)	100(2)	100(2)	100(2)
crystsyst	triclinic	monoclinic	monoclinic	triclinic
space group	*P*-1	*P*2(1)/n	*P*21/c	*P*-1
a[Å]	8.6769(11)	13.924(7)	23.2600(14)	15.0076(16)
b [Å]	15.920(2)	15.956(8)	20.2750(11)	16.2066(16)
c [Å]	17.935(3)	14.787(8)	8.2071(4)	17.9512(19)
α [deg]	115.794(4)	90.00	90.00	63.780(3)
β [deg]	103.951(3)	116.941(9)	94.156(4)	82.005(3)
γ [deg]	90.302(3)	90.00	90.00	79.629(3)
V [Å^3]	2147.5(5)	2929(3)	3860.3(4)	3844.1(7)
Z	2	4	2	2
D_c [g cm^{-3}]	1.385	1.799	1.642	1.627
radiation used	Mo Kα	Mo Kα	Cu Kα	Mo Kα
μ [mm^{-1}]	0.111	5.090	7.732	4.108
θ range [deg]	1.44–27.49	1.67–27.50	2.894–66.595	2.105–27.499
no. of unique data	28066	20375	27316	158525
max., min. transmn	09835, 0.9631	0.7898, 0.5489	0.7528, 0.6022	0.7457, 0.5929
final R indices	R1 = 0.0720,	R_1 = 0.0315,	R1 = 0.0794,	R_1 = 0.0563,
[$I > 2\sigma(I)$]	wR2 = 0.1545	wR_2 = 0.0685	wR2 = 0.1700	wR_2 = 0.1493
R indices (all data)	R1 = 0.1026,	R_1 = 0.0445,	R1 = 0.1296,	R_1 = 0.0767,
	wR2 = 0.1672	wR_2 = 0.0735	wR2 = 0.1936	wR_2 = 0.1603
goodness-of-fit	1.090	1.027	1.072	1.071
peak/hole [e Å^{-3}]	0.602/–0.315	1.624/–0.829	1.785/–1.091	6.166/–2.353

Continued…

	77$_{\mathbf{Bn}}$	**77**$_{\mathbf{Me}}$ $CHCl_3$	**78**$_{\mathbf{Me}}$·$6H_2O$	**82**·$1.4(CH_3)_2O$·$0.6CH_3CN$
formula	$C_{41}H_{39}Cl_2N_7O_2Pd$	$C_{29}H_{31}Cl_2N_7O_2Pd$ $CHCl_3$	$C_{29}H_{31}BClF_4N_7O_2Pd·6H_2O$	$C_{41}H_{37}AuClN_7O_2Pd·1.4(CH_3)_2O·0.6CH_3CN$
fw	839.09	806.27	846.36	1075.11
color, habit	colourless, block	pale-yellow, block	yellow, block	yellow, needle
cryst size [mm]	0.22×0.16×0.06	0.24×0.22×0.16	0.32×0.19×0.17	0.229×0.096×0.044
temp [K]	100(2)	100(2)	100(2)	100(2)
crystsyst	triclinic	monoclinic	triclinic	triclinic
space group	*P*-1	*P*21/n	P-1	P-1
a[Å]	12.8523(13)	9.43444(4)	10.9678(17)	10.0851(11)
b [Å]	13.2254(13)	17.7459(8)	11.3697(17)	15.0164(16)
c [Å]	13.9322(14)	19.0745(10)	15.235(2)	15.8093(18)
α [deg]	114.339(2)	90.00	83.845(3)	108.918(3)
β [deg]	109.288(2)	94.579(2)	69.378(3)	90.879(3)
γ [deg]	100.396(2)	90.00	84.171(3)	109.332(3)
V [Å^3]	1893.5(3)	3183.3(3)	1763.7(5)	2116.9(4)
Z	2	4	2	2
D_c [g cm^{-3}]	1.472	1.682	1.594	1.687
radiation used	Mo Kα	Mo Kα	Mo Kα	Mo Kα
μ [mm^{-1}]	0.677	1.045	0.681	3.998
θ range [deg]	1.79–27.50	2.338–27.498	1.99–25.00	2.391–28.353
no. of unique data	24851	30584	19103	70687
max., min. transmn	0.5629, 0.5155	0.7457, 0.7076	0.5629, 0.5236	0.7457, 0.5986
final R indices	R1 = 0.0494,	R_1 = 0.0587,	R1 = 0.0337,	R_1 = 0.0336,
[$I > 2\sigma(I)$]	wR2 = 0.1119	wR_2 = 0.1573	wR2 = 0.0842	wR_2 = 0.0565
R indices (all data)	R1 = 0.0664,	R_1 = 0.0881,	R1 = 0.0354,	R_1 = 0.0531,
	wR2 = 0.1192	wR_2 = 0.1712	wR2 = 0.0852	wR_2 = 0.0611
goodness-of-fit	1.048	1.047	1.097	1.017
peak/hole [e Å^{-3}]	0.844/–0.637	2.806/–1.851	0.778/–0.394	1.253/–0.723

Appendix

For complexes of which elemental analyses are not satisfactory, the ^{1}H and ^{13}C NMR spectra are displayed here.

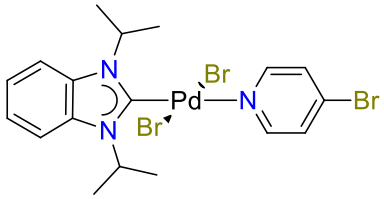

Complex **8**, ^{1}H NMR spectrum was shown in Figure 2.1. ^{13}C NMR spectrum (125.77 MHz, $CDCl_3$):

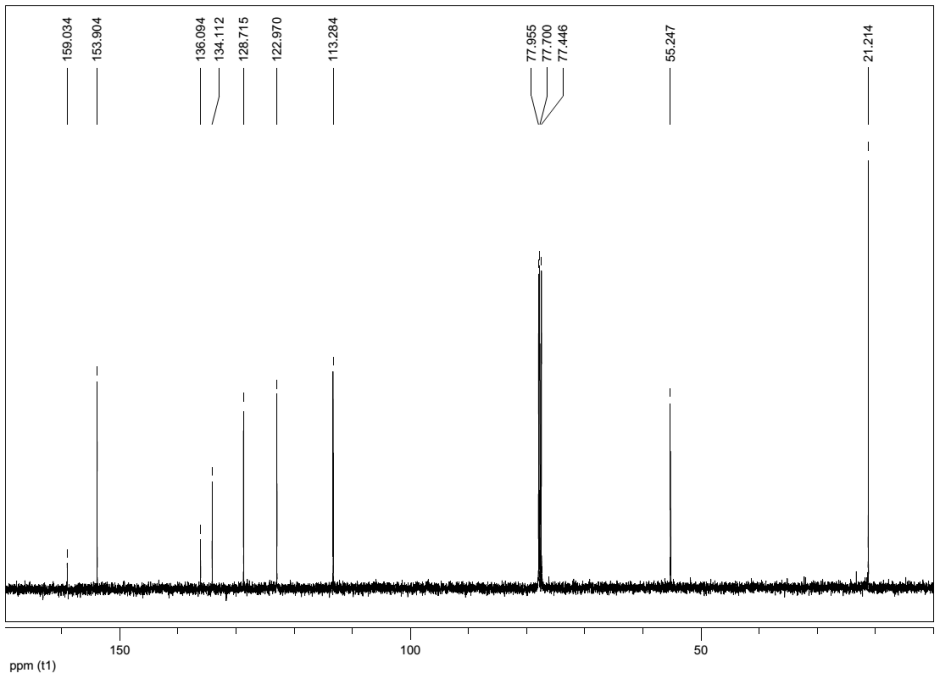

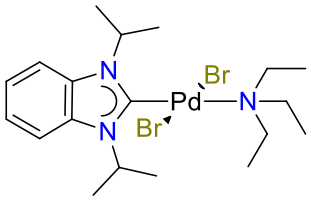

Complex **12**, ^{1}H NMR (300 MHz, $CDCl_3$) and ^{13}C NMR spectrum (75.48 MHz):

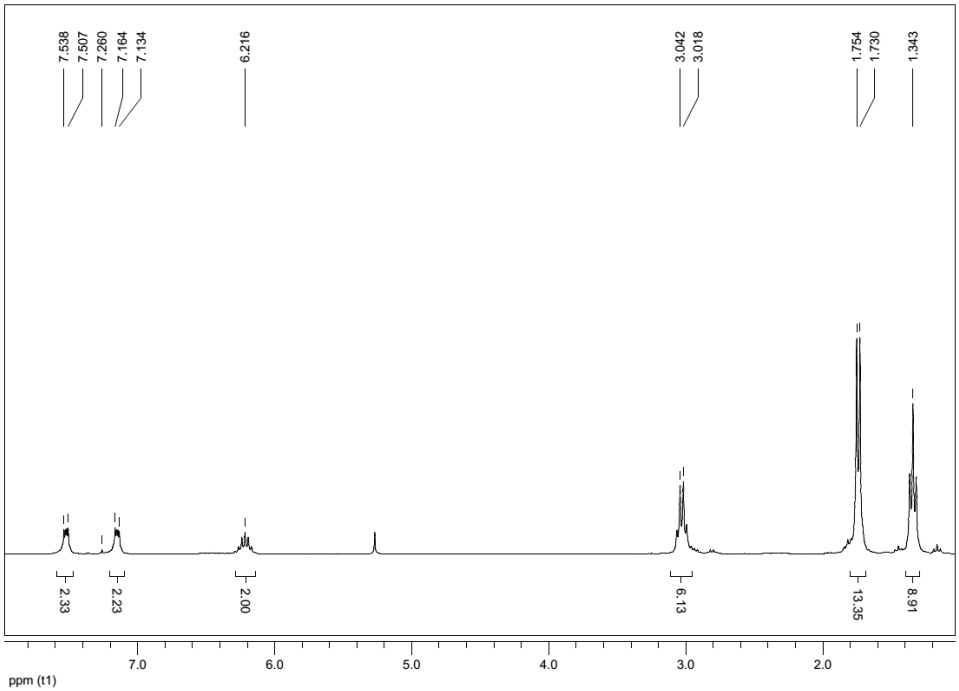

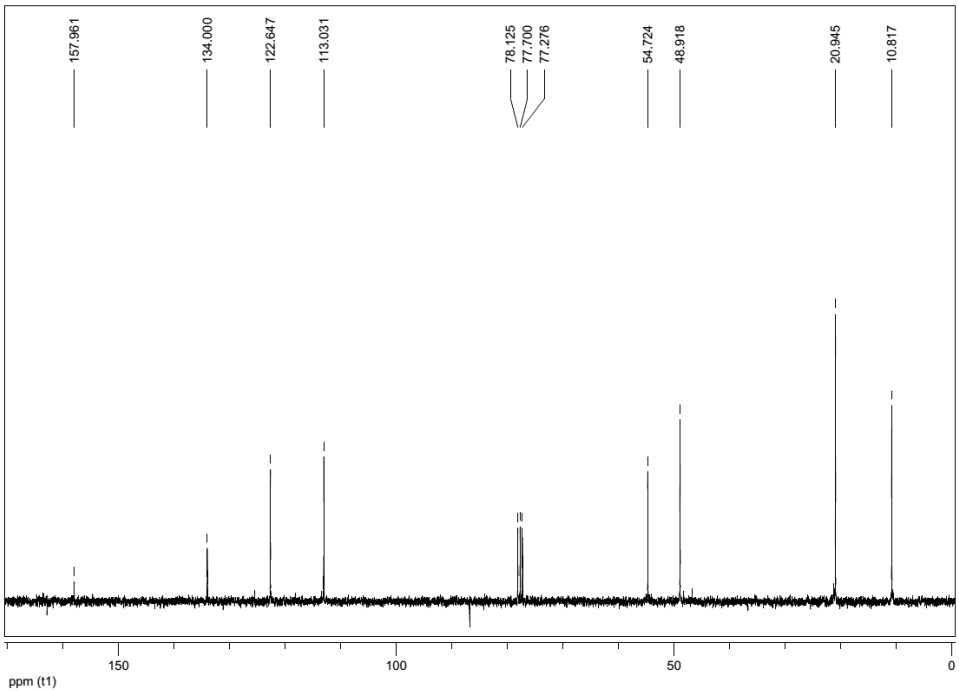

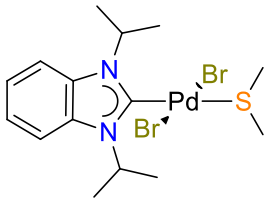

Complex **21**, ^{1}H NMR spectrum (500 MHz, $CDCl_3$) and ^{13}C NMR spectrum (125.77 MHz):

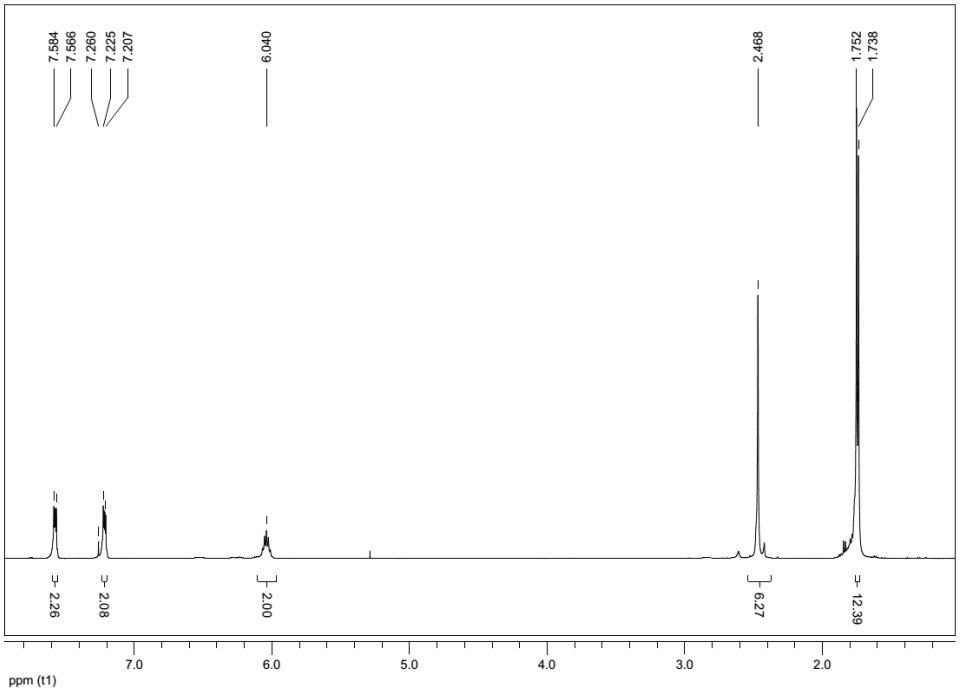

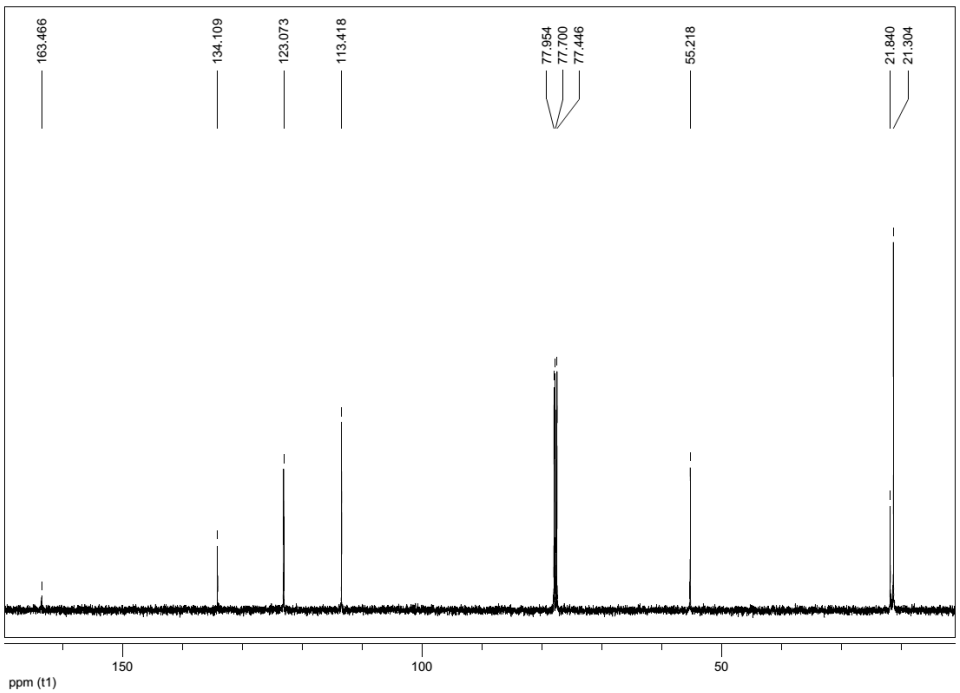

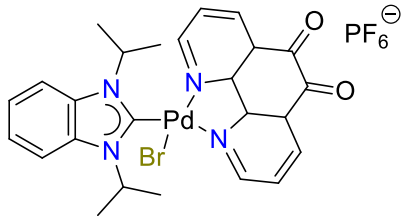

Complex **24**, ^{1}H NMR (500 MHz, CD_3CN) and ^{13}C NMR spectrum (125.77 MHz):

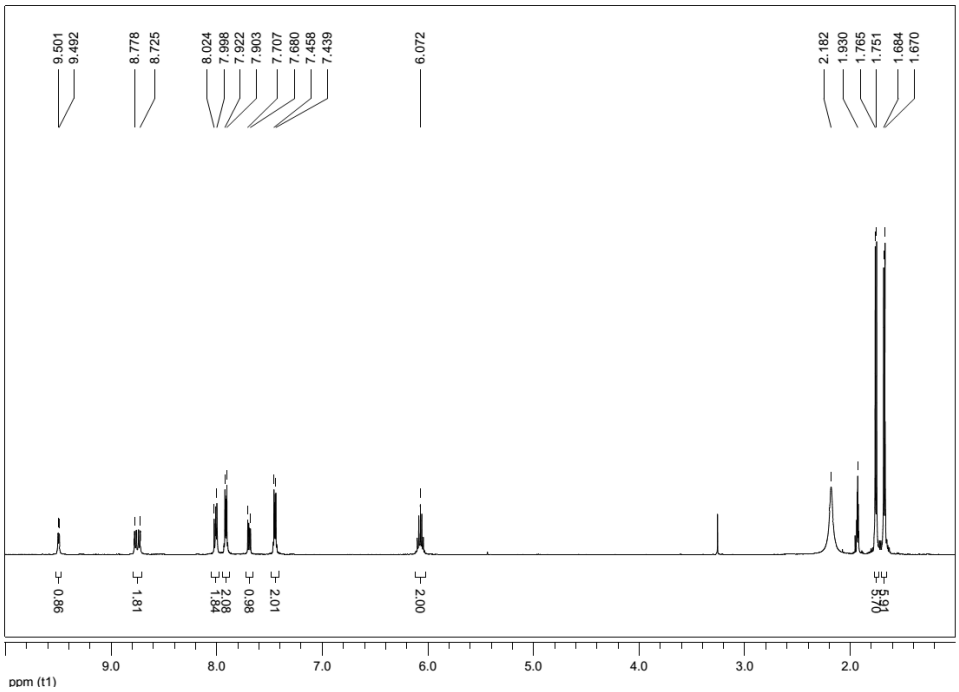

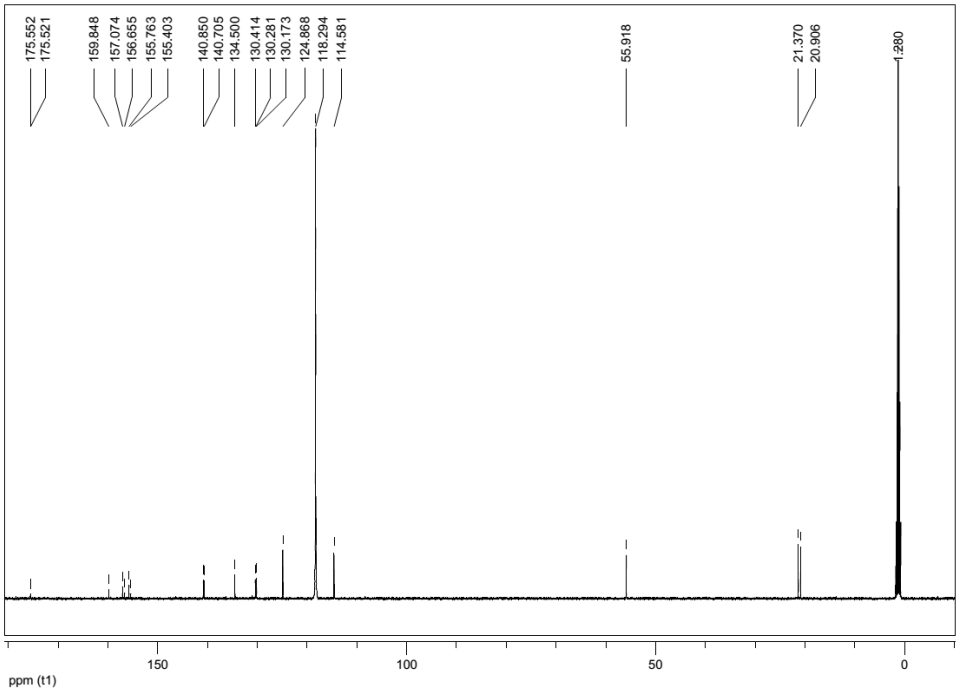

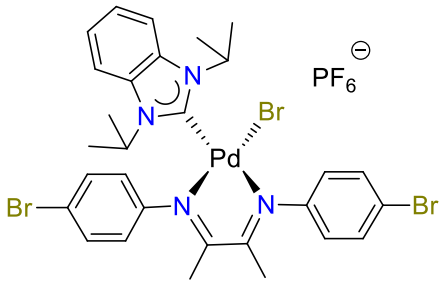

Compound **27**, ^{1}H NMR spectrum (500 MHz, $CDCl_3$) and ^{13}C NMR spectrum (125.77 MHz):

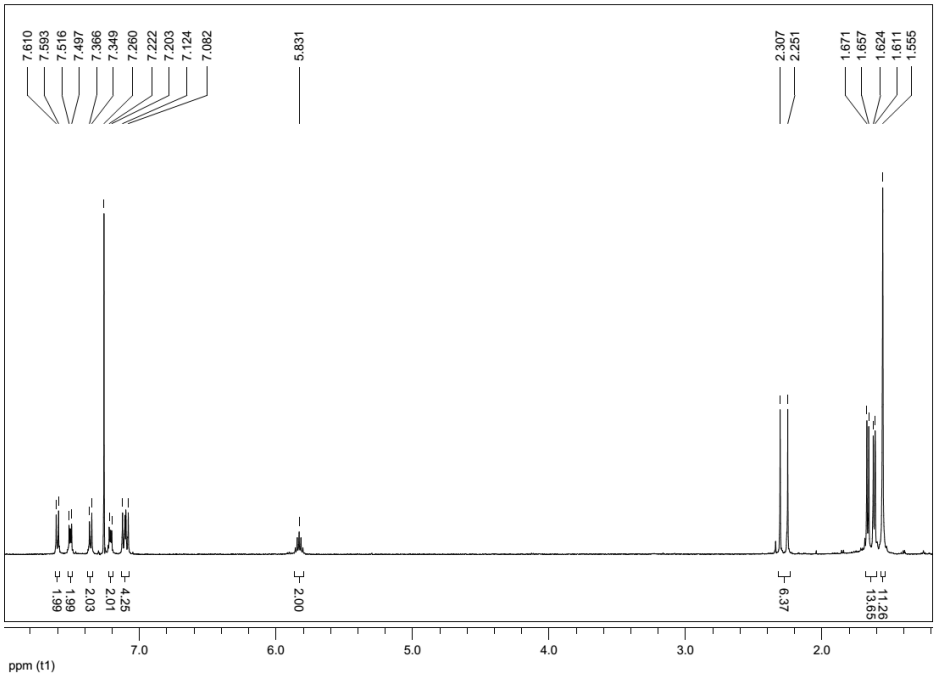

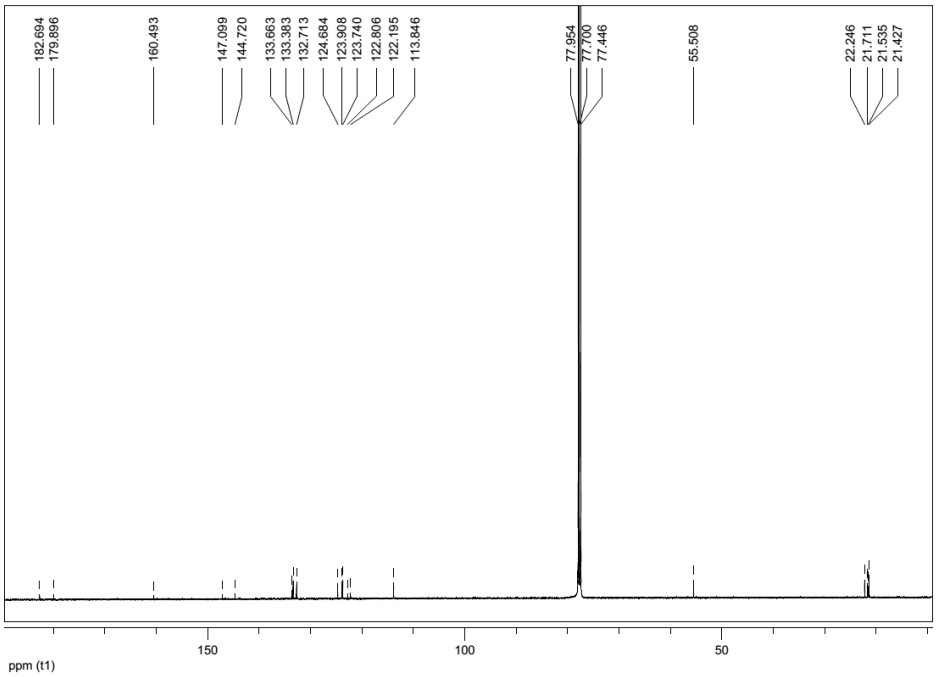

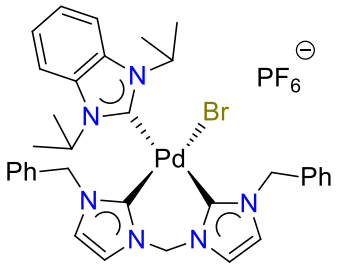

Compound **35**, ^{1}H NMR spectrum (500 MHz, $CDCl_3$) and ^{13}C NMR spectrum (125.77 MHz):

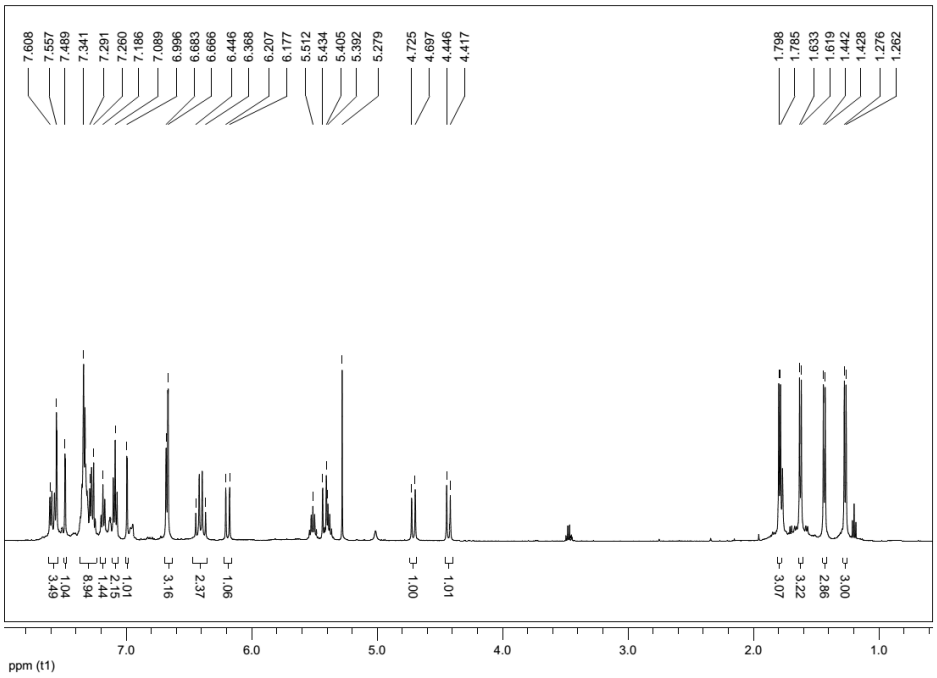

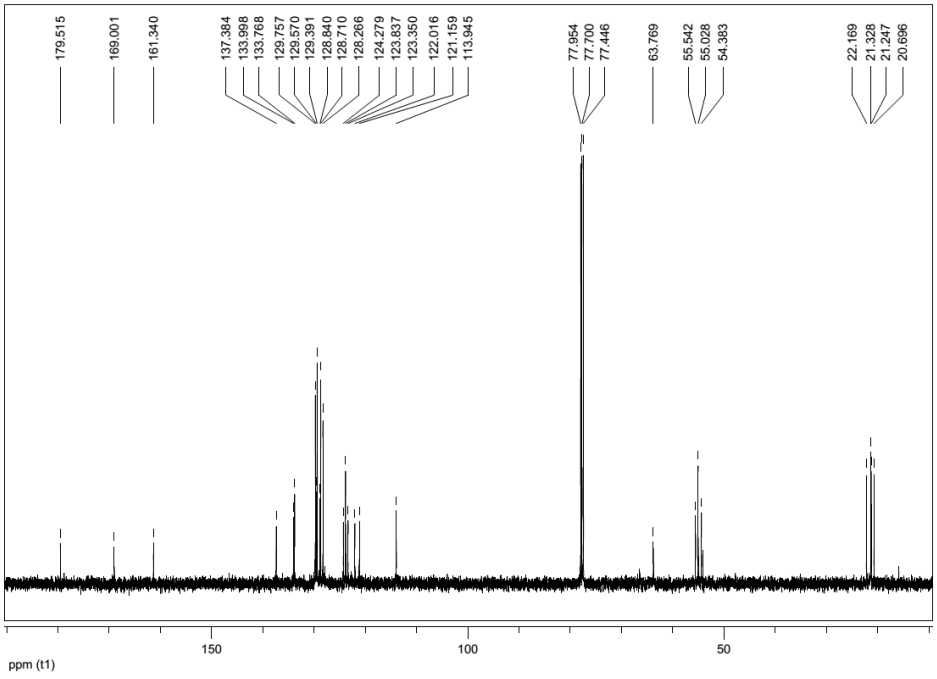

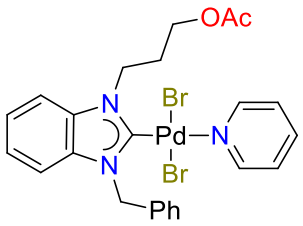

Compound **47**, ^{1}H NMR spectrum (300 MHz, $CDCl_3$) and ^{13}C NMR spectrum (75.48 MHz):

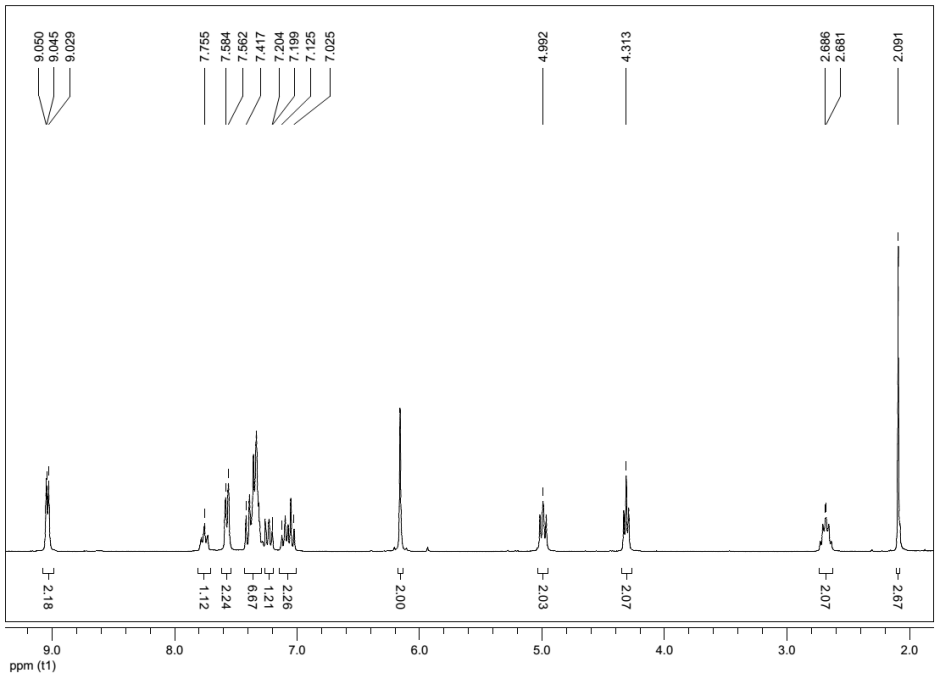

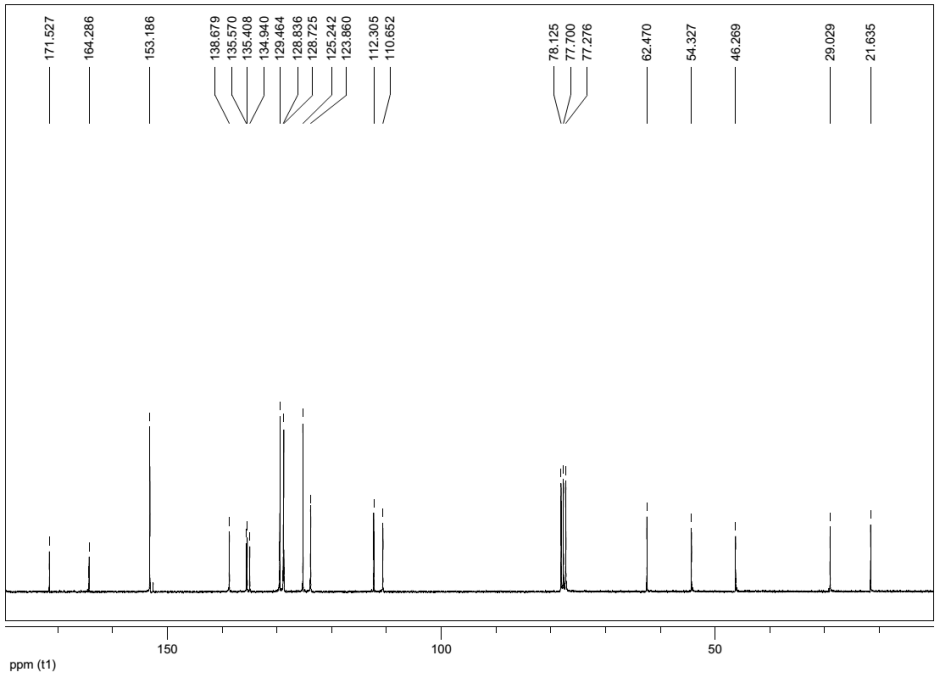

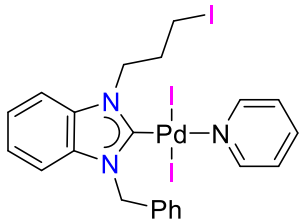

Compound **49**, ^{1}H NMR spectrum (500 MHz, $CDCl_3$) and ^{13}C NMR spectrum (125.77 MHz):

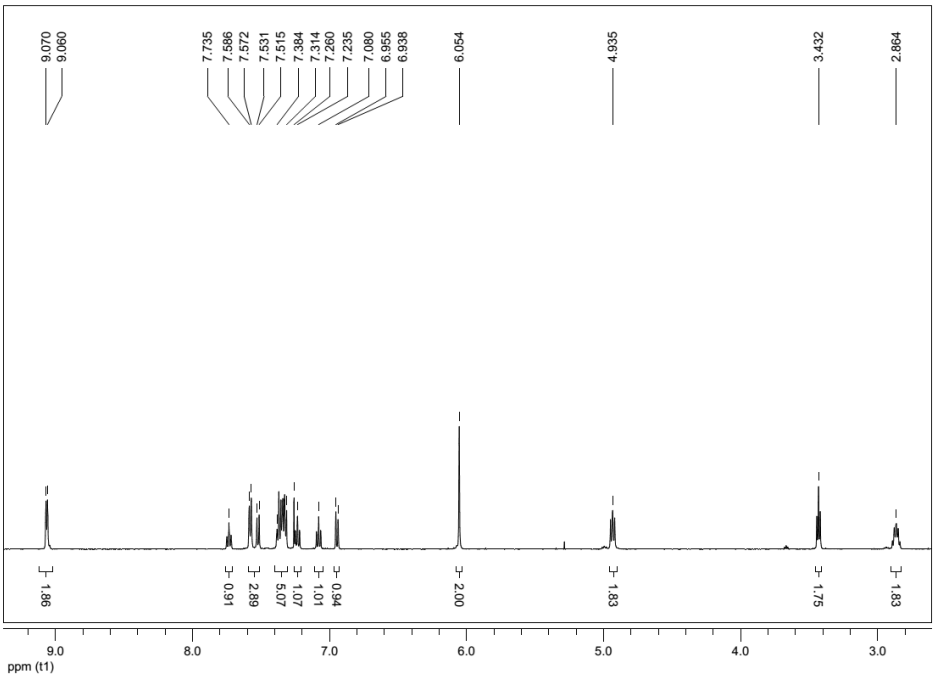

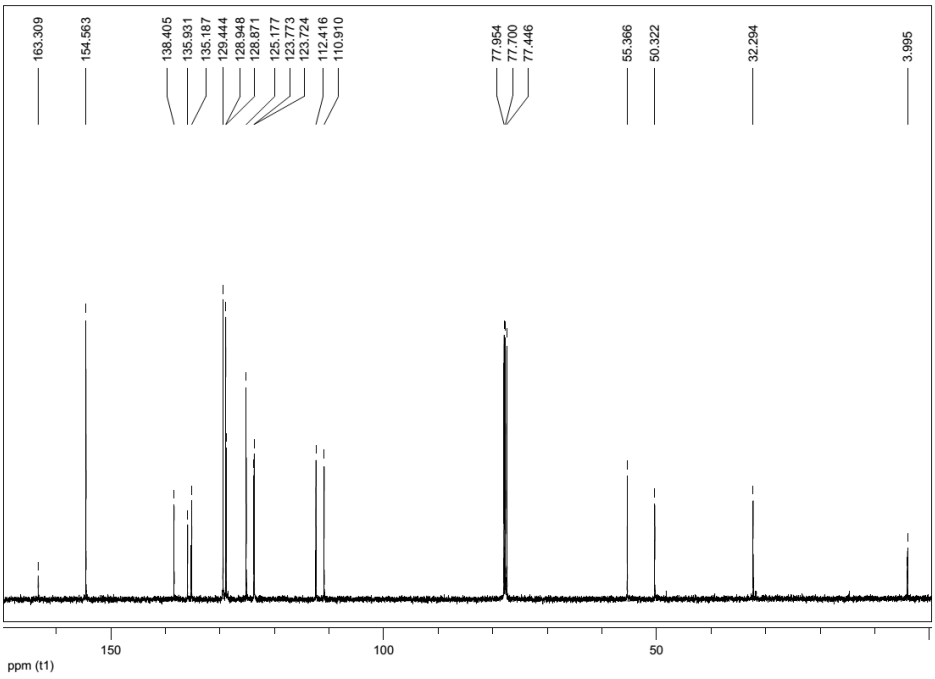

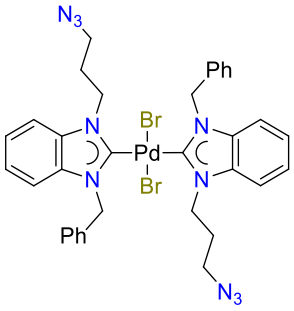

Compound **59**, ^{1}H NMR spectrum (500 MHz, $CDCl_3$) and ^{13}C NMR spectrum (125.77 MHz):

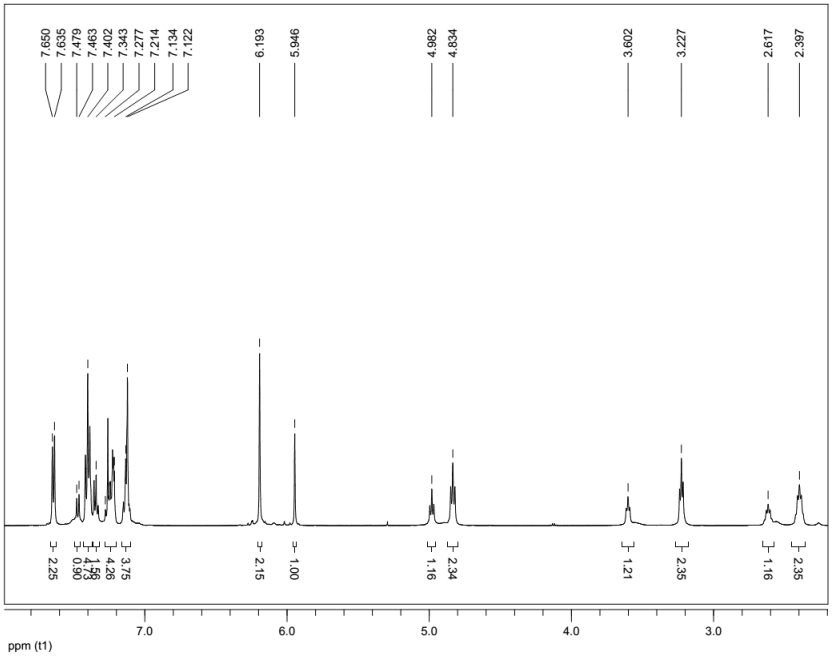

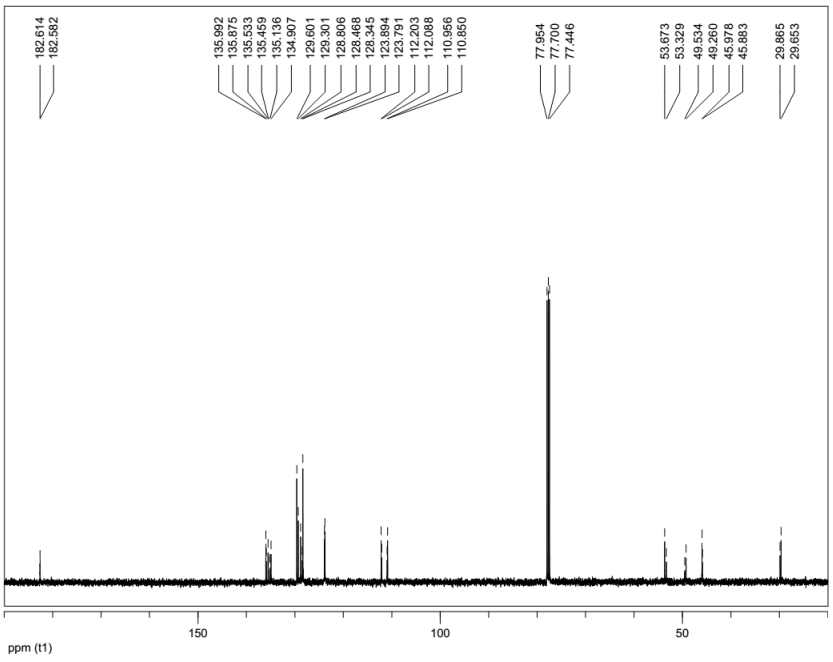

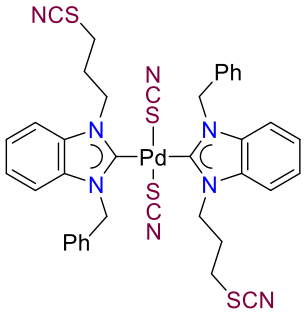

Compound **62**, ^{1}H NMR spectrum (500 MHz, $CDCl_3$) and ^{13}C NMR spectrum (125.77 MHz):

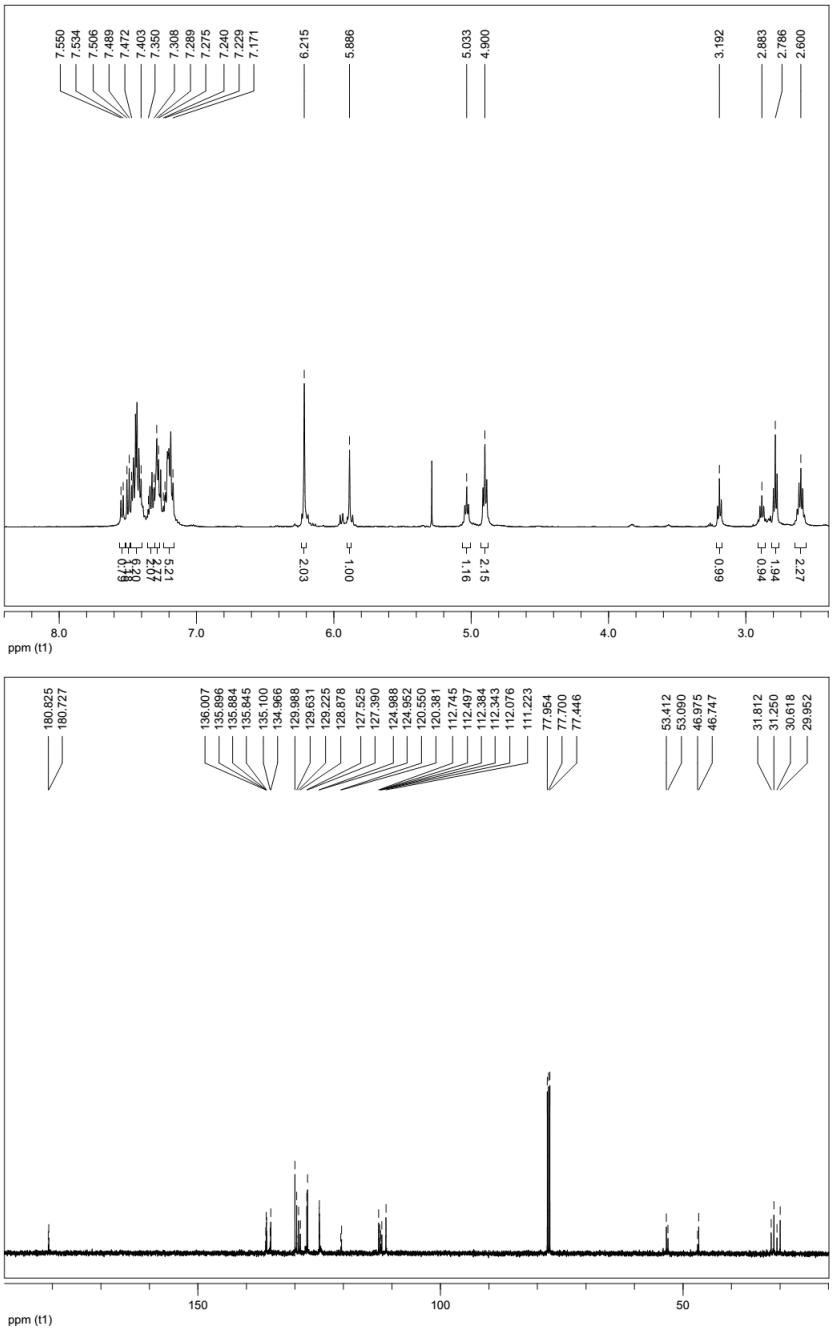

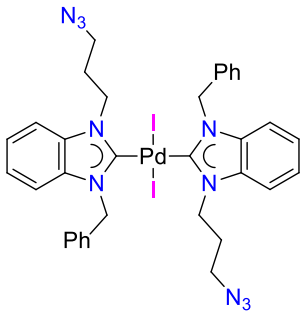

Compound **64**, ^{1}H NMR spectrum (500 MHz, $CDCl_3$) and ^{13}C NMR spectrum (125.77 MHz):

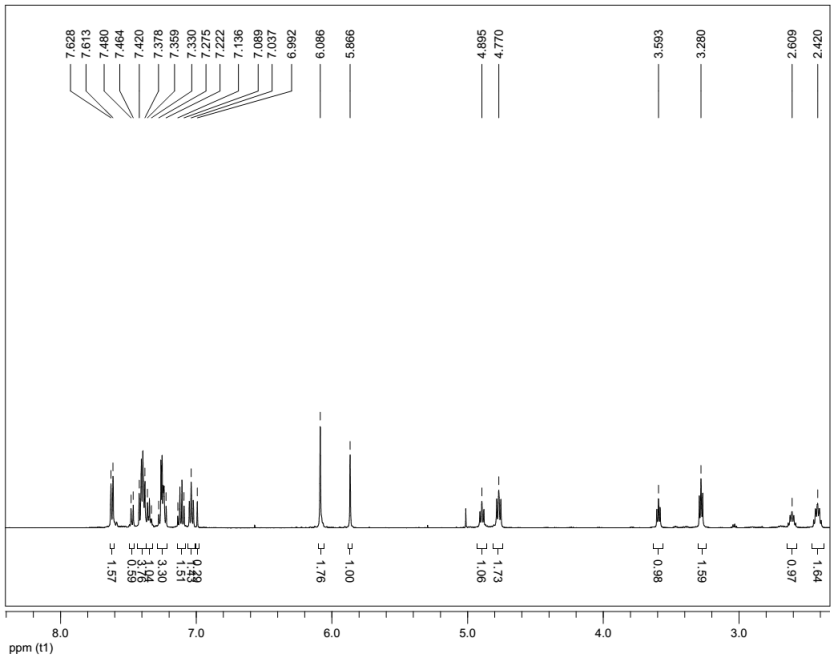

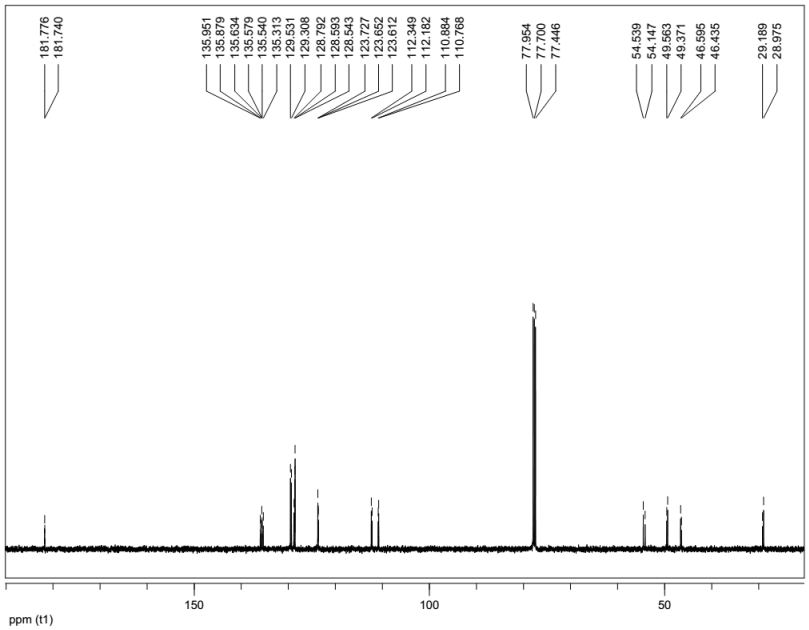

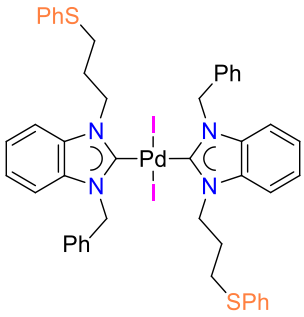

Compound **65**,[1]H NMR spectrum (500 MHz, $CDCl_3$) and [13]C NMR spectrum (125.77 MHz):

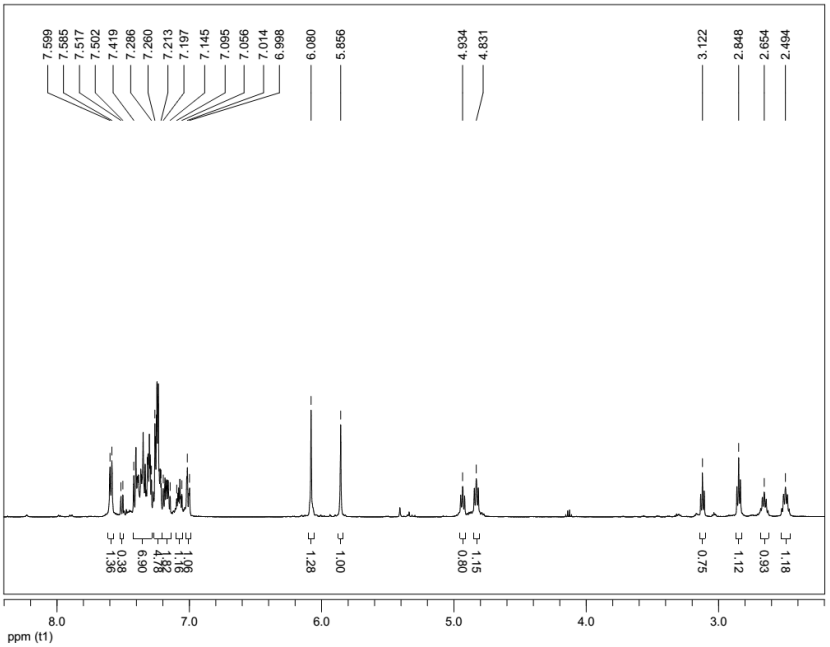

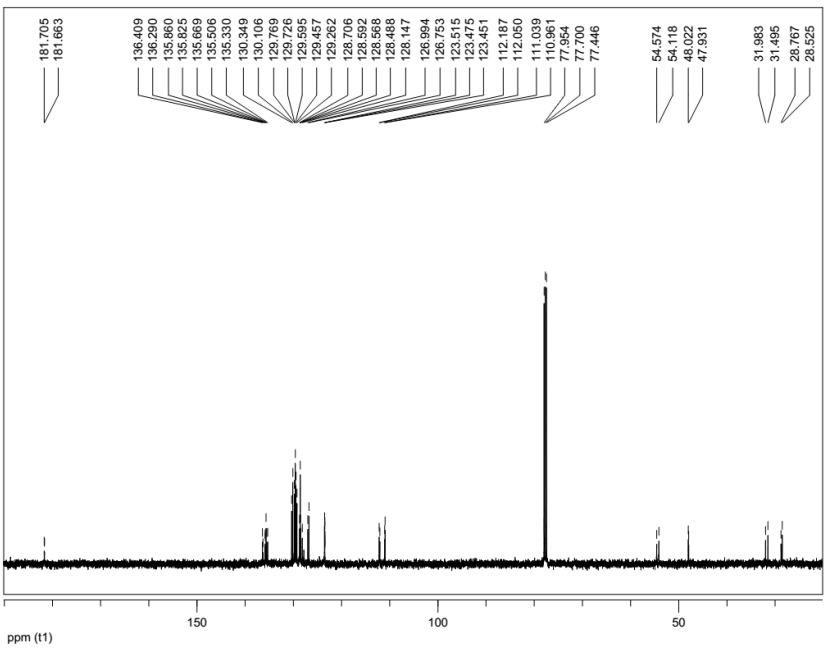

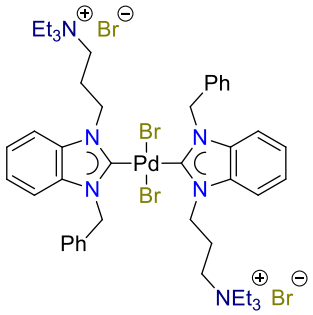

Compound **68**, ^{1}H NMR spectrum (500 MHz, d_6-DMSO) and ^{13}C NMR spectrum (125.77 MHz):

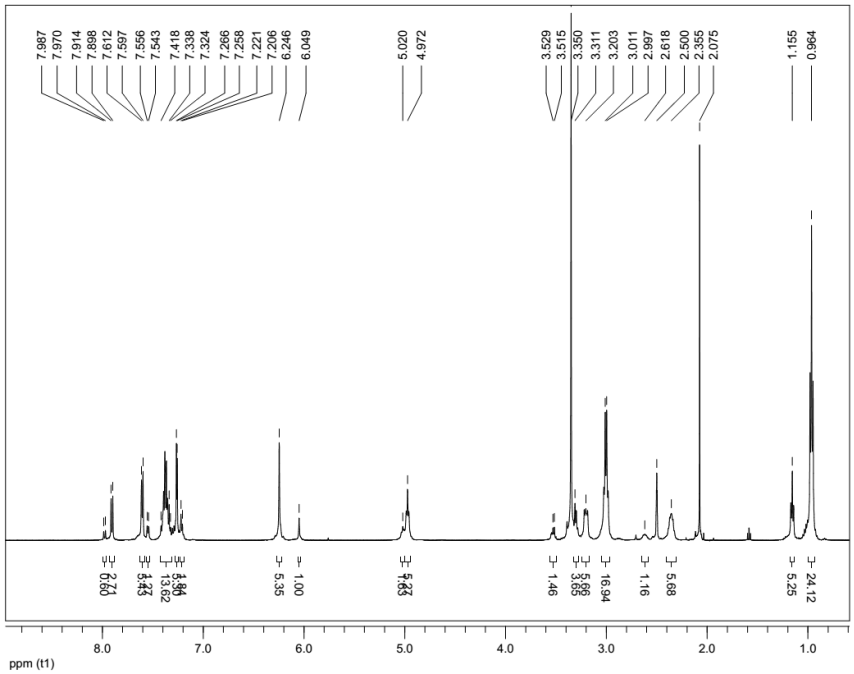

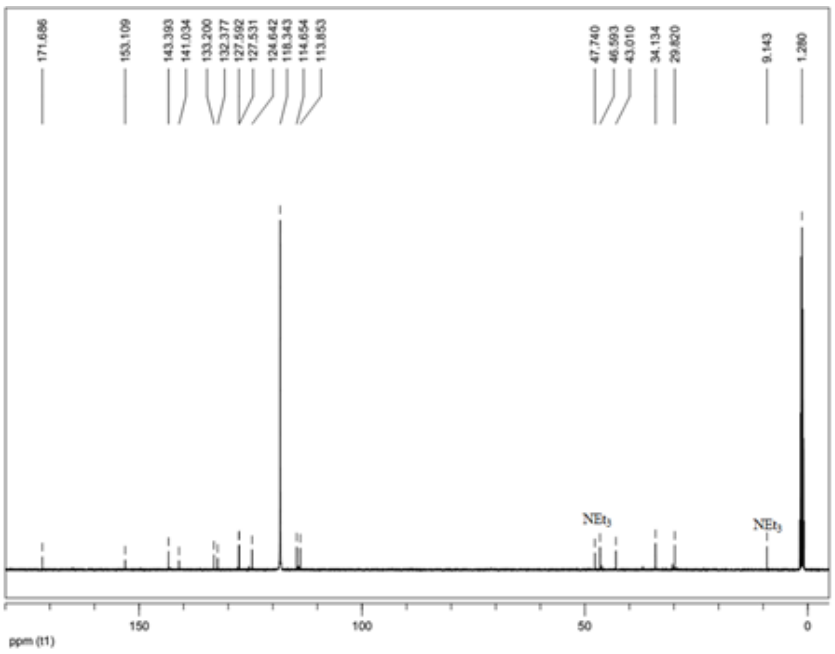

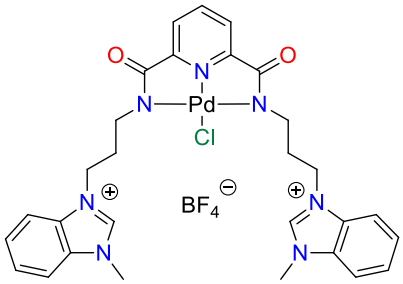

Compound **78$_{Me}$**, ^{1}H NMR spectrum (500 MHz, CD_3CN) and ^{13}C NMR spectrum (125.77 MHz):

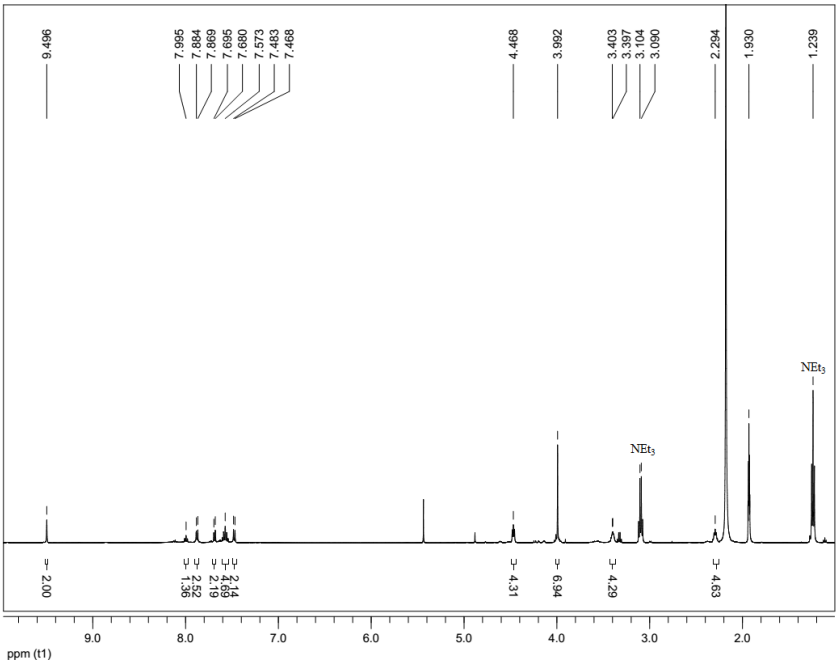

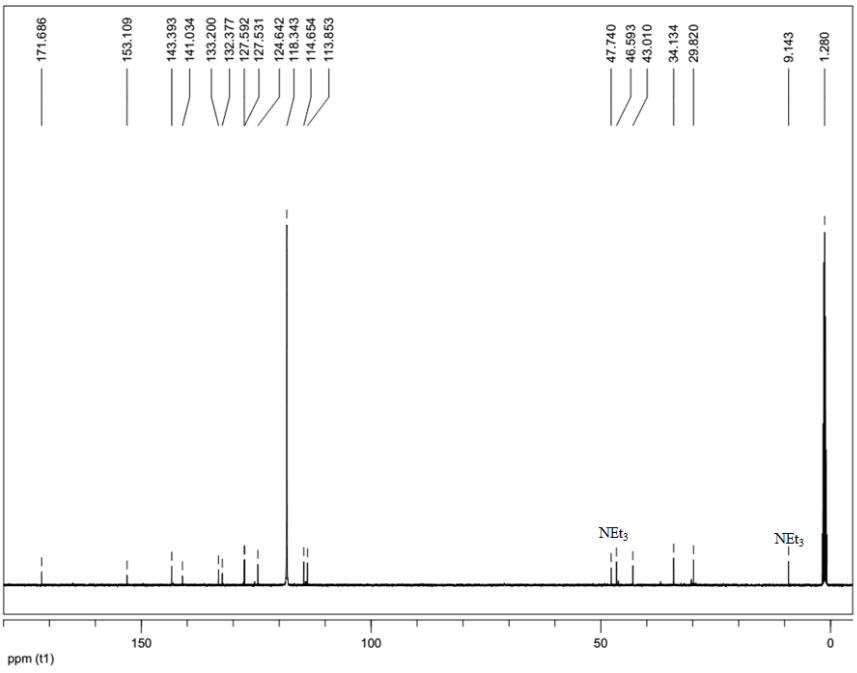

References

(1) IUPAC. Compendium of Chemical Terminology, 2nd ed. (the "Gold Book"). Compiled by A. D. McNaught, A. D. and Wilkinson, A. Blackwell Scientific Publications, Oxford (1997). XML on-line corrected version: http://goldbook.iupac.org (2006-) created by Nic, M., Jirat, J., Kosata, B.; updates compiled by Jenkins, A. ISBN 0-9678550-9-8. DOI: 10.1351/goldbook.

(2) Bourissou, D.; Guerret, O.; Gabba ï, F. P.; Bertrand, G. *Chem. Rev.* **2000**, *100*, 39.

(3) (a) Harrison, J. F. *J. Am. Chem. Soc.* **1971**, *93*, 4112; (b) Harrison, J. F.; Liedtke, R. C.; Liebman, J. F. *J. Am. Chem. Soc.* **1979**, *101*, 7162.

(4) (a) Hoffmann, R.; Zeiss, G. D.; Van Dine, G. W. *J. Am. Chem. Soc.* **1968**, *90*, 1485; (b) Baird, N. C.; Taylor, K. F. *J. Am. Chem. Soc.* **1978**, *100*, 1333.

(5) *Carbene Chemistry*, (Ed.: Bertrand, G.), Marcel Dekker, New York, **2002**.

(6) The first carbene that was stable under normal conditions and in bulk was prepared by Bertrand et al, see Igau, A.; Grutzmacher, H.; Baceiredo, A.; Bertrand, G. *J. Am. Chem. Soc.* **1988**, *110*, 6463.

(7) Hahn, F. E.; Jahnke, M. C. *Angew. Chem., Int. Ed.* **2008**, *47*, 3122.

(8) Wanzlick, H. W. *Angew. Chem., Int. Ed.* **1962**, *1*, 75.

(9) Arduengo III, A. J.; Harlow, R. L.; Kline, M. *J. Am. Chem. Soc.* **1991**, *113*, 361.

(10) (a) Arduengo III, A. J.; Dias, H. V. R.; Harlow, R. L.; Kline, M. *J. Am. Chem. Soc.* **1992**, *114*, 5530; (b) Arduengo III, A. J.; Goerlich, J. R.; Marshall, W. J. *J. Am. Chem. Soc.* **1995**, *117*, 11027; (c) Enders, D.; Breuer, K.; Raabe, G.; Runsink, J.; Teles, J. H.; Melder, J.-P.; Ebel, K.; Brode, S. *Angew. Chem., Int. Ed.* **1995**, *34*, 1021; (d) Herrmann, W. A.; Köcher, C.; Gooßen, L. J.; Artus, G. R. J. *Chem. Eur. J.* **1996**, *2*, 1627; (e) Herrmann, W. A.; Elison, M.; Fischer, J.; Köcher, C.; Artus, G. R. J. *Chem. Eur. J.* **1996**, *2*, 772; (f) Denk, M. K.; Thadani, A.; Hatano, K.; Lough, A. J. *Angew. Chem., Int. Ed.* **1997**, *36*, 2607; (g) Arduengo III, A. J.; Goerlich, J. R.; Krafczyk, R.; Marshall, W. J. *Angew. Chem., Int. Ed.* **1998**, *37*, 1963; (h) Hahn, F. E.; Wittenbecher, L.; Boese, R.; Bläser, D. *Chem. Eur. J.* **1999**, *5*, 1931; (i) Despagnet-Ayoub, E.;

Grubbs, R. H. *J. Am. Chem. Soc.* **2004**, *126*, 10198; (j) Krahulic, K. E.; Enright, G. D.; Parvez, M.; Roesler, R. *J. Am. Chem. Soc.* **2005**, *127*, 4142; (k) Dastgir, S.; Coleman, K. S.; Cowley, A. R.; Green, M. L. H. *Organometallics* **2006**, *25*, 300; (l) Berthon-Gelloz, G.; Siegler, M. A.; Spek, A. L.; Tinant, B.; Reek, J. N. H.; Markó, I. E. *Dalton Trans.* **2010**, *39*, 1444; (m) Lu, W. Y.; Cavell, K. J.; Wixey, J. S.; Kariuki, B. *Organometallics* **2011**, *30*, 5649; (n) Zhang, J.; Qin, X.; Fu, J.; Wang, X.; Su, X.; Hu, F.; Jiao, J.; Shi, M. *Organometallics* **2012**, *31*, 8275; (o) López-Gómez, M. J.; Martin, D.; Bertrand, G. *Chem. Commun.* **2013**, *49*, 4483.

(11) Wanzlick, H. W.; Schönherr, H.-J. *Angew. Chem., Int. Ed. Engl.* **1968**, *7*, 141.

(12) Öfele, K. *J. Organomet. Chem.* **1968**, *12*, P42.

(13) (a) Dorta, R.; Stevens, E. D.; Scott, N. M.; Costabile, C.; Cavallo, L.; Hoff, C. D.; Nolan, S. P. *J. Am. Chem. Soc.* **2005**, *127*, 2485; (b) Mas-Marzá, E.; Reis, P. M.; Peris, E.; Royo, B. *J. Organomet. Chem.* **2006**, *691*, 2708; (c) Nikiforov, G. B.; Roesky, H. W.; Jones, P. G.; Magull, J.; Ringe, A.; Oswald, R. B. *Inorg. Chem.* **2008**, *47*, 2171; (d) Ruddy, A. J.; Rupar, P. A.; Bladek, K. J.; Allan, C. J.; Avery, J. C.; Baines, K. M. *Organometallics* **2010**, *29*, 1362; (e) Xiang, L.; Xiao, J.; Deng, L. *Organometallics* **2011**, *30*, 2018; (f) Würtemberger, M.; Ott, T.; Döring, C.; Schaub, T.; Radius, U. *Eur. J. Inorg. Chem.* **2011**, 405.

(14) (a) Herrmann, W. A.; Böhm, V. P. W.; Gstöttmayr, C. W. K.; Grosche, M.; Reisinger, C.-P. Weskamp, T. *J. Organomet. Chem.* **2001**, *617-618*, 616; (b) Huynh, H. V.; Holtgrewe, C.; Pape, T.; Koh, L. L.; Hahn, F. E. *Organometallics* **2006**, *25*, 245; (c) Günay, M. E.; Gümüşada, R.; Özdemir, N.; Dinçer, M.; Çetinkaya, B. *J. Organomet. Chem.* **2009**, *694*, 2343; (d) Gaillard, S.; Nun, P.; Slawin, A. M. Z.; Nolan, S. P. *Organometallics* **2010**, *29*, 5402; (e) Duan, G.; Yam, V. W.-W. *Chem. Eur. J.* **2010**, *16*, 12642; (f) Lazreg, F.; Slawin, A. M. Z.; Cazin, C. S. J. *Organometallics* **2012**, *31*, 7969; (g) Guo, S.; Lim, M. H.; Huynh, H. V. *Organometallics* **2013**, *32*, 7225.

(15) Wang, H. M. J.; Lin, I. J. B. *Organometallics* **1998**, *17*, 972.

(16) (a) Garrison, J. C.; Yongs, W. J. *Chem. Rev.* **2005**, *105*, 3978; (b) Lin, I. J. B.; Vasam, C. S. *Coord. Chem. Rev.* **2007**, *251*, 642.

(17) Herrmann, W. A.; Elison, M.; Fischer, J.; Köcher, C.; Artus, G. R. J. *Angew. Chem., Int. Ed. Engl.* **1995**, *34*, 2371.

(18) Herrmann, W. A. *Angew. Chem., Int. Ed.* **2002**, *41*, 1290.

(19) (a) Ittel, S. D.; Johnson, L. K. *Chem. Rev.* **2000**, *100*, 1169; (b) Elsevier, C. J.; Reedijk, J.; Walton, P. H.; Ward, M. D. *Dalton Trans.* **2003**, 1869; (c) Speiser, F.; Braunstein, P.; Saussine, L. *Acc. Chem. Res.* **2005**, *38*, 784; (d) Hartwig, J. F. *Inorg. Chem.* **2007**, *46*, 1936; (e) Kumar, A.; Ghosh, P. *Eur. J. Inorg. Chem.* **2012**, 3955.

(20) (a) Tolman, C. A. *J. Am. Chem. Soc.* **1970**, *92*, 2953; (b) Bell, A. G.; Koźmiński, W.; Linden, A.; Philipsborn, W. V. *Organometallics* **1996**, *15*, 3124; (c) Chianese, A. R.; Li, X; Janzen, M. C.; Faller, J. W.; Crabtree, R. H. *Organometallics* **2003**, *22*, 1663; (d) Chianese, A. R.; Kovacevic, A.; Zeglis, B. M.; Faller, J. W.; Crabtree, R. H. *Organometallics* **2004**, *23*, 2461; (e) Kelly III, R. A.; Clavier, H.; Giudice, S.; Scott, N. M.; Stevens, E. D.; Bordner, J.; Samardjiev, I.; Hoff, C. D.; Cavallo, L.; Nolan, S. P. *Organometallics* **2008**, *27*, 202; (f) Wolf, S.; Plenio, H. *J. Organomet. Chem.* **2009**, *694*, 1487; (g) Rosen, E. L.; Varnado, C. D.; Tennyson, A. G.; Khramov, D. M.; Kamplain, J. W.; Sung, D. H.; Cresswell, P. T.; Lynch, V. M.; Bielawski, C. W. *Organometallics* **2009**, *28*, 6695; (h) Mathew, J.; Suresh, C. H. *Inorg. Chem.* **2010**, *49*, 4665. (i) Hudnall, T. W.; Tennyson, A. G.; Bielawski, C. W. *Organometallics* **2010**, *29*, 4569; (j) Dröge, T.; Glorius, F. *Angew. Chem. Int. Ed.* **2010**, *49*, 6940; (k) Jothibasu, R.; Huynh, H. V. *Chem. Commun.* **2010**, *46*, 2986; (l) Diebolt, O.; Fortman, G. C.; Clavier, H.; Slawin, A. M. Z.; Escudero-Adán, E. C.; Benet-Buchholz, J.; Nolan, S. P. *Organometallics* **2011**, *30*, 1668; (m) Braun, M.; Frank, W.; Ganter, C. *Organometallics* **2012**, *31*, 1927; (n) Makhloufi, A.; Frank, W.; Ganter, C. *Organometallics* **2012**, *31*, 2001; (o) Borguet, Y.; Zaragoza, G.; Demonceau, A.; Delaude, L. *Dalton Trans.* **2013**, *42*, 7287; (p) Varnado, C. D.; Rosen, E. L.; Coliins, M. S.; Lynch, V. M.; Bielawski, C. W. *Dalton Trans.* **2013**, *42*, 13251; (q) Nelson, D. J.; Collado, A.; Manzini, S.; Meiries, S.; Slawin, A. M. Z.; Cordes, D. B.; Nolan, S. P. *Organometallics* **2014**, *33*, 2048; (r) Sato, T.; Yoshioka, D.; Hirose, Y.; Oi, S. *J. Organomet. Chem.* **2014**, *753*, 20.

(21) Lever, A. B. P. *Inorg. Chem.* **1990**, *29*, 1271.

(22) Öfele, K.; Herrmann, W. A.; Mihalios, D.; Elison, M.; Herdtweck, E.; Scherer, W.; Mink, J. *J*. *Organomet*. *Chem*. **1993**, *459*, 177.

(23) Mercs, L.; Labat, G.; Neels, A.; Ehlers, A.; Albrecht, M. *Organometallics* **2006**, *25*, 5648.

(24) (a) Huynh, H. V.; Han, Y.; Jothibasu, R.; Yang, J. A. *Organometallics* **2009**, *28*, 5395; (b) Yuan, D.; Huynh, H. V. *Organometallics* **2012**, *31*, 405; (c) Bernhammer, J. C.; Huynh, H. V. *Dalton Trans*. **2012**, *41*, 8600; (d) Bernhammer, J. C.; Huynh, H. V. *Organometallics* **2012**, *31*, 5121; (e) Guo, S.; Sivaram, H.; Yuan, D.; Huynh, H. V. *Organometallics* **2013**, *32*, 3685.

(25) Cardin, D. J.; Cetinkaya, B.; Cetinkaya, E.; Lappert, M. F.; Randall, E. W.; Rosenberg, E.; *J. Chem. Soc*., *Dalton Trans*. **1973**, 1982.

(26) Xue, L.; Shi, L.; Han, Y.; Xia, C.; Huynh, H. V.; Li, F. *Dalton Trans.* **2011**, *40*, 7632.

(27) Anton, D. R.; Crabtree, R. H. *Organometallics* **1983**, *2*, 621.

(28) Poyatos, M.; McNamara, W.; Incarvito, C.; Clot, E.; Peris, E.; Crabtree, R. H. *Organometallics* **2008**, *27*, 2128.

(29) Perrin, L.; Clot, E.; Eisenstein, O.; Loch, J.; Crabtree, R. H. *Inorg*. *Chem*. **2001**, *40*, 5806.

(30) (a) Darensbourg, D. J.; Klausmeyer, K. K.; Mueller, B. L.; Reibenspies, J. H. *Angew*. *Chem*., *Int*. *Ed*. *Engl*. **1992**, *31*, 1503; (b) Darensbourg, D. J.; Klausmeyer, K. K.; Reibenspies, J. H. *Inorg*. *Chem*. **1996**, *35*, 1529; (c) Darensbourg, D. J.; Klausmeyer, K. K.; Reibenspies, J. H. *Inorg*. *Chem*. **1996**, *35*, 1535; (d) Darensbourg, D. J.; Draper, J. D.; Frost, B. J.; Reibenspies. J. H. *Inorg*. *Chem*. **1999**, *38*, 4705; (e) Rampersad, M. V.; Jeffery, S. P.; Golden, M. L.; Lee, J.; Reibenspies, J. H.; Darensbourg, D. J.; Darensbourg, M .Y. *J*. *Am*. *Chem*. *Soc*. **2005**, *127*, 17323; (f) Hess, J. L.; Conder, H. L.; Green, K. N.; Darensbourg, M. Y. *Inorg*. *Chem*. **2008**, *47*, 2056.

(31) Liaw, W.-F.; Hsieh, C.-K.; Lin, G.-Y.; Lee, G.-H. *Inorg*. *Chem*. **2001**, *40*, 3468.

(32) Hartl, F.; Rosa, P.; Ricard, L.; Floch, P. L.; Záliš, S. *Coord*. *Chem*. *Rev*. **2007**, *251*, 557.

(33) Jeletic, M. S.; Lower, C. E.; Ghiviriga, I.; Veige, A. S. *Organometallics* **2011**, *30*, 6034.

(34) Ogata, K.; Yamaguchi, Y.; Kurihara, Y.; Ueda, K.; Nagao, H.; Ito, T. *Inorg. Chim. Acta* **2012**, *390*, 199.

(35) (a) Hiltner, O.; Boch, F. J.; Brewitz, L.; Härter, P.; Drees, M.; Herdtweck, E.; Herrmann, W. A.; Kühn, F. E. *Eur. J. Inorg. Chem.* **2010**, 5284; (b) Canella, D.; Hock, S. J.; Hiltner, O. Herdtweck, E.; Herrmann, W. A.; Kühn, F. E. *Dalton Trans.* **2012**, *41*, 2110.

(36) (a) Smithback, J. L.; Helm, J. B.; Schutte, E.; Woessner, S. M.; Sullivan, B. P. *Inorg. Chem.* **2006**, *45*, 2163; (b) Kirillov, A. M.; Haukka, M.; Silva, M. F. C. G.; Pombeiro, A. J. L. *Eur. J. Inorg. Chem.* **2007**, 1556; (c) Marchetti, F.; Pettinari, C.; Cerquetella, A.; Cingolani, A.; Pettinari, R.; Monari, M.; Wanke, R.; Kuznetsov, M. L.; Pombeiro, A. J. L. *Inorg. Chem.* **2009**, *48*, 6096; (d) Erasmus, J. J. C.; Conradie, J. *Electrochim. Acta* **2011**, *56*, 9287; (e) Conradie, J. *Electrochim. Acta* **2013**, *110*, 718; (f) Al-Rawashdeh, N. A. F.; Chatterjee, S.; Krause, J. A.; Connick, W. B. *Inorg. Chem.* **2014**, *53*, 294.

(37) (a) Seo, H.; Kim, B. Y.; Lee, J. H.; Park, H.-J.; Son, S. U.; Chung,Y. K. *Organometallics* **2003**, *22*, 4783; (b) Huynh, H. V.; Wong, L. R.; Ng, P. S. *Organometallics* **2008**, *27*, 2231; (c) Yuan, D.; Tang, H. Y.; Xiao, L. F.; Huynh, H. V. *Dalton Trans.* **2011**, *40*, 8788; (d) Huynh, H. V.; Jothibasu, R. *J. Organomet. Chem.* **2011**, *696*, 3369; (e) Busetto, L,; Cassani, M. C.; Femoni, C.; Mancinelli, M.; Mazzanti, A.; Mazzoni, R.; Solinas, G. *Organometallics* **2011**, *30*, 5258.

(38) (a) Kühl, O. *Chem. Soc. Rev.* **2007**, *36*, 592; (b) John, A.; Ghosh, P. *Dalton Trans.* **2010**, *39*, 7183.

(39) Selected examples: (a) Fliedel, C.; Braunstein, P. *J. Organomet. Chem.* **2014**, *751*, 286; (b) Normand, A. T.; Cavell, K. J. *Eur. J. Inorg. Chem.* **2008**, 2781; (c) Bierenstiel, M.; Cross, E. D. *Coord. Chem. Rev.* **2011**, *255*, 574; (d) Huynh, H. V.; Yeo, C. H.; Tan, G. K. *Chem. Commun.* **2006**, 3833; (e) Huynh, H. V.; Yeo. C. H.; Chew, Y. X. *Organometallics* **2010**, *29*, 1479; (f) Jiménez, M. V.; Fernández-Tornos, J.; Pérez-Torrente, J. J.; Modrego, F. J.; Winterle, S.; Cunchillos, C.; Lahoz, F. J.; Oro, L. A. *Organometallics* **2011**, *30*, 5493.

(40) (a) Lemke, J.; Metzler-Nolte, N. *Eur. J. Inorg. Chem.* **2008**, 3359; (b) Chardon, E.; Puleo, G. L.; Dahm, G.; Guichard. G.; Bellemin-Laponnaz, S. *Chem. Commun.* **2011**, *47*, 5864; (c) Roland, S.; Jolivalt, C.; Cresteil, T.; Eloy, L.; Bouhours, P.; Hequet, A.; Mansuy, V.; Vanucci, C.; Paris, J. M. *Chem. Eur. J.* **2011**, *17*, 1442.

(41) (a) Hsu, T. H. T.; Naidu, J. J.; Yang, B. J.; Jang, M. Y.; Lin, I. J. B. *Inorg. Chem.* **2012**, *51*, 98; (b) Azua, A.; Sanz, S.; Peris, E. *Chem. Eur. J.* **2011**, *17*, 3963; (c) Li, G.; Yang, H. Q.; Li, W.; Zhang, G. L. *Green Chem.* **2011**, *13*, 2939; (d) Velazquez, H. D.; Verpoort, F. *Chem. Soc. Rev.* **2012**, *41*, 7032; (e) Schaper, L.-A.; Hock, S. J.; Herrmann, W. A.; Kühn, F. E. *Angew. Chem., Int. Ed.* **2013**, *52*, 270.

(42) (a) Cure, J.; Poteau, R.; Gerber, I. C.; Gornitzka, H.; Hemmert, C. *Organometallics* **2012**, *31*, 619; (b) Peñafiel, I.; Pastor, I. M.; Yus, M.; Esteruelas, M. A.; Oliván, M.; Oñate, E. *Eur. J. Org. Chem.* **2011**, 7174; (c) Yuan, D.; Huynh, H. V. *Dalton Trans.* **2011**, *40*, 11698.

(43) Yuan, D.; Huynh, H. V. *Organometallics* **2010**, *29*, 6020.

(44) Herrmann, W. A.; Gooβen, L. J.; Spiegler, M. *J. Organomet. Chem.* **1997**, *547*, 357.

(45) (a) Au, V. K. -M.; Wong, K. M. -C.; Zhu, N.; Yam, V. W. -W. *J. Am. Chem. Soc.* **2009**, *131*, 9076; (b) Ballarim, B.; Busetto, L.; Cassani, M. C.; Femoni, C.; Ferrari, A. M.; Miletto, I.; Caputo, G. *Dalton Trans.* **2012**, *41*, 2445; (c) Zou, T.; Lum, C. T.; Chui, S. S. -Y.; Che, C. -M. *Angew. Chem. Int. Ed.* **2013**, *52*, 2930; (d) Zhang, Y.; Blacque, O.; Venkatesan, K.; *Chem. Eur. J.* **2013**, *19*, 15689; (e) Liu, Y.; Harlang, T.; Canton, S. E.; Chábera, P.; Suárez-Alcántara, K.; Fleckhaus, A.; Vithanage, D. A.; Göransson, E.; Corani, A.; Lomoth, R.; Sundström, V.; Wärnmark, K. *Chem. Commun.* **2013**, *49*, 6412; (f) Zhang, Y.; Clavadetscher, J.; Bachmann, M.; Blacque, O.; Venkatesan, K. *Inorg. Chem.* **2014**, *53*, 756; (g) Ng, C. -O.; Yiu, S. -M.; Ko, C. -C. *Inorg. Chem.* **2014**, *53*, 3022; (h) Visbal, R.; Gimeno, M. C. *Chem. Soc. Rev.* **2014**, *43*, 3551.

(46) (a) Teyssot, M. -L.; Jarrousse, A. -S.; Manin, M.; Chevry, A.; Roche, S.; Norre, F.; Beaudoin, C.; Morel, L.; Boyer, D.; Mahiou, R.; Gautier, A. *Dalton Trans.* **2009**, 6894; (b) Budagumpi, S.; Haque, R. A.; Endud, S.; Rehman, G. U.; Salman, A. W. *Eur. J. Inorg. Chem.* **2013**, 4367; (c) Liu, W.; Gust, R. *Chem. Soc. Rev.* **2013**, *42*, 755; (d) Bertrand, B.; Casini, A. *Dalton Trans.* **2014**, *43*, 4209.

(47) (a) Poyatos, M.; Mata, J. A.; Peris, E. *Chem. Rev.* **2009**, *109*, 3677; (b) Mercs, L.; Albrecht, M. *Chem. Soc. Rev.* **2010**, *39*, 1903 and papers cited therein.

(48) (a) Rit, A.; Pape, T.; Hahn, F. E. *J. Am. Chem. Soc.* **2010**, *132*, 4572; (b) Rit, A.; Pape, T.; Hepp, A.; Hahn, F. E. *Organometallics* **2011**, *30*, 334; (c) Rit, A.; Pape, T.; Hahn, F. E.

Organometallics **2011**, *30*, 6393; (d) Blase, V.; Pape, T.; Hahn, F. E. *J. Organomet. Chem.* **2011**, *696*, 3337; (e) Maity, R.; Rit, A.; Schulte to Brinke, C.; Daniliuc, C. G.; Hahn, F. E. *Chem. Commun.* **2013**, *49*, 1011; (f) Maity, R.; Schulte to Brinke, C.; Hahn, F. E. *Dalton Trans.* **2013**, *42*, 12857; (g) Maity, R.; Koppetz, H.; Hepp, A.; Hahn, F. E. *J. Am. Chem. Soc.* **2013**, *135*, 4966; (h) Schulte to Brinke, C.; Pape, T.; Hahn, F. E. *Dalton Trans.* **2013**, *42*, 7330.

(49) (a) Boydston, A. J.; Williams, K. A.; Bielawski, C. W. *J. Am. Chem. Soc.* **2005**, *127*, 12496; (b) Varnado, C. D.; Lynch, V. M.; Bielawski, C. W. *Dalton Trans.* **2009**, 7253; (c) Williams, K. A.; Bielawski, C. W. *Chem. Commun.* **2010**, *46*, 5166.

(50) (a) Gonell, S.; Poyatos, M.; Mata, J. A. Peris, E. *Organometallics* **2011**, *30*, 5985; (b) Gonell, S.; Poyatos, M.; Mata, J. A.; Peris, E. *Organometallics* **2012**, *31*, 5606; (c) Gonell, S.; Poyatos, M.; Peris, E. *Angew. Chem., Int. Ed.* **2013**, *52*, 7009; (d) Segarra, C.; Linke, J.; Mas-Marzá, E.; Kuck, D.; Peris, E. *Chem. Commun.* **2013**, *49*, 10572.

(51) (a) Han, Y.; Lee, L. J.; Huynh, H. V. *Chem. Eur. J.* **2010**, *16*, 771; (b) Huynh, H. V.; Sim, W.; Chin, C. F. *Dalton Trans.* **2011**, *40*, 11690; (c) Yuan, D.; Huynh, H. V. *Inorg. Chem.* **2013**, *52*, 6627.

(52) (a) Mercs, L.; Neels, A.; Stoeckli-Evans, H.; Albrecht, M. *Inorg. Chem.* **2011**, *50*, 8188; (b) Cabeza, J. A.; Damonte, M.; García-Álvarez, P.; Hernández-Cruz, M. G.; Kennedy, A. R. *Organometallics* **2012**, *31*, 327; (c) Mechler, M.; Latendorf, K.; Fery, W.; Peters, R. *Organometallics* **2013**, *32*, 112; (d) Ahamed, B. N.; Dutta, R.; Ghosh, P. *Inorg. Chem.* **2013**, *52*, 4269.

(53) Hahn, F. E.; Raadloff, C.; Pape, T.; Hepp, A. *Organometallics* **2008**, *27*, 6408.

(54) Conrady, F. M.; Fröhlich, R.; Schulte to Brinke, C.; Pape, T.; Hahn, F. E. *J. Am. Chem. Soc.* **2011**, *133*, 11496.

(55) Hahn, F. E.; Radloff, C.; Pape, T.; Hepp, A. *Chem. Eur. J.* **2008**, *14*, 10900.

(56) Lehn, J.-M.; Rigault, A.; Siegel, J.; Harrowfield, J.; Chevrier, B.; Moras, D. Proc. *Natl. Acad. Sci. U. S. A.* **1987**, *84*, 2656.

(57) (a) Chen, J. C. C.; Lin, I. J. B. J. *Chem. Soc., Dalton Trans.* **2000**, 839; (b) Scheele, U. J.; Dechert, S.; Meyer, F. *Inorg. Chim. Acta* **2006**, *359*, 4891.

(58) Huynh, H. V.; Han, Y.; Ho, J. H. H.; Tan, G. K. *Organometallics* **2006**, *25*, 3267.

(59) (a) Han, Y.; Huynh, H. V; Koh, L. L. *J. Organomet. Chem.* **2007**, *692*, 3606; (b) Han, Y.; Huynh, H. V.; Tan, G. K. *Organometallics* **2007**, *26*, 4612; (c) Han, Y.; Huynh, H. V.; Tan, G. K. *Organometallics* **2007**, *26*, 6447.

(60) (a) Hammett, L. P. *Chem. Rev.* **1935**, *17*, 125; (b) Hammett, L. P. *J. Am. Chem. Soc.* **1937**, *59*, 96.

(61) Hansch, C.; Leo, A.; Taft, R. W. *Chem. Rev.* **1991**, *91*, 165.

(62) (a) Sabot, C.; Kumar, K. A.; Antheaume, C.; Mioskowski, C. *J. Org. Chem.* **2007**, *72*, 5001; (b) Karami, K.; Moghadam, Z. K.; Hosseini-Kharat, M. *Catal. Commun.* **2014**, *43*, 25; (c) Nowrouzi, N.; Tarokh, D.; Motevalli, S. *J. Mol. Catal. A: Chem.* **2014**, *385*, 13; (d) Singh, M.; Singh, S. B.; Fatma, S.; Ankit, P.; Singh, J. *New J. Chem.* **2014**, *38*, 2756.

(63) (a) Oakley, S. H.; Coles, M. P.; Hitchcock, P. B. *Inorg. Chem.* **2004**, *43*, 7564; (b) Oakley, S. H.; Soria, D. B.; Coles, M. P.; Hitchcock, P. B. *Dalton Trans.* **2004**, 537.

(64) Ishikawa, T. *Superbases for Organic Synthesis*, John Wiley & Sons, Ltd, 2009.

(65) Vicente, J.; Arcas, A.; Bautista, D. *Organometallics* **1997**, *16*, 2127.

(66) (a) Vicente, J.; Arcas, A.; Bautista, D.; Arellano, M. C. R. *J. Organomet. Chem.* **2002**, *663*, 164; (b) Crespo, M.; Granell, J.; Solans, X.; Font-Bardia, M. *J. Organomet. Chem.* **2003**, *681*, 143; (c) Vicente, J.; Arcas, A.; Gálvez-López, M.-D. *Organometallics* **2006**, *25*, 4247; (d) Casas, J. M.; Fornés, J.; Fuertes, S.; Martín, A.; Sicilia, V. *Organometallics* **2007**, *26*, 1674; (e) Vicente, J.; Arcas, A.; Gálvez-López, M.-D.; Julián-Hernández, F. *Organometallics* **2008**, *27*, 1582.

(67) Verkade, J. G. *Coord. Chem. Rev.* **1972**, *9*, 1.

(68) Delbeke, F. T.; Kenlen, G. P. V. D.; Eeckhout, Z. *J. Organomet. Chem.* **1974**, *64*, 265.

(69) Kuznik, N.; Wendt, O. F. *J. Chem. Soc., Dalton Trans.* **2002**, 3074.

(70) Braunstein, P.; Naud, F. *Angew. Chem. Int. Ed.* **2001**, *40*, 680.

(71) (a) Hissler, M.; McGarrah, J. E.; Connick, W. B.; Geiger, D. K.; Cummings, S. D.; Eisenberg, R. *Coord. Chem. Rev.* **2000**, *208*, 115; (b) O'Reilly, R. K.; Shaver, M. P.; Gibson, V.

C.; White, A. J. P. *Macromolecules* **2007**, *40*, 7441; (c) Shaver, M. P.; Allan, L. E. N.; Gibson, V. C. *Organometallics* **2007**, *26*, 4725; (d) Rillema, D. P.; Cruz, A. J.; Moore, C.; Siam, K.; Jehan, A.; Base, D.; Nguyen, T.; Huang, W. *Inorg. Chem.* **2013**, *52*, 596; (e) Zhu, L.; Fu, Z. S.; Pan, H. J.; Feng, W.; Chen, C. L.; Fan, Z. Q. *Dalton Trans.* **2014**, *43*, 2900.

(72) Arduengo III, A. J.; Krafczyk, R.; Schmutzler, R. *Tetrahedron* **1999**, *55*, 14523.

(73) Scherg, T.; Schneider, S. K.; Frey, G. D.; Schwarz, J.; Herdtweck, E.; Herrmann, W. A. *Synlett* **2006**, *18*, 2894.

(74) Lee, H. M.; Lu, C. Y.; Chen, C. Y.; Chen, W. L.; Lin, H. C.; Chiu, P. L.; Cheng, P. Y. *Tetrahedron* **2004**, *60*, 5807.

(75) For an example for a Pd complex with 3 monodentate NHCs see: Clement, N. D.; Cavell, K. J.; Jones, C.; Elsevier, C. J. *Angew. Chem. Int. Ed.* **2004**, *43*, 1277. For an example for a Pd complex with a triNHC ligand see: Paulose, T. A. P.; Wu, S.-C.; Quail, J. W.; Foley, S. R. *Inorg. Chem. Commun.* **2012**, *15*, 37.

(76) (a) Gardiner, M. G.; Herrmann, W. A.; Reisinger, C.-P.; Schwarz, J.; Spiegler, M. *J. Organomet. Chem.* **1999**, *572*, 239; (b) Herrmann, W. A.; Schwarz, J. *Organometallics* **1999**, *18*, 4082; (c) Heckenroth, M.; Neels, A.; Stoeckli-Evans, H.; Albrecht, M. *Inorg. Chim. Acta* **2006**, *359*, 1929; (d) Schneider, S. K.; Schwarz, J.; Frey, G. D.; Herdtweck, E.; Herrmann, W. A. *J. Organomet. Chem.* **2007**, *692*, 4560; (e) Taige, M. A.; Zeller, A.; Ahrens, S.; Goutal, S.; Herdtweck, E.; Strassner, T. *J. Organomet. Chem.* **2007**, *692*, 1519; (f) Huynh, H. V.; Seow, H. X. *Aust. J. Chem.* **2009**, *62*, 983; (g) Munz, D.; Allolio, C.; Döring, K.; Poethig, A.; Doert, T.; Lang, H.; Straßner, T. *Inorg. Chim. Acta* **2012**, *392*, 204.

(77) (a) Ahrens, S.; Zeller, A.; Taige, M.; Strassner, T. *Organometallics* **2006**, *25*, 5409; (b) Huynh, H. V.; Jothibasu, R. *J. Organomet. Chem.* **2011**, *696*, 3369.

(78) Jokić, N. B.; Straubinger, C. S.; Goh, S. L. M.; Herdtweck, E.; Herrmann, W. A.; Kühn, F. E. *Inorg. Chim. Acta* **2010**, *363*, 4181.

(79) (a) Zhang, D.; Zhou, S.; Li, Z.; Wang, Q.; Weng, L. *Dalton Trans.* **2013**, *42*, 12020; (b) Özdemir, I.; Gürbüz, N.; Kaloğlu, N.; Doğan, Ö.; Kaloğlu, M.; Bruneau, C.; Doucet, H. *Beilstein J. Org. Chem.* **2013**, *9*, 303.

(80) Huynh, H. V.; Wu, J. *J. Organomet. Chem.* **2009**, *694*, 323.

(81) The reaction of thiocyanato-functionalized azolium salts led to organic products that did not contain any Pd–NHC complexes.

(82) Ochs, C.; Hahn, F. E.; Fröhlich, R. *Chem. Eur. J.* **2000**, *6*, 2193.

(83) Huynh, H. V.; Yuan, D.; Han, Y. *Dalton Trans.* **2009**, 7262.

(84) Trost, B. M.; Curran, D. P. *Tetrahedron Lett.* **1981**, *22*, 1287.

(85) Leadbeater, N. E.; Marco, M. *Angew. Chem. Int. Ed.* **2003**, *42*, 1407.

(86) Magill, A. M.; McGuinness, D. S.; Cavell, K. J.; Britovsek, G. J. P.; Gibson, V. C.; White, A. J. P.; Williams, D. J.; White, A. H.; Skelton, B. W. *J. Organomet. Chem.* **2001**, *617-618*, 546.

(87) Amadio, E.; Scrivanti, A.; Bortoluzzi, M.; Bertoldini, M.; Beghetto, V.; Matteoli, U.; Chessa, G. *Inorg. Chim. Acta* **2013**, *405*, 188 and references cited therein.

(88) Peh, G. R.; Kantchev, E. A. B.; Zhang, C.; Ying, J. Y. *Org. Biomol. Chem.* **2009**, *7*, 2110.

(89) Bull, S. D.; Davies, S. G.; Smith, A. D. *J. Chem. Soc., Perkin Trans.* **2001**, *1*, 2931.

(90) (a) McGuinness, D. S.; Cavell, K. J. *Organometallics* **1999**, *18*, 1596; (b) Arnold, P. L.; Cloke, F. G. N.; Geldbach, T.; Hitchcock, P. B. *Organometallics* **1999**, *18*, 3228; (c) Böhm, V. P. W.; Gstöttmayr, C. W. K.; Weskamp, T.; Herrmann, W. A. *J. Organomet. Chem.* **2000**, *595*, 186; (d) Lee, E.; Yandulov, D. V. *J. Organomet. Chem.* **2011**, *696*, 4095.

(91) Huynh, H. V.; Ho, J .H. H.; Neo, T. C.; Koh, L. L. *J. Organomet. Chem.* **2005**, *690*, 3854.

(92) (a) Hirtenlehner, C.; Krims, C.; Hölbling, J.; List, M.; Zabel, M.; Fleck, M.; Berger, R. J. F.; Schoefberger, W.; Monkowius, U. *Dalton Trans.* **2011**, *40*, 9899; (b) Adhikary, S. D.; Jhulki, L.; Seth, S.; Kundu, A.; Bertolasi, V.; Mitra, P.; Mahapatra, A.; Dinda, J. *Inorg. Chim. Acta* **2012**, *384*, 239; (c) Sivaram, H.; Jothibasu, R.; Huynh, H. V. *Organometallics* **2012**, *31*, 1195; (d) Xu, X.; Kim, S. H.; Zhang, X.; Das. A. K.; Hirao, H.; Hong, S. H. *Organometallics* **2013**, *32*, 164; (e) Ghdhayeb, M. Z.; Haque, R. A.; Budagumpi, S. *J. Organomet. Chem.* **2014**, *757*, 42.

(93) (a) Marlin, D. S.; Olmstead, M. M.; Mascharak, P. K. *Inorg. Chem.* **1999**, *38*, 3258; (b) Marlin, D. S.; Olmstead, M. M.; Mascharak, P. K. *Inorg. Chem.* **2001**, *40*, 7003; (c) Singh, A. K.;

Balamurugan, V.; Mukherjee, R. *Inorg*. *Chem*. **2003**, *42*, 6497; (d) Dwyer, A. N.; Grossel, M. C.; Horton, P. N. *Supramol*. *Chem*. **2004**, *16*, 405; (e) Donoghue, P. J.; Tehranchi, J.; Cramer, C. J.; Sarangi, R.; Solomon, E. I.; Tolman, W. B. *J*. *Am*. *Chem*. *Soc*. **2011**, *133*, 17602; (f) Zhang, X.; Huang, D.; Chen, Y. -S.; Holm, R. H. *Inorg*. *Chem*. **2012**, *51*, 11017; (g) Rajput, A.; Mukherjee, R. *Coord*. *Chem*. *Rev*. **2013**, *257*, 350; (h) Tehranchi, J.; Donoghue, P. J.; Cramer, C. J.; Tolman, W. B. *Eur*. *J*. *Inorg*. *Chem*. **2013**, 4077; (i) Wnag, Q. -Q.; Day, V. W.; Bowman-James, K. *Chem*. *Commun*. **2013**, *49*, 8042.

(94) Janiak, C. *J. Chem. Soc., Dalton Trans*. **2000**, 3885.

(95) Lin, J. C. Y.; Huang, R. T. W.; Lee, C. S.; Bhattacharyya, A.; Hwang, W. S.; Lin, I. J. B. *Chem*. *Rev*. **2009**, *109*, 3561.

(96) Garrison, J. C.; Yongs, W. J. *Chem. Rev*. **2005**, *105*, 3978.

(97) (a) Wang, H. M. J.; Chen, C. Y. L.; Lin, I. J. B. *Organometallics* **1999**, *18*, 1216; (b) Jothibasu, R.; Hunyh, H. V.; Koh, L. L. *J*. *Organomet*. *Chem*. **2008**, *693*, 374.

(98) (a) Gale, P. A. *Coord. Chem. Rev*. **2003**, *240*, 191; (b) Xu, Z.; Kim, S. K.; Yoon, J. *Chem. Soc. Rev*. **2010**, *39*, 1457.

(99) Zhao, X.-F.; Zhang, C. *Synthesis* **2007**, *4*, 551.

(100) (a) Frémont, P. D.; Singh, R.; Stevens, E. D.; Petersen, J. L.; Nolan, S. P. *Organometallics* **2007**, *26*, 1376; (b) Gaillard, S.; Slawin, A. M. Z.; Bonura, A. T.; Stevens, E. D.; Nolan, S. P. *Organometallics* **2010**, *29*, 394; (c) Pažický, M.; Loos, A.; Ferreira, M. J.; Serra, D.; Vinokurov, N.; Rominger, F.; Jäkel, C.; Hashmi, A. S. K.; Limbach, M. *Organometallics* **2010**, *29*, 4448. (d) Sivaram, H.; Tan, J.; Huynh, H. V. *Organometallics* **2012**, *31*, 5875. (e) Huynh, H. V.; Guo, S.; Wu, W. Q. *Organometallics* **2013**, *32*, 4591.

(101) Ray, M.; Ghosh, D.; Shirin, Z.; Mukherjee, R. *Inorg*. *Chem*. **1997**, *36*, 3568.

(102) (a) Warsink, S.; Roodt, A. *Acta Cryst*. **2012**, *E68*, m1075; (b) Petko, K. I.; Kokhanovskii, Y. P.; Gutov, O. V.; Rusanov, E. B.; Yagupolskii, Y. I.; Yagupolskii, L. M. *J*. *Organomet*. *Chem*. **2013**, *739*, 11; (c) Szulmanowicz, M. S.; Gniewek, A.; Gil, W.; Trzeciak, A. M. *ChemCatChem* **2013**, *5*, 1152.

(103) (a) Gülcemal, S.; Kahraman, S.; Daran, J.-C.; Çetinkaya, E.; Çetinkaya, B. *J. Organomet. Chem*. **2009**, *694*, 3580; (b) Kamisue, R.; Sakaguchi, S. *J. Organomet. Chem*. **2011**, *696*, 1910; (c) Gupta, S.; Basu, B.; Das, S. *Tetrshedron* **2013**, *69*, 122.

(104) Haque, R. A.; Ghdhayeb, M. Z.; Budagumpi, S.; Salman, A. W.; Ahamed, M. B. K.; Majid, A. M. S. A. *Inorg. Chim. Acta* **2013**, *394*, 519.

(105) SMART version 5.628; Bruker AXS Inc.: Madison, WI, 2001.

(106) *SAINT+version 6.22a*; Bruker AXS Inc.: Madison, WI, 2001.

(107) Sheldrick, G. W. *SADABS version 2.10*; University of Göttingen, 2001.

(108) *SHELXTL version 6.14*; Bruker AXS Inc.: Madison, WI, 2000.

List of Publications

(1) Yuan Han, Dan Yuan, Qiaoqiao Teng, Han Vinh Huynh,* "**Reactivity Differences of Palladium(II) Dimers Bearing Heterocyclic Carbenes with Two, One, or No α-Nitrogen Atoms toward Isocyanides**", *Organometallics* **2011**, *30*, 1224.

(2) Han Vinh Huynh,* Qiaoqiao Teng, "**Highly Modular Access to Functionalised Metal-Carbenes *via* Post-Modifications of a Single Bromoalkyl-Substituted NHC-Pd(II) complex**", *Chem. Commun*. **2013**, *49*, 4244.

(3) Dan Yuan, Qiaoqiao Teng, Han Vinh Huynh,* "**Template-Directed Synthesis of Palladium(II) Sulfonate-NHC Complexes and Catalytic Studies in Aqueous Mizoroki-Heck Reactions**", *Organometallics* **2014**, *33*, 1794.

(4) Qiaoqiao Teng, Daniel Upmann, Sheena Ai Zi Ng Wijaya, Han Vinh Huynh,* "**Bis(functionalized NHC) Palladium(II) Complexes via a Postmodification Approach**", *Organometallics* **2014**, *33*, 3373.

(5) Qiaoqiao Teng, Han Vinh Huynh,* "**Determining the Electron Donating Properties of Bidentate Ligands by ^{13}C NMR Spectroscopy**", *Inorg. Chem*. **2014**, *53*, 10964.

(6) Qiaoqiao Teng, Han Vinh Huynh,* "**Controlled Access to a Heterometallic N-Heterocyclic Carbene-helicate**", *Chem Commun*. **2015**, 51, 1248.

(7) Qiaoqiao Teng, Han Vinh Huynh,* "**Selective and Catalytic Formation of Cyanamides via alkylation of a mixed NHC/carbodiimido complex**", in preparation.